COMPOSITE POWER SYSTEM ADEQUACY ASSESSMENT INVOLVING NON-UTILITY GENERATION AND POWER WHEELING

A Thesis

Submitted to the College of Graduate Studies and Research

in Partial Fulfilment of the Requirements

for the Degree of

Master of Science

in the

Department of Electrical Engineering

University of Saskatchewan

by

FRANCIS FOLI-MAWUSI GBEDDY

Saskatoon, Saskatchewan

June 1992

COPYRIGHT

ACKNOWLEDGEMENTS

The author of this thesis would like to extend his appreciation, gratitude and sincere thanks to Dr. Roy Billinton, his supervisor, for the guidance and consistent encouragement provided during the course of this research work.

This work was financed by the National Energy Board/Ministry of Energy of Ghana and by Dr. Billinton in the form of a research assistantship from a Natural Science and Engineering Research Council of Canada operating grant. Both financial supports are thankfully acknowledged.

Finally, special thanks to my wife, Diana, my two daughters, Spes and Stephanie, and my parents for their patience, constant encouragement and moral support during the study.

UNIVERSITY OF SASKATCHEWAN
Electrical Engineering Abstract 92A362

COMPOSITE POWER SYSTEM ADEQUACY ASSESSMENT INVOLVING NON-UTILITY GENERATION AND POWER WHEELING

Student: FRANCIS GBEDDY Supervisor: ROY BILLINTON

M.Sc. Thesis Presented to the
College of Graduate Studies and Research

June 1992

ABSTRACT

A significant component of the overall system electrical energy requirements of many power utilities is now being provided by Non-Utility Generators (NUGs) and power/energy purchases from neighbouring systems. A NUG is defined in this thesis as an independent power production facility or cogeneration facility, which is not owned by the utility in whose service area the facility is located. These facilities are small generating capacity components associated with load points within the utility system. NUG capacity additions can have considerable impact on adequacy at both the individual load points and the overall system.

The opportunity to wheel energy/power through the transmission facilities of one system in order to serve another system is one of the many possible uses and benefits of interconnection between neighbouring electric power systems. Wheeling of energy can also occur within a system when an independent power producer in a local utility system serves a load located at some other point in the system. Power wheeling transactions are recognised to have a definite impact on the utility's system losses depending upon the system topology, the amount of power/energy wheeled and the wheeling distance involved. These factors currently form the basis for determining service charges associated with power wheeling.

Quantification of the reliability impacts of NUGs and power wheeling transactions is also important in order to fully understand the impacts of these supply options. This

Table of Contents

List of Figures

List of Tables

LIST OF SYMBOLS

AC	Alternating Current
BPII	Bulk Power Interruption Index
COMREL	COMposite RELiability evaluation package
DC	Direct Current
EENS	Expected Energy Not Supplied
ELC	Expected Load Curtailed
HLI	Hierarchical Level I
HLII	Hierarchical Level II
HLIII	Hierarchical Level III
IPS	Intermediate Power System
KV	Kilo Volts
MECORE	Monte Carlo simulation and Enumeration COmposite Reliability Evaluation package
MW	Mega Watt
MWh	Mega Watt-hour
NUG	Non-Utility Generator
N	Number of random samples
U	Unavailability
λ	Failure rate
μ	Repair rate
σ	Standard deviation
α	Variance coefficient

1. INTRODUCTION

1.1. Power System Reliability Concepts

The fundamental objective of an electric power system is to supply customers, both large and small, with electrical energy as economically as possible and with an acceptable level of reliability. The increasing dependence of modern society on electrical energy puts a heavy pressure on electric power utilities to maintain a continuous supply to customers as and when required. This requirement is, however, not physically possible as it is not economically and practically justified to attempt to design and construct a power system with 100% reliability. Power system engineers, however, have always attempted to achieve the highest possible reliability at a reasonable and affordable cost. The value of power system reliability assessment in managerial decision-making both at the planning and operating stages of power system development is becoming increasingly important and many utilities around the world are showing increased interest in this form of assessment.

The term "reliability" can be generally defined as the overall ability of the system to perform its particular function. Reliability, however, has a wide range of meaning when applied to power systems. The reliability concerns in a power system can be classified into two basic functional categories: **Adequacy** and **Security** as shown in Figure 1.1.

System adequacy relates to the existence of sufficient generation, transmission and distribution facilities to satisfy customer load demands. Adequacy, therefore, is concerned with evaluations under static system conditions which do not involve system disturbances. System security, on the other hand, concerns the ability of the system to respond to disturbances and perturbations arising within it. System security analysis,

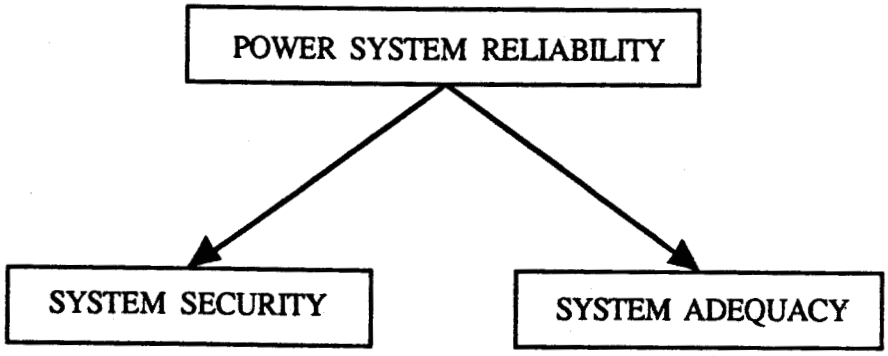

Figure 1.1: Subdivision Of Power System Reliability

therefore involves the dynamic behaviour of the system and may require dynamic studies such as transient stability analysis involving detailed modelling of power system control and protection equipment. It is therefore evident that adequacy assessment and security analysis deal with quite different reliability issues and involve different assessment techniques. The work described in this thesis is confined to the area of power system adequacy assessment.

The evaluation techniques used in adequacy assessment can be categorised in terms of their application to the three basic segments of a complete power system. These three segments, which can also be designated as functional zones of the power system are generation, transmission and distribution. Adequacy studies can be performed individually in each of these three zones. Sequential combinations of the functional zones define appropriate Hierarchical Levels as shown in Figure 1.2.

Hierarchical Level (HL) I is concerned with only the generation facilities. HLI adequacy evaluation forms a basic element of any power system planning process and is concerned with the assessment of the ability of the generation facilities to generate sufficient energy to give a reasonable level of assurance of satisfying the total system load demand. HLII analysis includes both generation and transmission facilities, and HLIII analysis involves all three functional zones in the assessment of consumer load point adequacy.

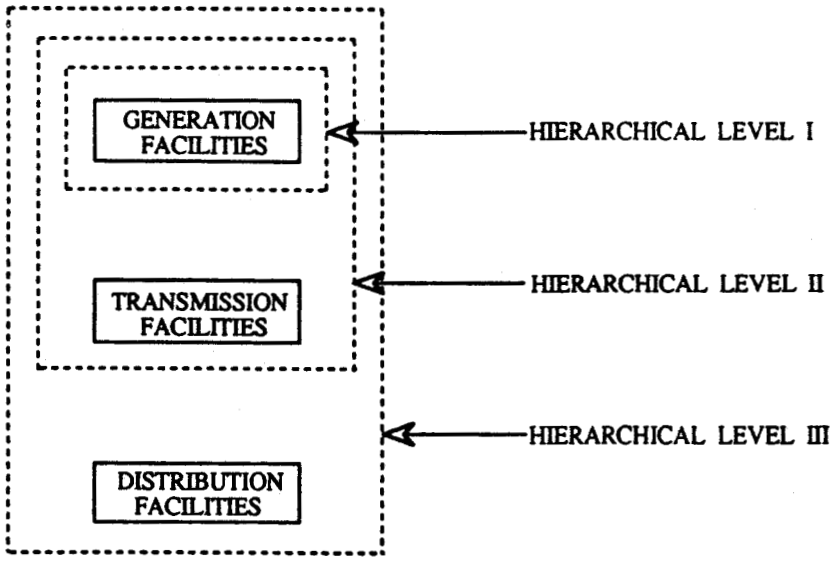

Figure 1.2: Power System Functional Zones And Hierarchical Level Structure

1.2. Scope and Objectives of Thesis

The work done in this thesis is primarily concerned with composite system (or HLII) adequacy evaluation. These assessments involve the total problem of evaluating the adequacy of the generation and transmission facilities to supply adequate, dependable and suitable electrical energy to the major system load points. The analysis recognises the role of the transmission network as the means by which energy from the generation locations is conveyed to the major system load points. Composite system adequacy assessment is still in its infancy and relatively little use is made of it at the present time in practical decision making. The need to possess the ability to quantitatively assess the adequacy of a composite system is, however, now widely recognised and interest is expanding. Recent advancements in the establishment of comprehensive data bases by utilities and the enhancement of computing facilities are gradually removing the barriers which artificially constrain the probabilistic nature of power systems into a deterministic framework. These advances have resulted in the relatively recent development of several computer programs [1, 2, 3, 4, 5, 6, 7, 8, 9] based on probabilistic principles for composite system adequacy analysis.

The tasks involved in power system planning are becoming increasingly complex as a result of the rising costs of conventional electrical energy supplies coupled with the uncertain global economic and political conditions and the increasing environmental concerns facing power utilities. System planners are therefore faced with limited choices and numerous supply constraints leading to a trend in which previously unconventional energy resources are beginning to play a significant role in the planning process as potentially viable supply options. In recent years, a significant component of overall electrical energy requirements of many utilities has been provided by independent power production facilities in the form of Non-Utility Generation (NUG) and energy from neighbouring systems. These supply options are becoming increasingly important in least cost energy planning. It is therefore important that computational tools be developed which are efficient and sufficiently flexible to incorporate these new technologies in the analyses.

The methods used for evaluating NUG and external energy options are normally based on the economic and system loss impacts associated with these options. Reliability considerations and other impacts associated with these options, such as those relating to system security, VAr requirements and voltage profiles [10] are also important factors which must be taken into consideration. This thesis is concerned with the reliability impacts of NUG and external energy transactions in utility systems.

The objectives of the work described in this thesis are:

1. to review the probabilistic methods used for composite system adequacy analysis with the object of highlighting the major differences, advantages and limitations associated with each method; and
2. to investigate the composite system reliability impacts associated with NUG and external power/energy transactions in a utility system.

It is believed that the concepts and studies described in this thesis provide significant insight to the quantification of the composite system reliability impacts associated with NUG and external energy transactions. The studies reported in this thesis and the analysis of the test systems used therefore enhance the methods currently used in evaluating these options.

1.3. Thesis Outline

The thesis is divided into two main parts consisting of seven chapters.

Following the introduction in Chapter 1, the first part of the thesis consisting of Chapters 2 and 3 provides a review of the probabilistic methods currently used for composite system adequacy evaluation. Two general approaches for HLII analysis are identified in Chapter 2. These are the analytical technique and Monte Carlo simulation. The analysis procedure in each case is outlined showing the various steps and how the different types of indices are computed and accumulated. The advantages and limitations of both methods are also stated. Two computer programs developed at the University of Saskatchewan for HLII analysis are also described in this chapter.

Chapter 3 briefly describes two test systems, the Roy Billinton Test System (RBTS) and the IEEE-Reliability Test System (RTS), which are used for the studies described in this thesis. The two computer programs described in Chapter 2 are utilised to compute the composite system indices of the RBTS and the IEEE-RTS in order to illustrate the basic features of the two methods of evaluation. These indices serve as base-case results for the two test systems in subsequent system studies.

The second part of the thesis consisting of Chapters 4, 5 and 6 deals with the required analysis to determine the reliability impacts associated with NUG and external energy transactions in utility systems.

System studies are illustrated in Chapter 4 to determine the composite system reliability impacts associated with various NUG options in the two test systems. The effects on both load point and overall system adequacy are discussed.

The effects of external power/energy transactions on the utility's composite system adequacy are investigated in Chapters 5 and 6. These external transactions, designated as "power wheeling" in this thesis, can either occur within the supply jurisdiction of the utility (termed Intra-system power wheeling) or come from neighbouring interconnected systems. Intra-system power wheeling concepts are introduced in Chapter 5. These concepts are further extended in Chapter 6 to examine the impacts of wheeling in

interconnected systems. The effects of various wheeling options in both cases on the composite system indices of the RBTS and the IEEE-RTS are discussed in Chapters 5 and 6.

The seventh chapter summarises the work in the thesis and presents the conclusions.

2. REVIEW OF COMPOSITE SYSTEM RELIABILITY EVALUATION METHODS AND INDICES

2.1. Introduction

A composite power system or bulk power system consists of two basic component types: generating units and transmission lines. Transformers in the system are treated as transmission elements with appropriate failure and repair data. The primary objective of composite or bulk power system planning is the economic development of the generation and transmission facilities required to satisfy the customer load demands at acceptable levels of quality and availability. Substations and switching stations also form an integral part of the bulk power system and are composed basically of circuit breakers, bus sections and transformers. Basic composite system adequacy evaluation can be extended to include the reliability effects of stations [11, 12, 13]. Station reliability performance is an important area of study and is normally considered as a separate entity. Bulk power system adequacy evaluation is primarily concerned with the total problem of assessing the ability of generation and transmission facilities to supply adequate, dependable and suitable electrical energy at the major system load points.

The available computer programs [1-9] for composite power system adequacy assessment are generally based on one of two fundamental evaluation techniques: the analytical approach and the Monte Carlo simulation technique. Irrespective of the approach, the general outline of the evaluation procedure is the same in both cases, although implementation methodologies of some of the steps involved differ in certain respects. The ultimate objective of any evaluation technique is to quantify supply adequacy both at the individual load buses and the overall system by producing appropriate indices. A wide range of indices can be produced and these are generally

classified as either load point indices or system indices. There is no general consensus in the power industry regarding which particular indices are the best. Although most of the indices can be produced using either approach, there are fundamental differences in the way they are accumulated. These differences, in one way or the other, can affect the level of accuracy of the indices obtained. Therefore making a decision on an appropriate set of indices or the suitable evaluation methodology to adopt, depends on a number of factors which are all principally influenced by the intent behind the evaluation process.

The analytical and simulation approaches to composite system adequacy assessment are discussed in this chapter. The main features of the two approaches are described showing the major differences and similarities as well as the advantages and limitations of each approach. Two computer programs developed at the University of Saskatchewan by the Power System Research Group, the COMREL and the MECORE programs based on the analytical and simulation methods of evaluation respectively, are also presented. The indices produced by the programs are also illustrated together with an example of how they are accumulated in each case.

2.2. General Outline of Composite System Adequacy Evaluation

Composite system adequacy evaluation using either the analytical or the simulation approach essentially consists of the steps shown schematically in Figure 2.1. These steps are general in principle, and are followed in the most frequently used methods in the analytical approach (State Enumeration method) and the simulation approach (Monte Carlo method).

Base case evaluation of the system should be performed prior to continuing with any form of contingency evaluation. This is necessary because if the base case is found to be unsatisfactory, then any system component outage cannot be expected to improve the situation and these initial conditions may be a totally unsuitable starting point. On the other hand, if the base case is satisfactory, then these data provide a datum for comparing the results of the various contingency cases.

There are some basic conceptual differences in the implementation methodologies

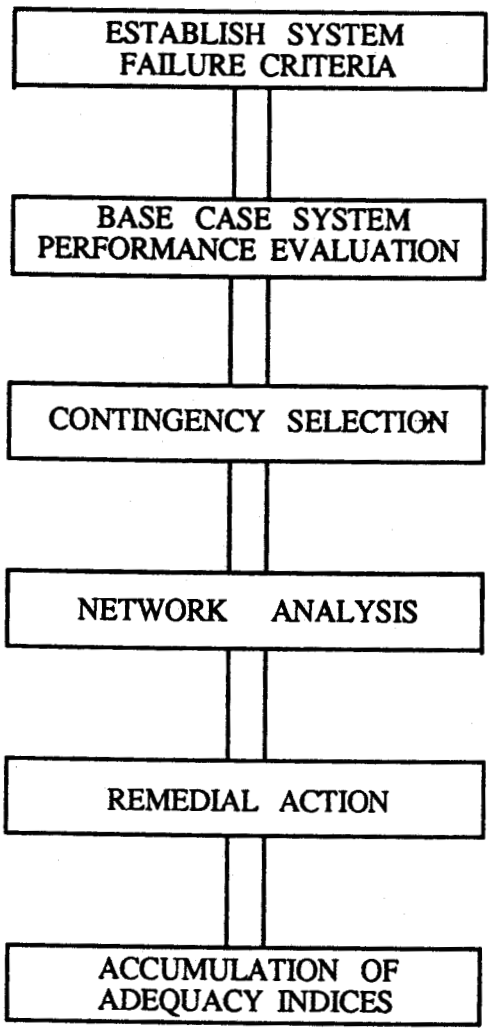

Figure 2.1: Schematic Outline Of Composite System Adequacy Evaluation

used in the two techniques. This is particularly true in connection with the system contingency selection stage which is largely influenced by the modelling approach of system components and operating policies. Differences also exist in the methodology for accumulating risk indices. These differences are discussed later in the chapter.

On the other hand, several aspects of composite system adequacy assessment are common and similar in both methods. The aspects of the analysis common to both methods include the establishment of system failure criteria, the network analysis and the need for remedial or corrective actions. The basic concepts and factors involved at each of these stages of the analysis are discussed in the following sections.

2.3. System Failure Criteria

Quantitative adequacy analysis in a composite system is performed based on a prescribed set of criteria by which the system must be judged as being in the success or failed state. Generally, a bulk power system is considered to be failed if the service at the load buses is interrupted or its quality becomes unacceptable. Such a condition arises if any of the following events occur:

1. Lack of sufficient generation in the system to meet load demand.
2. Interruption of continuity of power supply to a load point.
3. Overload of transmission facilities (e.g. Lines and transformers).
4. Violation of bus voltage tolerances.
5. Generating unit MVAr limit violations.
6. Ill-conditioned network situations.

Failure by any of these criteria does not necessarily mean the collapse of the entire system, although this could be recorded as a failure event. While it is possible for an overload condition to develop into a cascading sequence of events finally leading to the collapse of the system, it is more likely that such a catastrophe would be averted by taking appropriate corrective measures. It should therefore be appreciated that the system failure criteria are only a set of undesirable events which form a basis for the calculation of reliability indices.

2.4. Network Analysis

The adequacy analysis of a bulk power system generally involves the solution of the network configuration under selected outage conditions. Since the analysis normally involves many repetitive calculations for the various system contingency states to be examined, the efficiency and speed of the evaluation process depends appreciably on the load flow algorithm employed in the network analysis. Depending on the prescribed set of failure criteria which in turn depends on the intent behind the studies, various solution techniques are available, each producing a unique set of load point indices. The three network solution techniques normally used are:

- the Network Flow Method ;
- the DC Load Flow Method; and
- the AC Load Flow Method

2.4.1. Network Flow Method (Transportation Model)

The network flow method (or the Transportation Model) is basically concerned with the continuity of the power supply from the generation stations to the major load centres in order to satisfy load demand. The failure constraints addressed in the linear network flow model are limited availability of power at the generating stations to satisfy system load requirements and the continuity of power flow to the major load centres.

In the transportation model, capacity levels are assigned to every system component together with a probability corresponding to each capacity level. The network is solved using Kirchoff's First Law and max-flow or min-cut [14] concepts, ensuring that the line flows do not exceed the prescribed capacities. The indices obtained using this method are of a low level of accuracy, but may be acceptable in some applications.

2.4.2. DC Load Flow Method

Approximate linear power flow techniques such as the DC load flow algorithm can be used to enhance the computation speed in composite system adequacy assessment. In addition to recognising generation unavailability and lack of supply continuity as system constraints, the DC load flow solution technique also provides information regarding line overload conditions in the composite system and considers them to be system failure conditions when estimating the adequacy indices. This technique, like the transportation model, does not provide any estimate of the bus voltages and the reactive power limits of generating units.

2.4.3. AC Load Flow Method

AC load flow techniques are required when the continuity and the quality of power supply (i.e. proper bus voltage levels and the correct MVAr limits of the generating units) are important concerns in adequacy assessment of a composite system. The AC load flow technique is capable of recognising all the system failure criteria listed in Section 2.3 and produces indices that reflect the impact on adequacy of the operational characteristics of the power system. The conventional AC load flow techniques such as the Gauss-Siedel, Newton Raphson and more accurate second order load flow methods are, however, rarely used for adequacy studies, because they are computationally expensive and require large storage requirements. Several approximate versions of these algorithms, such as the decoupled and the fast decoupled AC load flow algorithms, which are faster and require less storage have been developed and are more frequently used to produce results with an acceptable degree of accuracy.

The selection of an appropriate network solution technique, therefore, is of prime importance and is basically an engineering decision. The selected technique, however, should be capable of satisfying the intent behind the studies from a management, planning and design point of view.

2.5. Remedial Actions

It is important to determine whether it is possible to eliminate a system problem by employing a remedial action (or corrective measure). On the basis of the system failure criteria, the broad categories of remedial actions that can be employed are as follows:

1. Generation rescheduling in the case of capacity deficiency in the system - applicable in all the three network solution techniques.
2. Handling of bus isolation and system splitting problems arising from transmission line(s) and transformer(s) outages - applicable in all the three network solution techniques.
3. Line overload alleviation - applicable in the DC and the AC load flow solution techniques.
4. Correction of generation unit MVAr limit violations - applicable only in the AC load flow solution technique.
5. Correction of a bus voltage problem and the solution of ill-conditioned network situations - applicable in only the AC load flow solution technique.

6. Load curtailment in the event of an unavoidable system problem - applied in all the network solution techniques.

Load curtailment is usually the last resort to eliminate a system problem and should be used when all relevant corrective measures fail to reverse an undesirable condition caused by an outage event in the bulk power system. It is therefore necessary to determine a suitable strategy (or philosophy) to direct the load curtailment action so that it reflects the operating policy of the system concerned. An outage event may affect a wide area of the system or perhaps a single bus depending on the component(s) on outage, the network configuration, the corrective measures taken and the load curtailment philosophy adopted. It is generally desirable for the load curtailment philosophy to be flexible and capable of ensuring that indices produced truly reflect the level of adequacy at the major load points. This necessitates the following policies:

1. to classify the load at each bus according to importance, so that, the least important loads are curtailed first, followed by the next least important and the most important loads last , if necessary; and
2. to assign each major load centre with some priority relative to the location of the outage event in order to confine load curtailment as much as possible to the problem area.

With these policies directing the load curtailment action, it is possible to confine load curtailment to a small area or allow it to spread to a wider area.

2.6. Analytical Modelling Methods

In the analytical method of composite system adequacy evaluation, mathematical models are used to represent the system and its operating policies. The models are derived based on specific assumptions which, at times, are limited in the amount of sophistication that can be accommodated in modelling the complex characteristics of practical power systems. The mathematical models can be developed using any of the following approaches:

- the Network Method; and
- the State-space Method

2.6.1. Network Method

The network method [15, 16, 17] of system reliability analysis is generally based on the solution of logic networks composed of logic block diagrams. A logic block diagram or reliability block diagram for a system describes the logical connections between system components indicating which combinations of component failures result in system failure. By assigning failure and repair data to each block, the logic network can be solved to produce the probability of failure as well as duration and frequency indices [16] though the latter indices do not associate well with this method. Logic block diagrams, however, can only be used to represent systems which consist of monotonic structures [17]; therefore only such systems can be analysed with the network method .

It is important to appreciate that the network method for reliability analysis is based solely on continuity as the single failure criterion. In a practical modern power system, complete component redundancy is not economically feasible and therefore system failure criteria take on a wider dimension covering several other aspects of service quality as noted earlier. The use of series/parallel reduction techniques are therefore inadequate for the analysis of a composite power system; because the method fails to recognise that component failure can result in a composite system failure in a conditional sense. It is however possible to extend the network method to incorporate conditional probability theories [18, 19] in order to recognise the conditional behaviour of system components.

2.6.2. State Space Method

In the state space method of composite system reliability analysis, a system is described by its states and the possible transitions between the states. The system state describes the states of the components and the environment in which the system is operating. The probability, frequency and mean duration of the individual system states are easily computed using Markovian Models which utilise constant transitions between states. The fact that the times-to-event have exponential distributions is an underlying assumption behind the provision of constant transition rates. The individual system states are tested with the prescribed set of system failure criteria to determine those states that result in system failure in order to combine them and calculate the relevant indices.

In order to illustrate the procedure for obtaining the frequency and duration indices of a combined state, consider the state space diagram in Figure 2.2 consisting of four different states which are partitioned into failed (F) and operating (W) system categories.

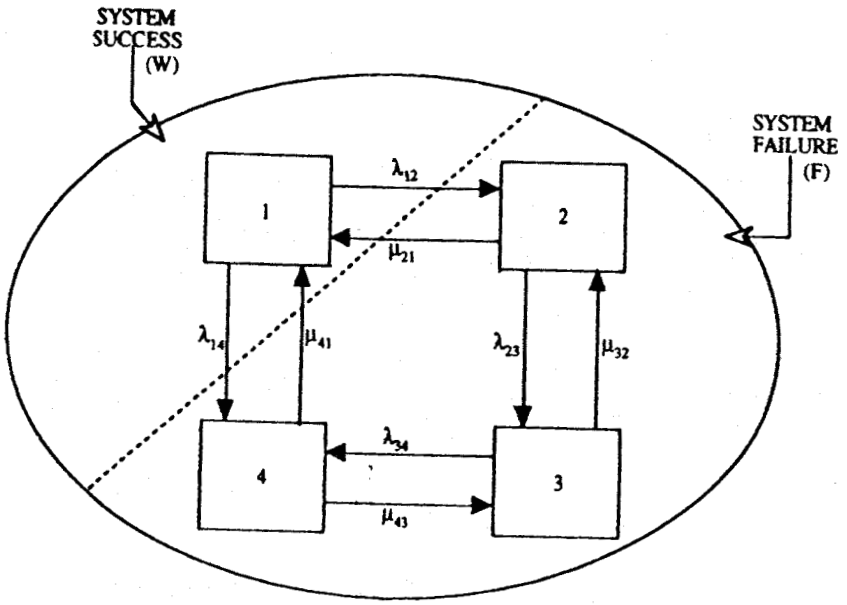

Figure 2.2: State Space Diagram Partitioned Into System Failure And Success Domains

States 2, 3 and 4 represent system failure modes whilst State 1 is the system success or operating mode. If P_i is the steady state probability of State i, and λ_{ij} and μ_{ij} are the departure rates from State i to State j, then:

$$\textit{Probability of System Failure}\,(P_F) = P_2 + P_3 + P_4 \tag{2.1}$$

$$\textit{Frequency of System Failure}\,(F_F) = P_2\mu_{21} + P_4\mu_{41} = P_1(\lambda_{12} + \lambda_{14}) \tag{2.2}$$

$$\textit{Duration of System Failure}\,(D_F) = \frac{P_F}{F_F} = \frac{P_2 + P_3 + P_4}{P_2\mu_{21} + P_4\mu_{41}} = \frac{P_2 + P_3 + P_4}{P_1(\lambda_{12} + \lambda_{14})} \tag{2.3}$$

Similarly,

$$\textit{Probability of System Success } (P_S) = P_1 \tag{2.4}$$

$$\textit{Frequency of System Success } (F_S) = P_1(\lambda_{12} + \lambda_{14}) \tag{2.5}$$

$$\textit{Duration of System Success } (D_S) = \frac{P_S}{F_S} = \frac{P_1}{P_1(\lambda_{12} + \lambda_{14})} = \frac{1}{\lambda_{12} + \lambda_{14}} \tag{2.6}$$

Equations 2.1 to 2.3 can be generalised for calculating system failure indices using Equations 2.7 to 2.9 as follows:

$$P_F = \sum_{i \in F} P_i \tag{2.7}$$

$$F_F = \sum_{i \in F} P_i \sum_{j \in W} \lambda_{ij} \tag{2.8}$$

$$D_F = \frac{\sum_{i \in F} P_i}{\sum_{i \in F} P_i \sum_{j \in W} \lambda_{ij}} \tag{2.9}$$

where

λ_{ij} : is the rate of transition from a state, i, in the failed domain to a state, j, in the success domain; and

F, W : are the system failure and success domains respectively.

2.6.3. State Enumeration Approach

The power and flexibility of the state space method are demonstrated in the State Enumeration Approach which is the most frequently used algorithm for implementing these concepts. The efficiency of the algorithm arises from the systematic manner in which contingency states are selected for evaluation, thus making it possible for the effects of each system component to be considered separately. However, the total number

of contingencies that must be evaluated can become enormous and it often becomes necessary in practical situations to limit the number by using some form of cut-off criteria.

The broad range of cut-off criteria normally employed include the following:

1. Predetermined contingency selection.
2. Frequency cut-off criterion.
3. Ranking of contingencies according to the impact on the system [10].

In the first method, the state space is truncated by specifying the contingency level to be considered (i.e. 1st Order, 2nd Order, etc.). This selection is based on the assumption that the probabilities of the states representing higher order overlapping outages are negligible compared with the lower order outages. The frequency cut-off alternative limits the evaluation to only contingencies which have a rate of occurrence above a certain predetermined value. The third criterion allows contingencies to be ranked according to their impact on the system and only those outage contingencies which result in severe system conditions are evaluated. The intention in all these methods of approximation is to curtail the list of events that can occur in a practical composite system in order to reduce the computational requirements of the analysis. These approximations, however, reduce the accuracy of the results obtained.

2.6.3.1. Accumulation of Risk Indices in the State Enumeration Approach

In the analytical methods, expected indices are calculated directly and are considered theoretically to be exact solutions based on the assumptions made. Figure 2.3 shows a flowchart for the accumulation of indices in the state enumeration algorithm.

Assume that a system contingency state s, has a probability $P(s)$, and the index function $F_i(s)$ at load point i is required. The mathematical expectation of the index function at load point i, $E(F_i)$, can be calculated by the state enumeration algorithm as follows :

$$E(F_i) = \sum_{s \in G} F_i(s) P(s) \tag{2.10}$$

where G is the set of system problem contingency states.

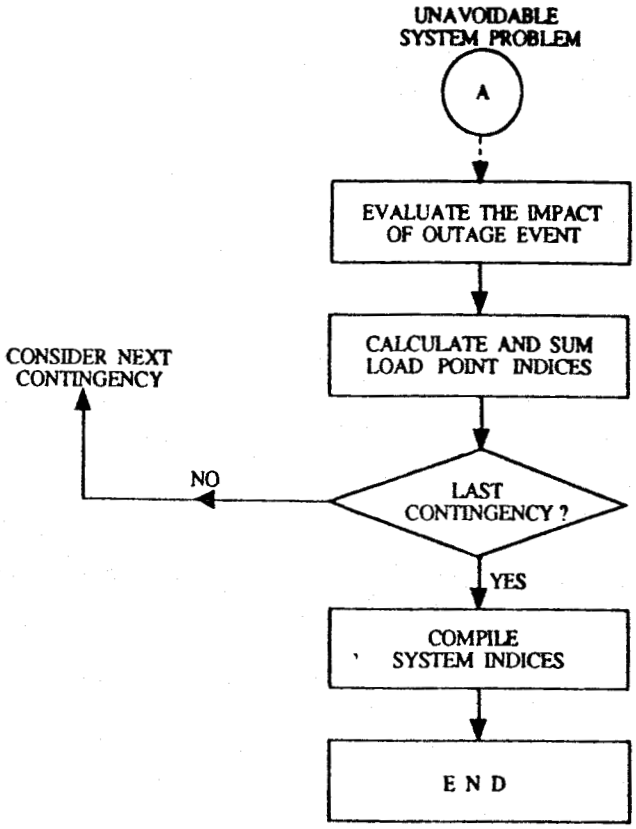

Figure 2.3: Flowchart For The Accumulation Of Reliability Indices In The State Enumeration Method

The index function $F_i(s)$ can be obtained from the results of the network analysis of the various contingency states. Equation 2.10 is used to accumulate indices for all the major load points in the system, each time a contingency is evaluated. The system indices can be calculated when all the contingencies have been considered

2.7. Monte Carlo Simulation Approach

The Monte Carlo simulation method of composite system adequacy analysis relies on statistical modelling techniques to represent the system and its operating policies. Random processes obeying predetermined probability distributions are used to simulate the various system states by recreating in each sample all the characteristics of the system. The system characteristics may include load levels, weather conditions, component availability, system protection behaviour, etc., thus theoretically enabling a realistic modelling of the features associated with a complex composite power system.

2.7.1. System Contingency Selection

The generation and selection of system contingency states for evaluation in the Monte Carlo method involves the sampling of equipment outages and load levels and can include common mode failures and dependent events, if required.

System component availability is generally modelled as a 2-state random variable using the component Forced Outage Rate (FOR) data. In cases where multi-state representation is required, the steady state probabilities of the various component states are used to define specific regions of the domain of the multi-state random variable corresponding to each state.

The traditional approach for determining the component availability is to sample a value from a uniform distribution [0,1] by the generation of a pseudorandom number [20]. The value of the number generated (in the range [0,1]) is compared with the defined regions of the domain of the random variable to determine the drawn state of the component. The two basic sampling approaches commonly used are :

- the State Duration Sampling Approach; and
- the State Probability Sampling Approach.

In the **State Duration Sampling Approach** the probability distribution of state duration for each component is sampled and the records of the chronological state transition process for each component is obtained over a suitable number of years. The chronological system state transition process can be obtained for system analysis by combining the chronological state transition process of all the system components. This approach can be used to sample time-dependent state probabilities as well as limiting state probabilities, but it involves relatively large computational requirements.

The **State Probability Sampling Approach** is a simpler and faster method and can be used when the sampling of limiting state probabilities is justified. In this approach, it is assumed that a system state depends on the combination of all component states. Therefore, each component state can be sampled using the state probability (or FOR) data of the component. The system state is obtained by repeating the sampling procedure for each component in the composite system.

2.7.2. System Analysis

The system analysis stage of adequacy assessment in the Monte Carlo method involves the network evaluation of the drawn state and the subsequent judgement of the state as representing either a system failure state or operating state. Due to the large computational requirements associated with the simulation of system contingency states, it is normally desirable to minimise, as much as possible, the computational requirements during the system analysis stage. Approximate linear power flow algorithms, such as DC load flow, are therefore normally preferred and used for the evaluation of the system performance in the Monte Carlo method. Although the approximate linear power flow models are limited in providing information relating to the quality of service at the load centres, their use in the Monte Carlo method is felt to be a reasonable and a necessary compromise between computational cost and the level of accuracy normally required of the calculated indices in planning studies [21].

2.7.3. Accumulation of Risk Indices in the Monte Carlo Method

The methodology by which risk indices are accumulated in the Monte Carlo Method consists of averaging the various experimental results in order to obtain an estimate of the expected value of the particular risk index. This involves keeping track of both the sample count and the system failure sample count. Figure 2.4 shows a flowchart for accumulating reliability indices in the Monte Carlo method.

Each time a sample is taken and analysed, indices are estimated and checked for accuracy using a suitable convergency criterion. If the error limit of the estimate falls within a predetermined threshold then the estimate is considered to be an acceptable estimate of the expected value and the simulation process is terminated. Otherwise, the process is repeated until an acceptable estimate is obtained.

Some basic characteristics of the indices obtained from the Monte Carlo method can be illustrated with an example in which an estimate of system *Unavailability (U)* is required. The Unavailability of a system is defined as the expected relative frequency of encountering the system failure states. This can be done in the Monte Carlo method by creating a system failure indicator, x_i, such that

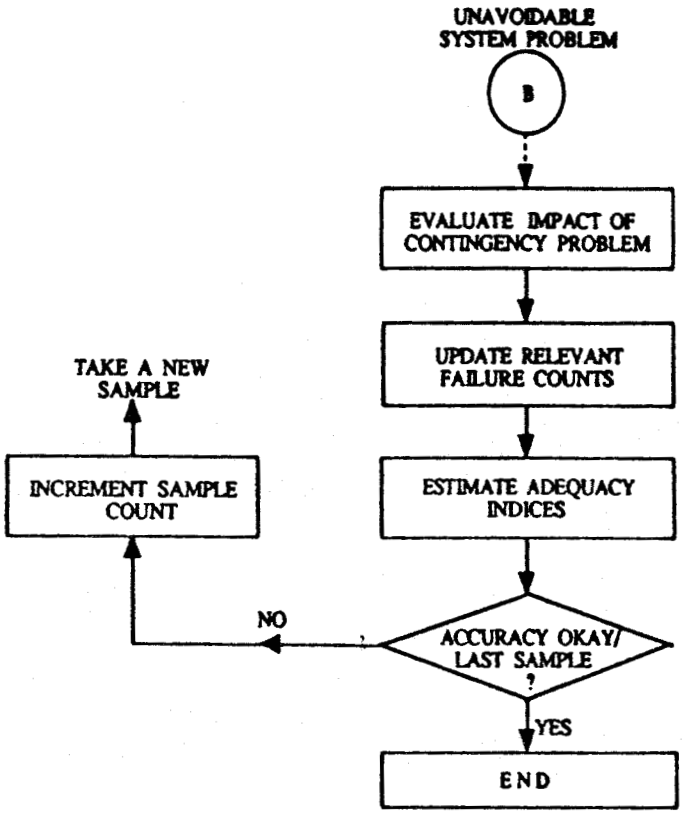

Figure 2.4: Flowchart For The Accumulation Of Reliability Indices In The Monte Carlo Method

$$x_i = \begin{cases} 0 & \text{for system success} \\ 1 & \text{for system failure} \end{cases} \tag{2.11}$$

The estimate of the system unavailability (U) is given by Equation 2.12 as follows:

$$U = \frac{\sum_{i=1}^{N} x_i}{N} \tag{2.12}$$

where N is the total number of trials or samples taken.

The Monte Carlo estimate of U has a variance, σ^2, which reflects the uncertainty associated with the estimate obtained with respect to the exact value. This variance is given by Equation 2.13:

$$\sigma^2=\frac{U(1-U)}{N} \tag{2.13}$$

where σ represents the standard deviation of the estimated sample.

2.7.3.1. Convergency Characteristics

The accuracy of the Monte Carlo method can be expressed in terms of the Variance Coefficient α, which is defined as:

$$\alpha=\frac{\sigma}{U} \tag{2.14}$$

Substituting for σ from Equation 2.13,

$$\alpha=\sqrt{\frac{U(1-U)}{NU^2}}=\sqrt{\frac{1-U}{NU}} \tag{2.15}$$

This parameter is normally used as the convergency criterion in a Monte Carlo sampling simulation. The convergence process is however not always monotonic as would perhaps be expected. Instead as the number of samples increases, the error limit of the estimate from the exact solution decreases. The level of accuracy of the Monte Carlo estimate is therefore highly dependent on the number of samples as well as the variance of the estimated sample.

Variance reduction techniques [20] can be employed to achieve a higher level of accuracy for a given number of samples in the convergency process. However, variance reduction cannot be realised beyond a certain point. Therefore, reduction of the error margin is a matter of compromise between reducing the variance and maintaining a reasonable number of samples in the simulation process. In practical situations, no matter how much effort is made to enhance the convergency process, the estimate never settles down completely to the exact expected value. Therefore there is always some uncertainty associated with the Monte Carlo estimate. It is the responsibility of the analyst to use

experience and judgement to decide when an estimate is considered accurate enough in order to terminate the simulation process.

2.7.3.2. Factors Affecting Computation Time

The number of required samples, N, in Equation 2.15 can be expressed in terms of the other variables as follows:

$$N=\frac{(1-U)}{\alpha^2 U} \tag{2.16}$$

The approximately inverse relationship between the number of samples (N) and system unavailability (U) as given in Equation 2.16 shows that the use of the Monte Carlo technique is not very effective computationally with very reliable systems (or systems with low Unavailability). In these cases, a large number of samples is required which can involve considerable computation time before an acceptable level of accuracy in the results can be obtained.

The large number of samples required in the Monte Carlo method and the large number of contingency states that must be analysed in the state enumeration technique have been identified as the major elements accounting for the large computational requirements in the different evaluation techniques. From Equation 2.16, it can be deduced that given a certain level of accuracy (α), the number of samples (N) required for the Monte Carlo analysis is independent of the system size. This is not the case in the state enumeration approach where the number of contingencies that has to be evaluated increases exponentially with the system size assuming no truncation approximations are made. On this basis, the Monte Carlo method can be considered to be the more viable technique for composite system adequacy assessment of practical power systems which are normally large in size and complex in nature. On the other hand, the complexity of the system analysis aspect of the Monte Carlo analysis has a direct relationship with the system size and this can offset the computing time savings of the sampling stage. However, other advantages of the simulation method such as its ability to effectively model complex characteristics of practical systems, may in some cases be used to justify the additional computational costs.

2.8. Features of the COMREL Program

The development of a digital computer program to perform HLII adequacy analysis was initiated at the University of Saskatchewan by Billinton in the 1960's. Extensive work done in this area in subsequent years by Billinton and Bhavaraju, Billinton and Medicherla [22], Billinton and Kumar [23] and Billinton and Khan [24] has resulted in a refined digital software package designated as COMREL which is now one of the innovative tools in the state of the art of composite system adequacy evaluation.

The COMREL program is based on state space analytical concepts of reliability evaluation and employs the state enumeration technique for the assessment of composite systems. The program can handle independent outages as well as common mode events and station-originated outages when required. It is equipped with all the three network solution techniques (i.e. the Transportation Model, the DC Load Flow Algorithm and the Fast Decoupled Load Flow Algorithm [25]) for analysing system contingencies. Any one of the solution techniques can be selected for evaluating the system performance depending on the prescribed set of system failure criteria. The basic structure of the state enumeration algorithm used in the COMREL program is illustrated by the flowchart in Figure 2.5. Some important features of the COMREL program are discussed in the following sections.

2.8.1. Contingency Selection and Evaluation

The large number of system contingency states that need to be evaluated has been emphasised as the major handicap of the state enumeration approach. In order to handle these problems, the COMREL program has been equipped with the following features, most of which seek to truncate the state space in order to reduce the computational requirements.

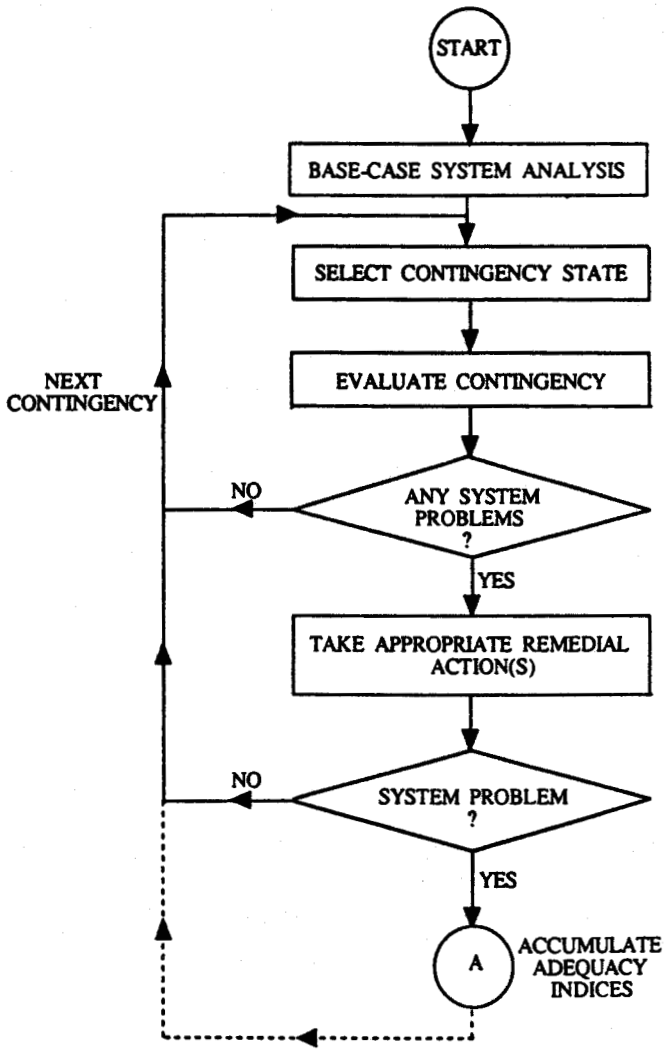

Figure 2.5: Flowchart For The COMREL Program

2.8.1.1. Predetermined Contingency Level

This feature provides for the truncation of the state space by selecting and specifying the order of overlapping outages to be considered. The COMREL program can consider simultaneous independent outages of generating units up to the 4^{th} level, of transformers/transmission lines up to the 3^{rd} level, and up to the 3^{rd} level for generating units together with transformer/transmission lines combined. The user is offered the flexibility of specifying as input data the appropriate levels within this range to suit the system and planning requirements. It is therefore possible and convenient to study the incremental effect of higher order overlapping outages on system adequacy in order to determine the optimum cut-off point for the particular system.

2.8.1.2. Ranking

In a recent update [24] of the program, a contingency ranking facility was provided to further enhance the truncation process by considering in the analysis, only those contingencies having a significant impact on the system.

2.8.1.3. Frequency Cut-off

In order to enhance the computational speed still further, the program employs a frequency cut-off criterion which automatically neglects those contingencies with a frequency of occurrence less than a prespecified value [26].

2.8.1.4. Sorting Facility

The sorting facility is a computational speed enhancement feature that avoids unnecessary repetitive evaluations of identical outage events. With this facility, the reliability indices are calculated based on the outcome of system analysis for only one of the identical contingency states. The contribution of other identical contingencies is computed by multiplying the indices obtained during that first calculation by the number of identical contingencies. This means that the repetition of load flow analysis for contingency states that would have ultimately produced identical effects is avoided, thus resulting in significant savings in CPU time. In the analysis, identical generating units are considered to be units with the same capacity rating, equal failure and repair rates and are located at the same generating station.

2.8.2. Remedial Actions in the COMREL Program

The COMREL program is equipped with the broad range of remedial actions listed in Section 2.5 . The selection of a corrective measure is dependent on the situation that causes an outage in the system. If a generating unit outage at a generation bus results in a capacity shortfall at that bus, then the generation at other generation buses with reserve capacity will be increased proportionately to make up the deficiency. However, if the system remains deficient even after supplying all the available reserve, load is curtailed at the relevant buses as dictated by the load curtailment philosophy.

When the AC load flow algorithm is used, voltage violation cases and

non-convergent situations are corrected by injecting reactive power and rescheduling generating units. Persistent ill-conditioned network problems are solved using heuristic algorithms developed to handle such cases [23].

2.8.2.1. Implementation of Load Curtailment Action

In the COMREL program, the two load curtailment policies introduced earlier in Section 2.5 are implemented using a deterministic approach. Load at each system load bus is classified into two categories: *firm load* and *curtailable load*. The proportion of curtailable load at each bus is pre-specified as a percentage of the total bus load and this information is made available to the program as input data. When there is a system problem, such as a deficiency in system generation capacity, that has to be alleviated by a load curtailment action, curtailable load is interrupted first followed by the interruption of firm load, if necessary.

The flexibility of either confining the load curtailment to the neighbourhood of the outage problem or distributing it over a wider area is implemented by defining three load curtailment passes, one of which must be selected by the analyst to indicate the preferred choice of confinement. The passes define sequential levels, each spreading the required curtailment over a wider area.

It is important to appreciate that the deterministic approach of implementing the two curtailment philosophies in the COMREL program gives the analyst considerable discretion over the confinement of load curtailment to a specific area. The provision for specifying the desired load curtailment pass and the proportion of curtailable load at each load bus as input data, particularly enhanced the modelling of network configurations for power wheeling analyses discussed in the latter part of this thesis. This feature considerably enhances the flexibility of the COMREL software and makes it adaptable for use in a wide range of power system operational studies.

2.9. Features of the MECORE Program

The contingency enumeration approach has been the traditional method used for composite system analysis at the University of Saskatchewan since the 1960's. The development of Monte Carlo-based analytical tools for HL2 adequacy analysis has however been given considerable attention in recent years [27]. Extensive work done in this area by Billinton and Li has led to the development of the MECORE program [9, 28, 29] which is predominantly a Monte Carlo-based computational tool for composite system adequacy evaluation.

MECORE is a digital computer program based on a hybrid Monte Carlo method and the Enumeration technique. The program utilises the basic random variable sampling approach typical of Monte Carlo simulation methods together with a direct analytical approach for system analysis. Figure 2.6 shows a simple flowchart for the MECORE program.

Generating unit states are modelled using multi-state random variables which consequently enables consideration of generating unit derated states, if required [29]. Other system conditions such as common cause outages, regional weather effects, bus load uncertainty and correlation can be easily incorporated in the analysis without any significant complexities and approximations in the system modelling. Considering all these effects simultaneously will, however, result in a significant increase in computation requirements.

2.9.1. Selection of Contingency States

The MECORE program is based on the state probability sampling modelling approach and employs the prime number congruential generator for the generation of uniformly distributed random numbers in the range [0,1] in order to simulate the occurrence of events in the composite system. Independent component outages are assumed. The possible states, S_i, of a component are defined using the component forced outage rate data to correspond to specific regions in the domain [0,1] of the random variable as follows:

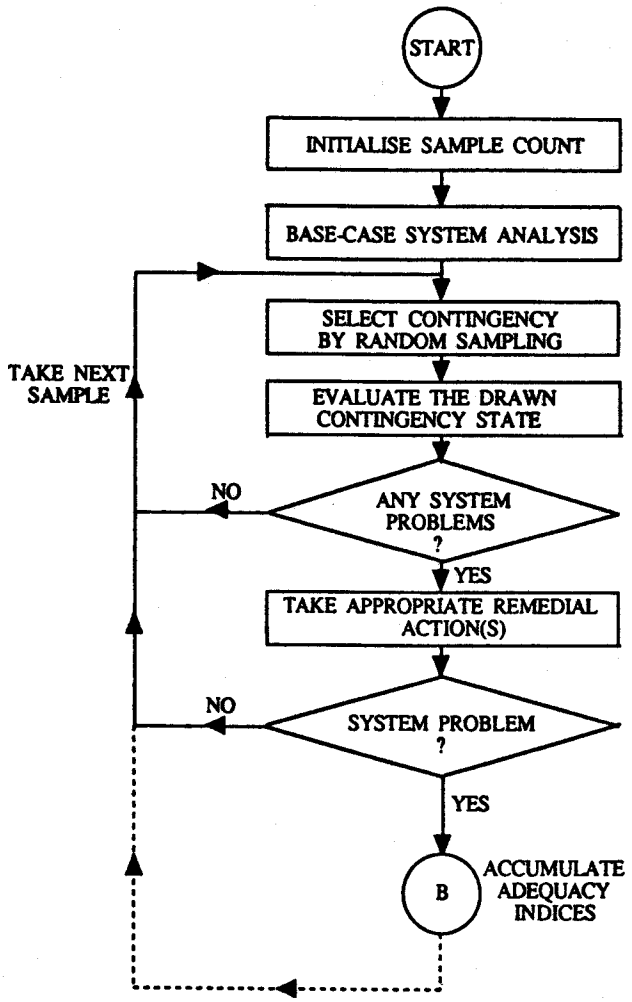

Figure 2.6: Flowchart For The MECORE Program

$$S_i = \begin{cases} 0 & \text{normal state } x > FOR_i \\ 1 & \text{failed state } 0 \le x < FOR_i \end{cases} \tag{2.17}$$

where

FOR_i : is the Forced Outage Rate of Component i; and

x : is the drawn value of the random number.

In a system containing t components, all the components are sampled by repeating the above procedure to obtain the system state, which can be represented by the vector S defined in Equation 2.18.

$$\mathbf{S} = (S_1, S_2, S_3, ...S_t) \tag{2.18}$$

If **S=0**, then the system is in the normal state otherwise it is in a contingent state. This process is repeated each time a system sample is taken.

In the MECORE program, the number of random samples required in a simulation is specified as input data. The variance coefficient of the Expected Demand Not Supplied index is calculated and displayed to indicate the level of accuracy of the results obtained for the specified number of samples. Depending on the level of accuracy desired, the analyst can vary the number of random samples until the desired level of accuracy is achieved.

2.9.2. System Analysis

In a practical power system, only a few of the drawn contingency states will possibly result in load curtailment and these can be easily identified without having to solve load flow equations. This basic concept was applied in the MECORE program to significantly reduce the computational requirements by avoiding the repeated solving of load flow equations for each selected contingency state. The program relies more on direct analytical assessment of situations wherever possible in the system analysis to identify contingencies which require load curtailment in order to alleviate an outage problem. Furthermore, by obtaining a DC load flow solution of the normal system state, the line flows of a contingency state involving line outages can be conveniently and speedily calculated from this base case result using standard mathematical formulae [28] available for the purpose. This further reduces the number of repeated load flow solutions and consequently results in significant savings in CPU time. Appropriate corrective measures are taken for the few contingency states in which a system problem has been established and the reliability indices estimated accordingly.

2.9.3. Remedial Actions in the MECORE Program

The MECORE program is equipped with the range of remedial actions that are applicable to linear power flow models. This includes generation rescheduling to alleviate a capacity deficiency or a line overload problem. If the problem persists, load curtailment is effected at appropriate load points as dictated by a linear programming minimisation model provided to direct the load curtailment action.

2.9.3.1. Implementation of Load Curtailment Action

The two load curtailment philosophies used in the COMREL program have been incorporated in the linear programming minimisation model provided to handle load curtailment in the MECORE program.

The implementation of the first philosophy is realised through the introduction of two or three load curtailment subvariables at each bus and assigning each subvariable with bus load percentages and weighting factors. The least important load at the bus carries the least weighting factor and the most important the largest. In the event where load curtailment is required, the least important load at the bus is curtailed first, followed by the next least important and the most important last, if necessary.

The second philosophy is also implemented by assigning weighting factors to each bus according to the location of the load bus relative to an outage element in each contingency state. The buses closest to the element(s) on outage have relatively small weighting factors and those further away from the outage element(s) have larger weighting factors. The assignment of weights is automatically realised in the resolution of the minimisation model and used to identify those buses which should suffer most of the effects of an outage condition. The ultimate objective of the linear programming minimisation model consisting of six different equations [28] is to minimise the total system load curtailment, simultaneously satisfying the system power balance, DC load flow mathematical relationships and the limits of line flows and generating unit outputs.

It is important to appreciate that, unlike the COMREL program, the MECORE program determines the specific load curtailment action required to alleviate a particular outage condition in accordance with the minimisation model. The user neither has the option of specifying the proportions of curtailable load at the system load buses, nor the option to vary the confinement of the load curtailment to a specific region. The values of all these parameters are automatically determined according to the original formulae embedded in the minimisation model. The MECORE program can therefore not be used to examine the effects of various load curtailment actions on the power system without restructuring the load curtailment algorithm. For example, when modelling a power

system network for power wheeling studies, it may be required to confine load curtailment to a specific area or to exempt, if possible, a particular bus from load curtailment. Before the MECORE program can be used for such an analysis, the minimisation model must be modified in order to achieve these objectives. On the other hand, by allowing more than two load classifications at the system load buses in the MECORE program, it becomes feasible to interrupt bus load in smaller steps. This feature helps to reduce the chance of curtailing too much load than may be necessary to alleviate a particular system problem. This is one main source of differences in the load point indices calculated by the COMREL and the MECORE programs as is illustrated in subsequent chapters of this thesis.

2.10. Composite System Reliability Indices Computed by the COMREL and MECORE Programs

Load point indices and system indices are produced by both the COMREL and MECORE programs. The load point indices are calculated for the major load points in the power system and are very useful in system design for comparing alternative system configurations and system alterations. They can also serve as input indices in the adequacy evaluation of distribution systems supplied from these bulk supply points. The system indices, on the other hand, are indicators of the overall adequacy of the composite system to meet the total system load demand and energy requirements and therefore are quite useful for the system planner. It is important to appreciate that the two sets of indices are not replacements for each other, but should be considered as complementary to each other. This is because neither of the two sets of indices alone can give the entire reliability picture of a power system.

The mathematical formulation of the indices produced in the COMREL and MECORE programs are presented in the following section.

2.10.1. Load Point Indices

PROBABILITY OF FAILURE (P_f)·

$$P_f[Comrel] = \sum_{j \in G} P_j P_{Kj} \tag{2.19}$$

$$P_f[Mecore] = \frac{1}{N_j} \sum_{j \in G} n_{Kj} \tag{2.20}$$

where

j : is an outage condition in the network;

P_j : is the state probability function or the probability associated with the j^{th} outage event;

P_{Kj} : is the probability of the load at bus K exceeding the maximum load that can be supplied at that bus during the j^{th} outage event.

n_{Kj} : is the number of samples in which the drawn outage contingency, j, resulted in load curtailment at bus K;

N : is the total number of samples taken; and

G : is the set of possible system contingency states.

FREQUENCY OF FAILURE (F_f)·

$$F_f[Comrel] = \sum_{j=1} F_j P_{Kj}\ Occurences/Year \tag{2.21}$$

$$F_f[Mecore] = \frac{1}{N_j} \sum_{j \in G} F_s n_{Kj}\ Occurences/Year \tag{2.22}$$

where

F_j : is the frequency of occurrence of the j^{th} outage event; and

F_s : is the failure frequency estimating function.

EXPECTED DURATION OF LOAD CURTAILMENT (*EDLC*)·

$$EDLC\ (Comrel) = \sum_{j \in x,y} D_{Kj} F_j = \sum_{j \in x,y} P_j 8760\ Hours \tag{2.23}$$

$$EDLC\ (Mecore) = \frac{1}{N} \sum_{j \in G} n_{Kj} 8760\ Hours \tag{2.24}$$

where

D_{Kj} : is the duration in hours of the load curtailment arising due to the j^{th} outage event or the duration in hours of the load curtailment at an isolated bus K due to outage event j;

x : represents the set of all contingencies resulting in line overloads which are alleviated by load curtailment at bus K; and

y : represents the set of all contingencies which result in isolation of bus K.

EXPECTED LOAD CURTAILED (*ELC*)

$$ELC\ (Comrel) = \sum_{j \in x,y} L_{Kj} F_j\ MW/Year \tag{2.25}$$

$$ELC\ (Mecore) = \frac{1}{N} \sum_{j \in G} L_{Kj} n_{Kj}\ MW/Year \tag{2.26}$$

where

L_{Kj} : is the load curtailment or simply the load not supplied at bus K due to the j^{th} outage event.

EXPECTED ENERGY NOT SUPPLIED (*EENS*)

$$EENS\ (Comrel) = \sum_{j \in x,y} L_{Kj} D_{Kj} F_j\ MWh/Year$$

$$= \sum_{j \in x,y} L_{Kj} P_j 8760\ MWh/Year \tag{2.27}$$

$$EENS\ (Mecore) = \frac{1}{N} \sum_{j \in G} L_{Kj} n_{Kj} 8760\ MWh/Year \tag{2.28}$$

2.10.2. System Indices

The system indices are derived from the set of load point indices as follows:

BULK POWER INTERRUPTION INDEX (*BPII*)

$$BPII\ (Comrel) = \frac{\sum_{K} \sum_{j \in x,y} L_{Kj} F_j}{L_s}\ MW/MW\text{-}Year \tag{2.29}$$

$$BPII\ (Mecore) = \frac{\sum_{K} \sum_{j \in G} L_{Kj} n_{Kj}}{NL_s}\ MW/MW\text{-}Year \tag{2.30}$$

where

L_s : is the total system load.

BULK POWER ENERGY CURTAILMENT INDEX (*BPECI*)

$$BPECI\ (Comrel) = \frac{\sum_{K} \sum_{j \in x,y} 60 L_{Kj} D_{Kj} F_j}{L_s}\ System\ Minutes \tag{2.31}$$

$$BPECI\ (Mecore) = \frac{\sum_{K} \sum_{j \in G} 60 L_{Kj} n_{Kj} 8760}{NL_s}\ System\ Minutes \tag{2.32}$$

The Bulk Power Energy Curtailment Index is also called the Severity Index and it is very useful in comparing the overall adequacy levels of different systems.

MODIFIED BULK POWER ENERGY CURTAILMENT INDEX (*MBPECI*)

$$MBPECI\ (Comrel) = \frac{\sum_{K} \sum_{j \in x,y} 60 L_{Kj} D_{Kj} F_j}{L_s 8760} \tag{2.33}$$

$$MBPECI\ (Mecore) = \frac{\sum_{K} \sum_{j \in G} 60 L_{Kj} n_{Kj} 8760}{N L_s 8760} \tag{2.34}$$

The full range of indices described in Reference [18] can also be obtained.

2.10.3. Annualised and Annual Indices

The indices calculated for a single fixed load level, normally the yearly peak, over a one year period are designated as **Annualised Indices**. In a practical system, however, the load does not remain constant throughout the year, but changes with the time-of-day as well as with the season. In a typical state enumeration evaluation approach, the effect of variable load can be accounted for by creating a multi-step load model in which loads are aggregated into levels and their probability of occurrence derived from the chronological data of the load duration curve. Annualised indices are then calculated for each load level and weighted by the corresponding load level probability of occurrence. The weighted indices are then summed up to produce a more representative set of indices designated as **Annual Indices**.

One of the advantages of the Monte Carlo Method is its ability to directly estimate annual indices which reflect the hourly variability of system load. This can be done by either sampling the loads directly from the bus load vector or sampling from the load duration curve. In both cases, annual indices are directly estimated with an appreciable level of accuracy. When annualised indices are required, a constant load level can be assumed during the sampling.

The multi-step load aggregation approach is used to calculate annual indices in the COMREL and MECORE programs. The accuracy of the annual indices obtained in this manner depends on the number of load steps assumed. The number of load steps which is appropriate in a particular case, depends upon the sensitivity of the composite system indices to load variations; but it is also limited by computational constraints. In this thesis, annual adequacy indices are calculated using appropriate load models. Detailed descriptions of the load models used are provided in Chapter 3.

2.11. Summary

The basic concepts of composite system adequacy assessment have been presented in this chapter. Two approaches to this form of analysis are introduced. The analytical methods produce exact solutions of the mathematical models developed to represent the composite system. The assumptions are, however, limited in their ability to effectively produce realistic models to represent a complex composite system and its operational policies. The Monte Carlo simulation methods are more effective in this regard, but can only provide estimates of the expected values of the indices. Depending upon a number of factors which include system complexity, the required level of accuracy and the power of the computational facilities available, one method may be found to be more appropriate and more convenient than the other in a given system study.

Two available computer programs, COMREL and MECORE based on the analytical method and Monte Carlo simulation respectively, have been described. The two programs constitute the computational tools utilised in this thesis for the quantitative analysis of composite system adequacy. The program features described show the different ways in which the primary objectives of composite system adequacy analysis can be realised.

3. RELIABILITY TEST SYSTEMS AND BASE CASE COMPOSITE SYSTEM ADEQUACY INDICES

3.1. Introduction

The experience of one power utility with its system may be different from that of another and therefore the characteristic features and capabilities of different computer programs for reliability assessment will differ according to the intent behind the development and utilisation. The establishment of an acceptable reliability test system is therefore extremely important, as it provides a reference network for testing the available programs in order to compare their capabilities and the results obtained using different solution techniques.

The IEEE-Reliability Test System (RTS), published in 1979 by the IEEE Subcommittee on the Application of Probability Methods (APM) [30], provides a consistent and generally acceptable set of data that can be used both in generation and composite system adequacy assessment. The nature of the IEEE-RTS reflects the essential characteristics of a practical power system. The Roy Billinton Test System (RBTS) [31] is a smaller reliability test system, which was developed at the University of Saskatchewan for educational purposes. The main objective in designing a reliability test system for educational purposes is to create a test system which is sufficiently small to permit the conduct of a large number of reliability studies with a reasonable solution time, but also sufficiently detailed to reflect the actual complexities involved in a practical reliability analysis. The two test systems are briefly described in this chapter. Both test systems are utilised in this thesis for composite system adequacy analysis. The complete data for the IEEE-RTS and the RBTS can be found in References [30] and [31] respectively.

3.2. Description of the Roy Billinton Test System (RBTS)

The single line diagram of the 6-bus RBTS is shown in Figure 3.1. The system has 2 generator (PV) buses, 4 load (PQ) buses, 9 transmission lines and 11 generating units. The minimum and the maximum ratings of the generating units are 5 MW and 40 MW respectively. The RBTS has a single transmission voltage level at 230 KV. The

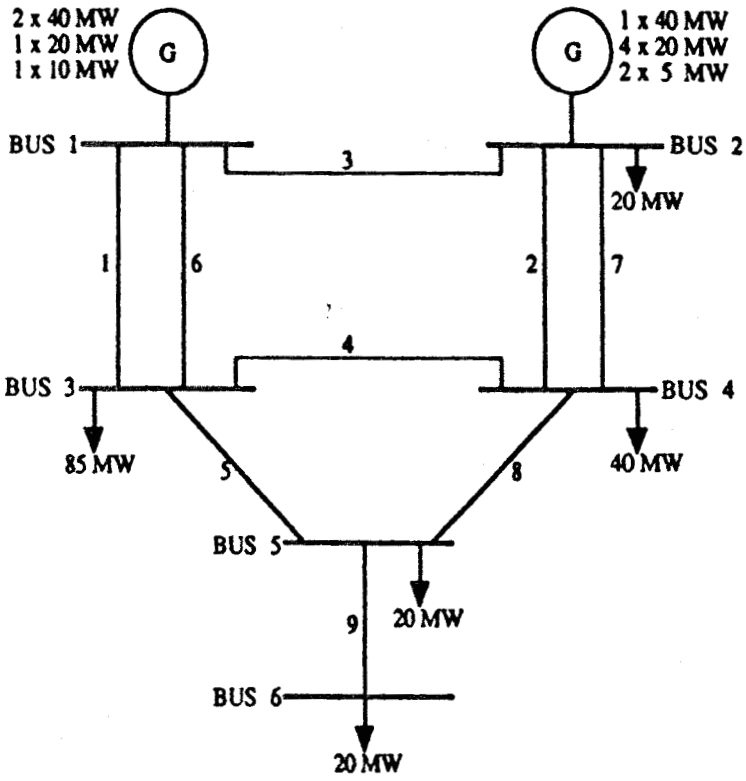

Figure 3.1: Single Line Diagram Of The RBTS

maximum and minimum voltage limits for the system buses are assumed to be 1.05 p.u. and 0.97 p.u. respectively. The system peak load is 185 MW and the total installed generation capacity is 240 MW. Approximately 89% of the system load is located at quite some distance away from the two generating stations. A considerable portion (46%) of this load is located at a single bus. This necessitates a relatively large movement of bulk power from the two generating stations located in the north to the major load points in the south. The power transfer distances range from 75 kilometers to beyond 200 kilometers in some cases. The bus data, line data and generator data for the RBTS are provided in Appendix A.

3.3. Description of the IEEE-Reliability Test System (RTS)

The single line diagram of the 24-bus IEEE-RTS is shown in Figure 3.2. The system has 10 generator (PV) buses, 10 load (PQ) buses, 33 transmission lines, 5 transformers and 32 generating units. The maximum and minimum ratings of the generating units are 12 MW and 400 MW respectively. There are two transmission voltage levels in the IEEE-RTS i.e. 230 KV in the north region and 138 KV in the south region. The maximum and minimum voltage limits of the system buses are assumed to be 1.05 p.u. and 0.95 p.u. respectively. The system peak load is 2850 MW supplied at the two voltage levels. Approximately 53% of the system load is supplied by the 230 KV system and the remaining 47% is supplied by the 138 KV system. From a geographic point of view, a considerable portion (74%) of the total load supplied at the 230 KV level is located in the north-west portion of the system. About 28% of the total load in the 138 KV system is supplied at two substations which are located close to the boundary with the 230 KV network. The remaining 72% is nearly equally distributed among the other eight buses in the region.

The total installed generating capacity is 3405 MW of which only 20% is supplied at the 138 KV level. Eight out of the ten generating stations are located relatively close to the load points and therefore no large power swings are expected. The 230 KV network is used to feed the load in the north-west part of the system and to transfer power to other system loads from the generating stations in the north-east part of the system. In these cases, power transfers generally do not exceed 30 miles except for one case in which the 230 KV network is used to transfer roughly 700 MW of power from the north to the main step down transformer station located in the mid-portion of the system approximately 70 miles south [32]. The transfer of power from the 230 KV network to the 138 KV network is concentrated at this transformer station. Some of this power is used to supply the local load at the substation and the rest is distributed to other load points in the 138 KV system. The average distance of power transfer in this case is generally less than 30 miles. The bus data, line data and generator data for the IEEE-RTS are provided in Appendix B.

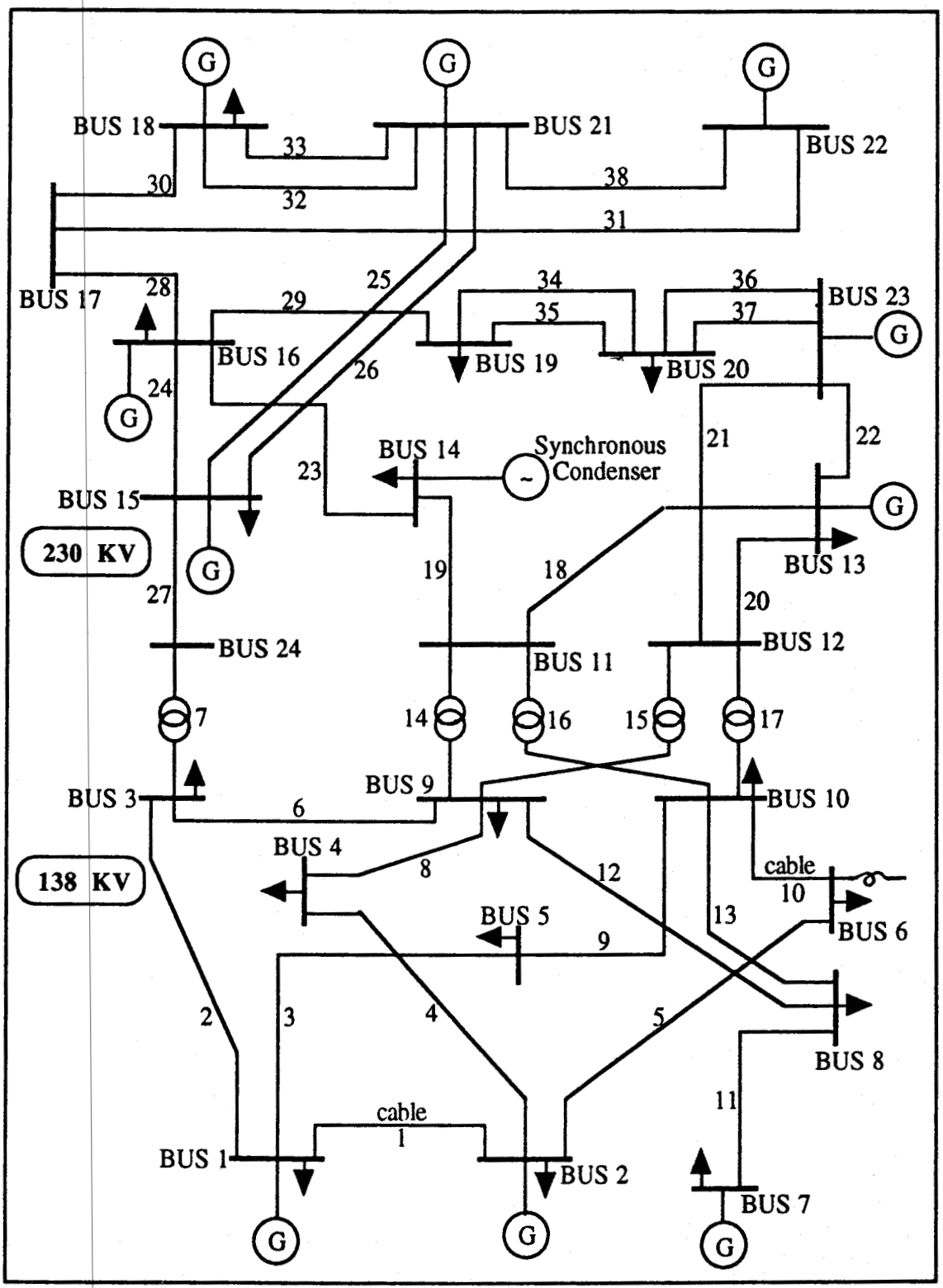

Figure 3.2: Single Line Diagram Of The IEEE-RTS

3.4. Load Model

The suggested annual peak load for the RBTS and the IEEE-RTS are 185 MW and 2850 MW respectively. Data on the weekly, daily and hourly loads for a one year period (8736 hours) are provided for the IEEE-RTS in Reference [30]. A load duration curve can be obtained by arranging the 8736 hourly peak loads data in descending order of load magnitude. A set of 100 data points that best represent this hourly peak load variation curve has been used as the load model for both the IEEE-RTS and the RBTS. The load data are expressed in per unit with the annual peak load as the base. The load duration curve obtained using these data points is shown in Figure 3.3. The actual data points are given in Appendix C.

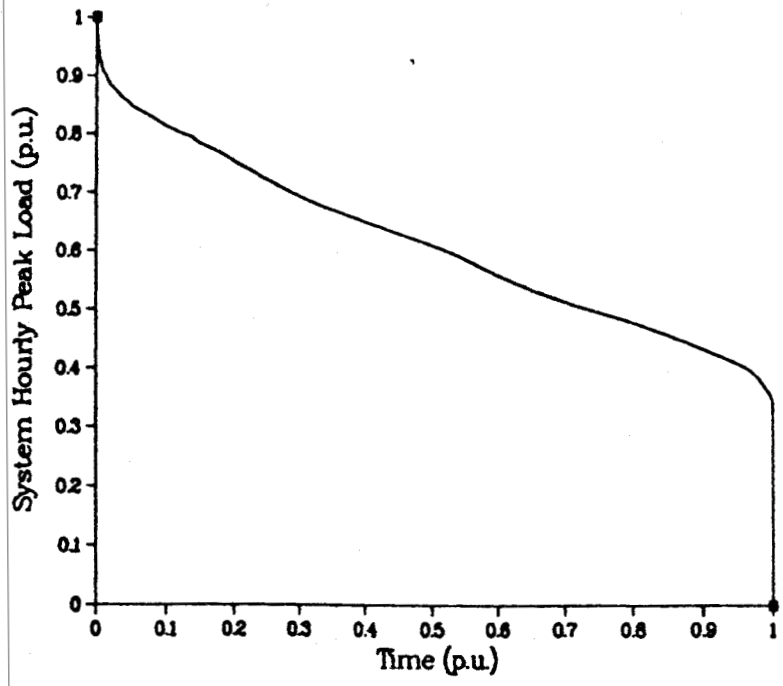

Figure 3.3: 100 Points Load Duration Curve

The load duration curve can be modified to obtain multiple discrete load levels to approximately represent the load model. This method of load model approximation is utilised in this thesis to obtain annual indices which reflect the variation of the system load over a year. The 7-step approximation of the load duration curve used in these studies is shown in Table 3.1. The load step size is assumed to be 5%. The probability and duration (in hours) of occurrence corresponding to each load level over a one year period are also provided.

Table 3.1: 7-step Load Model - (5% Step Size)

Step	Load (p.u.)	Load (MW) RBTS	IEEE-RTS	Duration (Hrs/year)	Probability
1	1.00	185.00	2850.00	19.2	0.00219780
2	0.95	175.75	2707.50	95.8	0.01096612
3	0.90	166.50	2565.00	313.8	0.03592033
4	0.85	157.25	2422.50	656.2	0.07511447
5	0.80	148.00	2280.00	727.7	0.08329899
6	0.75	138.75	2137.50	717.3	0.08210851
7	0.70	129.50	1995.00	6206.0	0.71039378
TOTAL				8736.0	1.00000000

The number of steps considered appropriate for the load aggregation approximation of the load model is dependent upon the sensitivity of the composite system indices to load variation [28]. The use of a large number of steps will result in excessive computing time. Fewer steps can be used with an attendant reduction in computing time, but with a loss in accuracy especially if the adequacy indices are very sensitive to load variation. Table 3.2 shows an alternative 4-step approximation of the load model with a step size of 10%.

The IEEE-RTS is noted to be highly sensitive to load variation [28], because a greater proportion of its inadequacy is caused by generation deficiencies. Adequacy indices are calculated for the RBTS and the IEEE-RTS using the 7-step and the 4-step load models shown in Tables 3.1 and 3.2 respectively. Both load models are utilised with the objective of verifying the sensitivity of the composite system indices of the two test systems to load variation.

Table 3.2: 4-step Load Model - (10% Step Size)

Step	Load (p.u.)	Load (MW) RBTS	IEEE-RTS	Duration (Hrs/year)	Probability
1	1.0	185.0	2850	115	0.01316392
2	0.9	166.5	2565	970	0.11103480
3	0.8	148.0	2280	1445	0.16540751
4	0.7	129.5	1995	6206	0.71039377
TOTAL				8736	1.00000000

3.5. Base Case Results

The indices computed for the original basic configuration of the RBTS and the IEEE-RTS are designated as the base case results. These results serve as a datum for comparing the effects of the modified forms of the two test systems in subsequent studies illustrated in this thesis. Load point indices and overall system indices are calculated using the COMREL and MECORE programs. The load point indices are computed for individual system load buses whilst the system indices serve as indicators of overall system adequacy. The indices considered in this analysis include the following.

Load Point Indices:

PLC :Probability of Load Curtailment.

ENLC :Expected Number of Load Curtailments or Failure Frequency (Occurrences/Year)

ELC :Expected Load Curtailed (MW/Year)

EENS :Expected Energy Not Supplied (MWh/Year)

System Indices:

ELC :Expected Load Curtailed (MW/Year)

EENS :Expected Energy Not Supplied (MWh/Year)

BPII :Bulk Power Interruption Index (MW/MW-Year)

BPECI :Bulk Power/Energy Curtailment Index (MWh/MW-Year)

SI :Severity Index (System Minutes)
MBECI :Modified Bulk Energy Curtailment Index

3.5.1. Selected Features of the COMREL and MECORE Programs

All the studies were conducted on a VAX-730 Mainframe Computer System using the COMREL and MECORE programs. The following features of COMREL and MECORE are utilised for this analysis and for subsequent studies in this thesis.

3.5.1.1. Contingency Selection

COMREL: Independent overlapping outages up to the 4^{th} level for generating units and up to the 3^{rd} level for transmission lines and/or transformers are considered. In the case of combined generator and line outages, situations involving up to two generating units and one line and one generating unit and two lines are considered. The sorting facility was utilised in order to reduce the computing time requirements in the case of the IEEE-RTS.

MECORE: Simulation trials were performed in the case of the MECORE program in order to select an appropriate number of samples that will generate indices with a reasonable level of accuracy and consistency for the RBTS and the IEEE-RTS. Figure 3.4 shows the severity index convergence characteristics of the MECORE program with the RBTS for two different seeds as the number of random samples used for the analysis is varied. A similar characteristic involving the IEEE-RTS is also shown in Figure 3.5.

Both figures illustrate that the MECORE program has an oscillatory convergence characteristic which is typical of the Monte Carlo technique. A reduction in the error limit of the estimates can be noted as the number of random samples used for the analysis is increased. It can be observed from Figure 3.4 that a minimum of about 40,000 samples is required for the RBTS analysis in order to obtain estimates which can be considered to be satisfactorily accurate, and which are reasonably independent of the seed used for the random number generation process. Similarly, the IEEE-RTS analysis requires at least 32,000 random samples in order to converge to the estimated value as can be seen from Figure 3.5. Based on the results of these analyses, 50,000 and 41,000 random samples

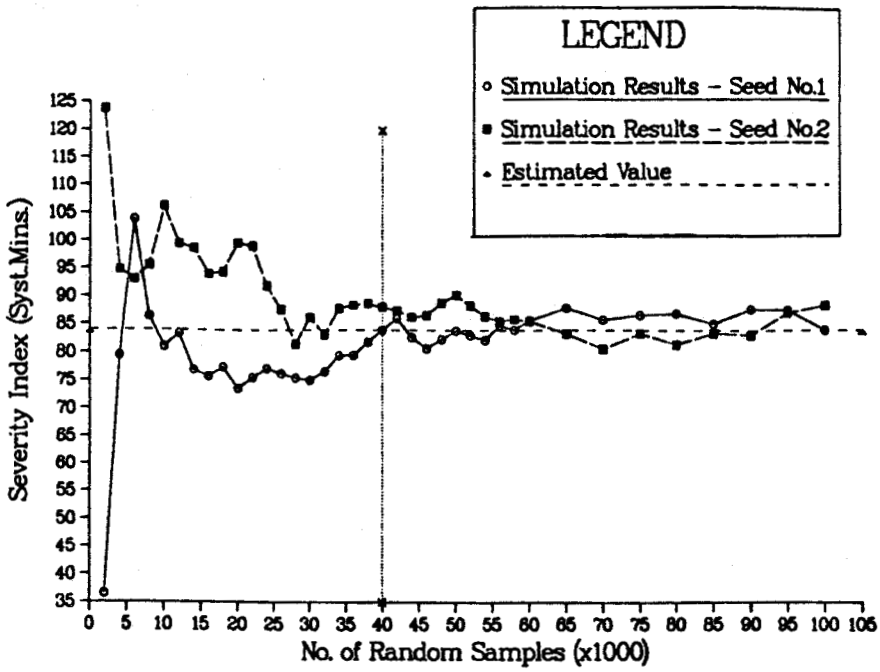

Figure 3.4: Convergence Characteristics Of The MECORE Program With The RBTS

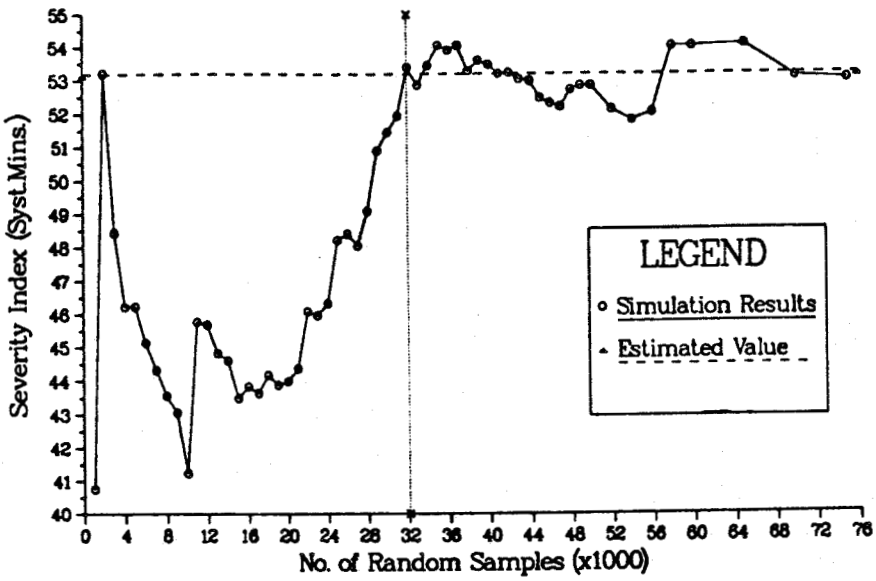

Figure 3.5: Convergence Characteristics Of The MECORE Program With The IEEE-RTS

were used for analyses involving the RBTS and the IEEE-RTS respectively in this thesis. It is, however, important to note that the convergence process does not settle down completely to a specific value for either of the two systems studied. It should therefore be recognised that although the error in a Monte Carlo estimate can be reduced to acceptable limits by using a large number of samples, it is quite unrealistic to expect an exact solution from a Monte Carlo-based analysis.

3.5.1.2. Network Analysis and Failure Criteria

The DC load flow solution technique was employed for network analysis in both programs. Bus failure under an outage condition is defined as the inability of the system to meet the load requirements at the bus. This condition can be caused by outage combinations leading to line overloads, split networks, bus isolation or generation deficiencies.

3.5.1.3. Remedial Actions

Swing bus overload conditions are alleviated by curtailing load at various load buses in both programs. Line or transformer overload conditions are alleviated by generation rescheduling and/or load curtailment, if necessary, at the appropriate buses.

3.5.1.4. Load Curtailment

COMREL: Curtailable load at each system load bus was assumed to be 20% of the total load at the bus. The load curtailment pass was specified to be one (1). This confines load curtailment to load points adjacent to the immediate location of the system problem.

MECORE: The load curtailment action is directed by a linear programming minimisation model which recognises up to 20% of the total load at each bus as curtailable load. The procedure involves sequential interruption of load in several small steps according to the importance attached to each proportion of load until the outage problem is alleviated.

3.5.2. Results for the RBTS

Tables 3.3 and 3.4 show the load point indices produced by the COMREL and the MECORE programs for the RBTS using the 4-step and the 7-step load model approximations respectively. The corresponding system indices produced by both programs are also shown in Table 3.5.

Table 3.3: Load Point Indices For The RBTS Using The 4-step Load Model

Bus No.	PLC	ENLC	ELC	EENS
a. COMREL:				
2	0.00030	0.14487	0.2693	4.8578
3	0.00044	0.22098	2.1777	36.8739
4	0.00031	0.15134	0.6376	10.7223
5	0.00001	0.01211	0.0526	0.2699
6	0.00114	1.12871	16.7537	148.1483
b. MECORE:				
2	0.00003	0.01563	0.0393	0.5563
3	0.00007	0.04554	0.4791	6.9677
4	0.00015	0.08583	0.4862	7.4841
5	0.00045	0.21195	0.6027	10.8036
6	0.00167	1.39202	18.2331	172.7652

It can be observed from Tables 3.3 and 3.4 that the load point indices produced by the two programs differ in magnitude and also in relative adequacy of the load points. Whilst bus 5 is portrayed by the COMREL program as the most adequate load point of the RBTS, bus 2 is judged to be the most adequate load point by the MECORE program. Both programs however agree on bus 6 as the least adequate in the system which is obvious from the RBTS layout. Bus 6 is located at a considerable distance away from the

Table 3.4: Load Point Indices For The RBTS Using The 7-step Load Model

Bus No.	PLC	ENLC	ELC	EENS
a. COMREL:				
2	0.00028	0.13386	0.1547	2.6013
3	0.00040	0.19843	1.2473	20.3628
4	0.00028	0.13909	0.3688	5.7911
5	0.00001	0.01118	0.0444	0.2202
6	0.00114	1.12865	16.5632	146.4656
b. MECORE:				
2	0.00002	0.01101	0.0307	0.43561
3	0.00007	0.03790	0.2914	4.03795
4	0.00013	0.07431	0.4036	6.28107
5	0.00022	0.11394	0.3601	5.98068
6	0.00145	1.29349	17.6615	163.47768

two generating stations in the RBTS and is connected to the rest of the system by a single radial link. Bus 6 therefore suffers complete isolation, and consequently load curtailment, whenever this radial connection is on outage.

The discrepancies in the magnitude of the load point indices and in the relative adequacy of the load buses can be attributed largely to differences in the philosophies directing the load curtailment action in the two programs. As noted in Chapter 2, the policy of confining load curtailment to the problem area of the system is more rigidly enforced in COMREL than MECORE. When load curtailment pass one (1) is specified, buses in the problem area are those adjacent to the immediate location of the system problem. Therefore buses 5 and 6, for example, are generally not affected by generating unit outages, because they are outside the defined problem area. Based on this assumption and its strategic location, bus 5 is rarely found to be in difficulty when the

Table 3.5: System Indices For The RBTS

System Indices	COMREL 4-step	Results 7-step	MECORE 4-step	Results 7-step
ELC	19.8905	18.3782	19.8404	18.7474
	(19.8778)	(18.3657)	-	-
EENS	200.8722	175.4410	198.5769	180.2130
	(200.8158)	(175.3854)	-	-
BPII	0.1408	0.1332	0.1418	0.1367
	(0.1407)	(0.1332)	-	-
BPECI	1.3920	1.2570	1.3983	1.3042
	(1.3916)	(1.2566)	-	-
MBPECI	0.00016	0.00014	0.00016	0.00015
	(0.00016)	(0.00014)	-	-
SI	83.519	75.418	83.900	78.251
	(83.495)	(75.393)	-	-
CPU TIME	24.88	43.22	43.200	74.290
(Seconds)	(44.83)	(77.03)	-	-

NB:Results obtained without using the sorting facility are in parenthesis.

COMREL program is used. Another factor noted to be accountable for the discrepancies is that in the COMREL program, loads are classified as either firm or curtailable at the various system load buses. Hence load curtailment can only be effected in a maximum of two steps, if necessary. This can lead to a situation of excessive load cuts beyond the limits considered adequate to alleviate an outage problem. On the other hand, load shedding is optimised in the MECORE program by curtailing load in several small steps followed by intermittent checks for system problem persistence. This reduces the possibility and magnitude of excessive load cuts to alleviate a system problem in the MECORE program.

It can be observed from Table 3.5 that the overall system indices obtained from the COMREL and MECORE programs are quite comparable. This observation is an indication of the fact that both programs are essentially doing the same thing but in different ways. The two programs are able to effectively assess the overall level of adequacy of the test system, although the amount of load curtailment at the various system load buses during the process may be different. This shows that the implementation methodology of the load curtailment philosophy has relatively little influence on overall system adequacy compared to load point adequacy.

It is observed by comparing the results for the two load models that the inadequacy indices computed for the individual load points and the overall system using the 7-step load model are slightly lower than those obtained with the 4-step load model. This trend is expected, because the effects of higher load levels generally last for a shorter duration in the 7-step load model which is a better reflection of the practical situation. It is however important to note from the results shown in Table 3.5 that the calculations utilising the 7-step load model require an additional 72% increment in computing (CPU) time for both programs. The improvements achieved in the results of the 7-step load model may or may not be considered significant enough to warrant the associated incremental computational costs, depending upon the particular situation. A decision regarding this must be made by the analyst for the specific conditions.

The CPU time results shown in Table 3.5 also indicate that less computing time is required for the RBTS analysis when the COMREL program is used with the sorting facility than when using the MECORE program for the analysis. The CPU time noted for the COMREL program without the sorting facility is however observed to be almost the same as that noted for the MECORE program. This demonstrates the power of the sorting facility in reducing computational costs of the COMREL analyses without significantly affecting the level of accuracy. It should be appreciated that the RBTS is a relatively simple system. Analytical evaluation techniques are therefore favoured over simulation techniques for such systems.

3.5.3. Results for the IEEE-RTS

The indices produced by the COMREL and MECORE programs for the IEEE-RTS are shown in Tables 3.6-3.10 for both the 4-step load model and the 7-step load model. Tables 3.6 and 3.7 respectively show the load point indices for the IEEE-RTS as computed by the COMREL and MECORE programs using the 4-step load model. Tables 3.8 and 3.9 show similar results for the 7-step load model.

Table 3.6: Load Point Indices For The IEEE-RTS Using The 4-step Load Model - COMREL Results

Bus No.	PLC	ENLC	ELC	EENS
1	0.00071	0.49186	3.9940	49.6264
2	0.00133	0.91395	7.4373	92.4063
3	0.00072	0.49599	8.0421	101.0893
4	0.00071	0.49352	3.7557	47.1493
5	0.00071	0.49352	3.1706	39.7761
6	0.00072	0.49481	6.9499	87.0449
7	0.00055	0.38128	4.3889	55.2932
8	0.00056	0.38520	8.0034	101.4241
9	0.00006	0.03992	0.6328	7.8301
10	0.00006	0.04017	0.6962	8.6556
13	0.00146	0.96364	34.4411	462.9061
14	0.00027	0.19954	4.3517	51.6992
15	0.00229	1.43846	59.7115	833.9764
16	0.00081	0.60095	10.0755	98.2522
18	0.00296	1.87049	95.3412	1377.9177
19	0.00035	0.28247	9.0518	84.1525
20	0.00161	1.05369	24.5741	341.4712

Table 3.7: Load Point Indices For The IEEE-RTS Using The 4-step Load Model - MECORE Results

Bus No.	PLC	ENLC	ELC	EENS
1	0.00007	0.06346	1.2155	12.0739
2	0.00008	0.07403	1.2819	12.6440
3	0.00010	0.09037	2.7801	27.6988
4	0.00011	0.09880	1.3126	13.0704
5	0.00012	0.10557	1.3221	13.1218
6	0.00016	0.13152	3.0750	31.2612
7	0.00018	0.15095	3.1173	32.4070
8	0.00025	0.21495	5.9442	62.0351
9	0.00040	0.30998	8.0133	84.2448
10	0.00047	0.37834	12.4268	137.7644
13	0.00064	0.51510	21.8626	238.8709
14	0.00087	0.66472	21.7136	246.3791
15	0.00134	0.99716	48.7440	571.8274
16	0.00149	1.11142	19.7199	231.9638
18	0.00222	1.66228	86.4821	1018.3367
19	0.00288	2.13212	63.8321	750.6681
20	0.00326	2.42645	54.3941	643.0109

As observed in the case of the RBTS, discrepancies exist in the magnitude of the load point indices for the IEEE-RTS and also in the relative adequacy of the various system load buses when the COMREL and the MECORE results are compared. Buses 9 and 10 located at the mid-portion of the system where bulk power exchanges between the north and south regions of the IEEE-RTS occur are shown to be the most adequate buses from the COMREL results. On the other hand, the MECORE results which are calculated

Table 3.8: Load Point Indices For The IEEE-RTS Using The 7-step Load Model - COMREL Results

Bus No.	PLC	ENLC	ELC	EENS
1	0.00033	0.22895	1.8147	23.0882
2	0.00063	0.43355	3.3846	43.0720
3	0.00033	0.23010	3.4891	44.5981
4	0.00033	0.22979	1.6479	20.9786
5	0.00033	0.22969	1.3813	17.5825
6	0.00033	0.23043	3.0682	38.8570
7	0.00026	0.18165	2.0164	25.6012
8	0.00026	0.18334	3.5949	45.9581
9	0.00002	0.01143	0.2314	2.7384
10	0.00002	0.01148	0.2493	3.0000
13	0.00085	0.55966	17.2434	229.7640
14	0.00015	0.11045	2.1114	24.3649
15	0.00129	0.80740	30.9902	441.1565
16	0.00044	0.35014	7.1722	62.2997
18	0.00161	1.01277	47.9518	694.4162
19	0.00020	0.18178	6.8350	55.9016
20	0.00092	0.59152	12.6803	177.8581

based on the policy of minimising the overall system load curtailment show buses 1 and 2 located in the very southern part of the system as the most adequate load points. The reason for these discrepancies is attributed mainly to the differences in the implementation methodology of the load curtailment policies for the two programs. Both programs, however, show bus 18 as having the lowest adequacy. Most of the inadequacy at bus 18 is accounted for by several swing bus overload conditions that arise in the system as a result of many outage combinations involving the generating unit connected at bus 18 and any other relatively large generators in the system.

Table 3.9: Load Point Indices For The IEEE-RTS Using The 7-step Load Model - MECORE Results

Bus No.	PLC	ENLC	ELC	EENS
1	0.00003	0.03129	0.5595	5.3714
2	0.00004	0.03976	0.6358	5.9858
3	0.00005	0.05065	1.4793	13.8947
4	0.00006	0.05471	0.7075	6.7482
5	0.00007	0.06300	0.7763	7.7013
6	0.00009	0.07425	1.7029	17.0491
7	0.00010	0.09064	1.7595	17.7773
8	0.00014	0.12183	3.2661	32.6517
9	0.00019	0.15661	4.2426	42.7754
10	0.00025	0.20531	6.3072	66.4580
13	0.00035	0.28966	11.5018	122.4009
14	0.00046	0.36903	11.5111	124.0162
15	0.00074	0.58655	26.9742	300.6957
16	0.00086	0.67089	11.1326	124.0049
18	0.00131	1.00738	49.8425	571.4524
19	0.00171	1.30068	37.4865	435.0436
20	0.00194	1.47342	31.8475	370.0538

It can be observed from Table 3.10 that the overall system indices obtained for the IEEE-RTS from both programs are quite comparable especially when higher level outage effects are considered by using the more-off states facility of the COMREL program. (A more-off state at a given contingency level is a state in which at least one more component is out of service in addition to those already out at that level.) It is important to appreciate that the evaluation of a composite system involves the analysis of all

Table 3.10: System Indices For The IEEE-RTS

System Indices	COMREL 4-step	Results 7-step	MECORE 4-step	Results 7-step
ELC	284.6183	145.8622	357.2370	201.7328
	(312.7791)	(167.5581)	-	-
EENS	3840.6707	1951.2350	4127.3813	2264.0801
	(4082.5383)	(2123.0564)	-	-
BPII	0.1072	0.0570	0.1363	0.0796
	(0.1197)	(0.0671)	-	-
BPECI	1.4374	0.7539	1.5642	0.8865
	(1.5405)	(0.8320)	-	-
MBPECI	0.00016	0.00009	0.00018	0.00010
	(0.00018)	(0.00009)	-	-
SI	86.247	45.237	93.851	53.189
	(92.431)	(49.919)	-	-
CPU TIME	44.04	75.39	5.05	8.63
(Minutes)	(44.23)	(75.18)	-	-

NB:COMREL results in parenthesis are obtained when more-off outage combinations are considered.

possible contingency states. This of course is not feasible in practice and therefore there is a need to limit the number of outage combinations considered. The inclusion of high level contingencies using more-off states can make a significant impact on the calculated adequacy indices especially when the analysis involves a large power network. This is illustrated by the two sets of COMREL results shown in Table 3.10 for the IEEE-RTS. The COMREL program (and for that matter analytical evaluation methods in general), however, possess the advantage of providing the analyst with insights on the relationships between input variables and final results. With the COMREL program, for example, it is

possible to investigate the effects of higher level outage combinations on the calculated adequacy indices. Such an analysis can help the analyst to make a decision concerning the outage combinations necessary for consideration in a particular analysis depending upon the level of accuracy required and the computational constraints.

The results obtained for the IEEE-RTS for both programs, using the 7-step load model, show a considerable (more than 50%) reduction in the value of inadequacy both at the individual load points and for the overall system compared to the results obtained with the 4-step load model. This observation underscores the high sensitivity of the composite system indices of the IEEE-RTS to the load duration curve, as reported in Reference [28]. The higher level of accuracy in the results of the 7-step load model is obtained at a considerable incremental computational cost. A 72% increase in computing time over that required by the 4-step load model is needed for the calculation involving the 7-step load model in both programs. The incremental gain in accuracy of the annual indices for the IEEE-RTS as a result of using the 7-step load model can be considered to be sufficiently significant to warrant the attendant increment in computational costs.

The superiority of the MECORE program regarding computational efficiency can be clearly seen from Table 3.10. The CPU time recorded for the MECORE program is about 11% of the time required by the COMREL program (i.e. even with the sorting facility) for the analysis involving the IEEE-RTS with either the 4-step or the 7-step load model. This indicates that the MECORE program (simulation approach) is more effective computationally than the COMREL program (state enumeration approach) for composite system analysis of relatively large and complex systems.

3.6. Summary

Two reliability test systems, the RBTS and the IEEE-RTS, utilised for composite system adequacy analysis in this thesis are described in this chapter. Base case load point and overall system indices were computed for the test systems utilising the COMREL and MECORE programs. These base case values serve as the datum for comparing results of subsequent studies involving modified forms of the test systems. Differences in the implementation methodology of load curtailment action in the two programs account

for the discrepancies noted in the set of load point indices. These differences diminish when overall system indices are determined.

Some of the basic characteristics of the analytical and simulation methods for composite system adequacy evaluation are illustrated in this chapter through the application of the COMREL and MECORE programs to the RBTS and the IEEE-RTS. The MECORE program, which is based on Monte Carlo simulation, is shown to be computationally more effective than the COMREL program in the IEEE-RTS analysis. The IEEE-RTS is a relatively large and complex system with the same basic characteristics as a practical power system. The COMREL program, which utilises the state enumeration approach, requires considerable computational requirements for the analysis of the IEEE-RTS; but it is the better tool when the analysis involves a small and relatively simple system like the RBTS.

The two sets of results obtained using the 4-step and 7-step load models show the RBTS to be relatively insensitive to the load duration curve and the IEEE-RTS to be very sensitive to the curve. Subsequent system studies described in this thesis were therefore conducted using the 4-step load model for the RBTS and the 7-step load model for the IEEE-RTS.

4. EFFECTS OF NON-UTILITY GENERATORS ON COMPOSITE SYSTEM ADEQUACY EVALUATION

4.1. Introduction

Energy is the driving force behind the survival of many national economies in the world today. The effectiveness of energy utilisation makes a considerable impact on the consumer in terms of availability and the cost of goods and services. Increasing costs and environmental concerns regarding conventional generating sources have given considerable impetus to the development of non-conventional energy sources and the adoption of energy conservation and efficient energy utilisation measures.

Independent power production in the form of Non-utility Generators (NUGs) and Cogeneration facilities is considered to be an important component in meeting future electrical energy requirements. NUGs can be defined as those generation facilities owned and operated by electricity producers other than the main power utility and may include relatively small private and municipal utilities in addition to other independent power producers. Cogeneration, which is also a form of independent power production, is normally associated with an industry in which a significant requirement for electrical energy is coupled with a large demand for process heat, normally in the form of steam.

In recent years, a significant component of the overall system electrical energy requirements of many utilities has been provided by independent power production facilities. This trend can be attributed partially to the increasing costs of conventional electrical energy supplies coupled with uncertain global economic and political conditions and the increasing environmental concerns facing many power utilities. In addition to providing some measure of flexibility and diversity in the electrical energy

supply, the introduction of independent power production facilities provides opportunities to utilise renewable energy resources and therefore assures the orderly, economic and efficient utilisation of natural energy resources.

Most of the existing literature on independent power production [33, 34, 35, 36, 37, 38] has, in the past, been focused on the economic effects of this form of power production on the utility, or on the customer, or on the ownership regarding the operation of the installations. None of these excellent analyses, however, has considered the reliability impacts of NUGs and cogeneration facilities on the utility systems. The reliability impacts of independent power production facilities can be quite significant on both load point adequacy and overall power system adequacy. In a study undertaken at the University of Saskatchewan [39], several methodologies for evaluating the impact of cogeneration sources on the overall capability of the generation system to meet the total system load requirement have been proposed. These analyses however do not recognise the relative locations of the generation facilities within the system. Injection of electrical energy due to NUG development can occur at locations in the system which would not normally be considered by the electric power utility as conventional sites for generation development. It is therefore necessary that the reliability evaluation techniques used to assess these impacts should involve the examination of both generation and transmission facilities (i.e. HLII Analysis) in order to capture these effects. The impact of NUGs on load point adequacy was examined in Reference [40] with respect to their insertion in a distribution network configuration. One of the main objectives of this thesis is to examine the impact of NUGs on the utility's composite system adequacy utilising existing computational tools for bulk power system adequacy assessment.

This chapter discusses the impact of NUGs on the composite system adequacy indices of the Roy Billinton and the IEEE-Reliability test systems. The effects are examined in regard to the individual load point and overall system adequacy indices of the test systems. The analyses were performed utilising the COMREL and the MECORE programs as the computational tools.

4.2. System Modelling Considerations

Independent power production facilities are essentially small private electric power business operations which often utilise natural resources such as small hydro, wood waste, peat, natural gas, the wind and other forms of renewable energy resources for the production of electrical energy. The NUGs can therefore be modelled as small capacity components that are modular in nature and with relatively low Forced Outage Rate (FOR) values compared to their conventional generating unit counterparts. With regard to cogeneration facilities, it is important to recognise that the production of by-product electric power is essentially a secondary industrial operation. The capacity components of cogeneration facilities are therefore determined by the available industrial process steam supply and this is usually dependent upon the level of production which is generally variable. It is therefore operationally more economical to install multiple small capacity components of cogenerating units which can be run in stages as sufficient steam becomes available, than to have a single large unit installation that can only be operational when industrial output is at its maximum level.

The standard designs of the RBTS and the IEEE-RTS were modified to include independent power generation facilities at specific locations in order to examine their impact on HLII adequacy indices. The NUGs can be inserted at a number of locations in the utility system where their basic function is to supply relatively small amounts of electrical energy to the overall system. Under normal conditions, the NUGs tend to reduce system operating cost by reducing system transmission losses. They can also be used to provide energy to system loads which cannot be supplied due to conventional generating capacity deficiencies. The NUGs, because of their locations within the system, can also be used to serve system loads which cannot be supplied because of transmission capacity limitations, load point isolation or other related split network situations arising from system outage conditions.

Apart from a few instances, such as those involving small hydro sources which are site specific in nature, NUGs are usually located close to system load points. For the purposes of this study, the NUGs are considered to be introduced at the system load points. When a "pure" load bus of a test system is selected to serve as a non-utility

generation point, its definition is changed from a PQ-bus to a PV-bus. Therefore all of its relevant parameters such as bus voltage, scheduled generation etc. are modified to conform with those of the other system PV-buses. Due to the nature of NUG operations and the small size of the units involved, the electrical energy produced by NUGs cannot be dispatched by the utility. The scheduled real power generation associated with a NUG is therefore assumed to be fixed and equal to the value of the rated capacity of the unit whenever the unit is available.

4.3. System Studies

The procedure and assumptions used for running the COMREL and MECORE programs are the same as those used to obtain the base case results in Chapter 3. In the studies performed, an increasing number of 2-MW and 10-MW capacity NUGs with assumed FOR values of 2% were introduced at different locations respectively in the RBTS and the IEEE-RTS. This produces different impacts on the load point and the overall system adequacy indices. Like most Monte Carlo-based computational tools, the MECORE program possesses that inherent nature of being highly sensitive to changes in network configurations which in this case arises as the number of NUGs injected into the test system is increased. The increment of the number of system components tends to distort the random number generation sequence in the Monte Carlo method, and consequently produces inconsistent estimates of the indices with varying levels of accuracy. In order to eliminate this inconsistency of the estimates from the MECORE program and also to keep the estimated indices within a narrow error limit, it is necessary to maintain a constant number of system components throughout the scenario. This assures the generation of a reasonably uniform sequence of random numbers for the simulation process during the analyses.

4.4. Discussion of Results

The impact of NUGs on load point and overall system adequacy of the RBTS and the IEEE-RTS are discussed in this section. The impacts on the Failure Probability, the Failure Frequency, the Expected Load Curtailed (ELC) and the Expected Energy Not Supplied (EENS) indices at the various load points of the test systems are considered.

The effects on the system Expected Load Curtailed, the system Expected Energy Not Supplied, the Bulk Power Interruption Index (BPII) and the Severity Index are also considered to illustrate the impacts on the overall power system adequacy. The results obtained from using the COMREL and MECORE programs are both presented. All the results shown are Annual Indices which reflect the variations in load level over a year. The 4-step (10% load step) load model was used for the RBTS analysis and the 7-step (5% load step) load model was used for the analyses involving the IEEE-RTS.

4.4.1. Results for the RBTS

4.4.1.1. Load Point Indices

Figures 4.1-4.12 show the results obtained for the five load points of the RBTS when up to ten (10) identical 2-MW NUGs are sequentially introduced at buses 2, 3 and 6 respectively. Figures 4.1 - 4.6 show the variations in the load point failure probability and frequency indices as the number of NUGs introduced at the specified locations is increased. Similar variations in the ELC and EENS at the individual load points of the RBTS are also shown in Figures 4.7-4.12.

The results show a general tendency towards reduction in the load point indices as the number of NUGs injected into the system is increased. From Figure 4.1-4.6, the failure probability and failure frequency indices for most of the load points appear to be insensitive initially to unit additions, especially in the case of the COMREL results. This is because the additional generation made available by the NUGs was not sufficient initially to completely alleviate the problems associated with a significant proportion of the outage events responsible for the inadequacies at the load points. The addition of a highly available NUG will, to some extent, alleviate the severity or intensity of an outage problem affecting a particular load point. This can be seen from Figures 4.7-4.12 which show reductions in the expected load and energy curtailed at most of the load points from the early stages of the unit additions. However unless the unit additions are enough to entirely eliminate all the problems associated with the particular outage event, that event will still count as a problem contingency and has to be considered when accumulating the failure probability indices for the load point.

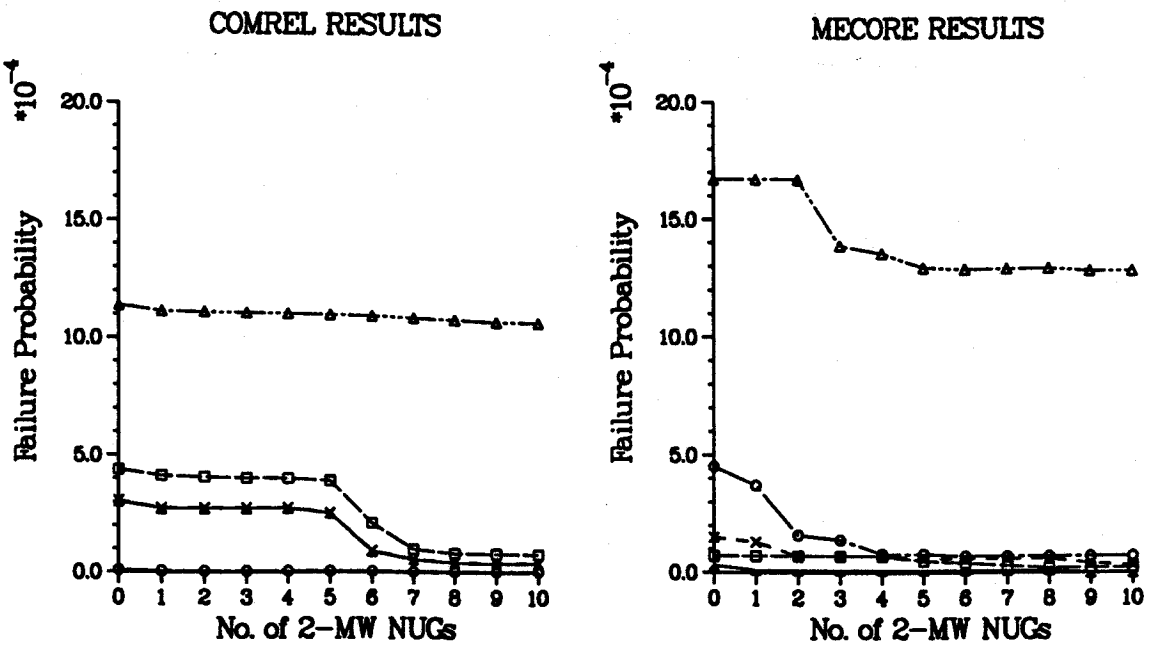

Figure 4.1: Variation In Load Point Failure Probability As Identical 2-MW NUGs Are Incrementally Introduced At Bus 2 Of The RBTS

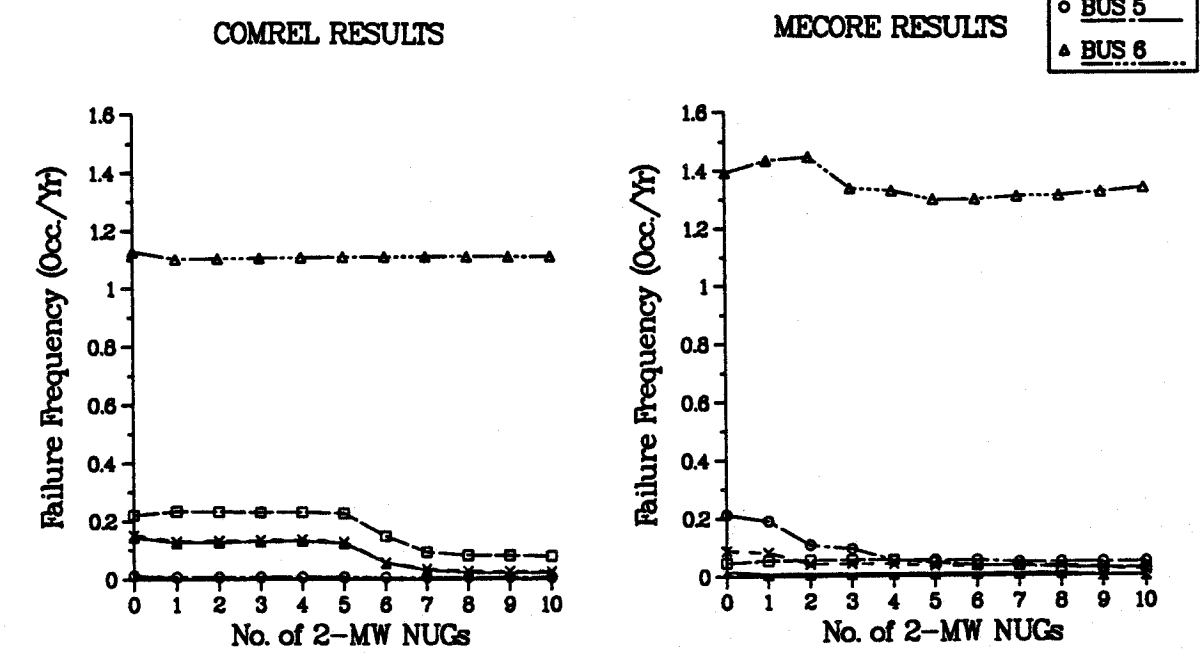

Figure 4.2: Variation In Load Point Failure Frequency As Identical 2-MW NUGs Are Incrementally Introduced At Bus 2 Of The RBTS

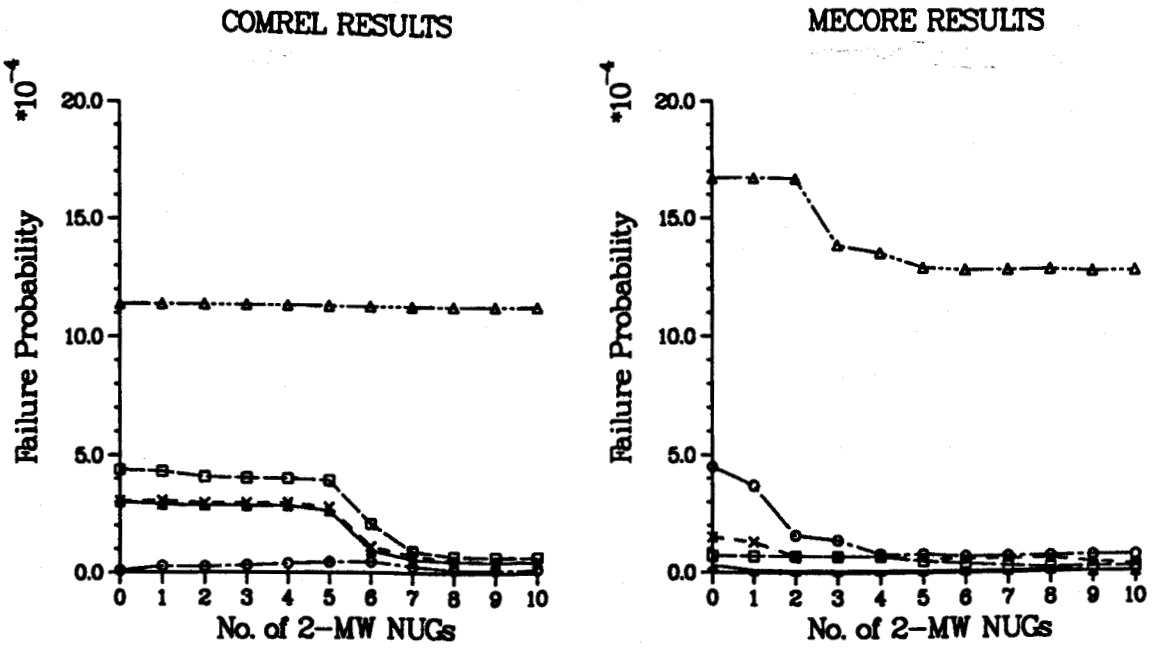

Figure 4.3: Variation In Load Point Failure Probability As Identical 2-MW NUGs Are Incrementally Introduced At Bus 3 Of The RBTS

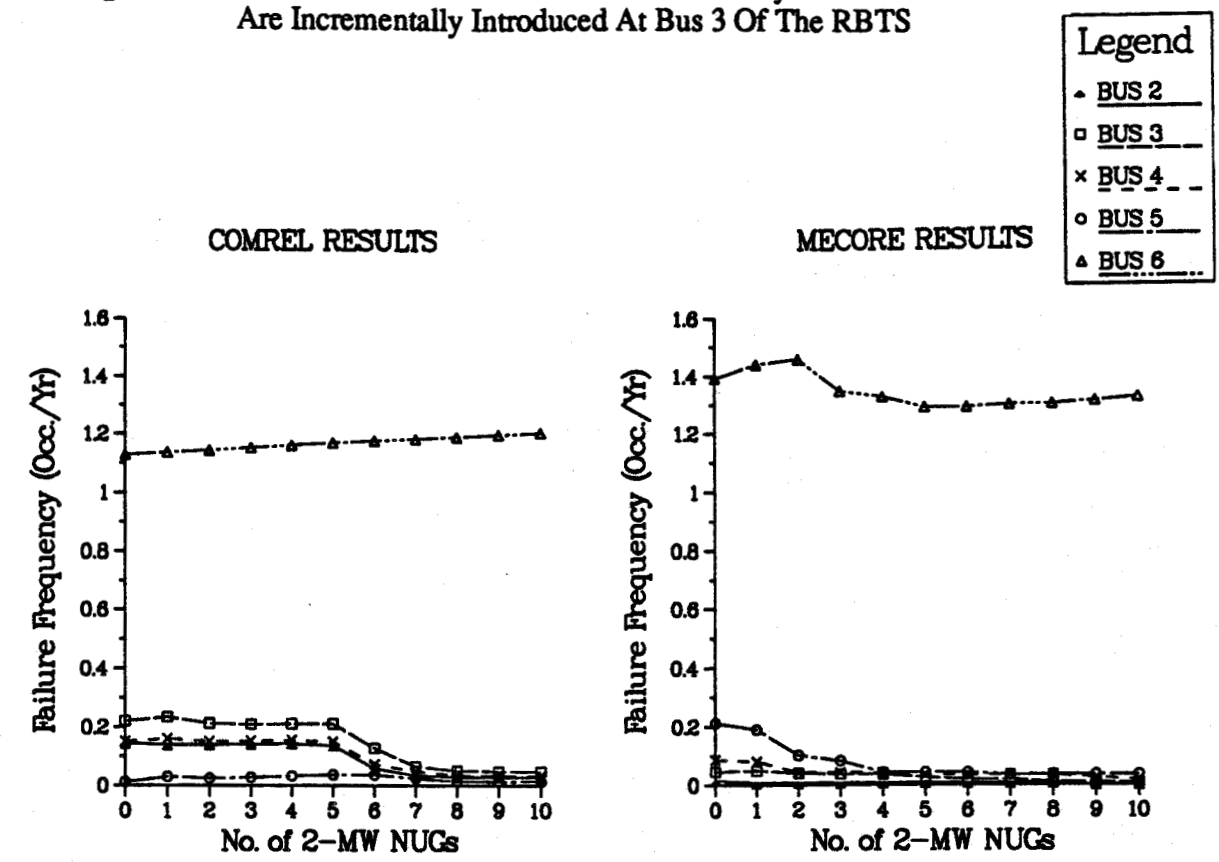

Figure 4.4: Variation In Load Point Failure Frequency As Identical 2-MW NUGs Are Incrementally Introduced At Bus 3 Of The RBTS

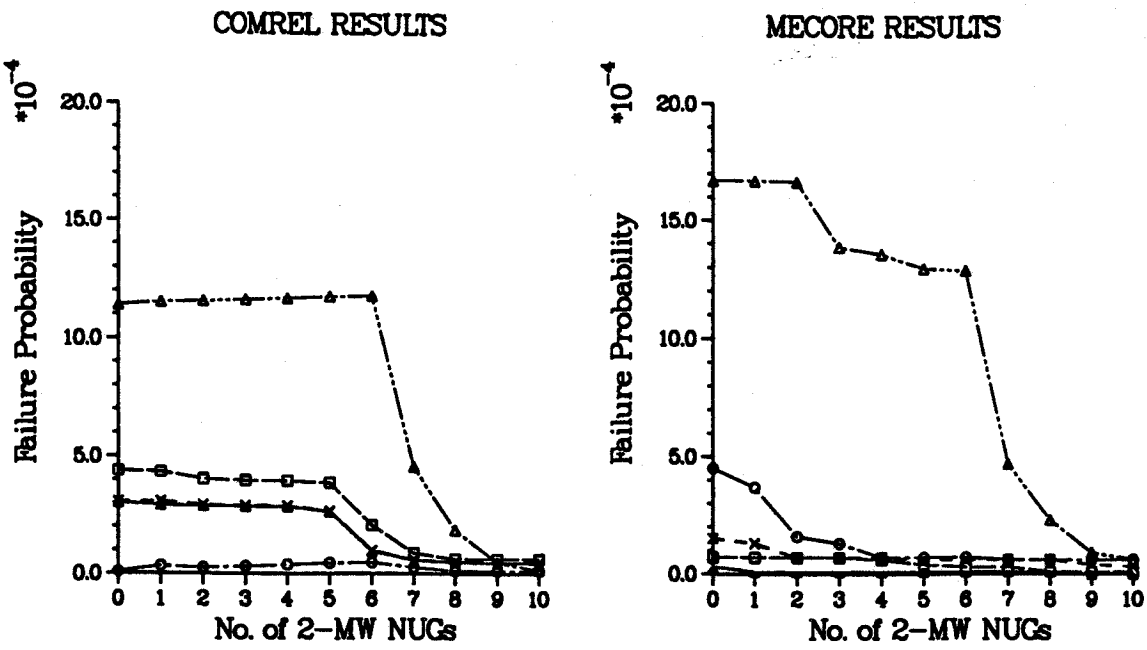

Figure 4.5: Variation In Load Point Failure Probability As Identical 2-MW NUGs Are Incrementally Introduced At Bus 6 Of The RBTS

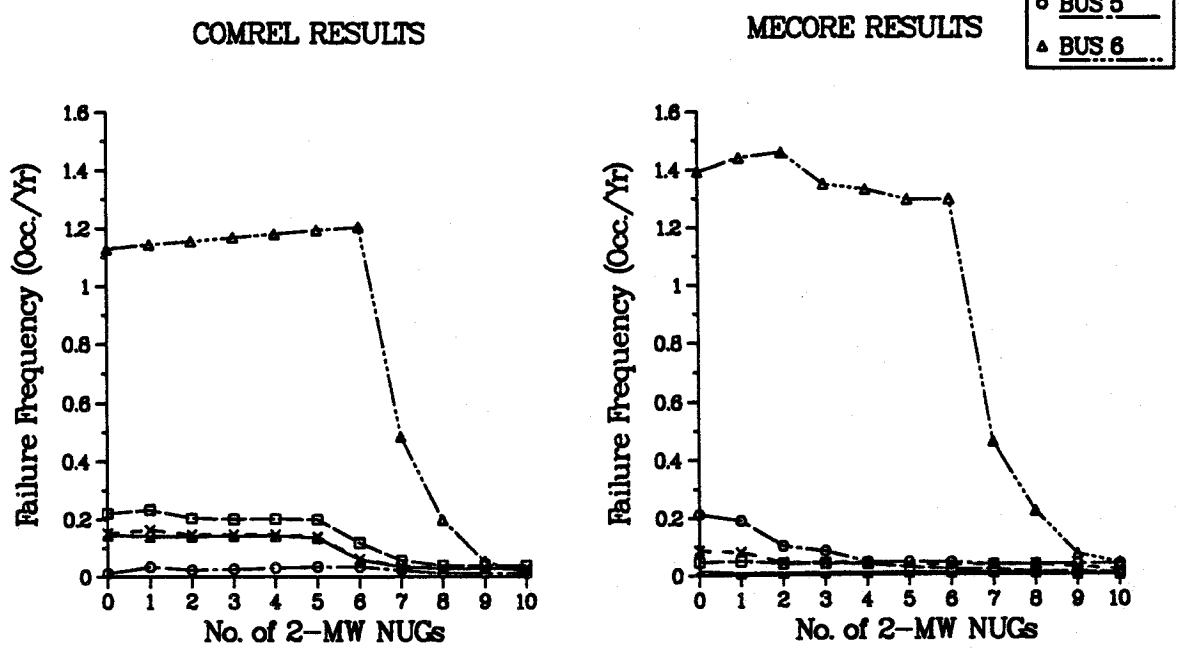

Figure 4.6: Variation In Load Point Failure Frequency As Identical 2-MW NUGs Are Incrementally Introduced At Bus 6 Of The RBTS

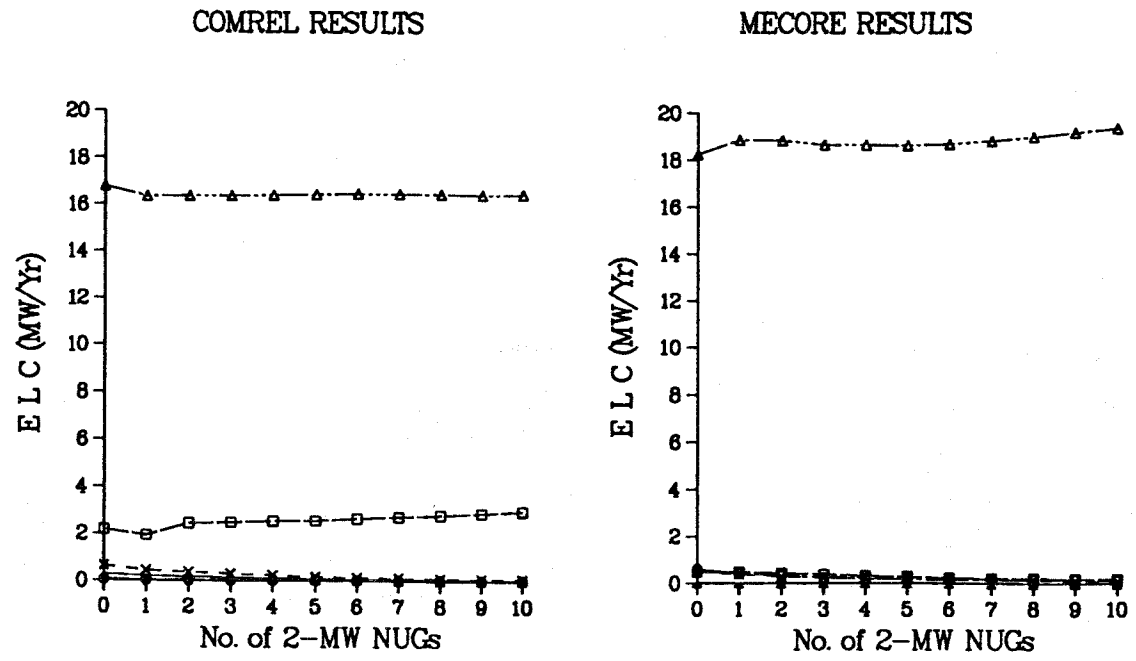

Figure 4.7: Variation In ELC At The Load Points As Identical 2-MW NUGs Are Incrementally Introduced At Bus 2 Of The RBTS

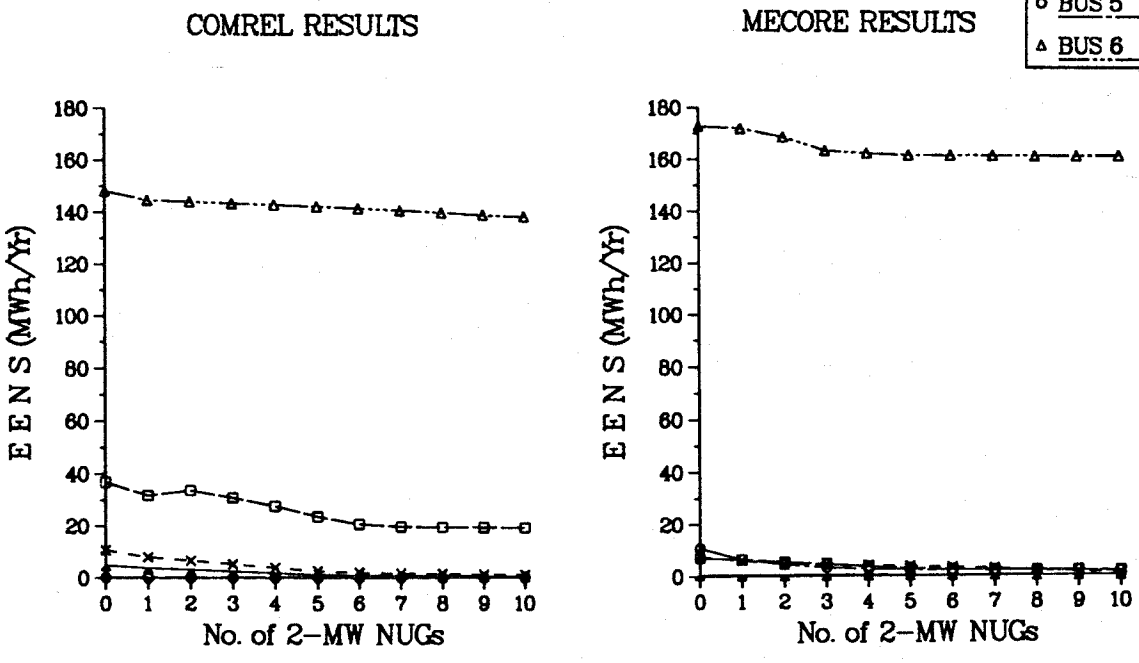

Figure 4.8: Variation In EENS At The Load Points As Identical 2-MW NUGs Are Incrementally Introduced At Bus 2 Of The RBTS

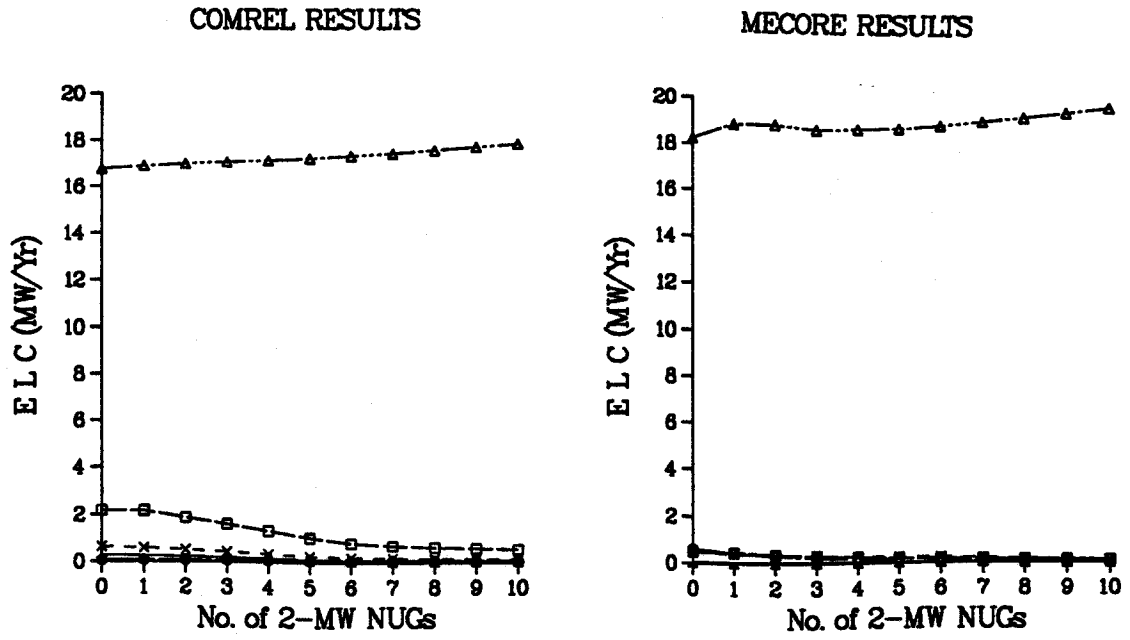

Figure 4.9: Variation In ELC At The Load Points As Identical 2-MW NUGs Are Incrementally Introduced At Bus 3 Of The RBTS

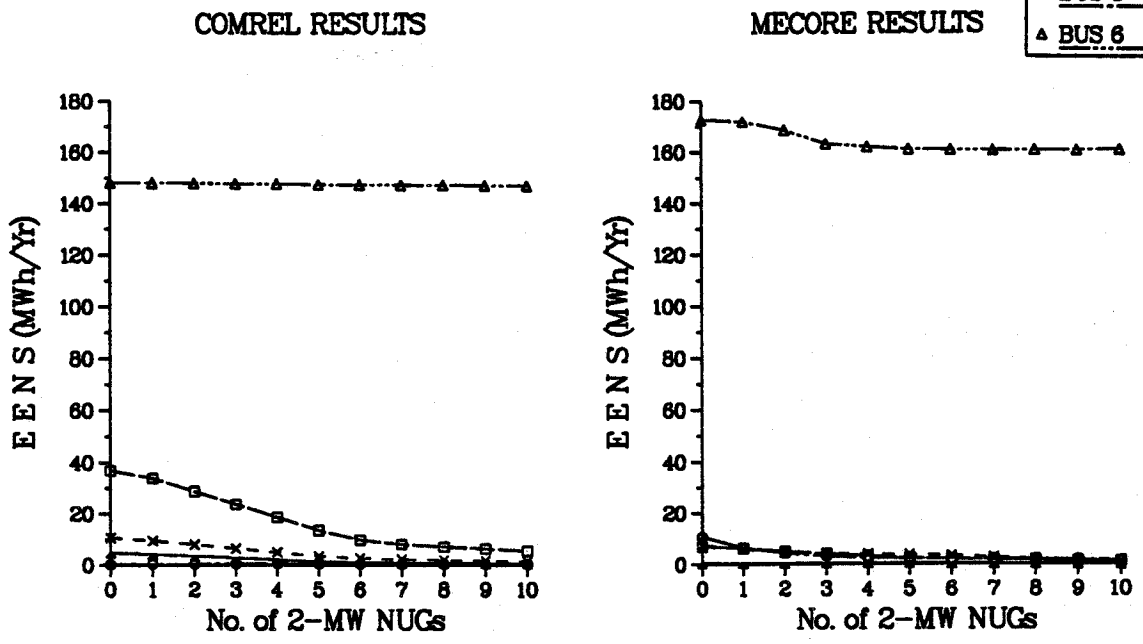

Figure 4.10: Variation In EENS At The Load Points As Identical 2-MW NUGs Are Incrementally Introduced At Bus 3 Of The RBTS

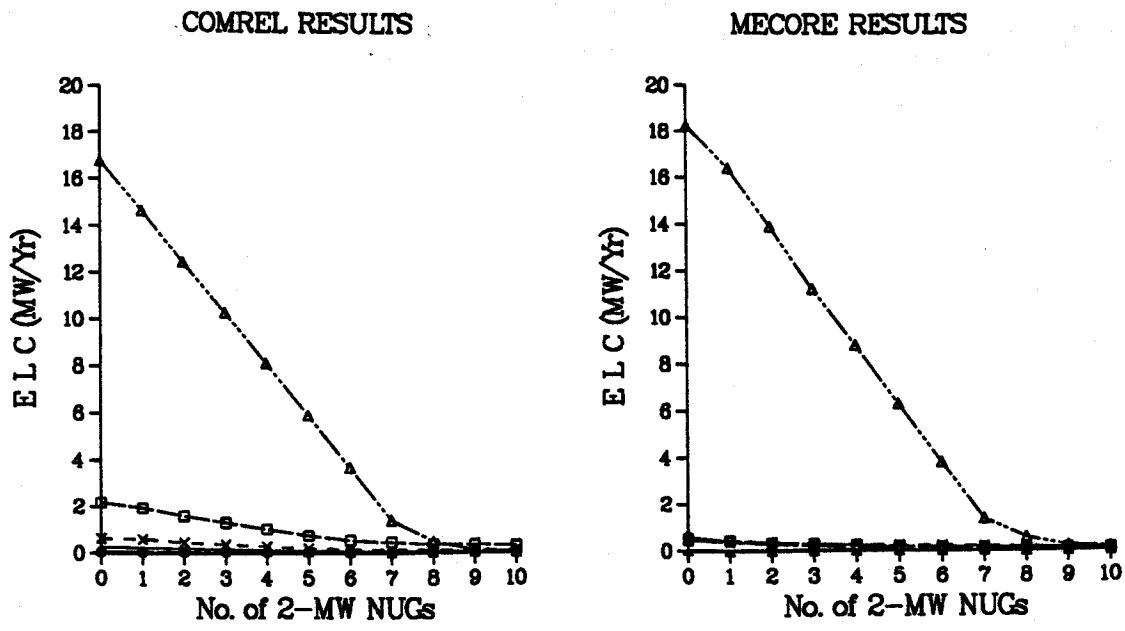

Figure 4.11: Variation In ELC At The Load Points As Identical 2-MW NUGs Are Incrementally Introduced At Bus 6 Of The RBTS

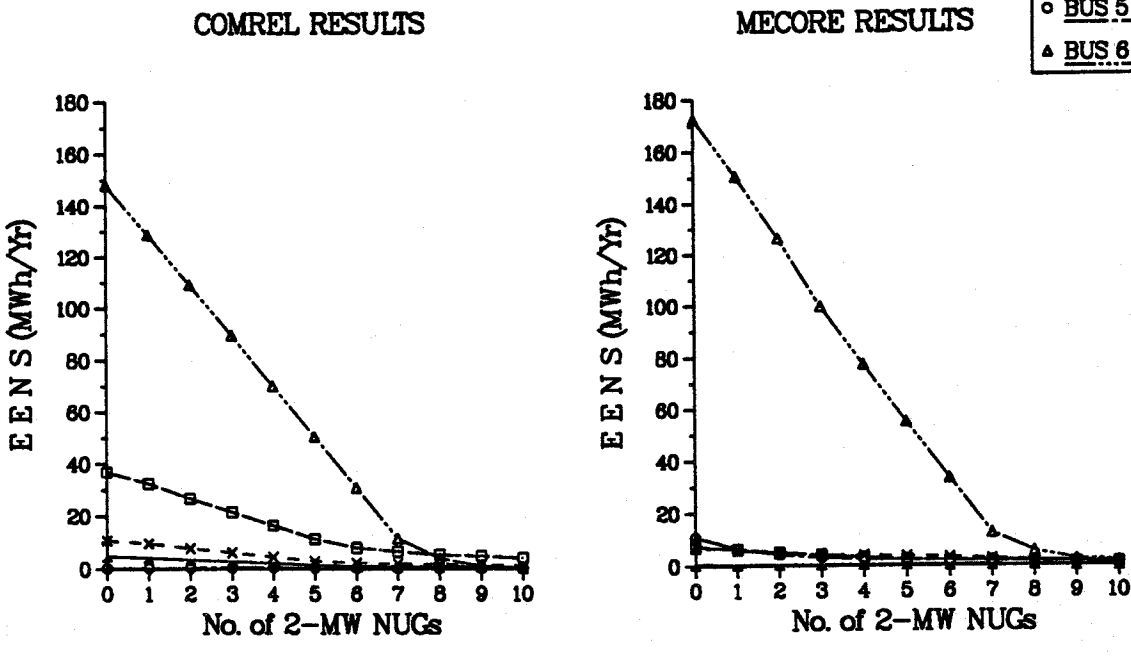

Figure 4.12: Variation In EENS At The Load Points As Identical 2-MW NUGs Are Incrementally Introduced At Bus 6 Of The RBTS

It can therefore be concluded from this analysis that the ELC and the EENS are more responsive indices for measuring the impacts of NUGs on load point adequacy. It is also possible to use these indices, especially the EENS index, as a basis to evaluate the reliability worth associated with the NUGs.

The load point indices at bus 6 are unaffected by the unit additions except when the NUGs are introduced at that bus itself. As mentioned in Chapter 3, bus 6 is the most unreliable load point in the RBTS because of the frequent isolation problems it experiences whenever its single-line radial connection with the rest of the test system is on outage. Introduction of additional generation facilities anywhere beyond the radial connection does not improve the situation at bus 6, because the isolation problems are not addressed by such actions. However, when the NUGs are introduced at bus 6, generation from the NUGs can be used locally to supplement supplies to the load point and therefore produces significant increases in the load point adequacy.

From Figure 4.7 the load curtailment situation at bus 3 persistently deteriorates as more units are introduced at bus 2 of the RBTS. These adverse effects at bus 3 are caused by the increased frequency of overloading experienced on line 3 (as a result of NUGs introduction at bus 2) which serves as the major route of generation supply from bus 2 to bus 3. The corresponding energy curtailment situation at bus 3, however, improves marginally, because the expected duration (or probability) of the load curtailment at the bus reduces considerably as a result of the unit additions. The inherent increasing trend in the ELC and the EENS at bus 6 as shown in Figures 4.7-4.10 can be attributed to the increased number of outage combinations that contribute to the problems at the bus when the NUGs are introduced at bus 2 or bus 3.

The higher flexibility associated with the implementation of load curtailment action in the MECORE program accounts for the relatively higher sensitivity of the MECORE results to unit additions. The linear programming minimisation model provided to handle load curtailment in that (MECORE) program is observed to be more responsive to the penetration of the additional generation from the NUGs than in the COMREL program where the load curtailment action is more rigidly enforced.

4.4.1.2. System Indices

Figures 4.13 and 4.14 respectively show variations in the system Expected Load Curtailed (ELC) and the system Expected Energy Not Supplied (EENS) as NUGs are incrementally introduced at the specified locations within the RBTS. The variations in the Bulk Power Interruption Index and the Severity Index which are derived from the system ELC and EENS respectively are also shown in Figures 4.15 and 4.16.

Gradual improvements in the overall system adequacy can be observed from all the figures as the number of NUGs introduced at a particular location is increased. The rate of improvement however reduces with the unit additions, and the indices settle at different levels of adequacy for the different NUG locations examined. It is important to appreciate that composite system inadequacy, in addition to direct generation deficiencies and bus isolation due to transmission failures, is also related to the composite problem of generation and transmission outages. As already noted in the case of the RBTS, the weak transmission link to bus 6 minimises the benefit to bus 6 of the additional NUG generation introduced at either bus 2 or bus 3. The principal benefits of the NUG additions at these locations is to alleviate generating capacity deficiencies prevailing in the north section of the system which constitutes only a small portion of the overall RBTS inadequacy. Therefore, though overall system inadequacy remains relatively high when a total of 12 MW of NUG capacity is introduced at either bus 2 or 3, relatively little further improvement is achieved from subsequent unit additions. Introduction of the NUGs at bus 6 however produces significant drops in the inadequacy indices as the NUGs can now directly supply the load point during normal system operation and when the load point is isolated from the conventional generation sources. Independent power production therefore, in this case, offers a technically feasible alternative to transmission system reinforcement as a measure for improving overall system adequacy.

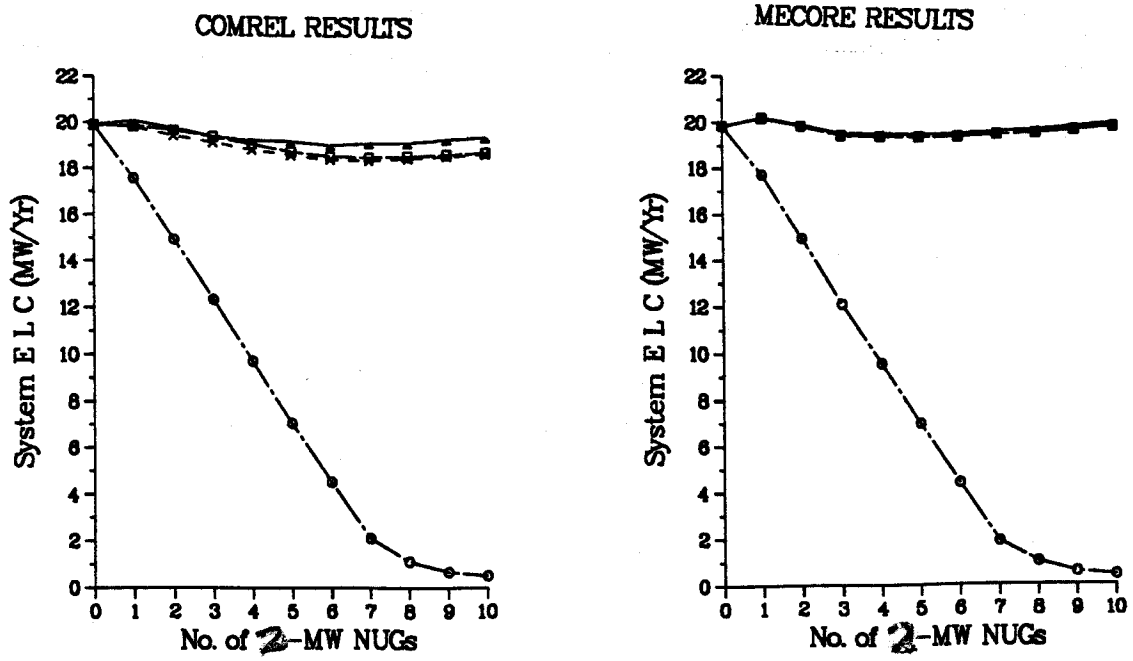

Figure 4.13: Variation In System ELC As Identical 2-MW NUGs Are Incrementally Introduced At Buses 2, 3 And 6 Of The RBTS Respectively

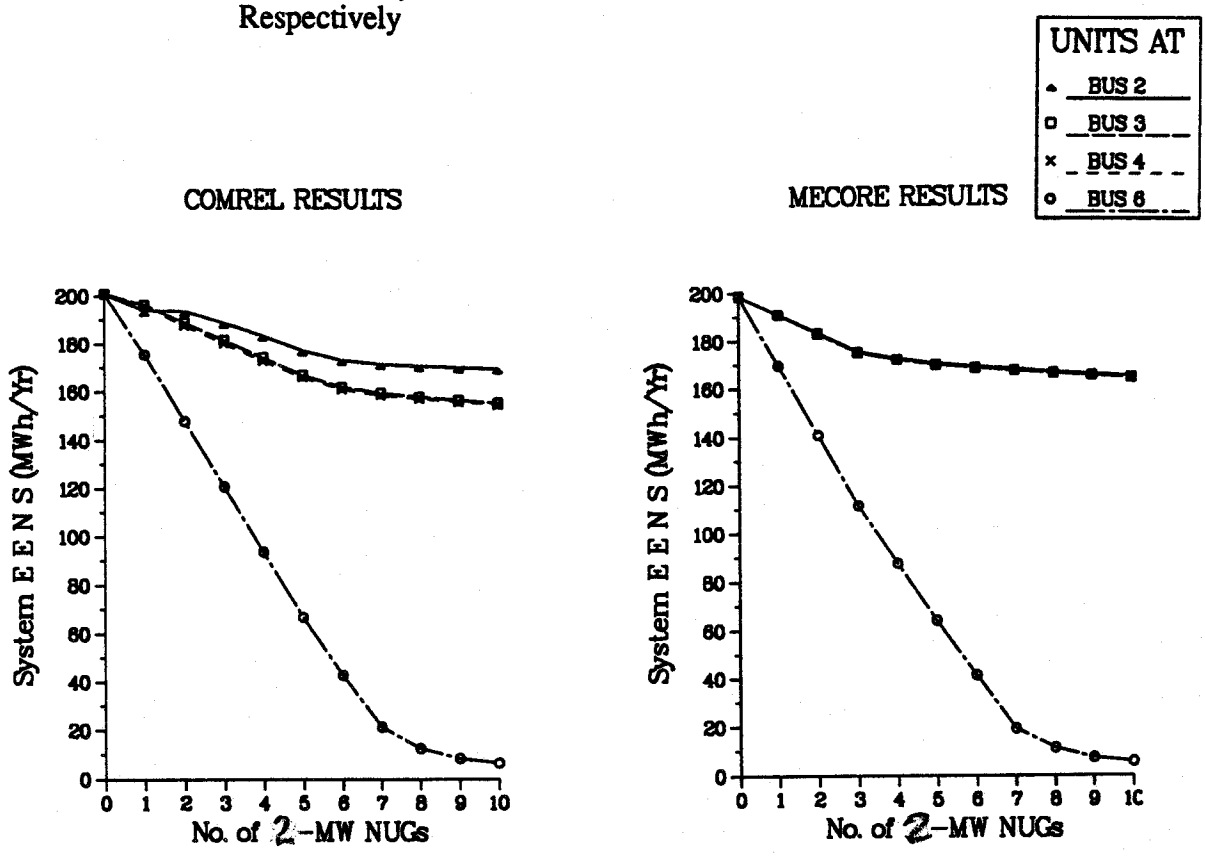

Figure 4.14: Variation In System EENS As Identical 2-MW NUGs Are Incrementally Introduced At Buses 2, 3 And 6 Of The RBTS Respectively

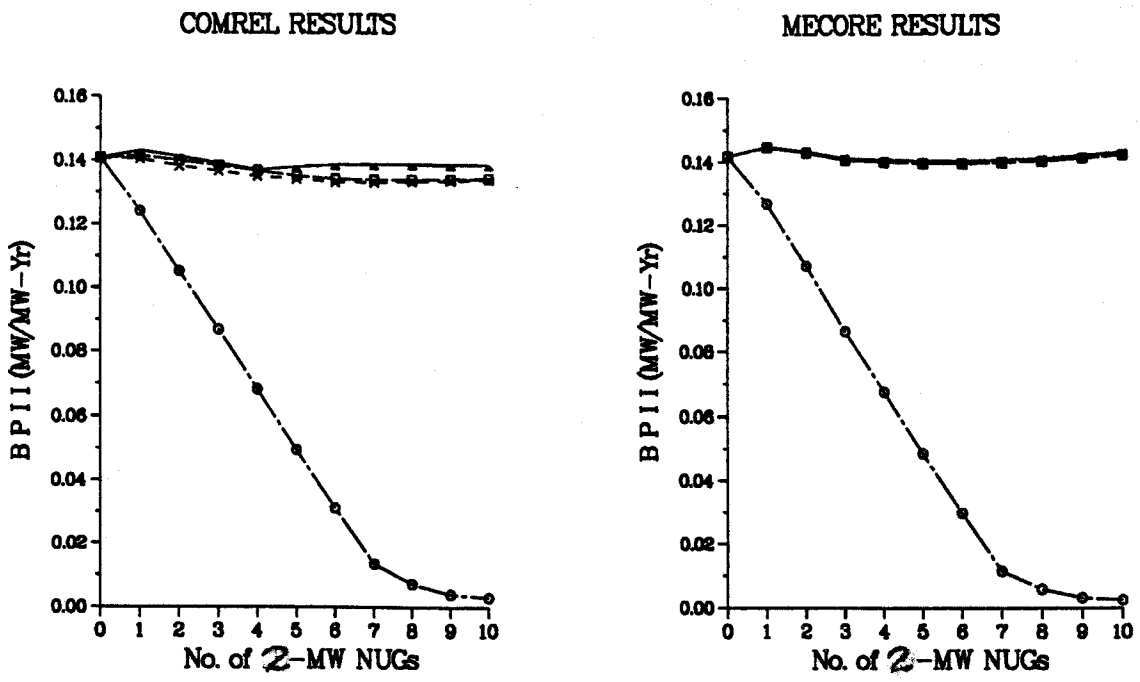

Figure 4.15: Variation In BPII As Identical 2-MW NUGs Are Incrementally Introduced At Buses 2, 3 And 6 Of The RBTS Respectively

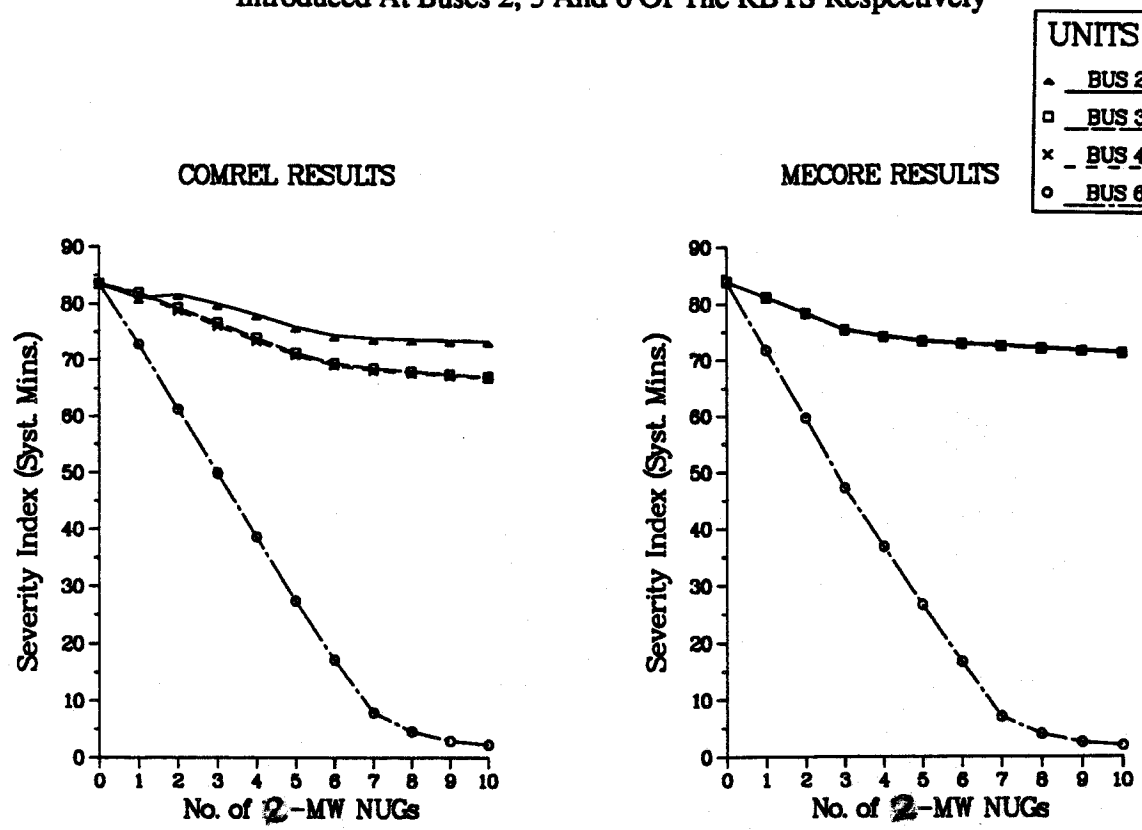

Figure 4.16: Variation In Severity Index As Identical 2-MW NUGs Are Incrementally Introduced At Buses 2, 3 And 6 Of The RBTS Respectively

4.4.2. Results for the IEEE-RTS

4.4.2.1. Load Point Indices

Figures 4.17-4.32 show the results obtained for the IEEE-RTS when up to 100 MW of additional generation from identical 10 MW NUGs are sequentially introduced at buses 1 and 8 in the south region and at buses 13 and 18 in the north region of the IEEE-RTS. The variations in the failure probability and the failure frequency indices are shown in Figures 4.17-4.24 and similar variations in the ELC and the EENS indices are also shown in Figures 4.25- 4.32 for the 17 load points of the IEEE-RTS.

A general decreasing trend in the indices for most of the load points can be seen immediately with the unit additions. This indicates that generation deficiency is the major cause of inadequacy at the load points in the IEEE-RTS. The comprehensive nature of the IEEE-RTS transmission network enhances the effective penetration of generation from the NUGs so that a number of outage contingencies which originally made a significant contribution to load point inadequacy are virtually eliminated. The largest improvement in adequacy occurred at the load points in the north region which are most affected by the generation capacity deficiencies. Therefore, additional NUG generation provided is used to alleviate a significant portion of these generation deficiency problems.

The COMREL results however show some load points to be adversely affected by the unit additions, depending upon the location of the NUG facilities. Bus 19, for example, is adversely affected in all the cases except when the NUGs are introduced at bus 13 from where additional supplies made available by the NUGs can easily reach it. Otherwise, as the number of unit additions increases, bus 19 becomes exposed to the effects of an increased number of generating unit outage combinations that lead to swing bus overload conditions affecting the load point. A similar situation arises when the NUGs are introduced at bus 18 in which case bus 16 is also adversely affected in addition to bus 19. Introduction of NUG facilities at bus 8 also causes a slight deterioration in the level of adequacy at buses 9 and 10. It can be recalled that these buses were shown by the COMREL program to be the most reliable buses in the IEEE-RTS. This deterioration occurs because, as the number of NUGs introduced at bus 8 increases, buses 9 and 10

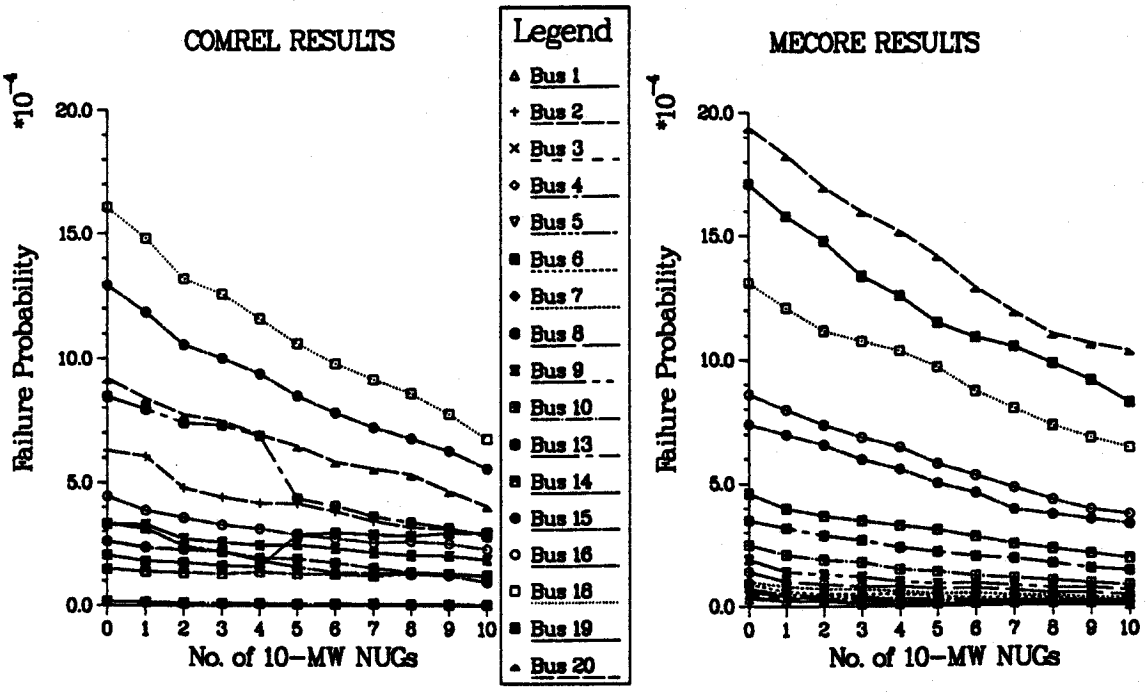

Figure 4.17: Variation In Load Point Failure Probability As Identical 10-MW NUGs Are Incrementally Introduced At Bus 1 Of The IEEE-RTS

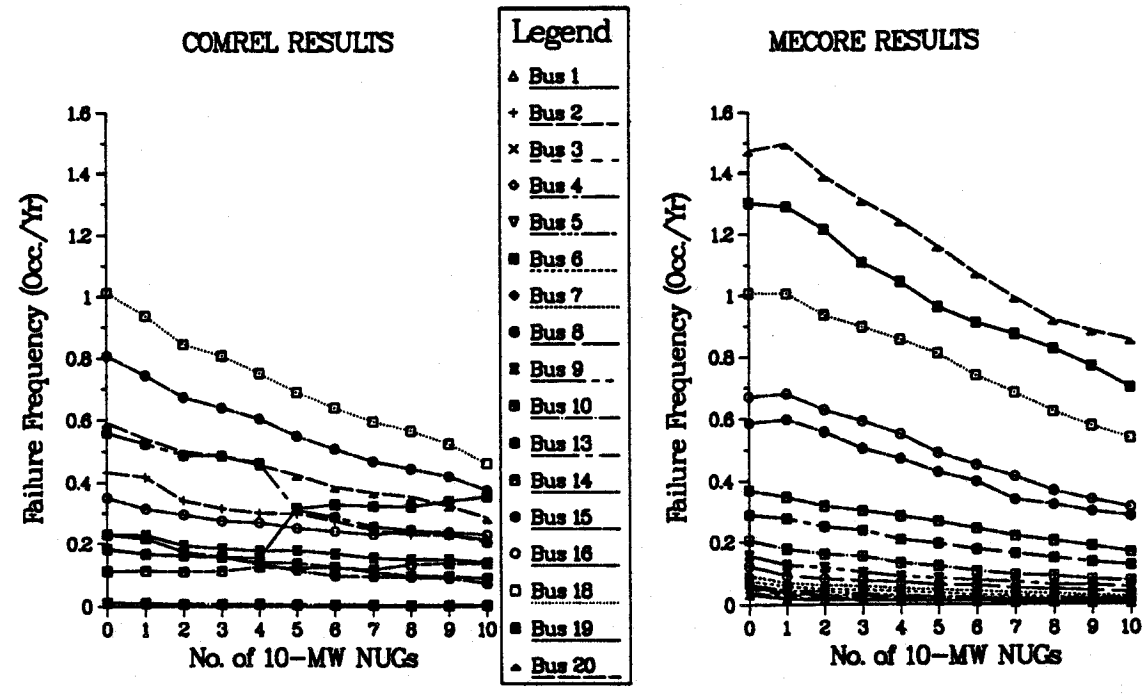

Figure 4.18: Variation In Load Point Failure Frequency As Identical 10-MW NUGs Are Incrementally Introduced At Bus 1 Of The IEEE-RTS

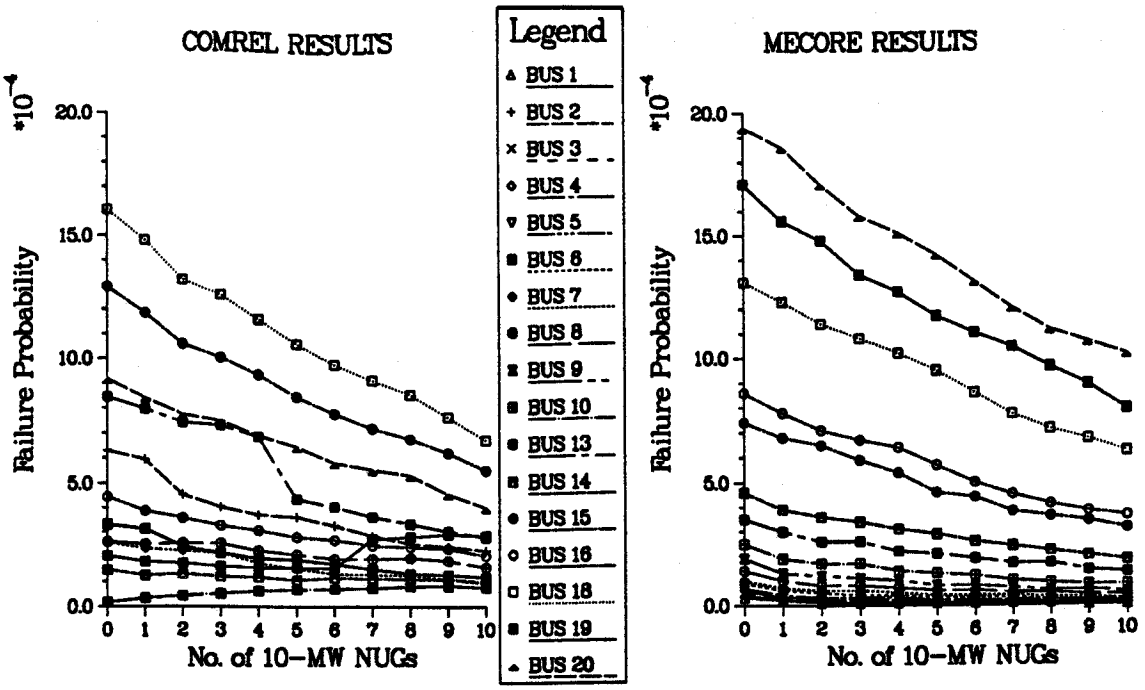

Figure 4.19: Variation In Load Point Failure Probability As Identical 10-MW NUGs Are Incrementally Introduced At Bus 8 Of The IEEE-RTS

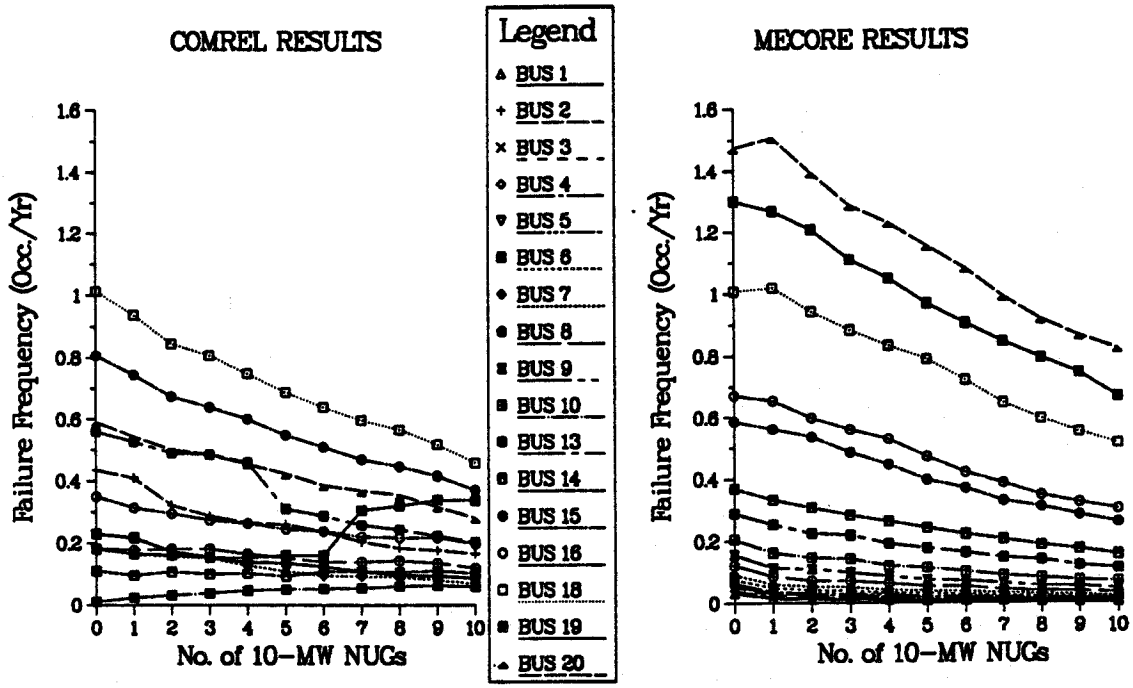

Figure 4.20: Variation In Load Point Failure Frequency As Identical 10-MW NUGs Are Incrementally Introduced At Bus 8 Of The IEEE-RTS

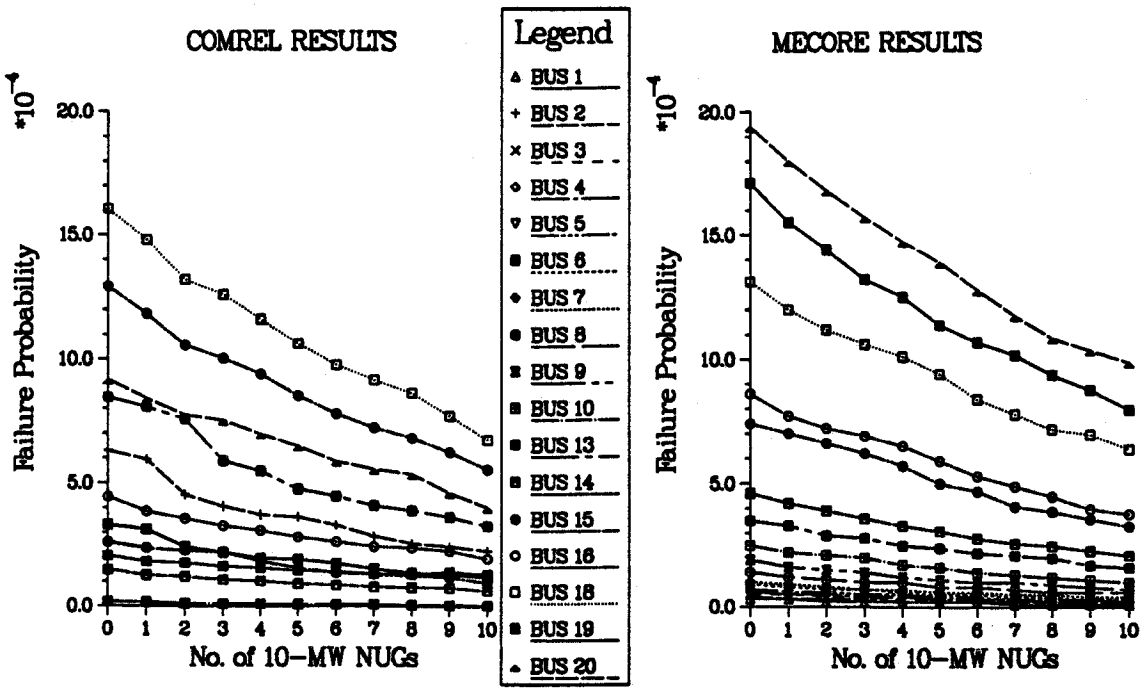

Figure 4.21: Variation In Load Point Failure Probability As Identical 10-MW NUGs Are Incrementally Introduced At Bus 13 Of The IEEE-RTS

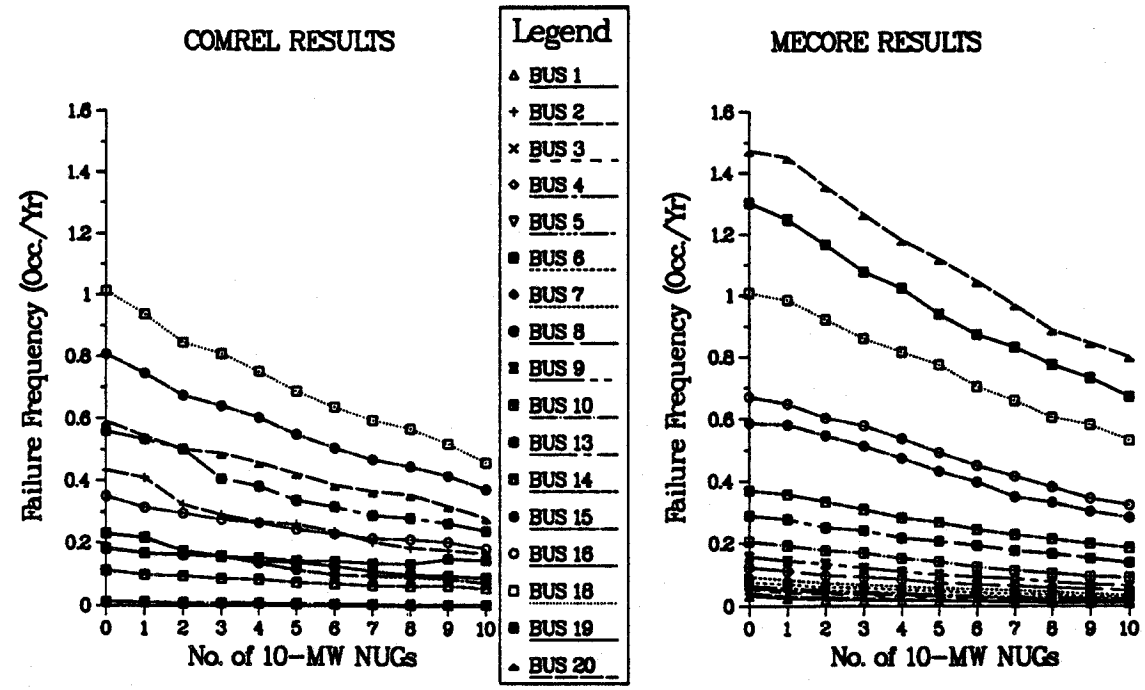

Figure 4.22: Variation In Load Point Failure Frequency As Identical 10-MW NUGs Are Incrementally Introduced At Bus 13 Of The IEEE-RTS

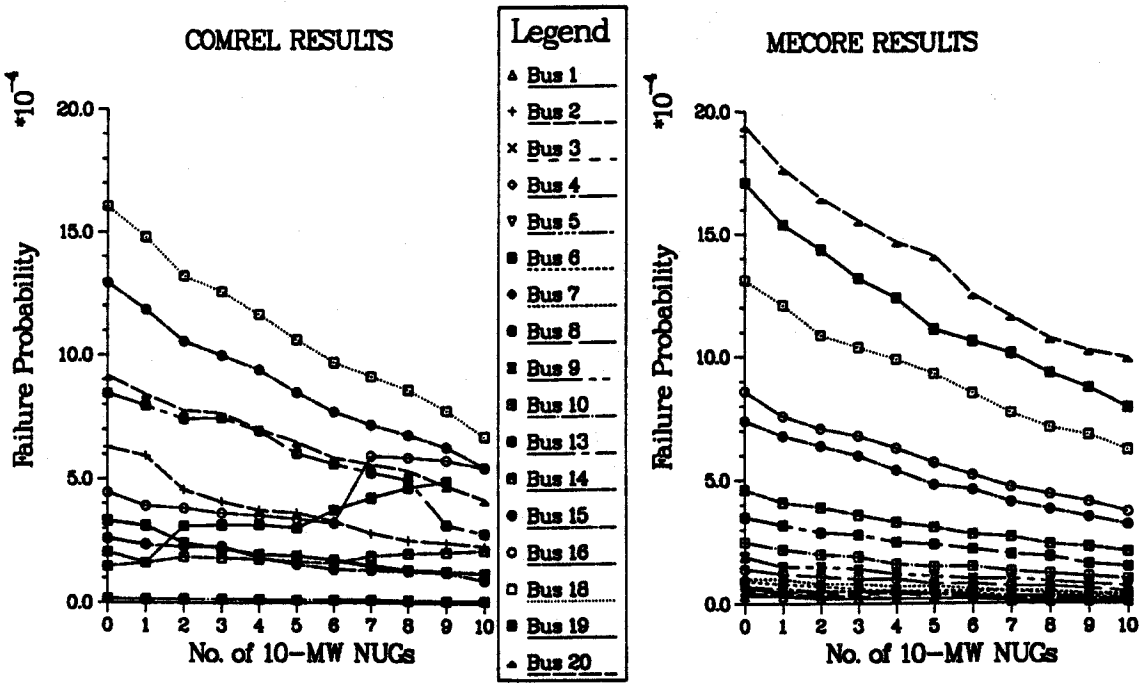

Figure 4.23: Variation In Load Point Failure Probability As Identical 10-MW NUGs Are Incrementally Introduced At Bus 18 Of The IEEE-RTS

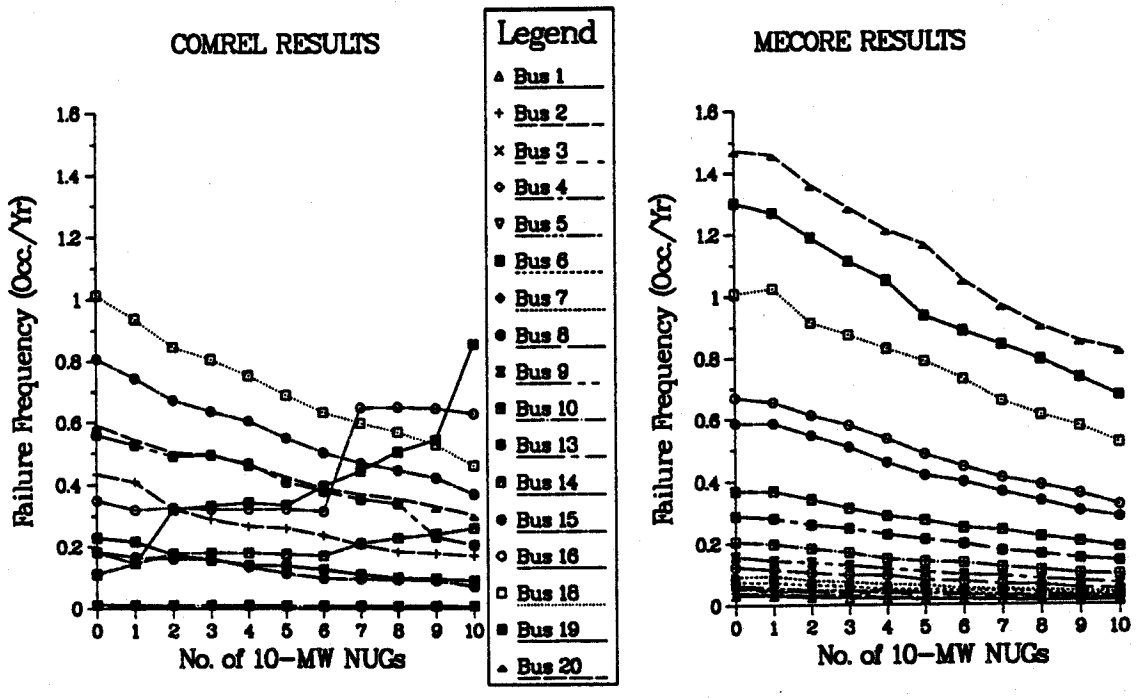

Figure 4.24: Variation In Load Point Failure Frequency As Identical 10-MW NUGs Are Incrementally Introduced At Bus 18 Of The IEEE-RTS

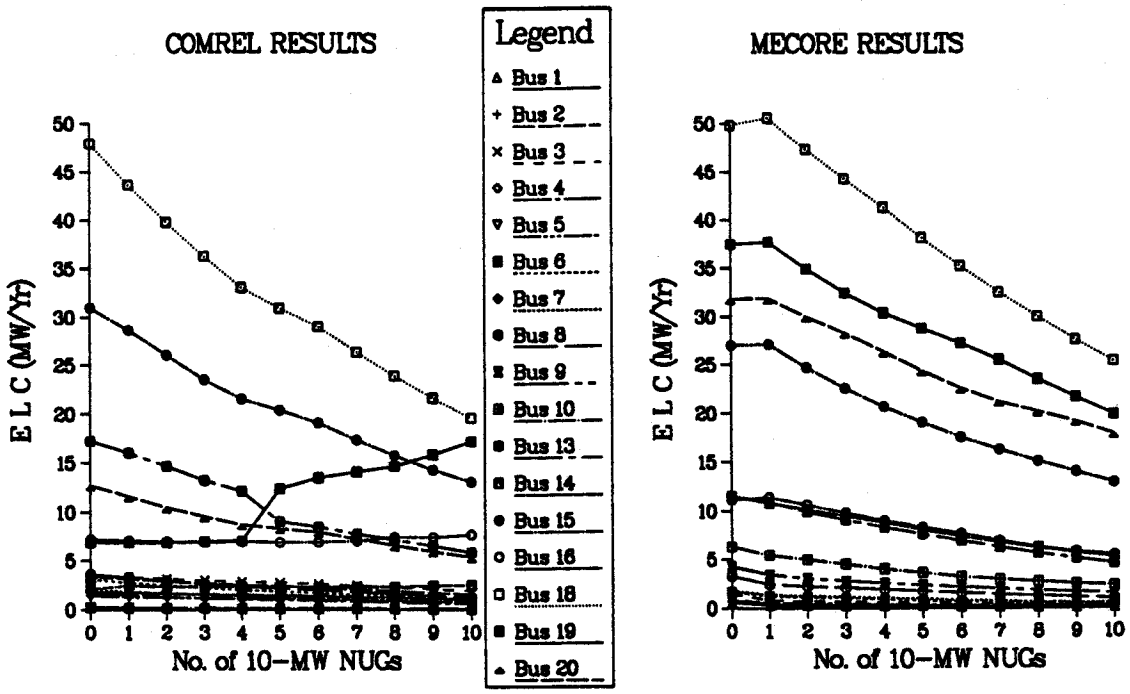

Figure 4.25: Variation In ELC At The Load Points As Identical 10-MW NUGs Are Incrementally Introduced At Bus 1 Of The IEEE-RTS

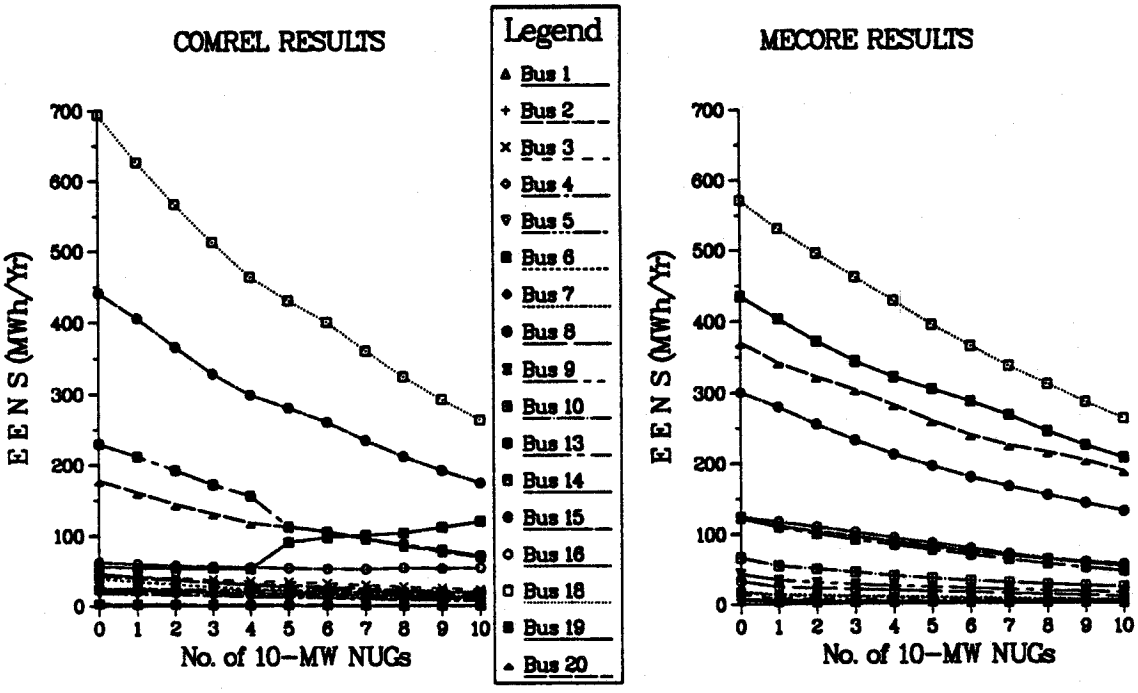

Figure 4.26: Variation In EENS At The Load Points As Identical 10-MW NUGs Are Incrementally Introduced At bus 1 Of The IEEE-RTS

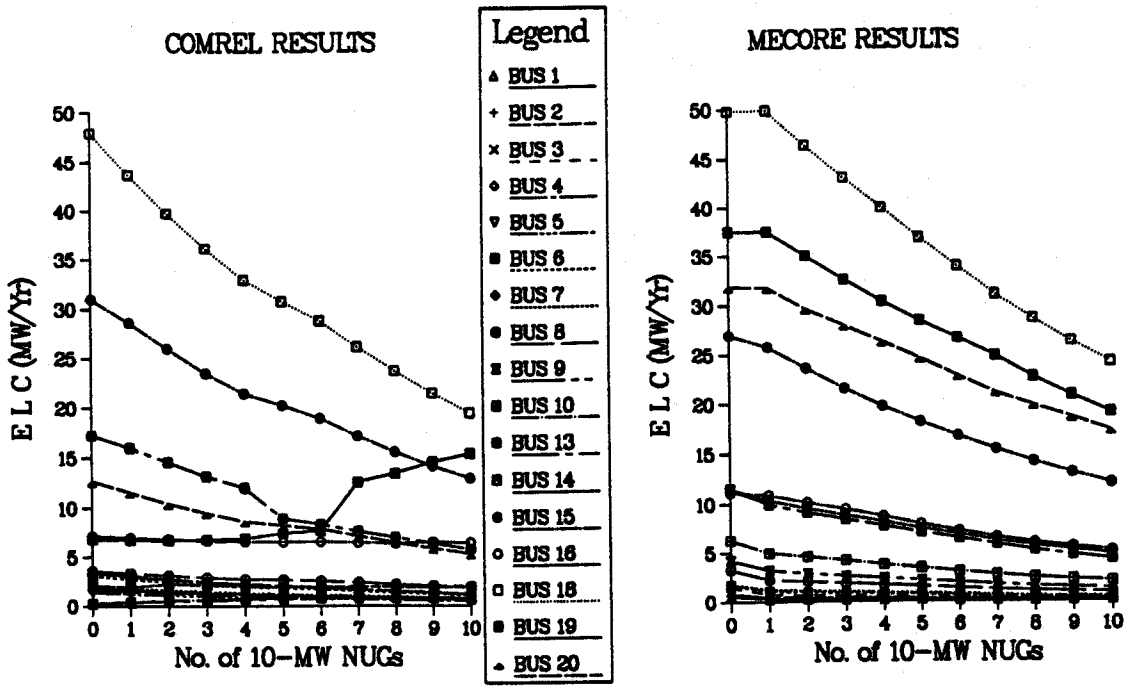

Figure 4.27: Variation In ELC At The Load Points As Identical 10-MW NUGs Are Incrementally Introduced At Bus 8 Of The IEEE-RTS

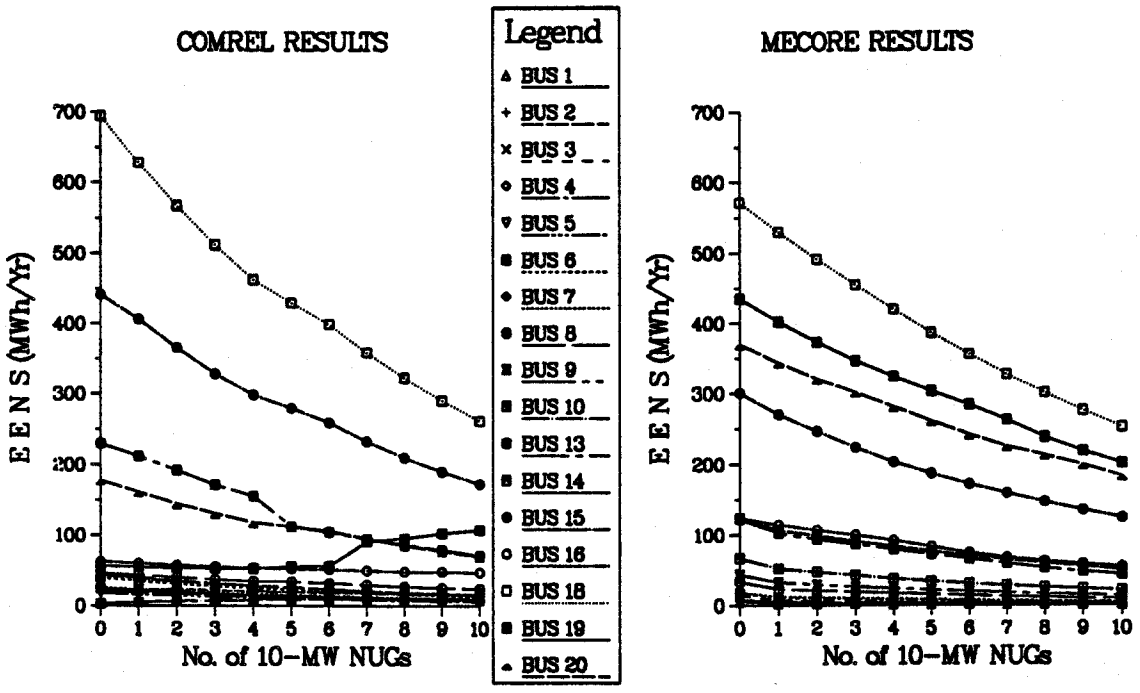

Figure 4.28: Variation In EENS At The Load Points As Identical 10-MW NUGs Are Incrementally Introduced At Bus 8 Of The IEEE-RTS

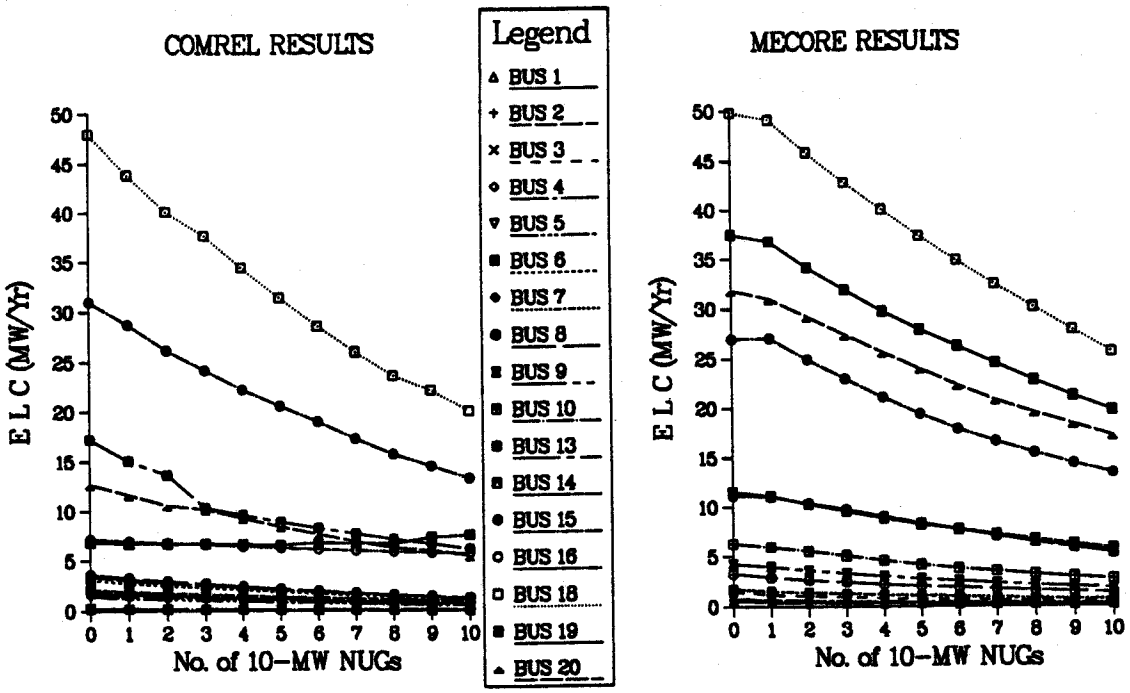

Figure 4.29: Variation In ELC At The Load Points As Identical 10-MW NUGs Are Incrementally Introduced At Bus 13 Of The IEEE-RTS

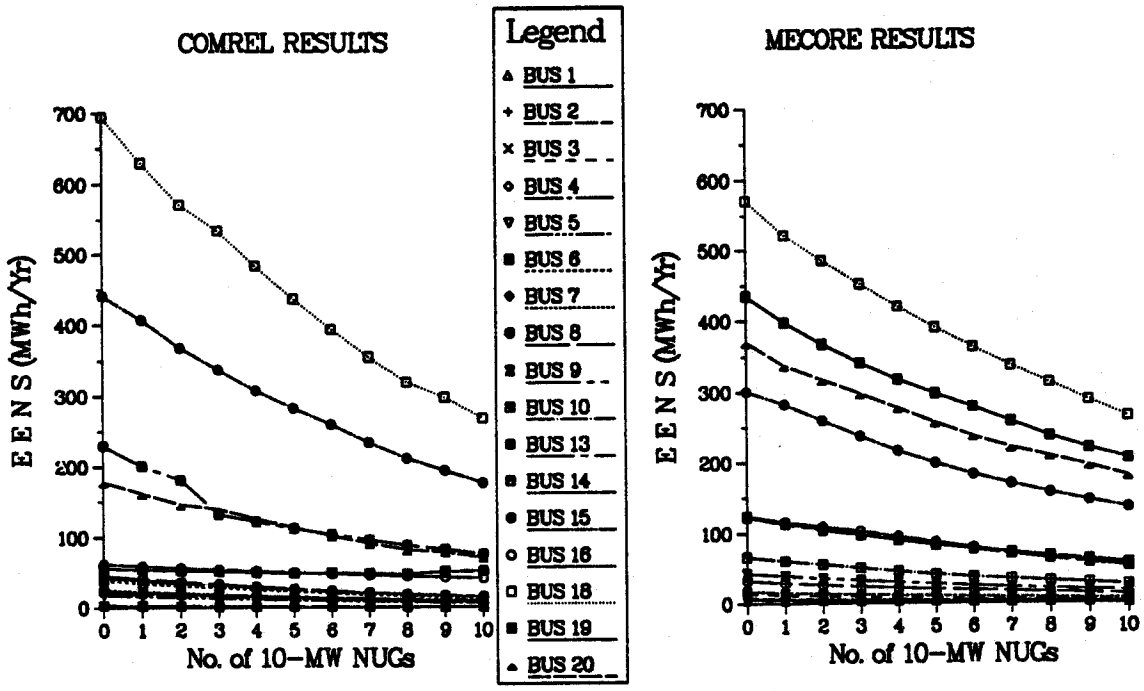

Figure 4.30: Variation In EENS At The Load Points As Identical 10-MW NUGs Are Incrementally Introduced At Bus 13 Of The IEEE-RTS

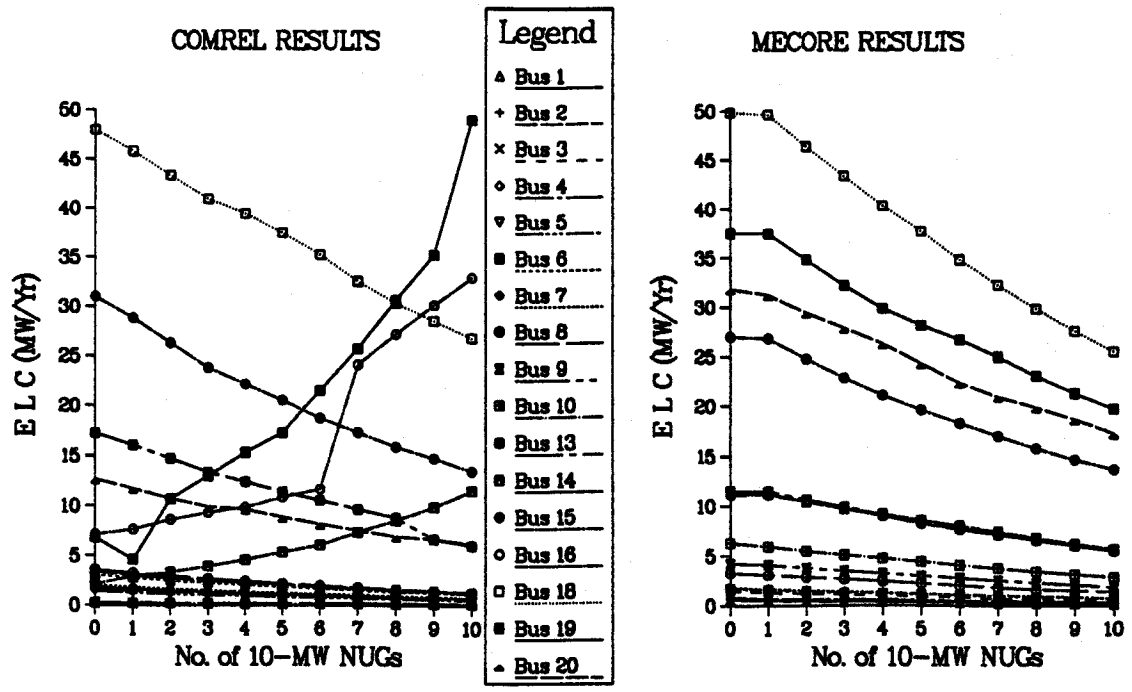

Figure 4.31: Variation In ELC At The Load Points As Identical 10-MW NUGs Are Incrementally Introduced At Bus 18 Of The IEEE-RTS

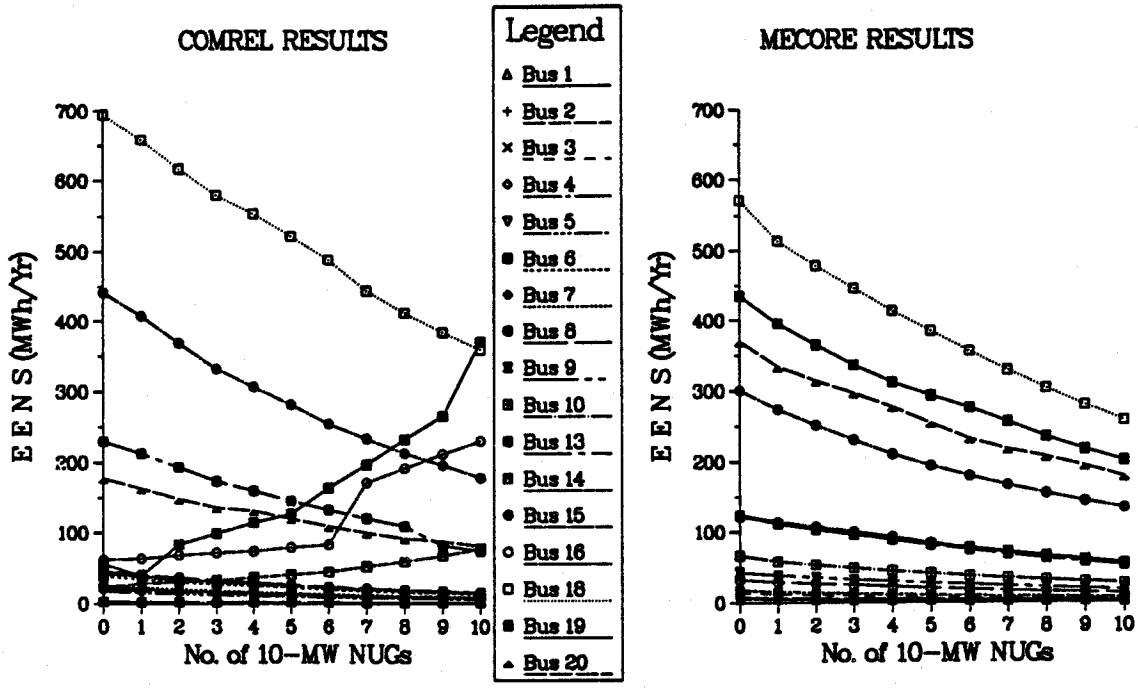

Figure 4.32: Variation In EENS At The Load Points As Identical 10-MW NUGs Are Incrementally Introduced At Bus 18 Of The IEEE-RTS

which are adjacent to bus 8 become exposed to the effects of an increasing number of generating unit outage combinations resulting in load curtailment at both buses. These trends are however absent from the MECORE results because of the linear programming minimisation model which tends to spread the load curtailment more evenly among a larger number of the system load points in an attempt to minimise the overall system load curtailment. The MECORE results therefore show consistent uniform reductions in inadequacy at all the load points of the IEEE-RTS as the NUGs are injected into the system.

4.4.2.2. System Indices

The variations in the system ELC, EENS, the Bulk Power Interruption Index (BPII) and the Severity Index (SI) for the IEEE-RTS when the NUGs are introduced at buses 1, 8, 13 and 18 are respectively shown in Figures 4.33-4.36.

The trends obtained show a general drop in the overall system indices as the NUGs are injected into the system. It should be noted that unlike the RBTS, the bulk of the inadequacies within the IEEE-RTS comes from generation deficiencies which frequently lead to swing bus overload conditions. The remedial actions taken to solve this type of problems ultimately involves load curtailment at system load points, particularly those in the north region. The introduction of NUGs therefore provides additional generation to the system to minimise these problems. Further unit additions at buses 8 and 13 after introducing 100 MW of additional NUG generation into the system, could have produced further improvements in the overall system adequacy. This can be attributed to the comprehensive nature of the IEEE-RTS transmission network which allows effective penetration of generation to most parts of the system, particularly from the east where the bulk supplies in the IEEE-RTS originate. Additional NUG supplies made available at bus 13 are used to reinforce supplies from the east region consequently reducing the frequency of the overload conditions experienced by the swing bus. Similarly, introduction of NUGs at either bus 1 or bus 8 in the south region also reduces that region's dependence on supplies from the north thus releasing substantial supplies for use in suppressing the occurrence of swing bus overload conditions. This accounts for the appreciable levels of improvements recorded when the unit additions are made at buses 1 and 8 in the south region of the IEEE-RTS.

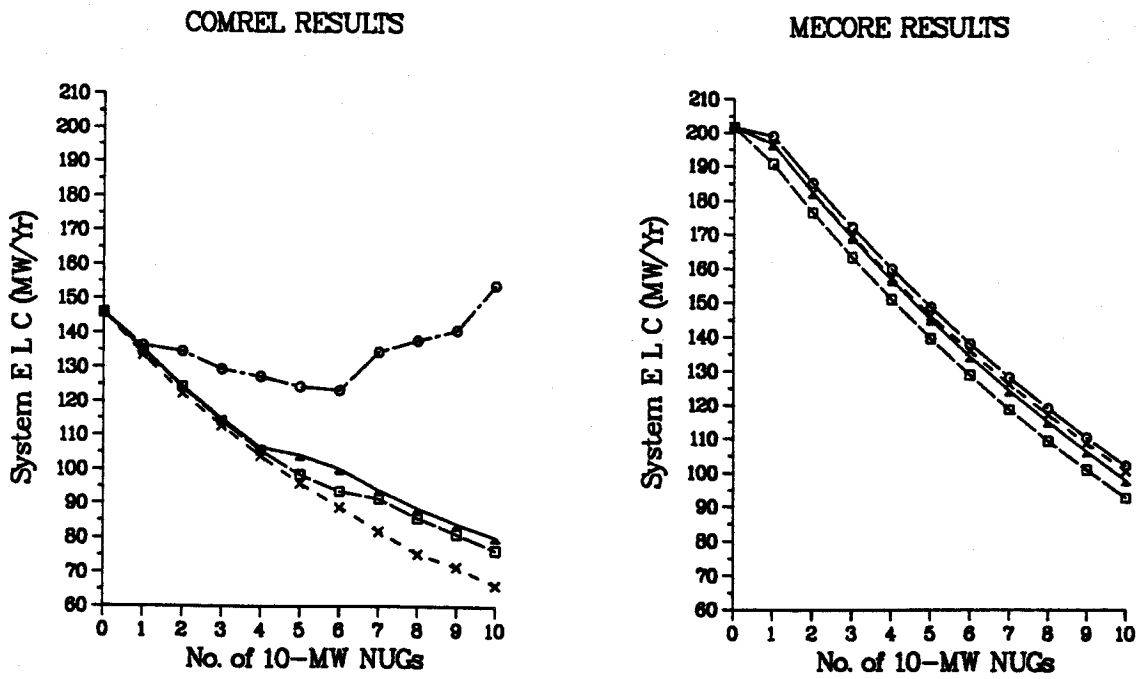

Figure 4.33: Variation In System ELC As Identical 10-MW NUGs Are Incrementally Introduced At buses 1, 8, 13 And 18 Of The IEEE-RTS Respectively

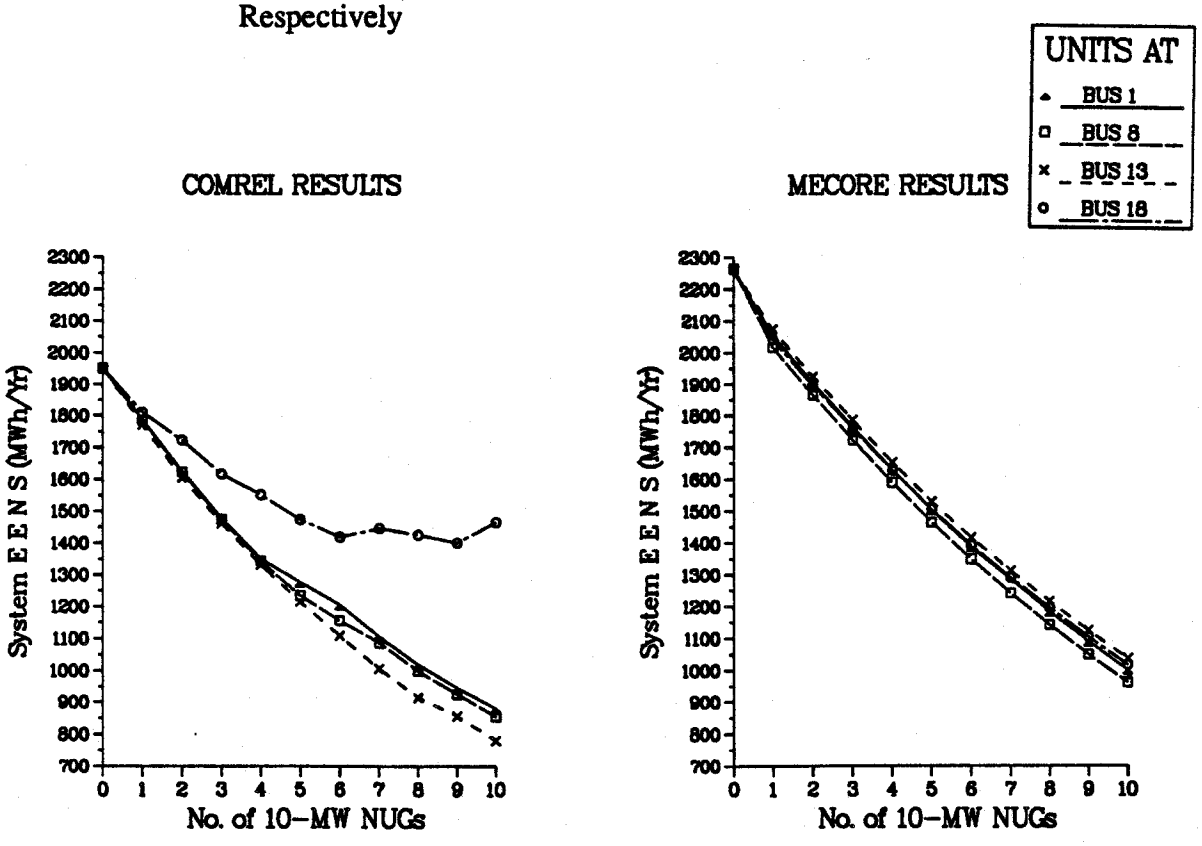

Figure 4.34: Variation In System EENS As Identical 10-MW NUGs Are Incrementally Introduced At Buses 1, 8, 13 And 18 Of The IEEE-RTS Respectively

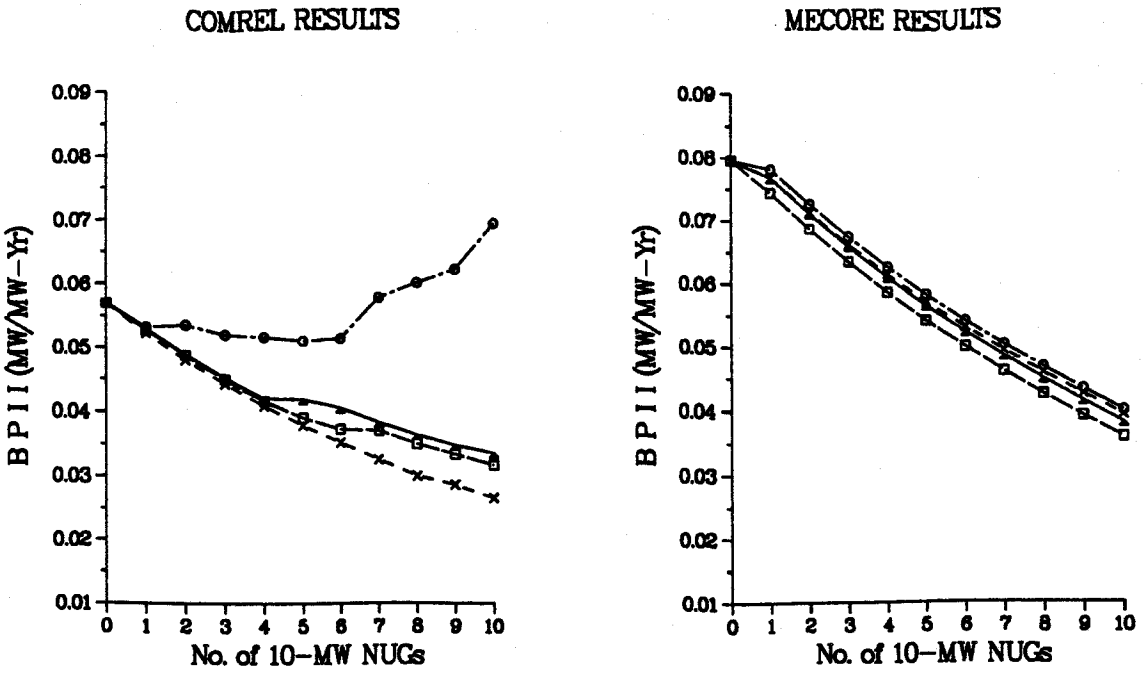

Figure 4.35: Variation In BPII As Identical 10-MW NUGs Are Incrementally Introduced At Buses 1, 8, 13 And 18 Of The IEEE-RTS respectively

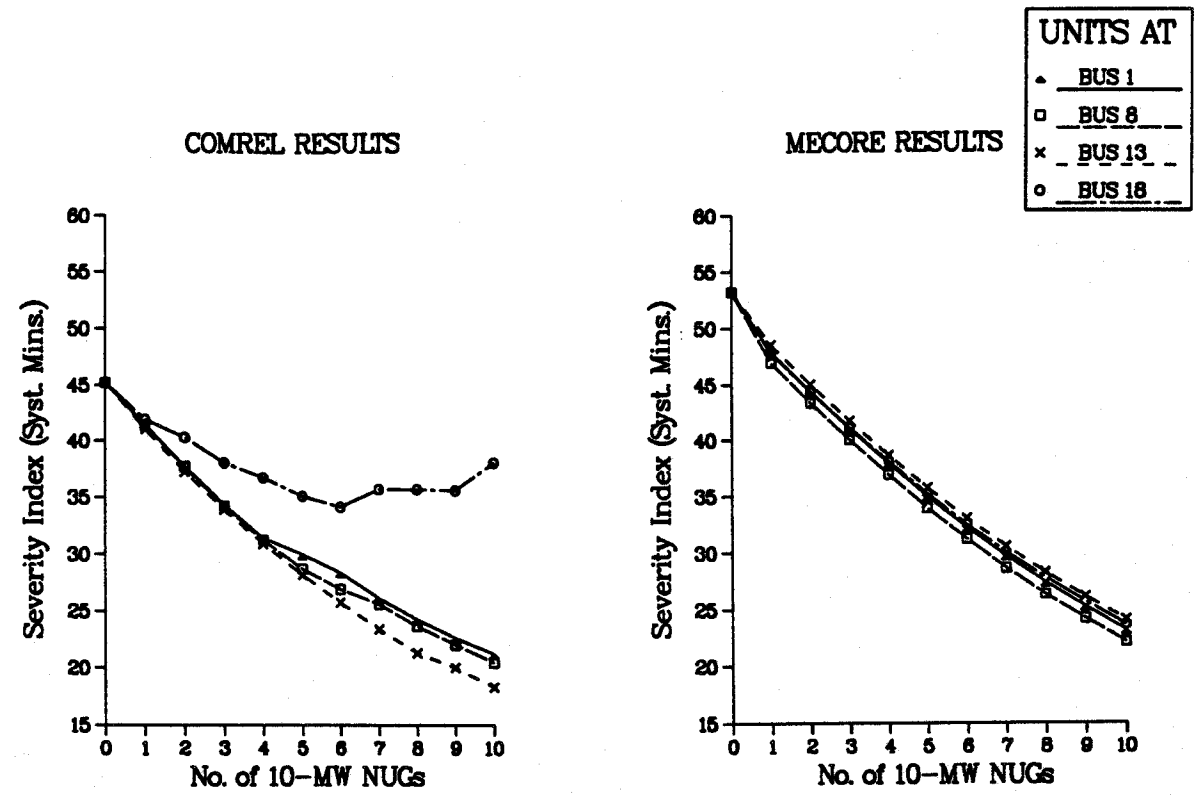

Figure 4.36: Variation In Severity Index As Identical 10-MW NUGs Are Incrementally Introduced At Buses 1, 8, 13 And 18 Of The IEEE-RTS Respectively

On the other hand when the NUGs are introduced at bus 18, the additional supplies made available are used up locally to minimise the curtailment effects at that load point caused by the swing bus overload conditions instead of attempting to prevent the occurrence of such conditions. In the long run, since other buses are also adversely affected by these system conditions, the adverse effects of the swing bus overload conditions at these neighbouring buses surpass the gains made at bus 18 and therefore reverse the initial trend of improvement in overall system adequacy. These observations are not apparent in the MECORE results because the program relies on the principle of minimising the overall system load curtailment. The MECORE results also show the NUG impacts on overall system adequacy to be virtually the same irrespective of the NUG locations. This can be attributed to the relaxation of the load curtailment confinement policy coupled with the comprehensive transmission system of the IEEE-RTS which makes effective penetration of the additional NUG supplies possible.

It can be concluded from these discussions that, taking advantage of NUGs in a large power system like the IEEE-RTS can produce significant improvements in overall composite system adequacy. Because of the strong transmission network of the IEEE-RTS, effective penetration of the additional supplies from the NUGs is assured from most of the injection points studied. The extent to which the siting of the NUGs is able to effectively influence inadequacy resulting from swing bus overload conditions is the major factor responsible for the differences in the impacts on the overall system adequacy of the IEEE-RTS.

4.5. Sensitivity Analyses

Sensitivity analysis is an important tool for supporting power system design and operation decisions and it can be used to estimate the impact of varying data on the performance measures of the system. Such an analysis is particularly essential in electric power system expansion planning because of the high variability of the component performance data resulting from uncertainties regarding the future due to the long planning horizon. Sensitivity analyses have been performed as part of this study to verify the impact of Forced Outage Rate (FOR) variations of single and multiple capacity NUGs with equivalent total installed capacity on the composite system reliability indices of the RBTS.

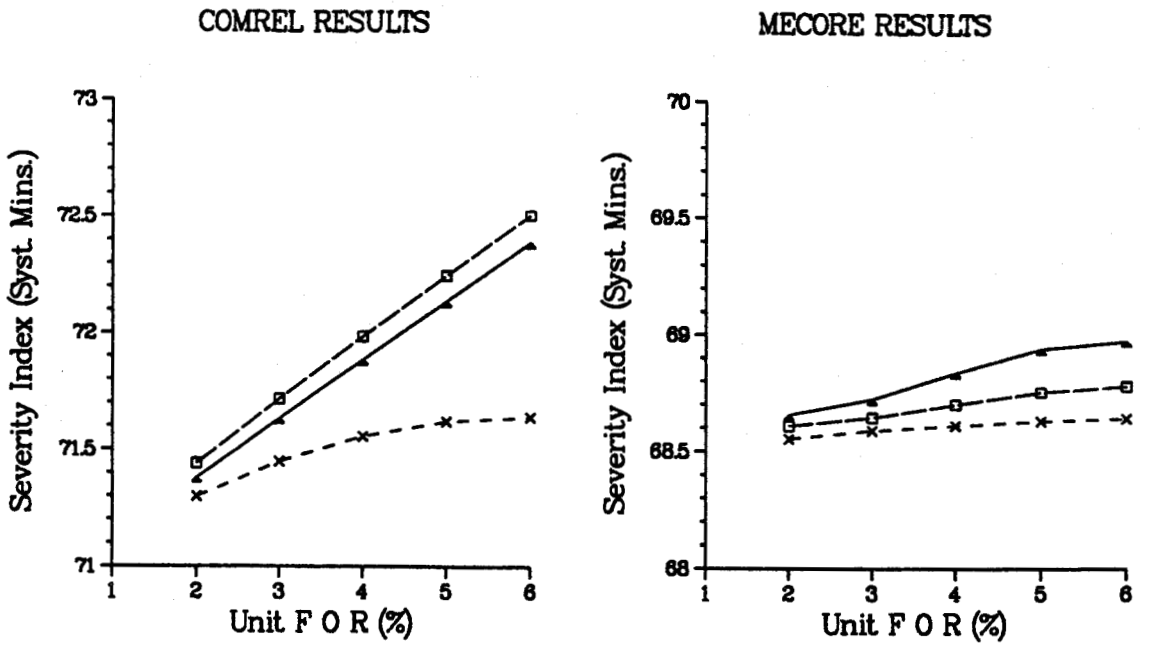

Figure 4.37: Sensitivity Study: Effects Of FOR Variation On Severity Index Of Single And Multiple NUGs With Total Capacity Of 10 MW When The Units Are Introduced At Bus 3 Of The RBTS

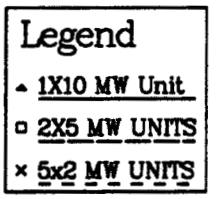

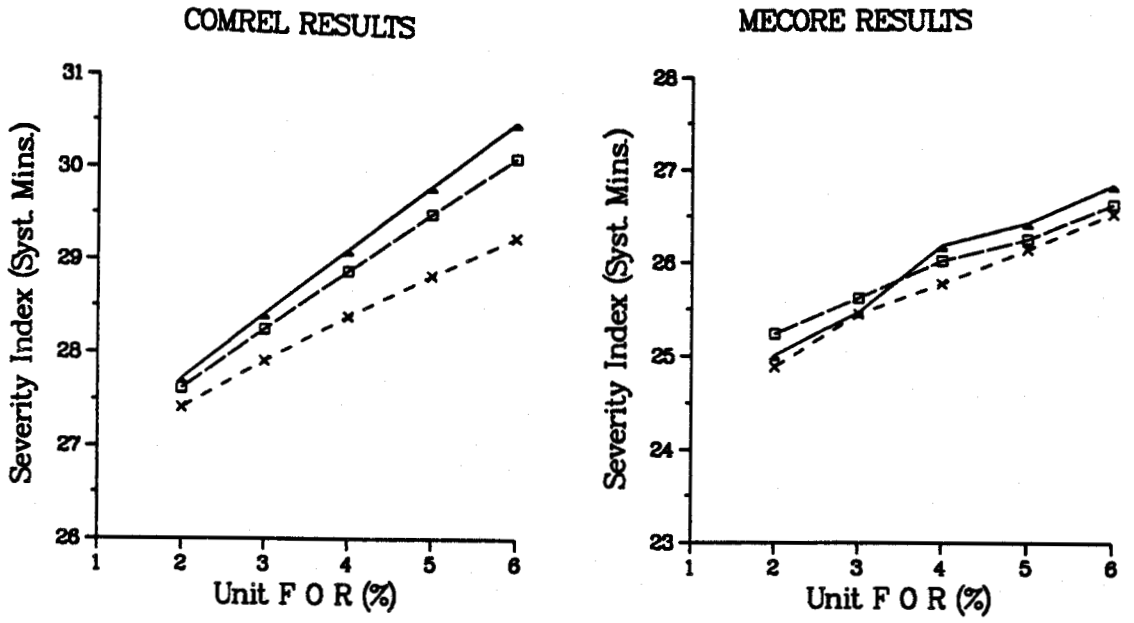

Figure 4.38: Sensitivity Study: Effects Of FOR Variation On Severity Index Of Single And Multiple NUGs With Total Capacity Of 10 MW When The Units Are Introduced At Bus 6 Of The RBTS

4.6. Summary

Composite system adequacy assessment involving NUGs has been introduced in this chapter utilising the COMREL and MECORE programs as the computational tools. Suitable methods for modelling the NUGs and the necessary network modelling modifications required to accommodate non-utility generation facilities have also been described. It has been shown by utilising the COMREL and the MECORE programs that, non-utility generators can serve as suitable alternatives to conventional power system reinforcement in the form of utility generation and transmission facilities. The results of the studies performed show that the introduction of NUGs at different locations in a utility system have different impacts on both load point adequacy and the overall system adequacy depending upon the existing composite generation and transmission configuration of the utility system. The results of sensitivity studies performed also show that multiple small capacity components of NUGs are generally more effective in producing lower system risk than relatively larger capacity components of NUGs.

The results obtained using the two programs illustrate that a power utility's operational practices and philosophies, such as the load curtailment policy, can have considerable influence on the benefits accruing from non-utility generation sources. The influence is most significant when the adequacy of the load points are determined.

5. INTRA-SYSTEM POWER WHEELING CONSIDERATIONS IN COMPOSITE SYSTEM ADEQUACY EVALUATION

5.1. Introduction

The discussion in the previous chapter regarding utilisation of the power produced from non-utility generators (NUGs) was based on the assumption that the local utility would be willing to purchase the independently produced power and use it to supplement its own supplies from conventional generation sources in the system. The local utility, for one reason or the other, may not be interested in purchasing the power produced from the NUGs. The factors [41] which account for this unwillingness on the part of the utility may include the following :

1. the utility may feel it has adequate generation capacity to meet the projected system load demand;
2. the utility may be concerned about its lack of adequate control over the independent power production facilities;
3. a desire on the part of the utility to discourage independent power production;
4. it may be the utility's traditional operational policy not to engage in such power purchasing transactions; or
5. the utility may believe that it can produce the required power and energy at a lower cost than the NUG purchase price.

In some of these cases, however, another utility or a particular customer might be interested in purchasing the available energy from the NUGs thus giving rise to the need to wheel the power over the transmission facilities of the local utility. The term "wheeling" is used to denote the transmission of electrical energy from one producer to a second party over the transmission facilities of a third party. The most common application of the wheeling technique involves the distribution of power from power

generating companies to relatively small private, municipal, or public etc. utilities which then market the power. The development of large generation facilities in recent years has also encouraged the wheeling of power; especially in the case of joint ownership of large, high capital plants by several utilities where the wheeling technique is used to transport the power produced back to the plant's owners for marketing. It therefore becomes important to examine the impact of wheeling operations on both the economic and technical performance of the systems involved in power wheeling.

Two forms of power wheeling can be identified: INTRA-SYSTEM power wheeling and INTER-SYSTEM power wheeling. Composite system reliability considerations associated with INTRA-SYSTEM power wheeling operations are discussed in this chapter.

5.2. Intra-System Power Wheeling Concepts

Intra-system power wheeling can be defined as the transmission of power from an independent power producing facility located at one point in a utility system to a second party located at another point in the same system over the transmission facilities of a third party which is usually the power utility. As noted earlier, this situation can arise when an independent power producer signs a contract to supply energy to a load point (or consumer) located some distance away from the NUG. Energy is then supplied into the utility system by the NUG and received at the load point. The intra-system power wheeling concept is illustrated in Figure 5.1 which shows a rectangular area representing the supply jurisdiction of the main power utility.

An independent power producing facility at location *A* may wish to supply a prospective customer with electrical energy at location *B* somewhere in the utility system. As there is no direct connection between *A* and *B* other than the transmission facilities of the main power utility, an agreement with the main utility is required to use its transmission facilities to transport the power from the producer at location *A* to the customer at location *B*. The required power to be wheeled from *A* will be injected into the utility's power system and passed on to the prospective customer at location *B* by the utility in accordance with the terms of the agreement or contract.

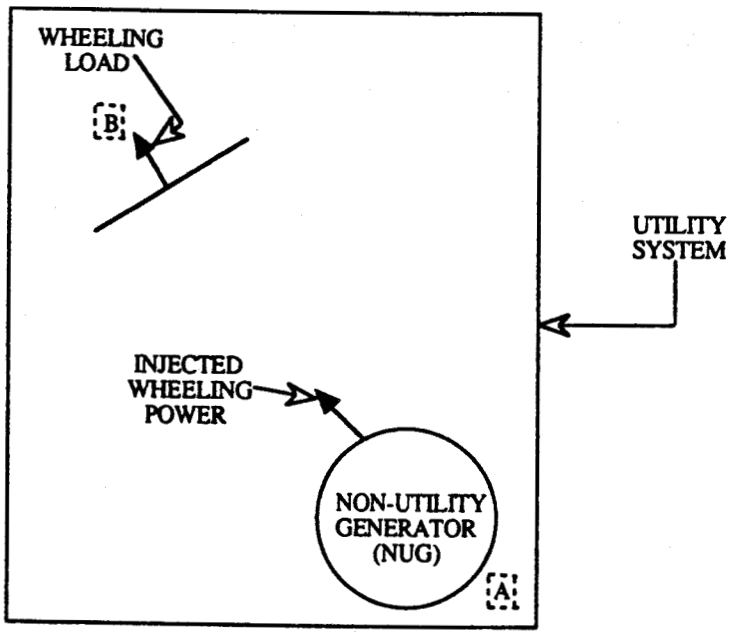

Figure 5.1: Illustration Of Intra-system Power Wheeling Concept

The involvement of a power utility in power wheeling transactions will have an impact on the utility's system losses depending upon the amount of power wheeled and the wheeling distance involved. These factors currently form the basis for determining the service charges associated with power wheeling. The reliability impacts of power wheeling, however, must be quantified before they can provide any meaningful input to the determination of the service charges for power wheeling. This chapter presents composite system adequacy analyses performed to provide some insight into the quantification of the reliability impacts of intra-system power wheeling.

5.3. Modelling Considerations for Intra-system Power Wheeling

The modelling techniques used to represent intra-system power wheeling situations have been developed to suit the structure of the COMREL program which was used for the wheeling analyses. Highlights of the modelling procedure used are as follows.

5.3.1. Wheeling Source and Power

The power to be wheeled is assumed to originate from an independent power producing facility located at a load point in the main utility's power system. This point is designated as the "wheeling source". When a PQ-bus is selected to serve as a wheeling source, its characteristics are redefined as a PV-bus with scheduled power generation appropriately assigned .

The power to be wheeled is designated as the "wheeling power" and is modelled as a 100% available single non-utility generator (NUG) with a capacity rating equivalent to the amount of wheeling power involved. The scheduled power generation associated with the NUG is assumed to be equal to the rated capacity of the unit.

5.3.2. Wheeling Sink and Load

The load point scheduled to receive the wheeling power is designated as the "wheeling sink" and is located somewhere in the utility system. The load to be supplied is also designated as the "wheeling load". The introduction of wheeling power of a certain capacity at the wheeling source is matched simultaneously with an equivalent increase in load at the designated wheeling sink. The incremental component of load at the wheeling sink represents the wheeling load and is regarded as firm load. This therefore leads to a reduction in the proportion of curtailable load at that load point. The COMREL program is structured to accept a specification of the percentage of curtailable load at every system load point as input data. When an outage event requires load curtailment as the ultimate remedial action, curtailable load is interrupted first followed by firm load, if necessary. Firm loads are therefore also interruptible, but only as a last resort to alleviate persistent outage events. This feature of the COMREL program allows the analyst to provide appropriate signals that indicate an increase in the firm component of load at a specific load point which is expected to be serviced by a dedicated wheeling power supply. The wheeling load is considered to be external to the utility system demand, and therefore the wheeling component of load at the wheeling sink is not utilised when computing the system peak load.

5.3.3. Load Model and System Analysis

Annual indices were calculated using the 4-step and 7-step load models described in Chapter 3. The 4-step load model was used for the RBTS and the 7-step load model for the IEEE-RTS. The wheeling load is, however, assumed to be constant at all load levels and its dedicated supply is considered to be continuously available in the same amount throughout the study period.

DC load flow analysis was used as the network solution technique during the power wheeling studies in order to avoid the problem of accounting for system losses arising from the power wheeling operations. There is currently no general agreement regarding how these losses should be handled. The procedures and other assumptions, such as relating to contingency selection etc., used in running the COMREL program in these studies are the same as those used in Chapter 3 to obtain the base case results.

5.4. Discussion of Results

Study results showing the impact of intra-system power wheeling on the composite system indices of the RBTS and the IEEE-RTS are illustrated and presented in this section. The impact of wheeling to and from different parts of the test systems are examined. The load point indices considered in the discussion are the failure probability, failure frequency, Expected Load Curtailed (ELC) and the Expected Energy Not Supplied (EENS) indices. The overall system indices considered are the Bulk Power Interruption Index (BPII) and the Severity Index (SI).

5.4.1. Results for the RBTS

5.4.1.1. Load Point Indices

Figures 5.2-5.13 show the impact on the indices at the load points of the RBTS when up to 50 MW of power is wheeled from one part of the RBTS to supply wheeling loads at specific locations in the system. The results shown in Figures 5.2-5.5 indicate the variation in the failure probability, failure frequency, ELC and the EENS at the five load points when wheeling is done from different locations to supply wheeling loads at bus 2 in the northern section of the RBTS. It can be observed that the indices for most of the

RBTS load points remained virtually unaffected throughout the power wheeling scenario in most of the cases studied. This shows that the RBTS is able to accommodate the range of wheeling power considered without causing any significant adverse impacts on adequacy at the load points. Wheeling from the south to the north of the RBTS generally assures a more effective re-distribution of power flow in the RBTS network. This accounts for the system's ability to cope with the entire range of wheeling power capacity examined. Approximately 90% of the RBTS load is located in the southern section of the system. Wheeling power imports in the south can therefore be used effectively to supply the loads in that part of the system with minimum transmission requirements. This reduces, to some extent, the region's dependence on conventional generation supplies which have to be transported from the north (from buses 1 and 2) to the south over transmission facilities which are exposed to the risk of failure. Meanwhile the wheeling load located in the north region is also supplied effectively from the conventional generation sources in that region. Wheeling from bus 6 produces significant drops in the value of the indices at that load point, because the wheeling supply made available at the bus is used to supplement utility supply both during normal system operation and when the load point is isolated from the conventional generation sources.

Supplying a wheeling load located at bus 2 from additional generation supplies provided at the swing bus (bus 1) leads to a deterioration in adequacy at bus 3 where about 46% of the RBTS load is located. This effect becomes most significant when the wheeling load introduced exceeds 35 MW, at which stage the increase in the number of swing bus overload conditions causes a considerable increase in both the number of load curtailment events and the amount of load curtailed at bus 3. This system condition occurs whenever at least one of the lines connecting bus 3 to the swing bus is on outage in combination with generating unit outages and/or outage of any other transmission line connecting the two generation buses in the north to the heavily loaded southern section of the RBTS.

Similar observations can be made from Figures 5.6-5.9 and Figures 5.10-5.13 which show the impacts on the load point indices when intra-system power wheeling operations are carried out to supply wheeling loads located at buses 3 and 5 of the RBTS

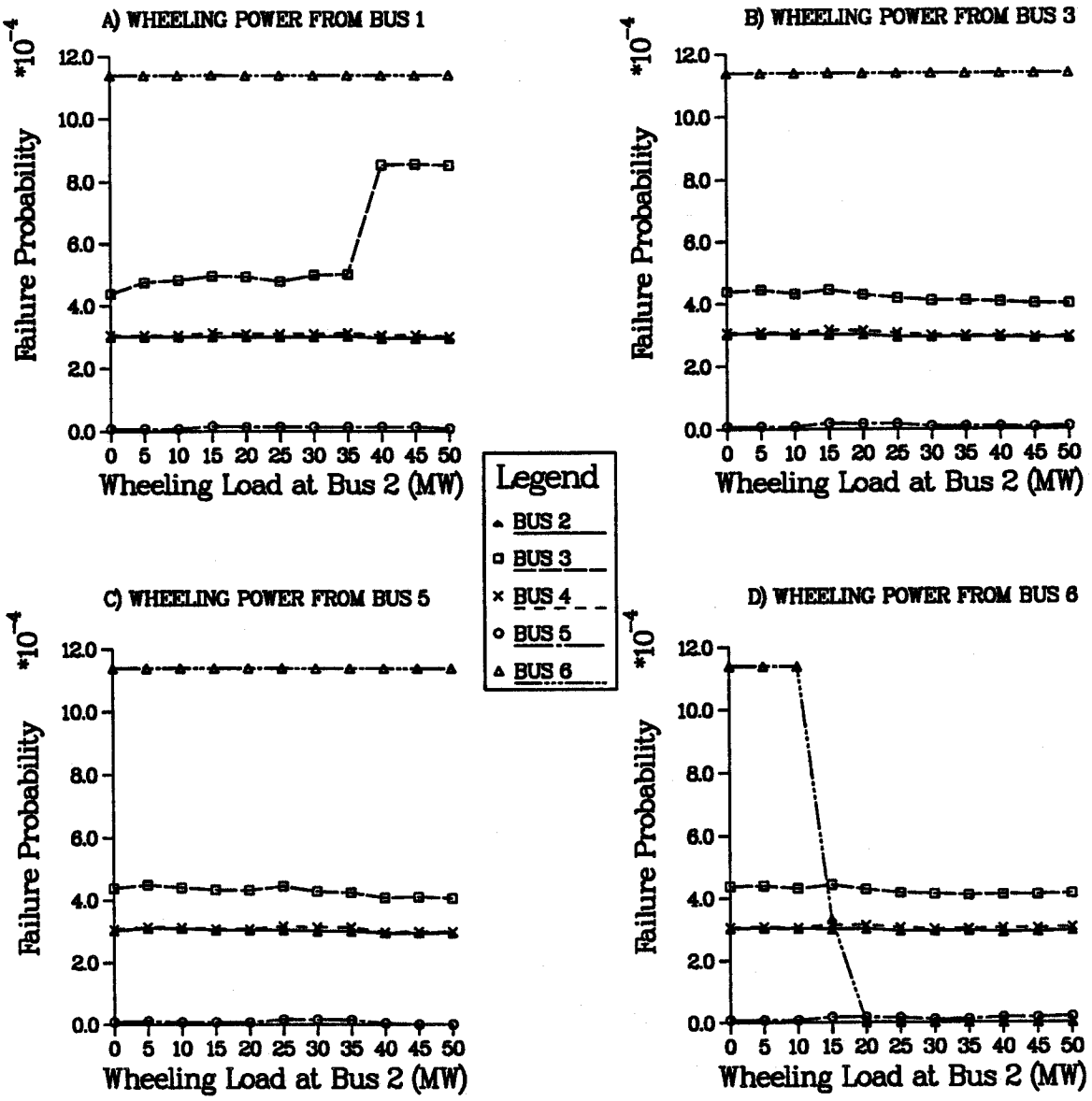

Figure 5.2: Variation In Load Point Failure Probability With Intra-system Wheeling Power To Supply Wheeling Load At Bus 2 Of The RBTS

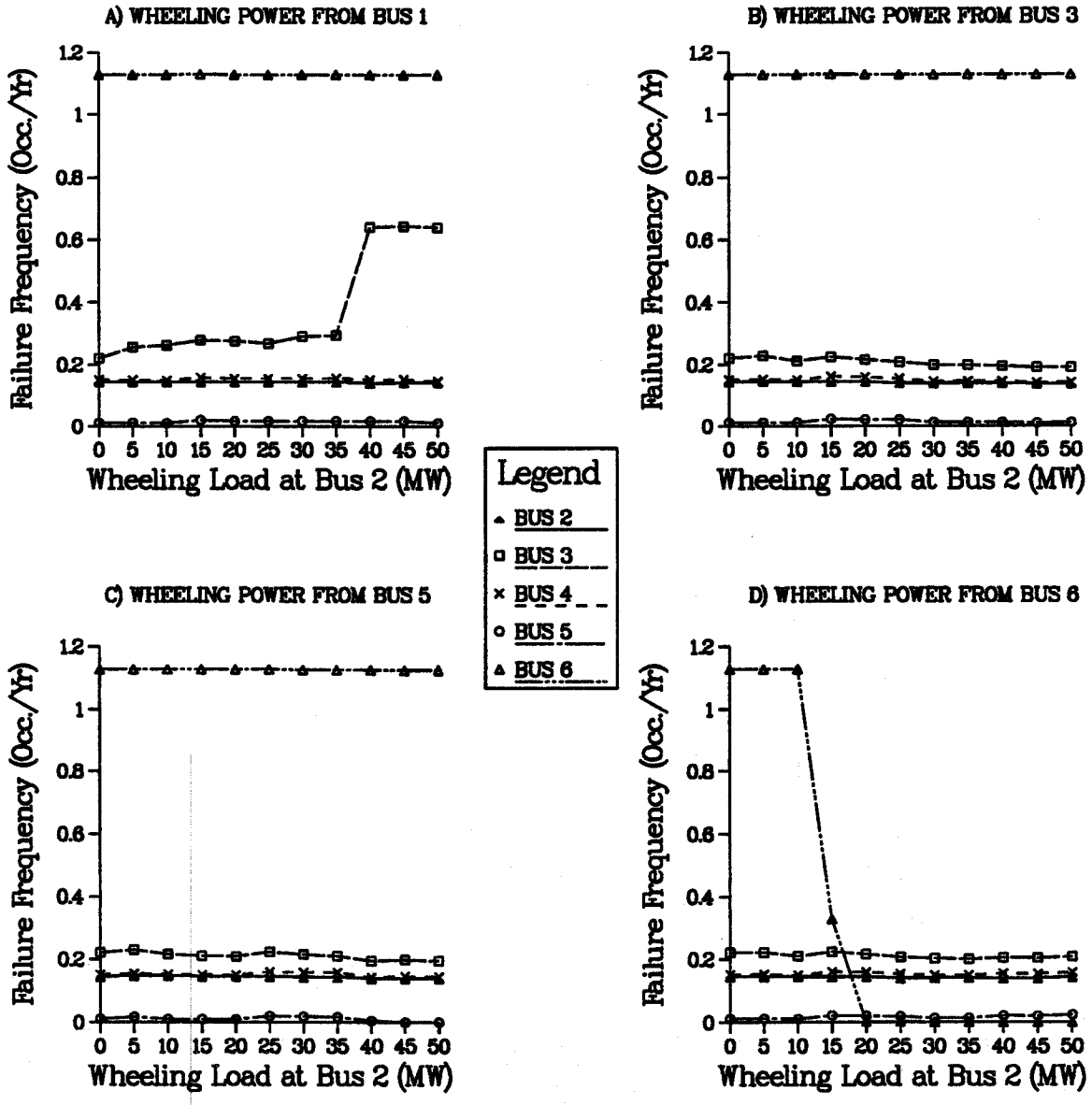

Figure 5.3: Variation In Load Point Failure Frequency With Intra-system Wheeling Power To Supply Wheeling Load At Bus 2 Of The RBTS

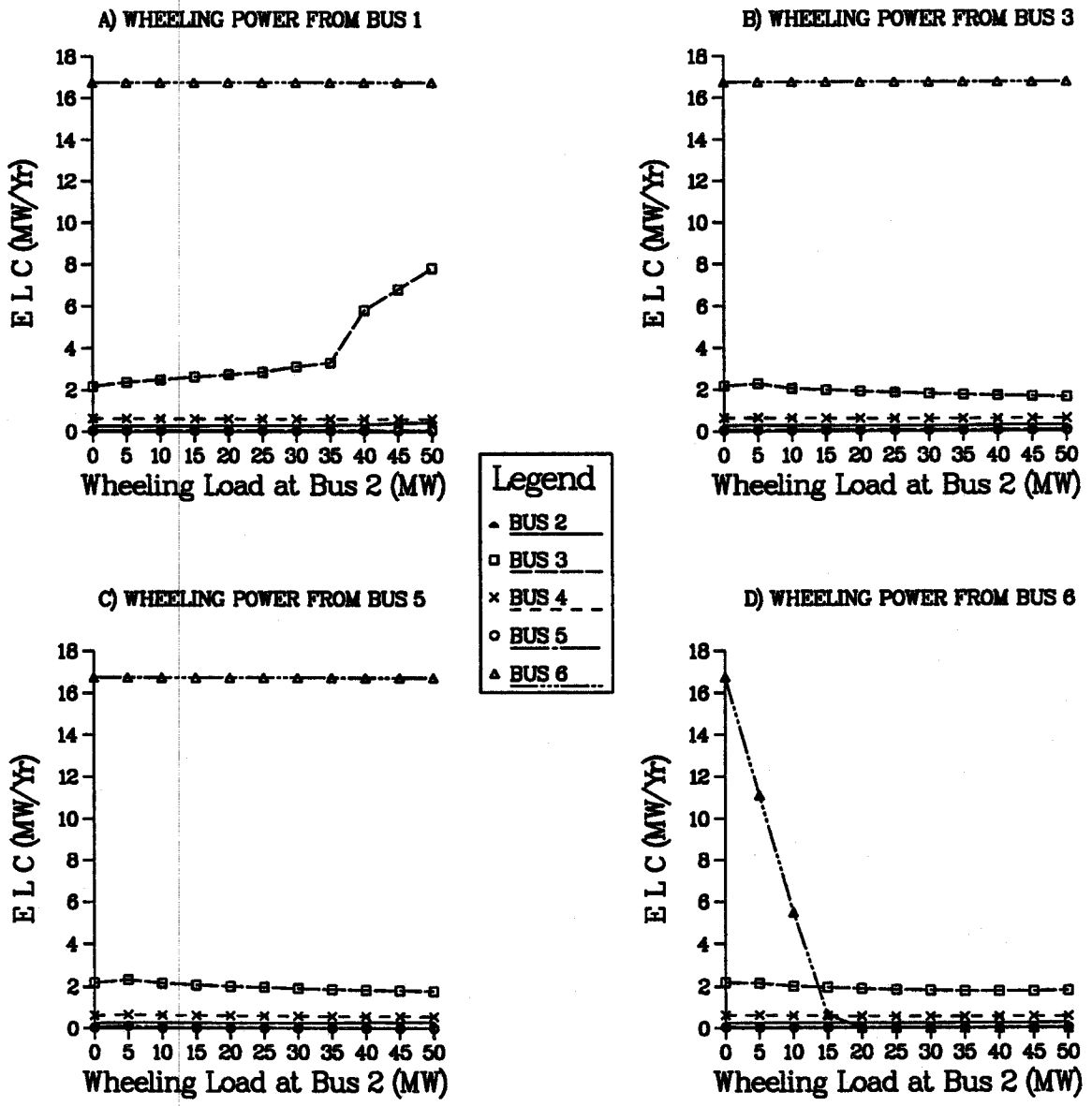

Figure 5.4: Variation In ELC At The Load Points With Intra-system Wheeling Power To Supply Wheeling Load At Bus 2 Of The RBTS

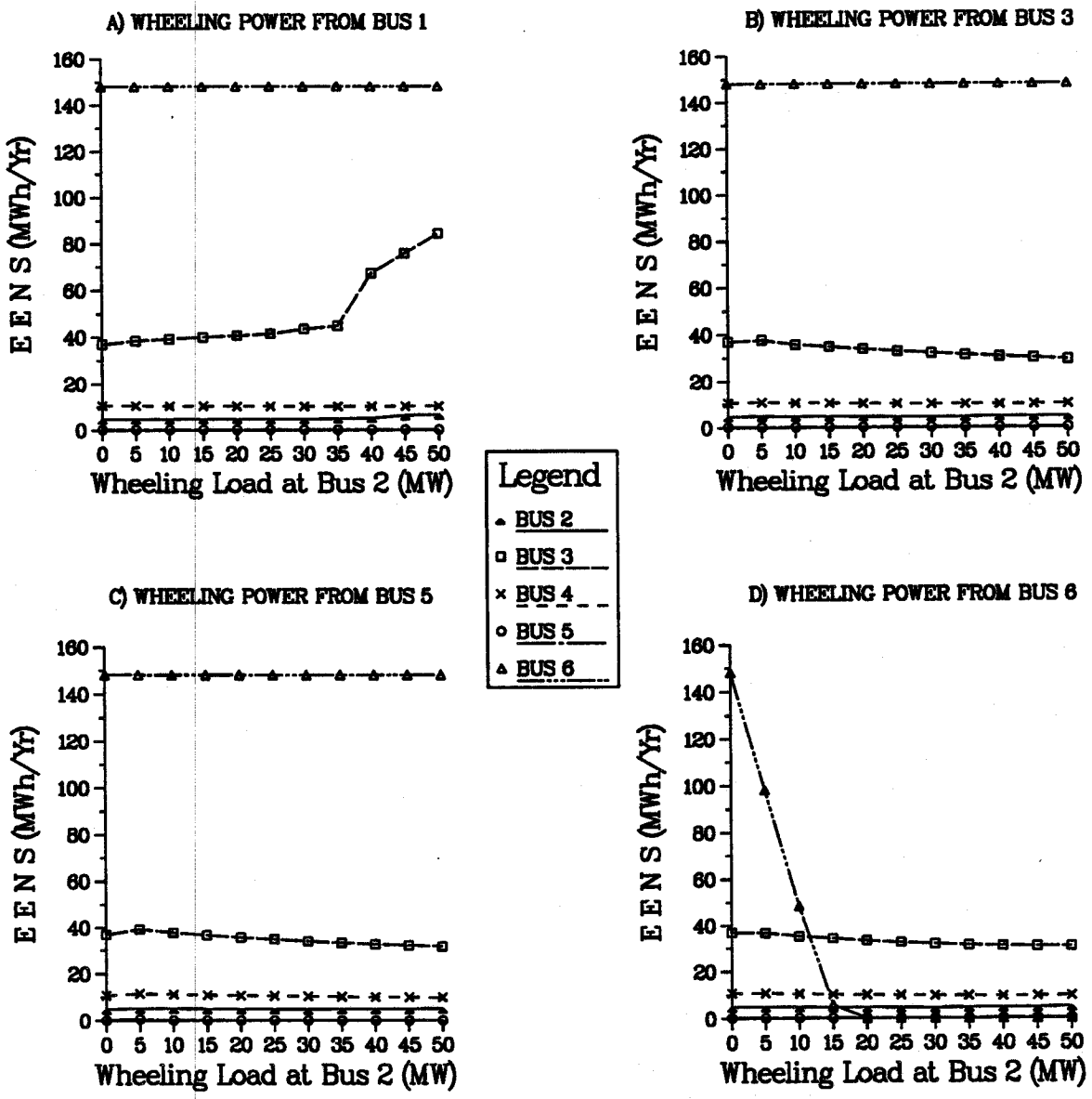

Figure 5.5: Variation In EENS At The Load Points With Intra-system Wheeling Power To Supply Wheeling Load At Bus 2 Of The RBTS

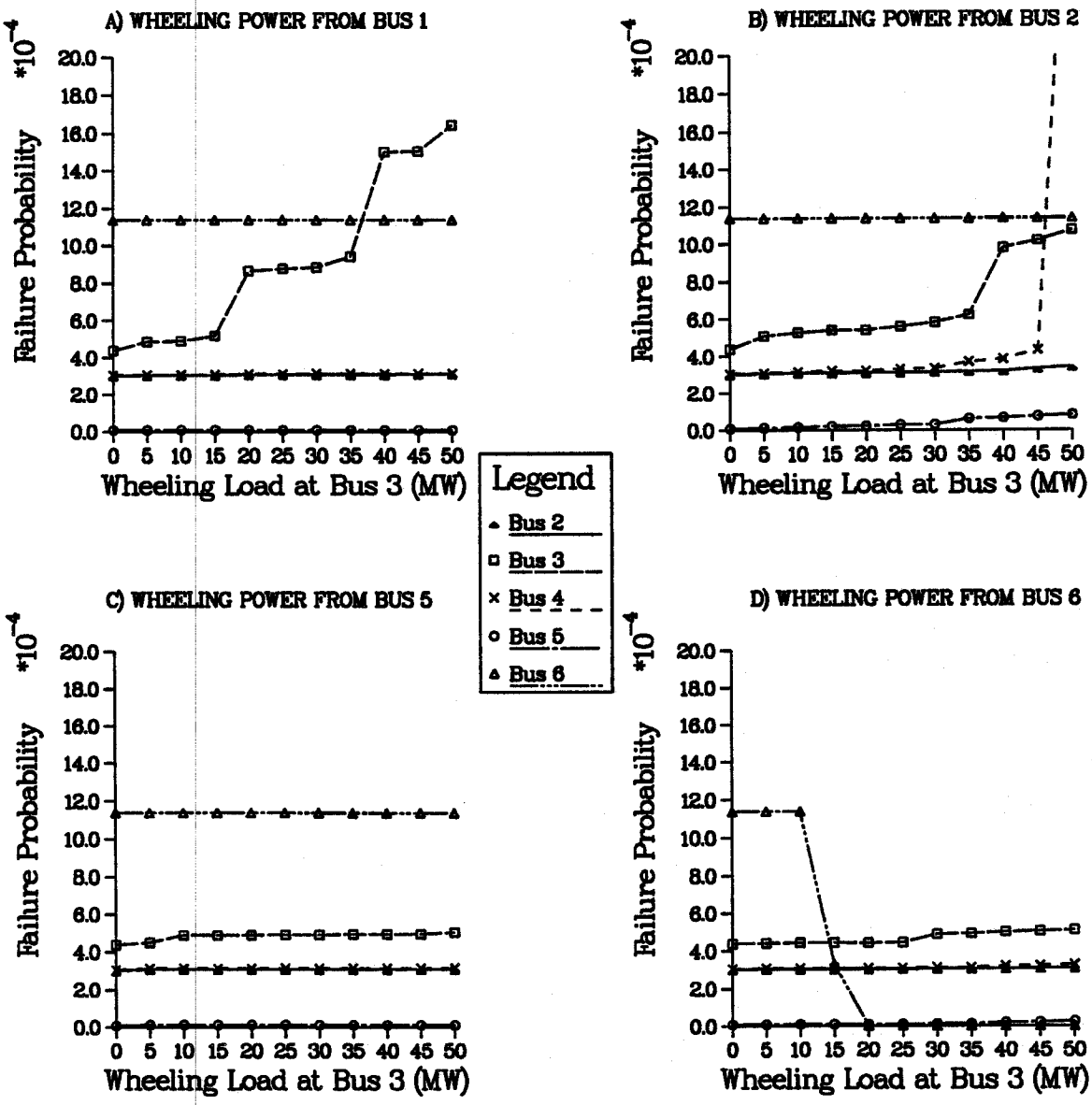

Figure 5.6: Variation In Load Point Failure Probability With Intra-system Wheeling Power To Supply Wheeling Load At Bus 3 Of The RBTS

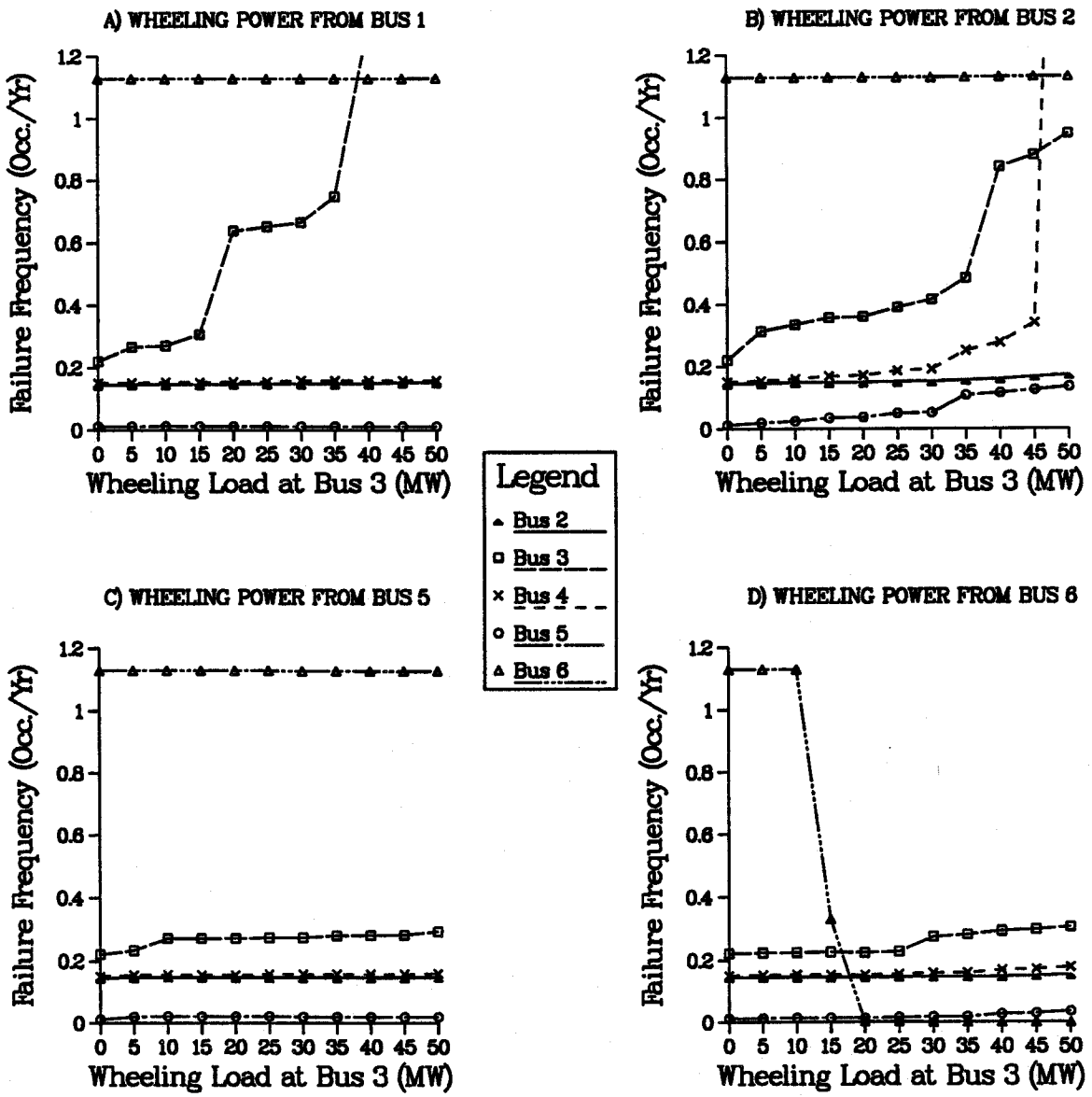

Figure 5.7: Variation In Load Point Failure Frequency With Intra-system Wheeling Power To Supply Wheeling Load At Bus 3 Of The RBTS

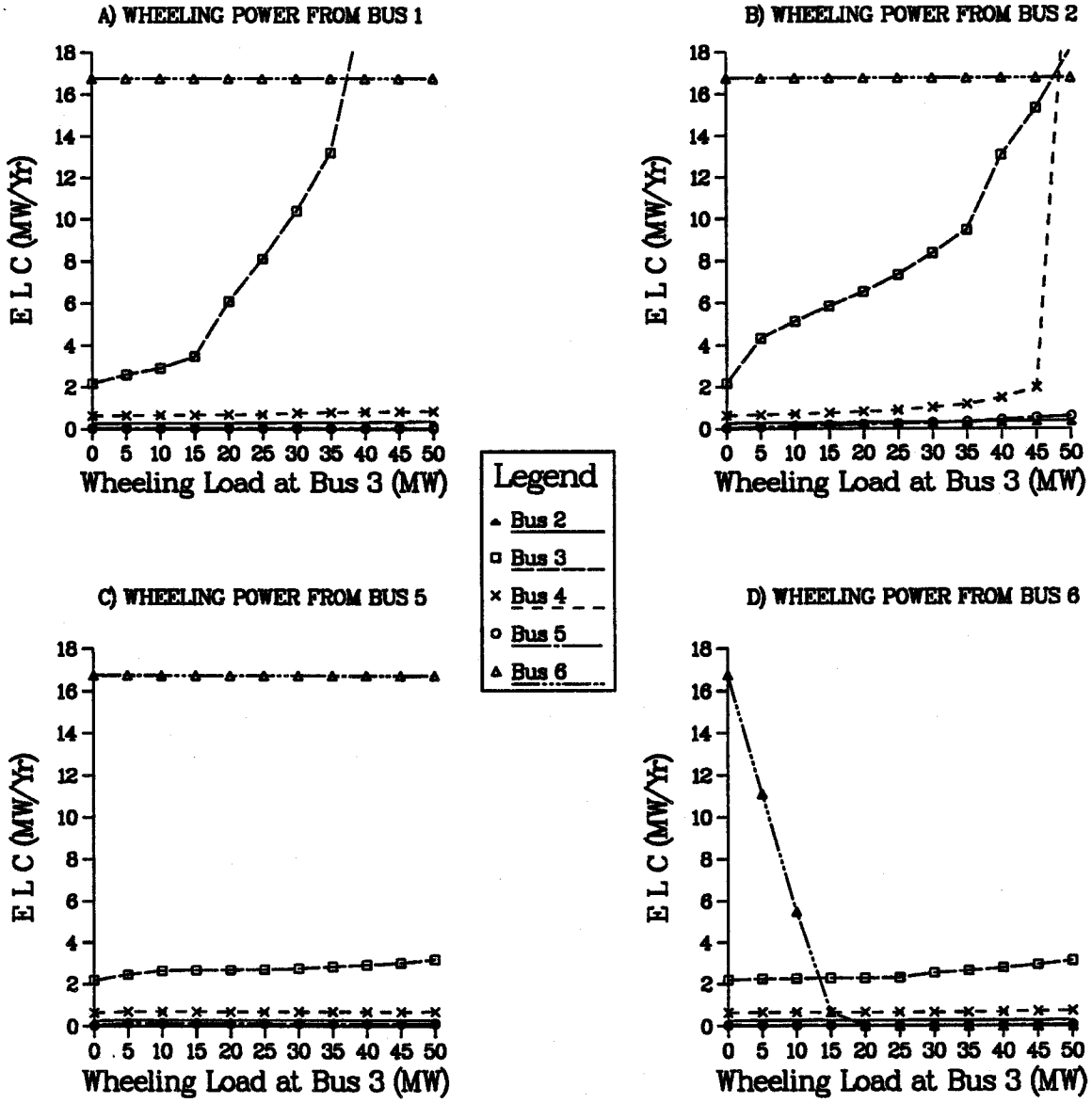

Figure 5.8: Variation In ELC At The Load Points With Intra-system Wheeling Power To Supply Wheeling Load At Bus 3 Of The RBTS

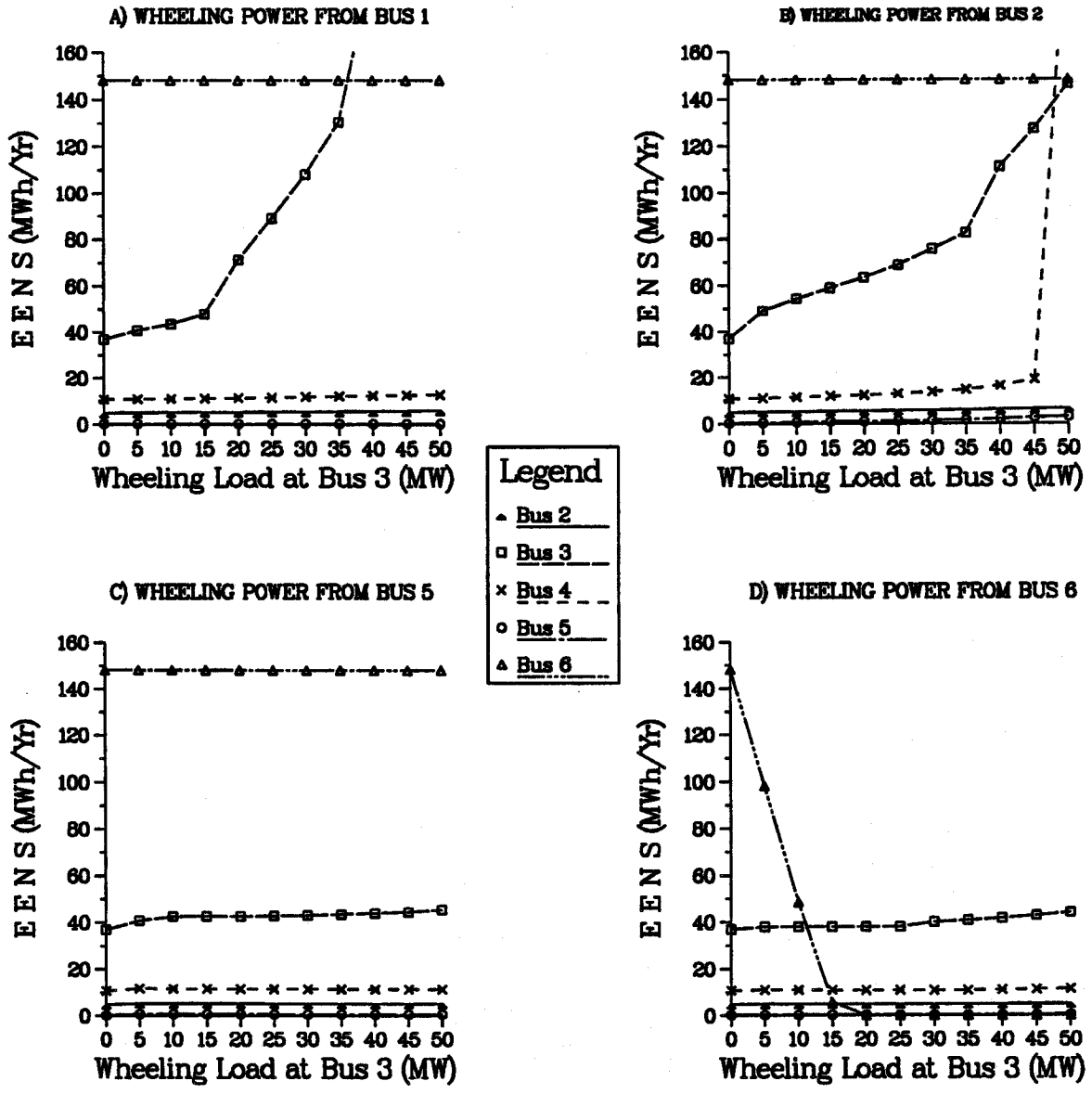

Figure 5.9: Variation In EENS At The Load Points With Intra-system Wheeling Power To Supply Wheeling Load At Bus 3 Of The RBTS

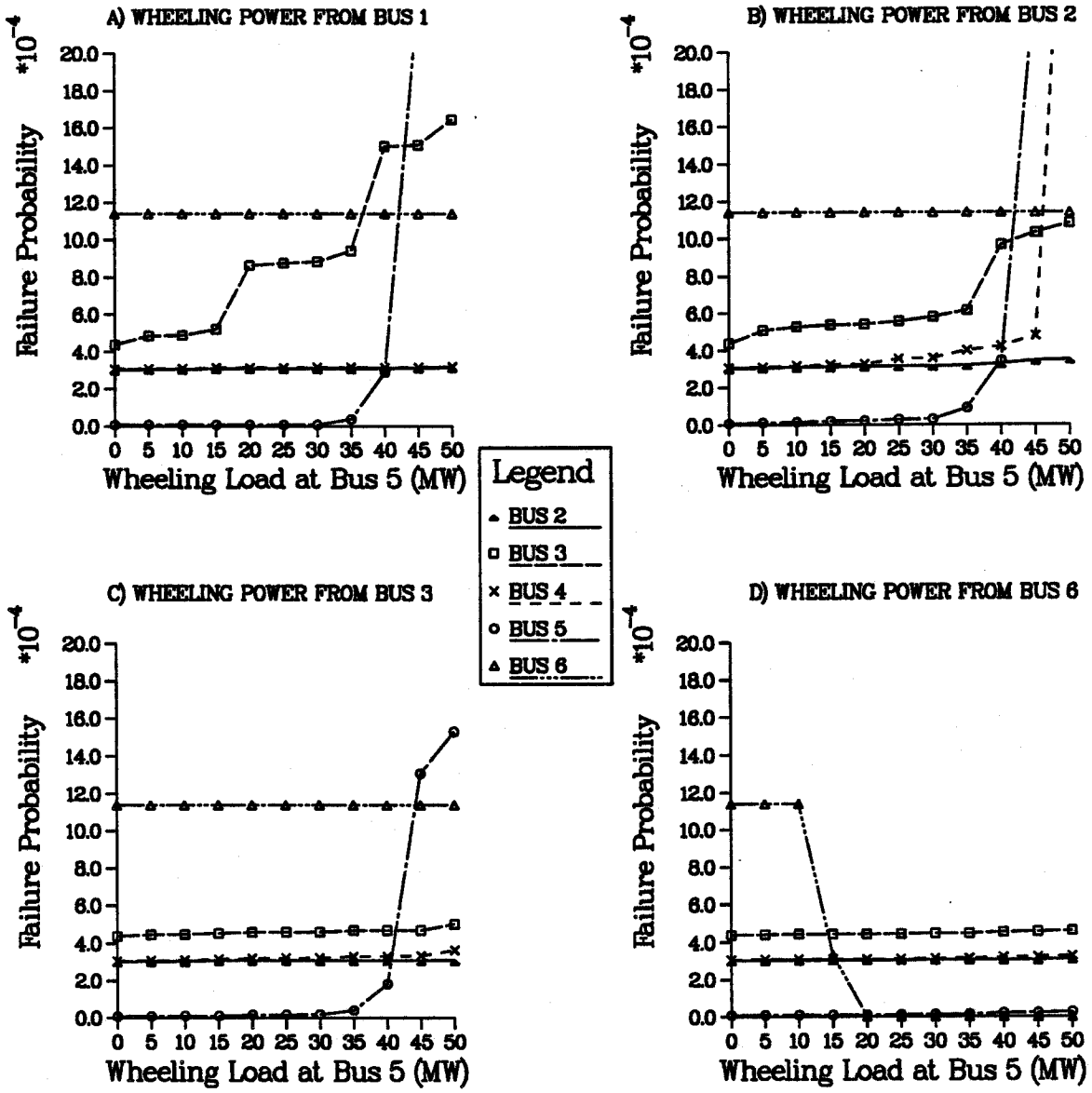

Figure 5.10: Variation In Load Point Failure Probability With Intra-system Wheeling Power To Supply Wheeling Load At Bus 5 Of The RBTS

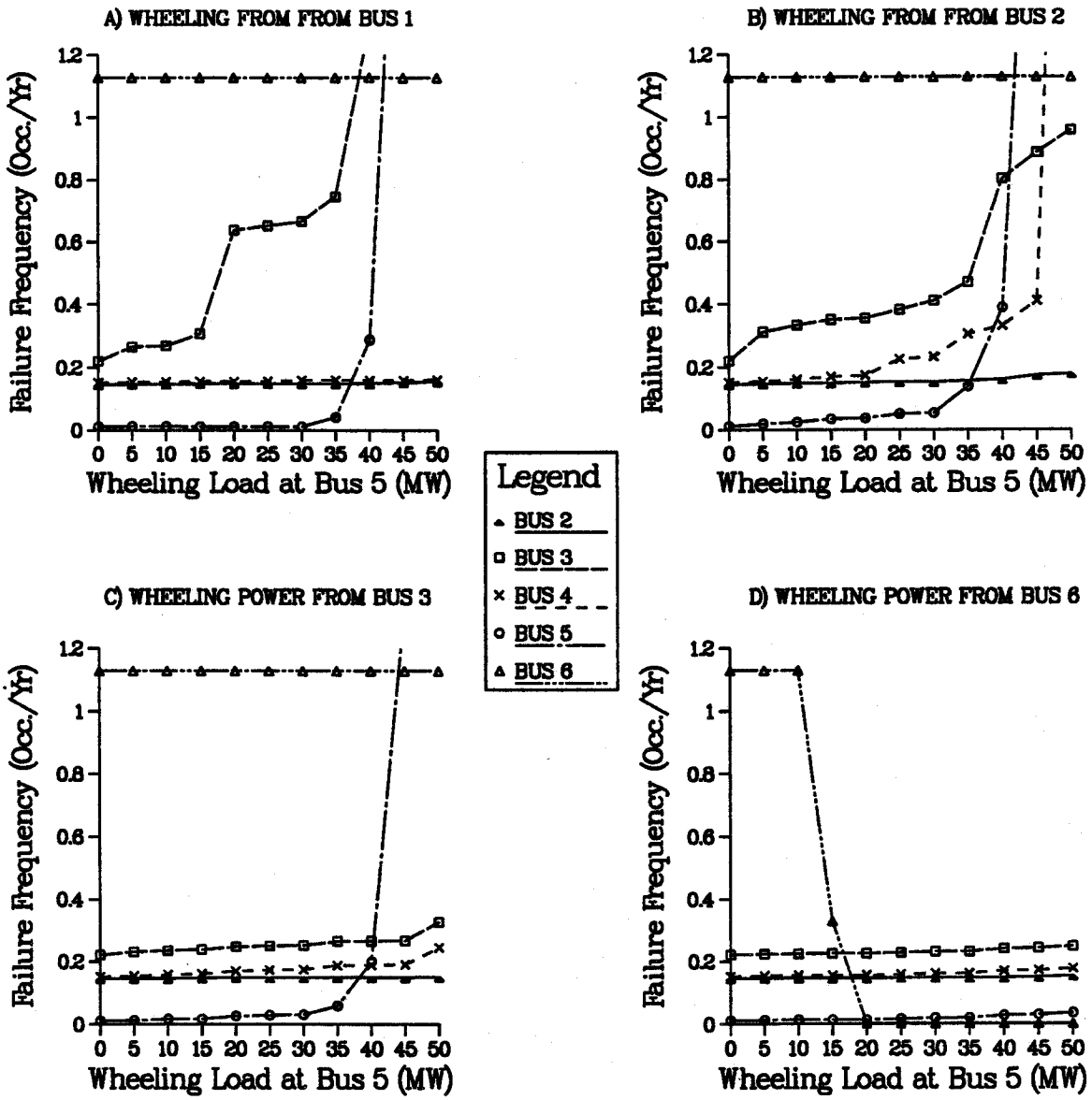

Figure 5.11: Variation In Load Point Failure Frequency With Intra-system Wheeling Power To Supply Wheeling Load At Bus 5 Of The RBTS

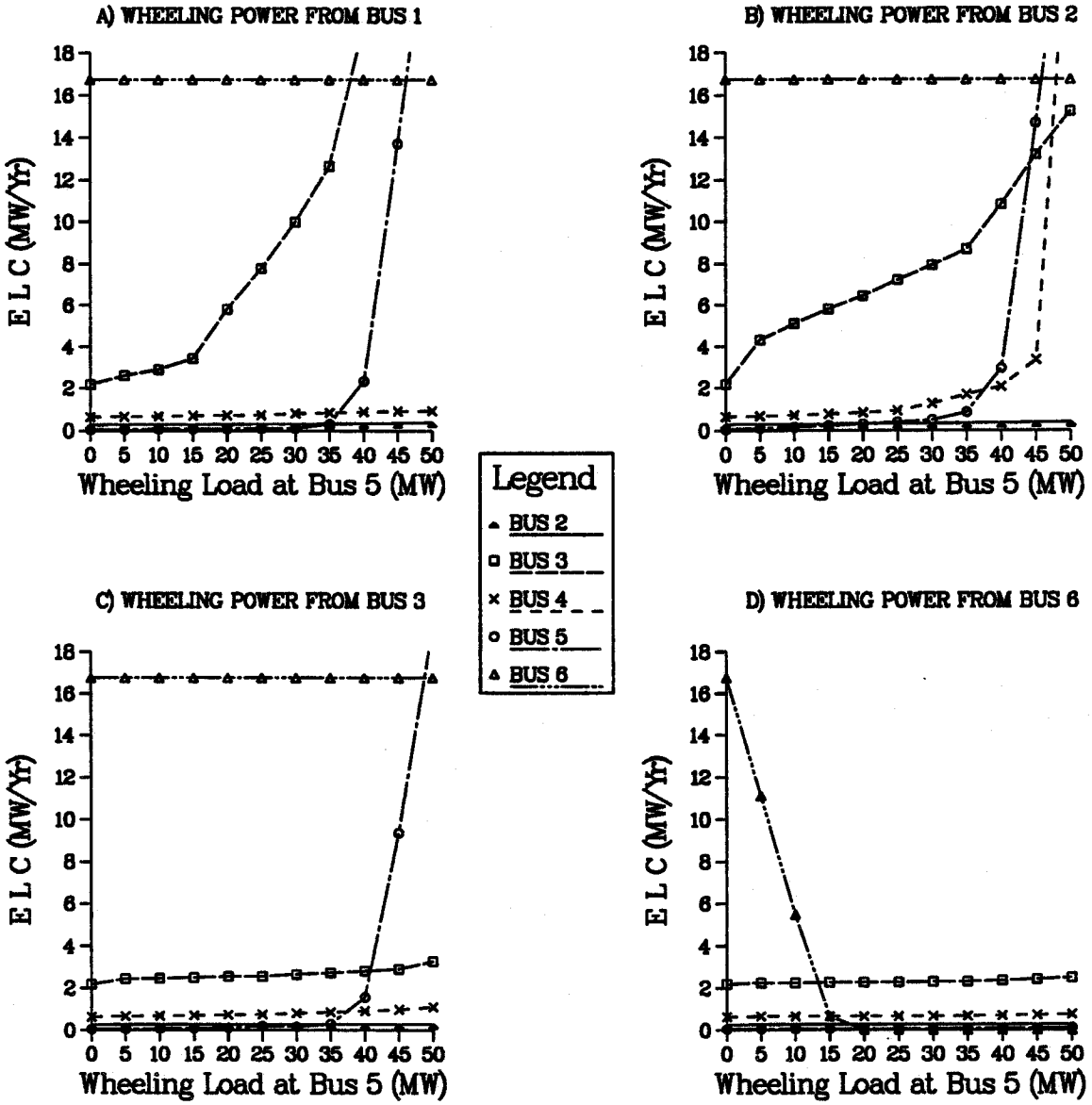

Figure 5.12: Variation In ELC At The Load Points With Intra-system Wheeling Power To Supply Wheeling Load At Bus 5 Of The RBTS

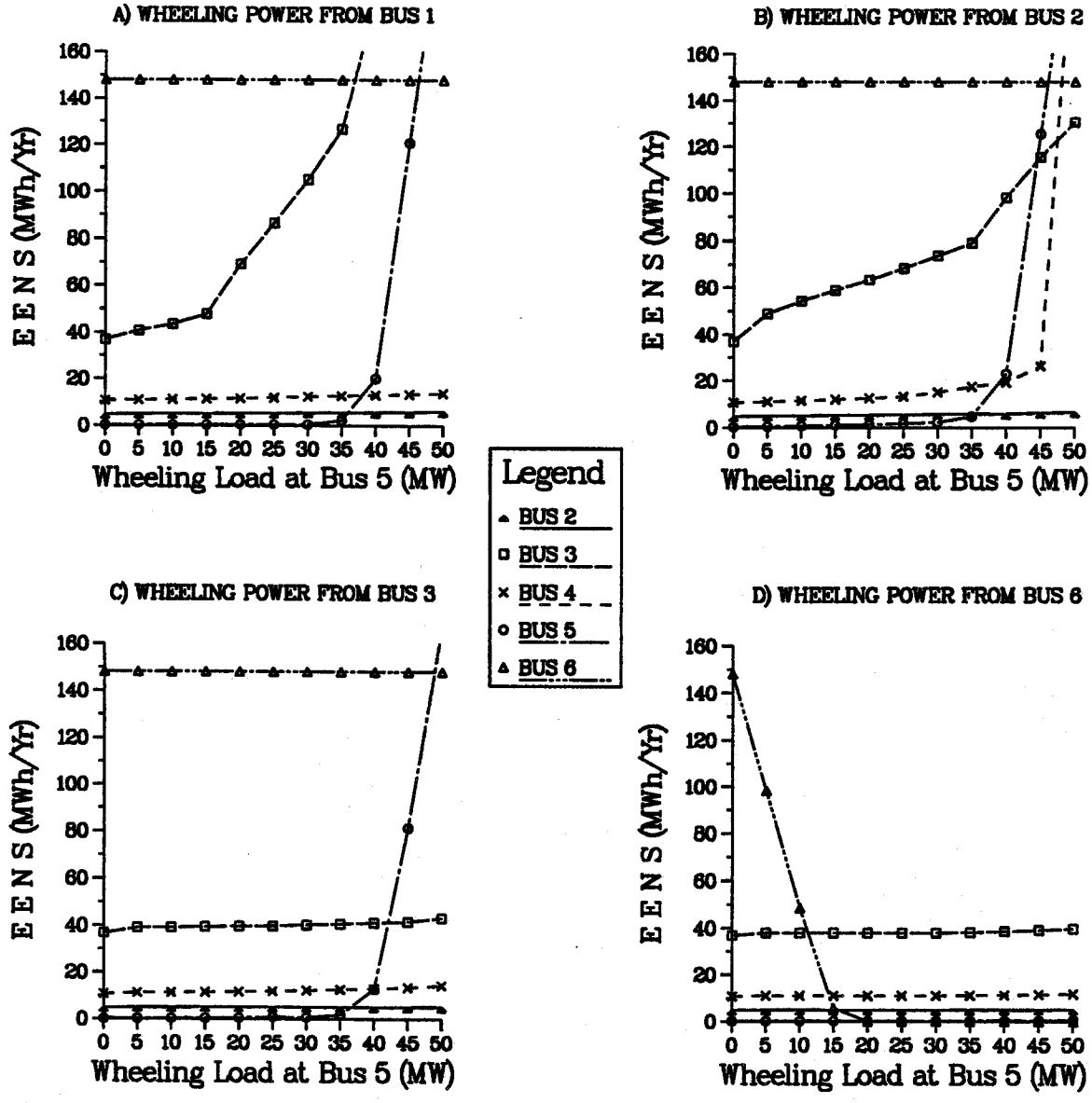

Figure 5.13: Variation In EENS At The Load Points With Intra-system Wheeling Power To Supply Wheeling Load At Bus 5 Of The RBTS

respectively. The impact on the indices when the wheeling operations involve only buses within the heavily loaded section of the RBTS are relatively minimal compared to when the wheeling loads are supplied directly from the conventional generation supply locations in the north. For example, from Figures 5.6-5.13, wheeling from bus 2 to supply wheeling loads at either bus 3 or bus 5 adversely affects bus 3 from the onset of wheeling and this effect spreads to buses 4 and 5 as the wheeling power (or load) increases. Supplying the wheeling load at these locations from the swing bus produces even worse impacts on adequacy at the load points. It can therefore be concluded that wheeling from the north section of the RBTS is generally not suitable, because the available transmission capacity is inadequate to effectively transport the increased supply requirements of the south region (created by the added wheeling load) from the generating facilities in the north. As the wheeling distance increases there is also an increase in the number of transmission facilities whose capacity limitations can obstruct power wheeling operations and this causes the adverse impacts of the wheeling operations to spread out affecting a larger number of load points in the system.

In all the cases considered, the load point indices at bus 6 remained virtually unaffected throughout the entire wheeling scenario except when the wheeling power is from that bus. This is expected because wheeling operations beyond the radial link do not address the isolation problems basically responsible for inadequacy at the bus.

5.4.1.2. System Indices

Figures 5.14 and 5.15 respectively show the variation in the Bulk Power Interruption Index (BPII) and the system Severity Index (SI) when up to 50 MW of power is wheeled from different locations to supply wheeling loads located at buses 2, 3 and 5 of the RBTS.

It can be observed from the figures that wheeling to and from different parts of the RBTS produced different and varying degrees of impact on the overall system indices. Figures 5.14 and 5.15 show a consistent drop in the value of the system indices when wheeling is done from most parts of the test system to supply wheeling loads at bus 2. This indicates an improvement in the overall system adequacy compared to the level of system adequacy that existed prior to the start of the wheeling operations.

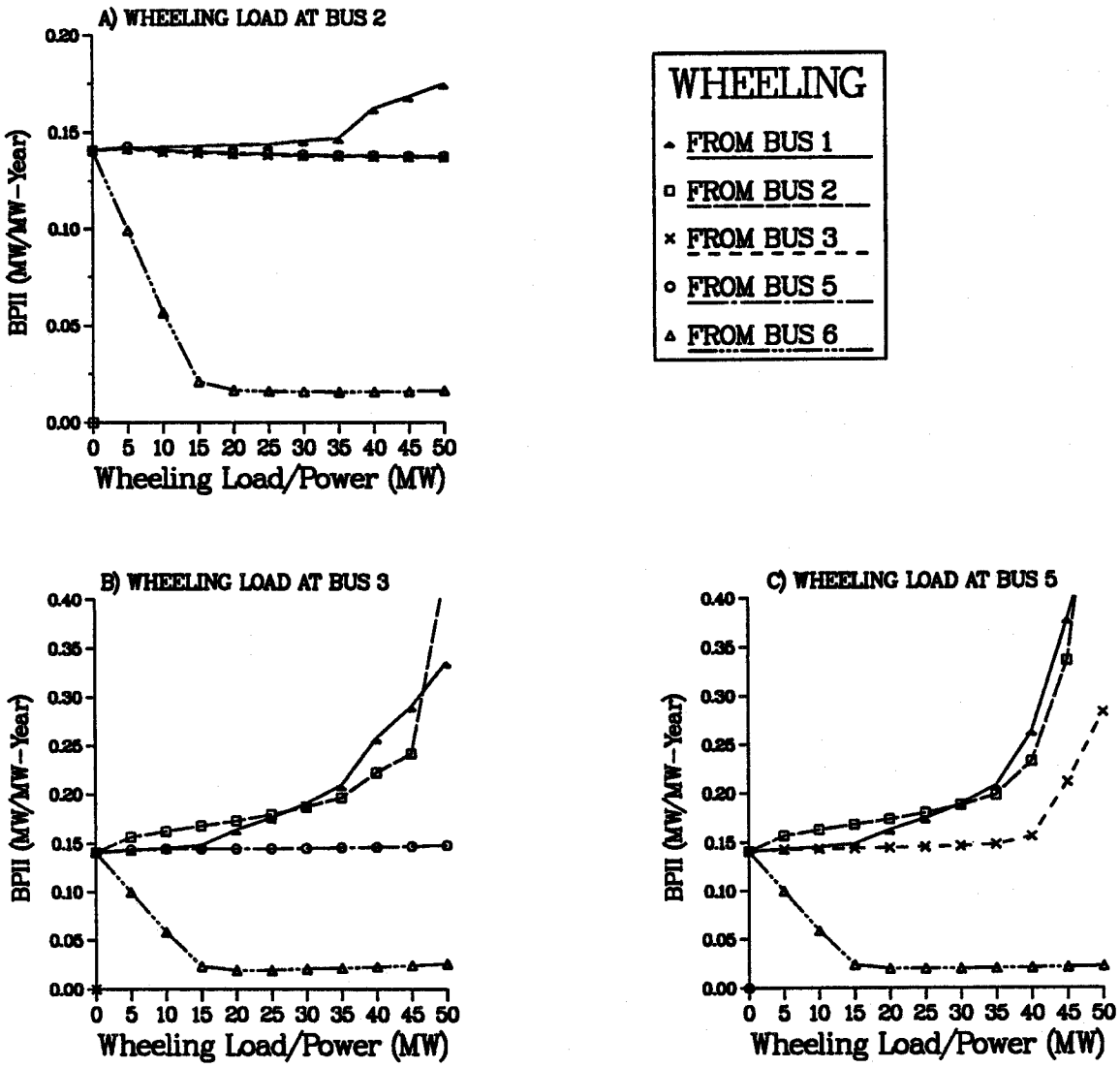

Figure 5.14: Variation In BPII With Intra-system Wheeling Power To Supply Wheeling Load At Buses 2,3 And 5 Of The RBTS Respectively

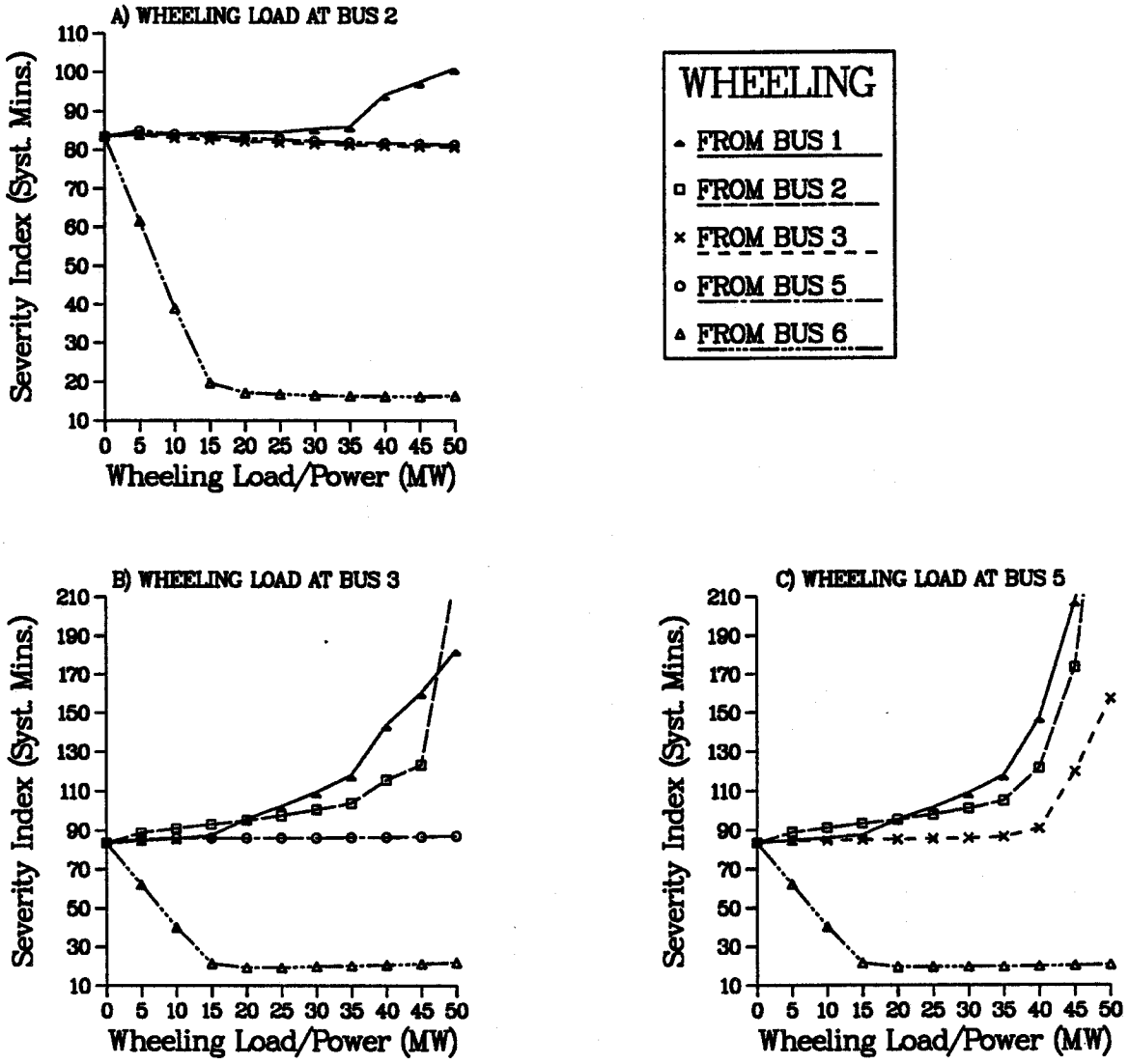

Figure 5.15: Variation In Severity Index With Intra-system Wheeling Power To Supply Wheeling Load At Buses 2,3 And 5 Of The RBTS Respectively

On the other hand, wheeling to buses 3 and 5 produced mixed impacts on system adequacy over the same range of wheeling power, as shown in Figures 5.14 and 5.15. The most significant improvement in overall system adequacy is obtained when power is wheeled from bus 6. This is expected because when wheeling supplies are made available at bus 6, the isolation problems experienced at the bus no longer lead to load curtailment at that load point as the wheeling supplies can be used to supply the bus loads. Wheeling from the north (predominant generation locations) towards the southern section (predominant load centres) of the RBTS produced the least desirable impacts on the overall system indices. This condition, as noted earlier, is due to capacity limitation problems faced by the lines responsible for bulk power movement from the north to the south as they are unable to effectively accommodate the entire range of wheeling power imposed on the RBTS.

5.4.2. Results for the IEEE-RTS

The impact on load point and overall system indices of wheeling up to 100 MW of power from one part of the IEEE-RTS to supply a wheeling load located at another part of the system are presented and illustrated in this section. The IEEE-RTS has ten of its load points (buses 1-10) interconnected in the 138 KV network (South region) in addition to seven other load points in the 230 KV network (North region). The results for the load points in the two regions of the IEEE-RTS are presented separately for each wheeling operation examined. The wheeling operations considered in the studies include wheeling within each region separately and wheeling across the north-south boundary in both directions.

5.4.2.1. Load Point Indices

Figures 5.16-5.19 show the impact of wheeling operations involving buses 3 and 8 (located in the south region) on the Failure Probability, Failure Frequency, ELC and EENS indices respectively at the various load points of the IEEE-RTS. The impact of similar wheeling operations involving buses 13 and 18 (in the north region) on the IEEE-RTS load point indices are also shown in Figures 5.20-5.23.

Comparing the two sets of results, it can be seen that the impact of the wheeling

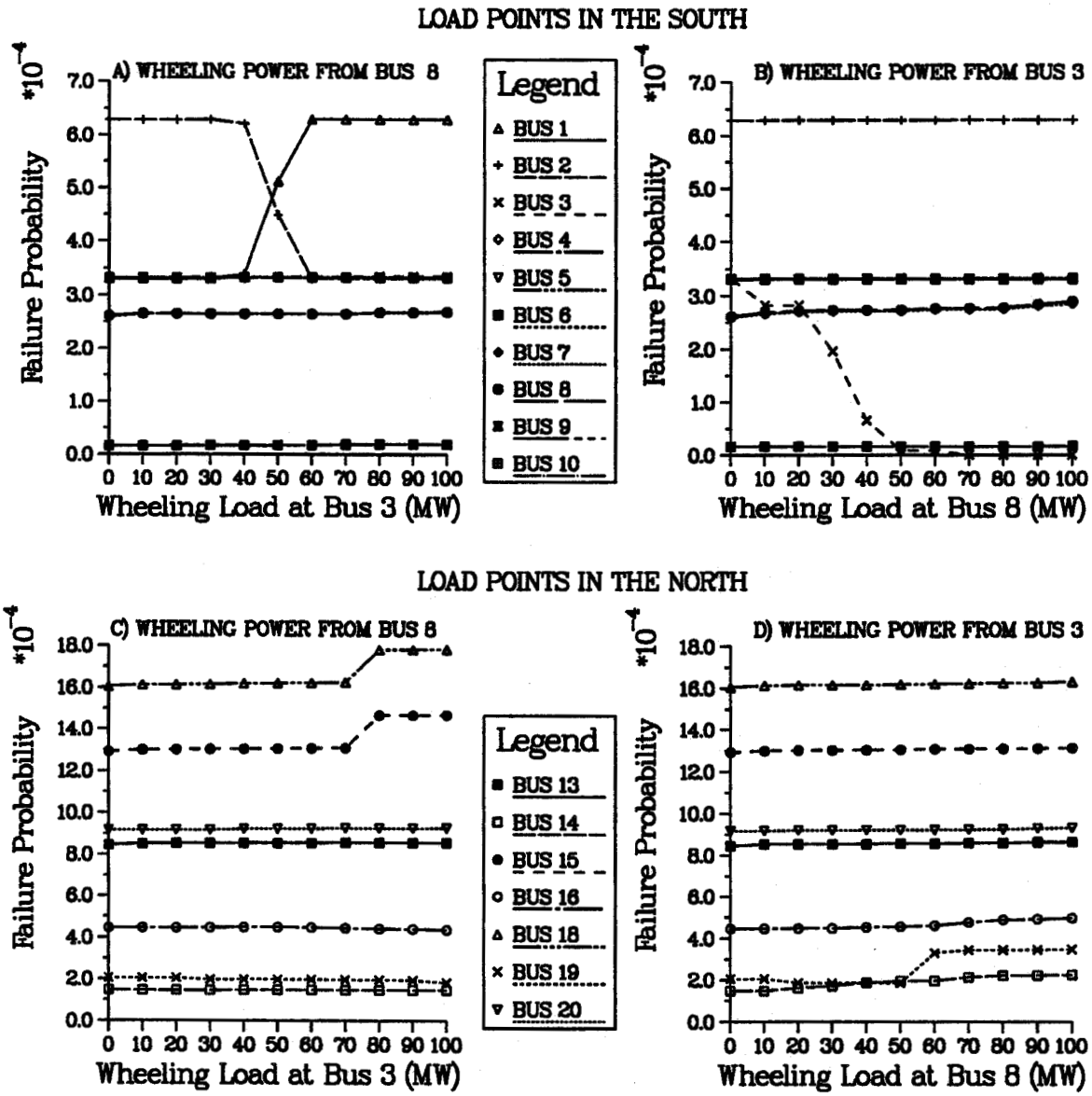

Figure 5.16: Variation In Load Point Failure Probability With Intra-system Wheeling Power Within The South Region Of The IEEE-RTS

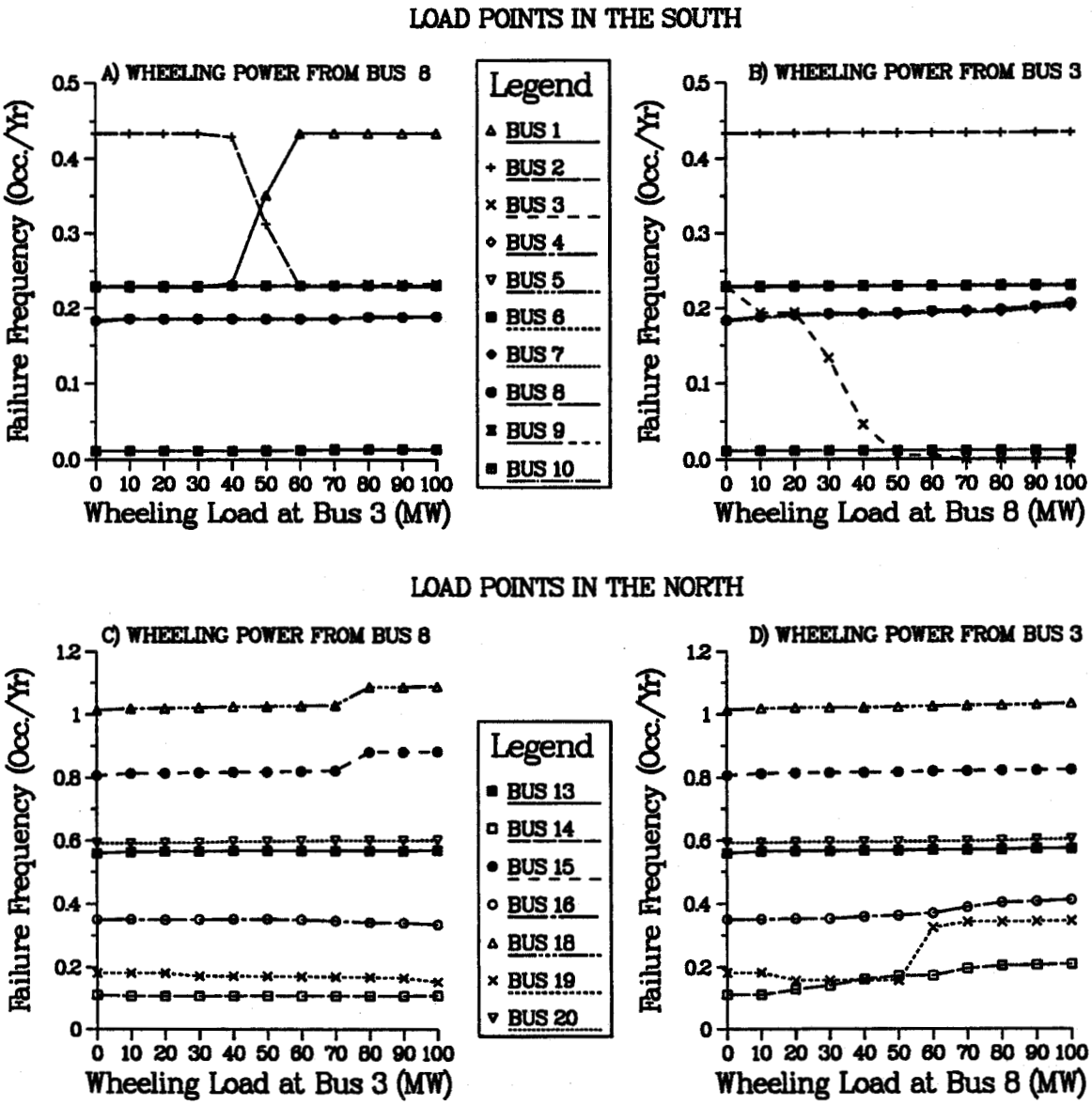

Figure 5.17: Variation In Load Point Failure Frequency With Intra-system Wheeling Power Within The South Region Of The IEEE-RTS

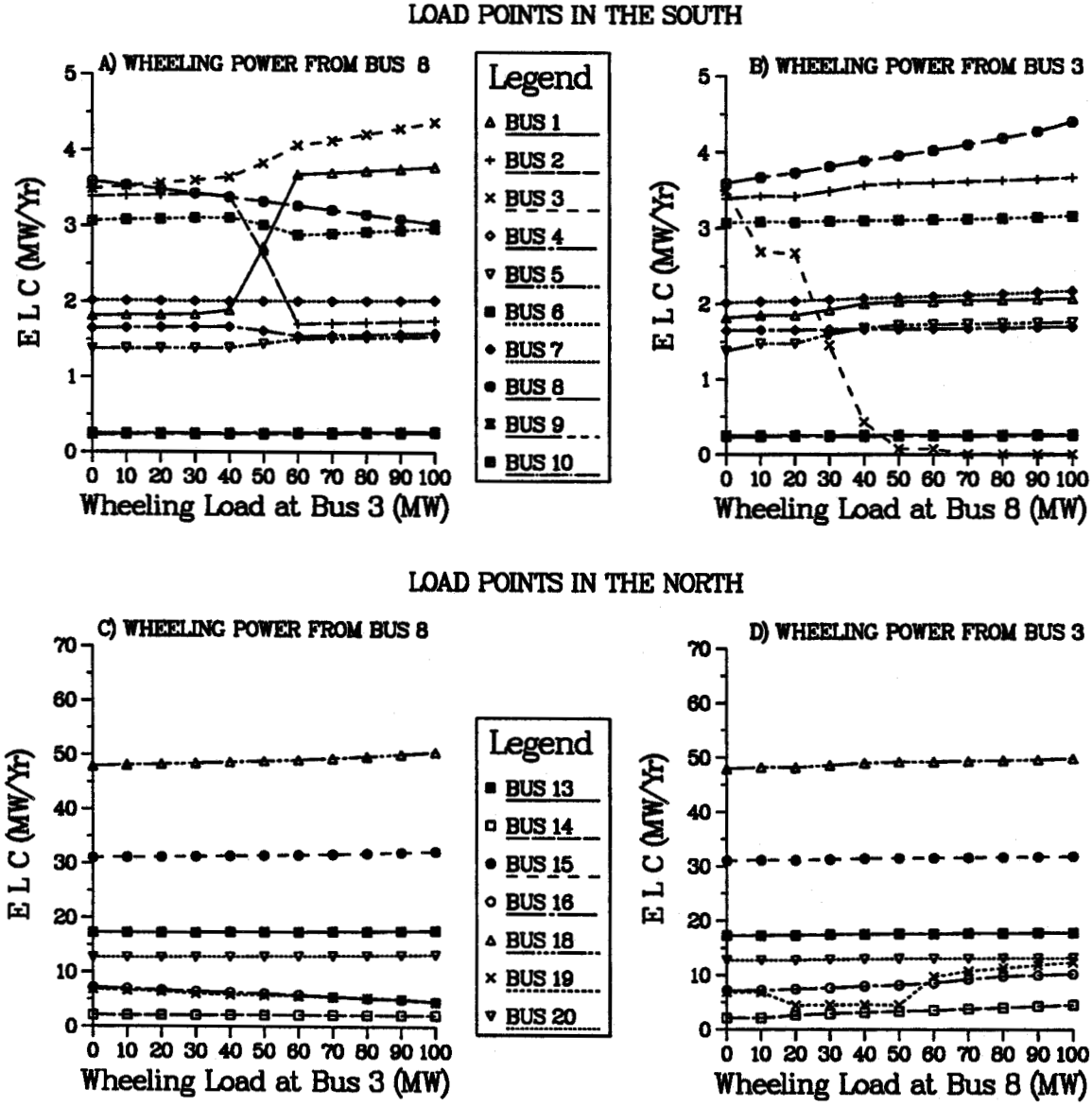

Figure 5.18: Variation In ELC At The Load Points With Intra-system Wheeling Power Within The South Region Of The IEEE-RTS

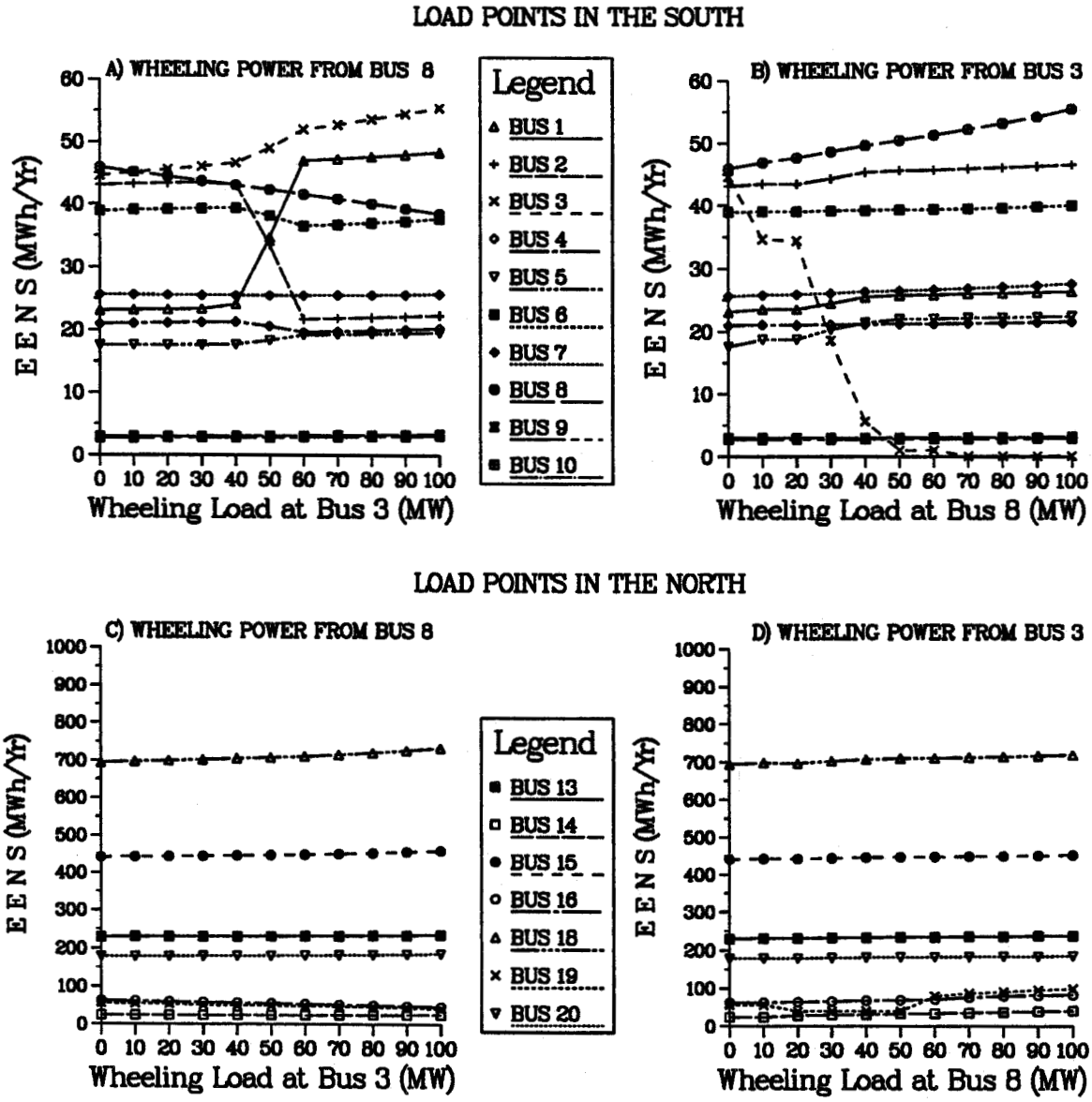

Figure 5.19: Variation In EENS At The Load Points With Intra-system Wheeling Power Within The South Region Of The IEEE-RTS

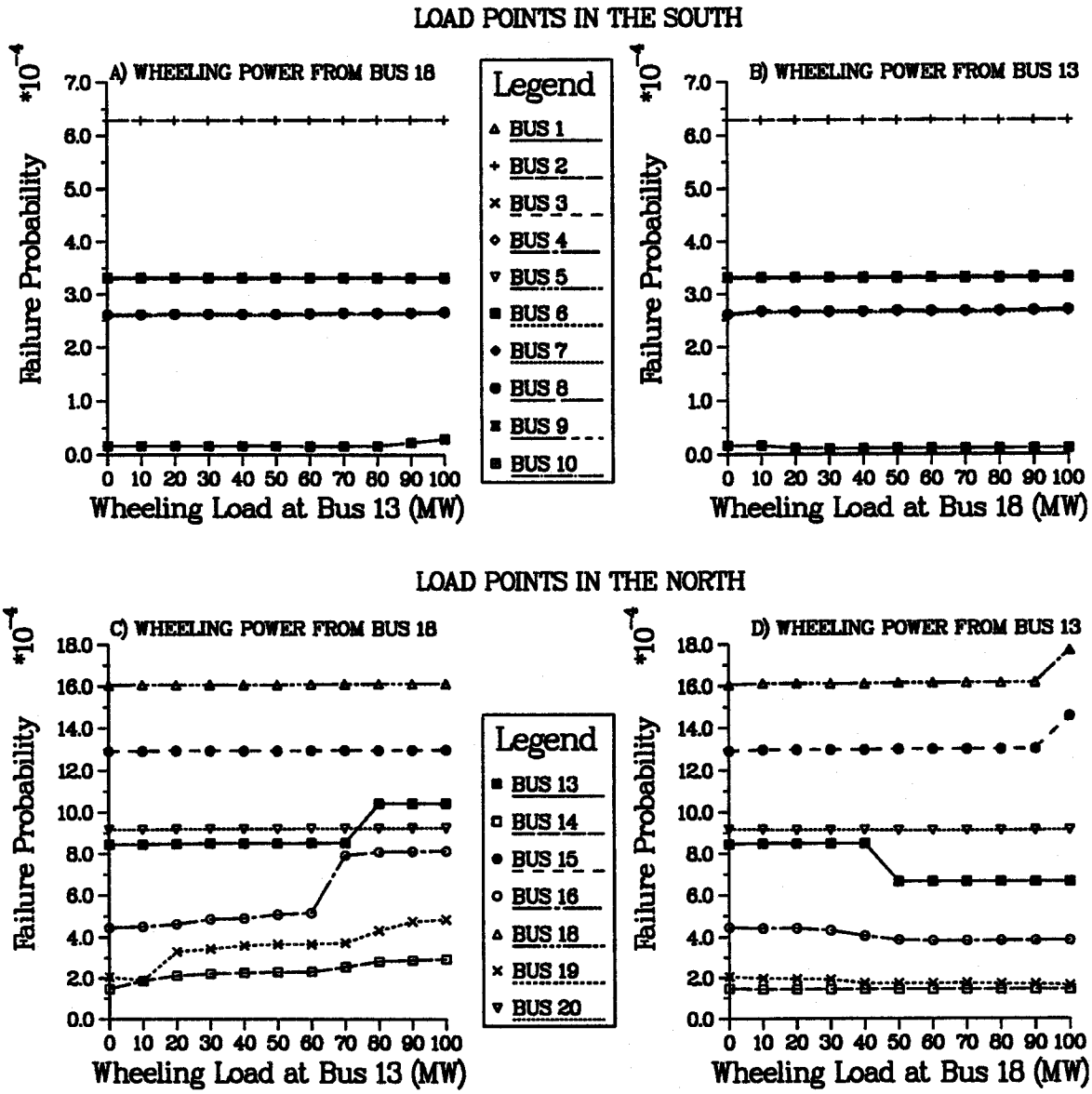

Figure 5.20: Variation In Load Point Failure Probability With Intra-system Wheeling Power Within The North Region Of The IEEE-RTS

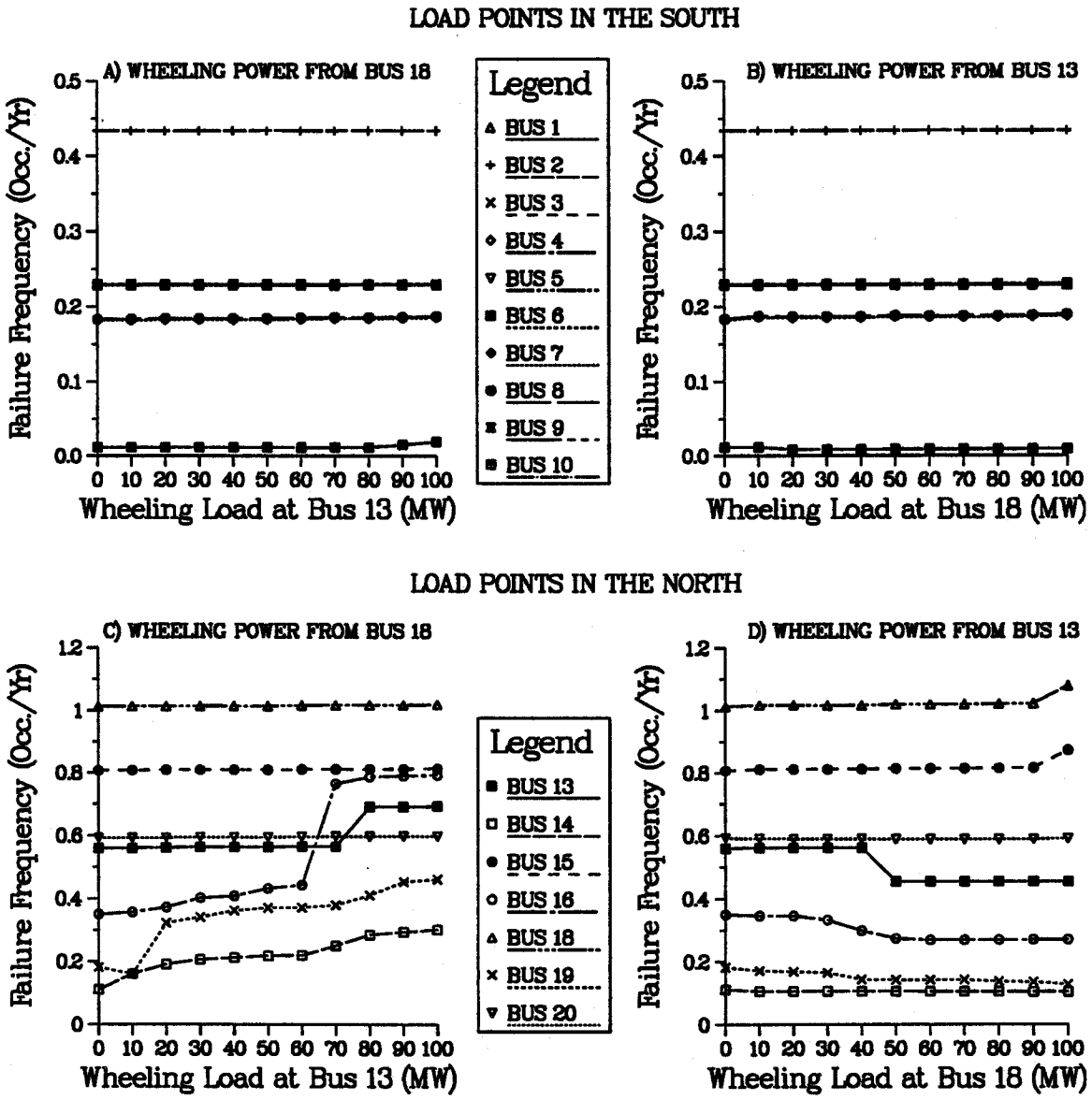

Figure 5.21: Variation In Load Point Failure Frequency With Intra-system Wheeling Power Within The North Region Of The IEEE-RTS

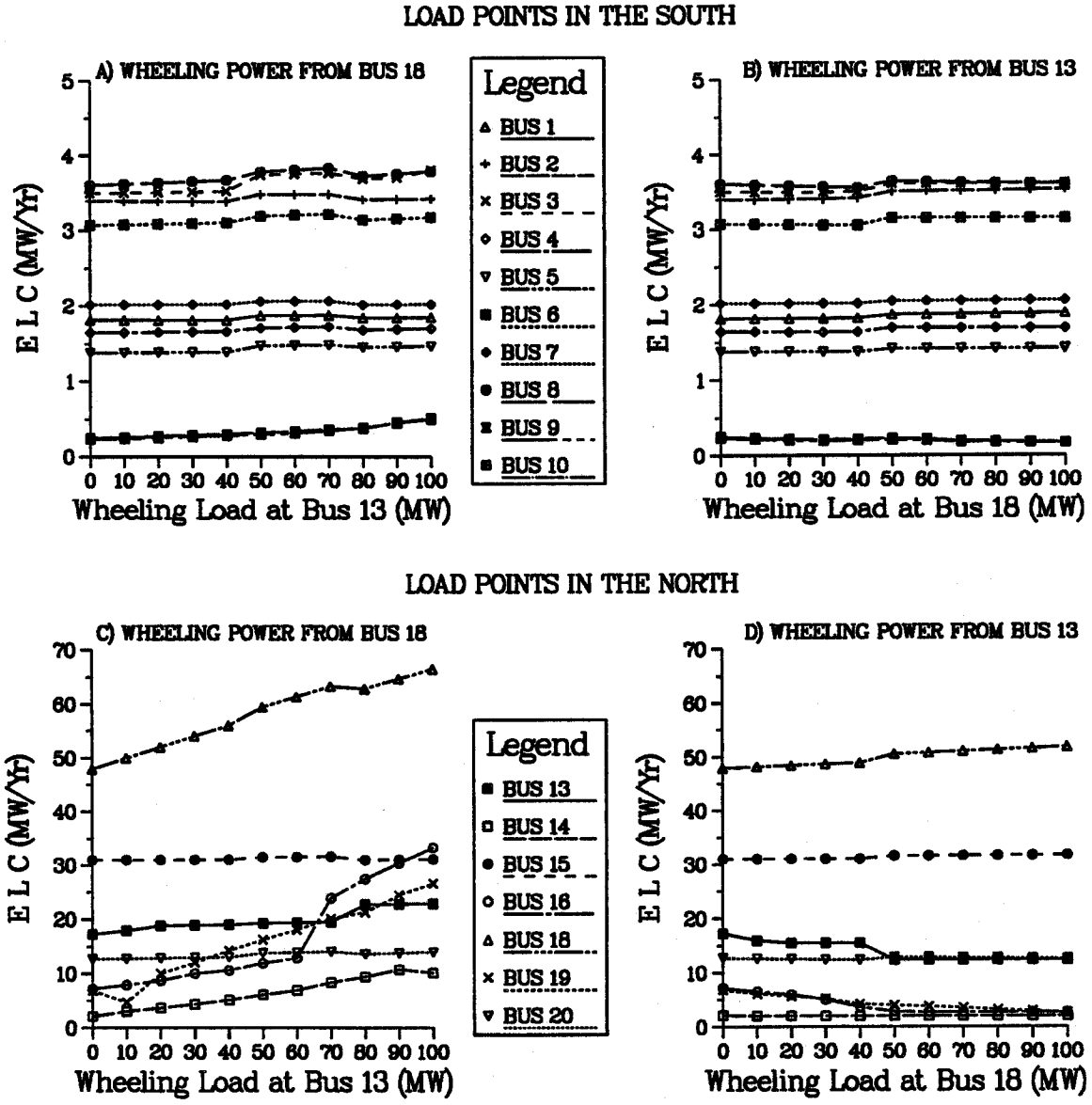

Figure 5.22: Variation In ELC At The Load Points With Intra-system Wheeling Power Within The North Region Of The IEEE-RTS

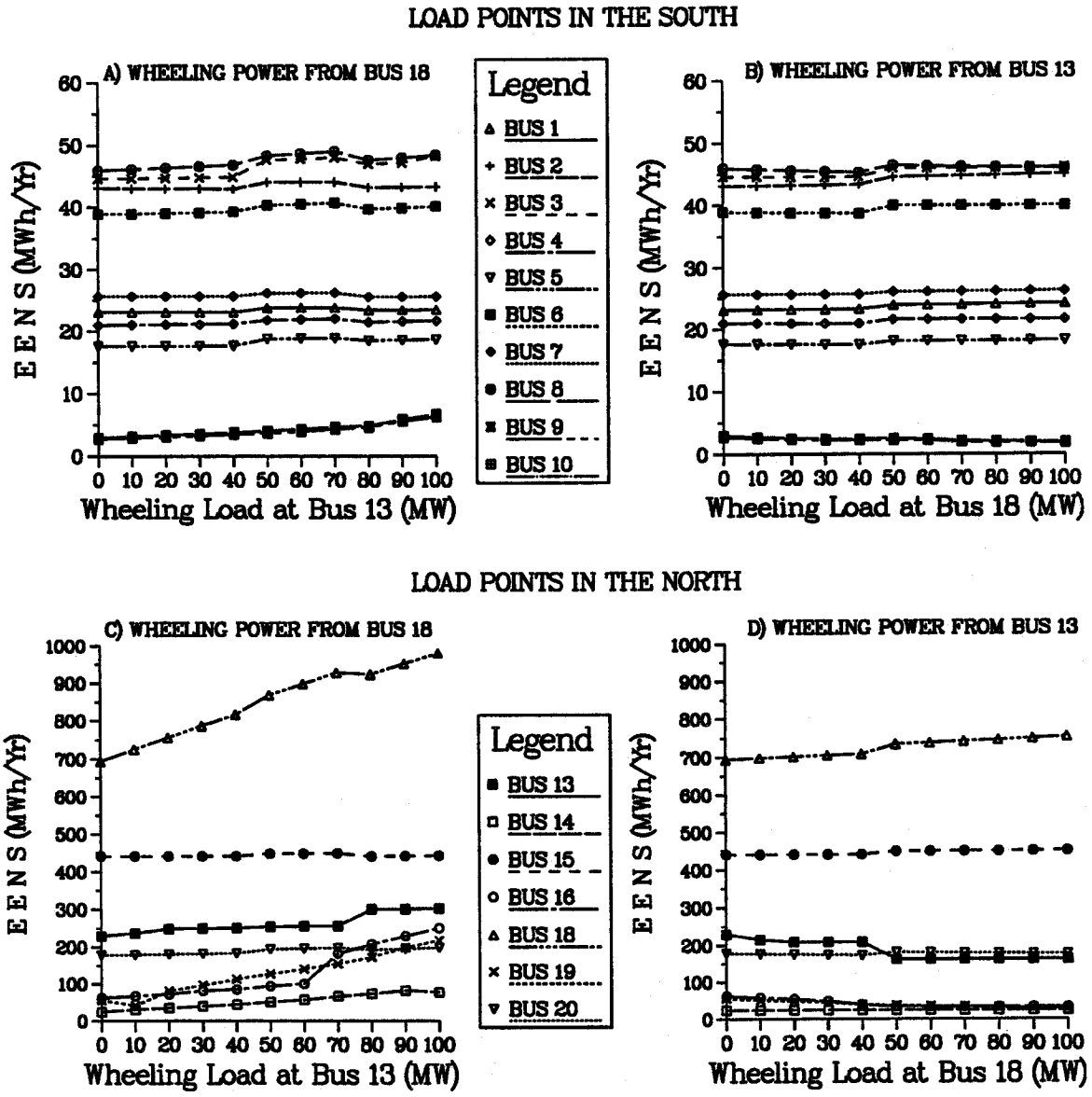

Figure 5.23: Variation In EENS At The Load Points With Intra-system Wheeling Power Within The North Region Of The IEEE-RTS

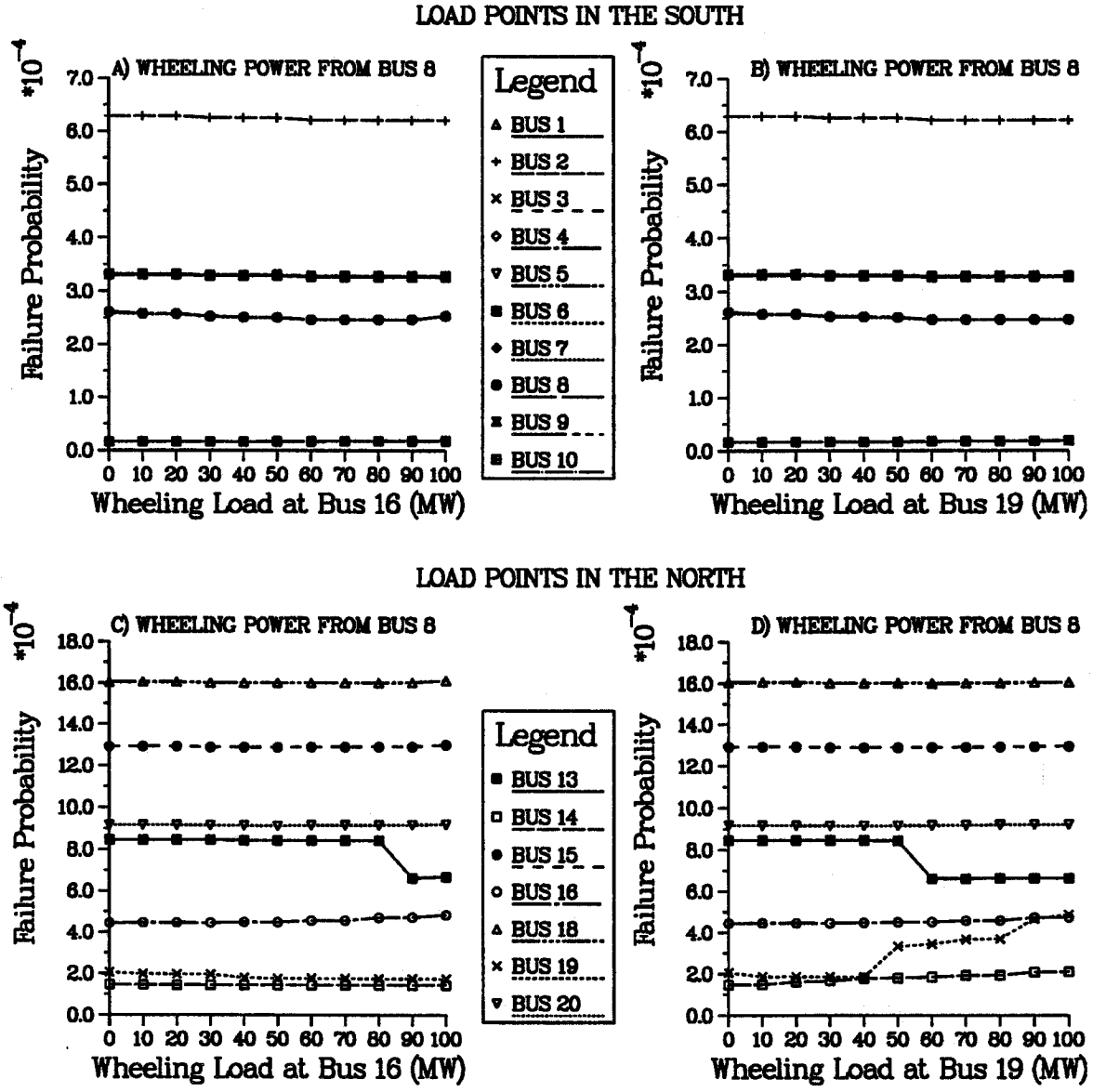

Figure 5.24: Variation In Load Point Failure Probability With Intra-system Wheeling Power From The South Region To The North Region Of The IEEE-RTS

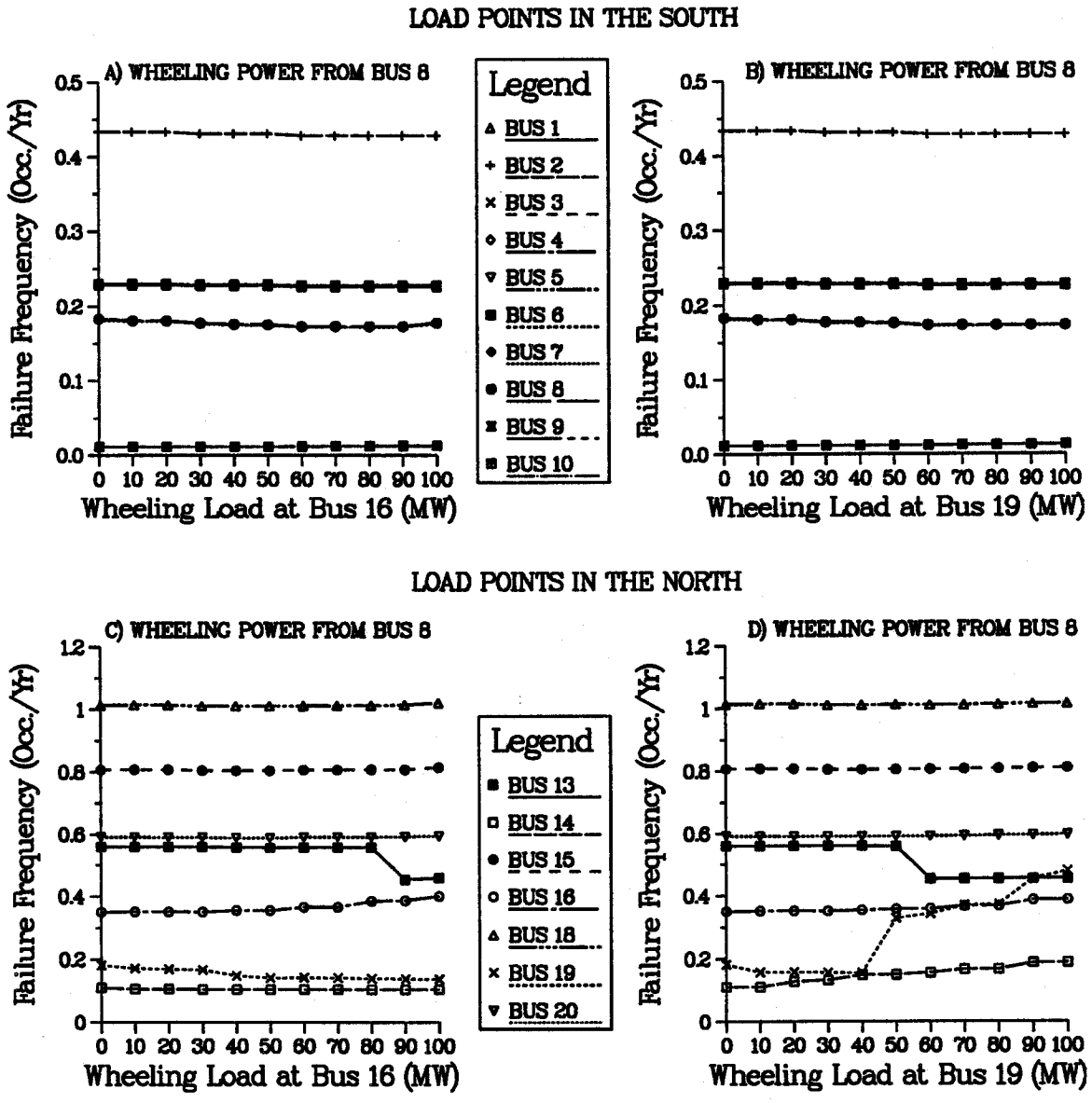

Figure 5.25: Variation In Load Point Failure Frequency With Intra-system Wheeling Power From The South Region To The North Region Of The IEEE-RTS

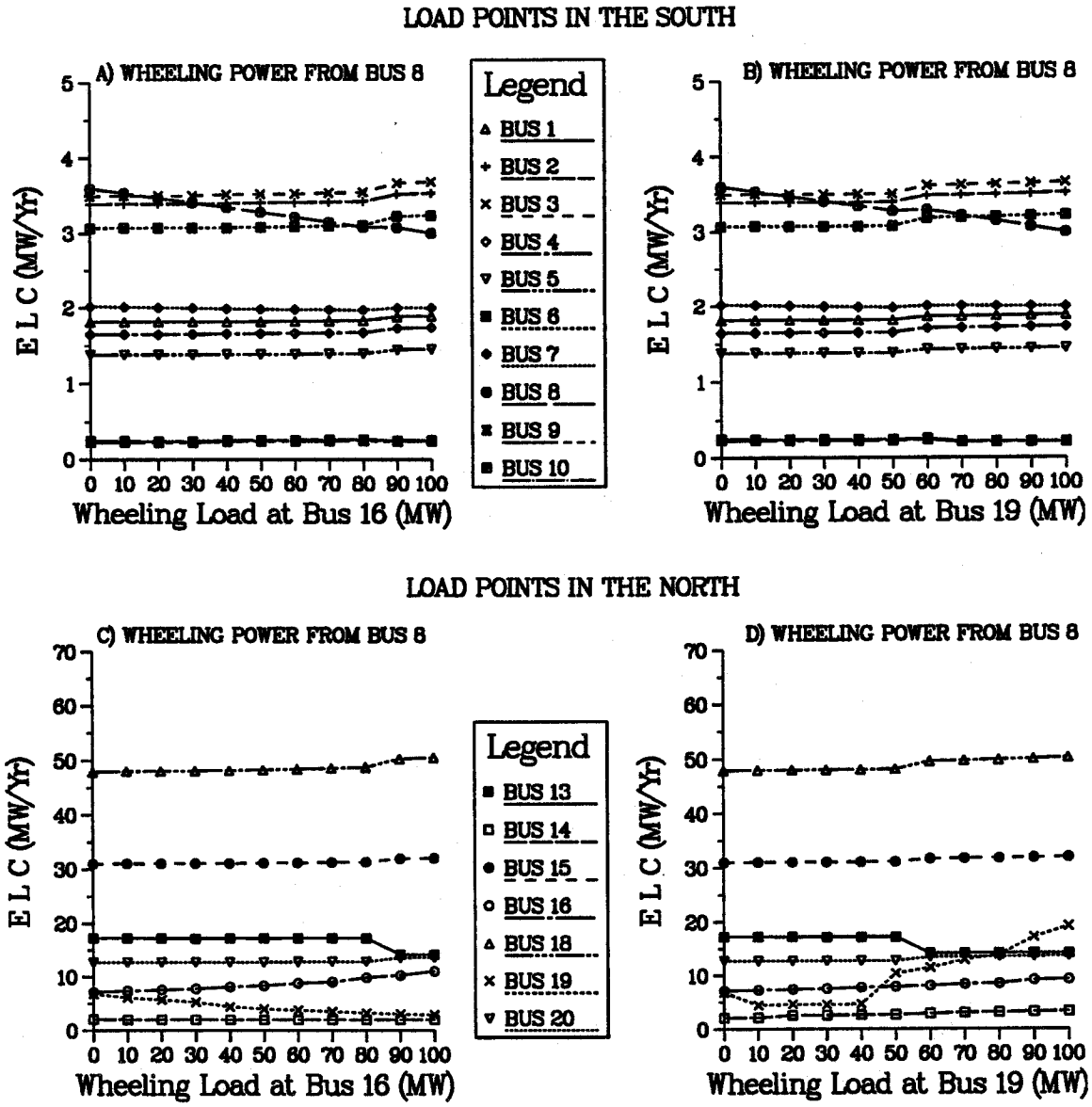

Figure 5.26: Variation In ELC At The Load Points With Intra-system Wheeling Power From The South Region To The North Region Of The IEEE-RTS

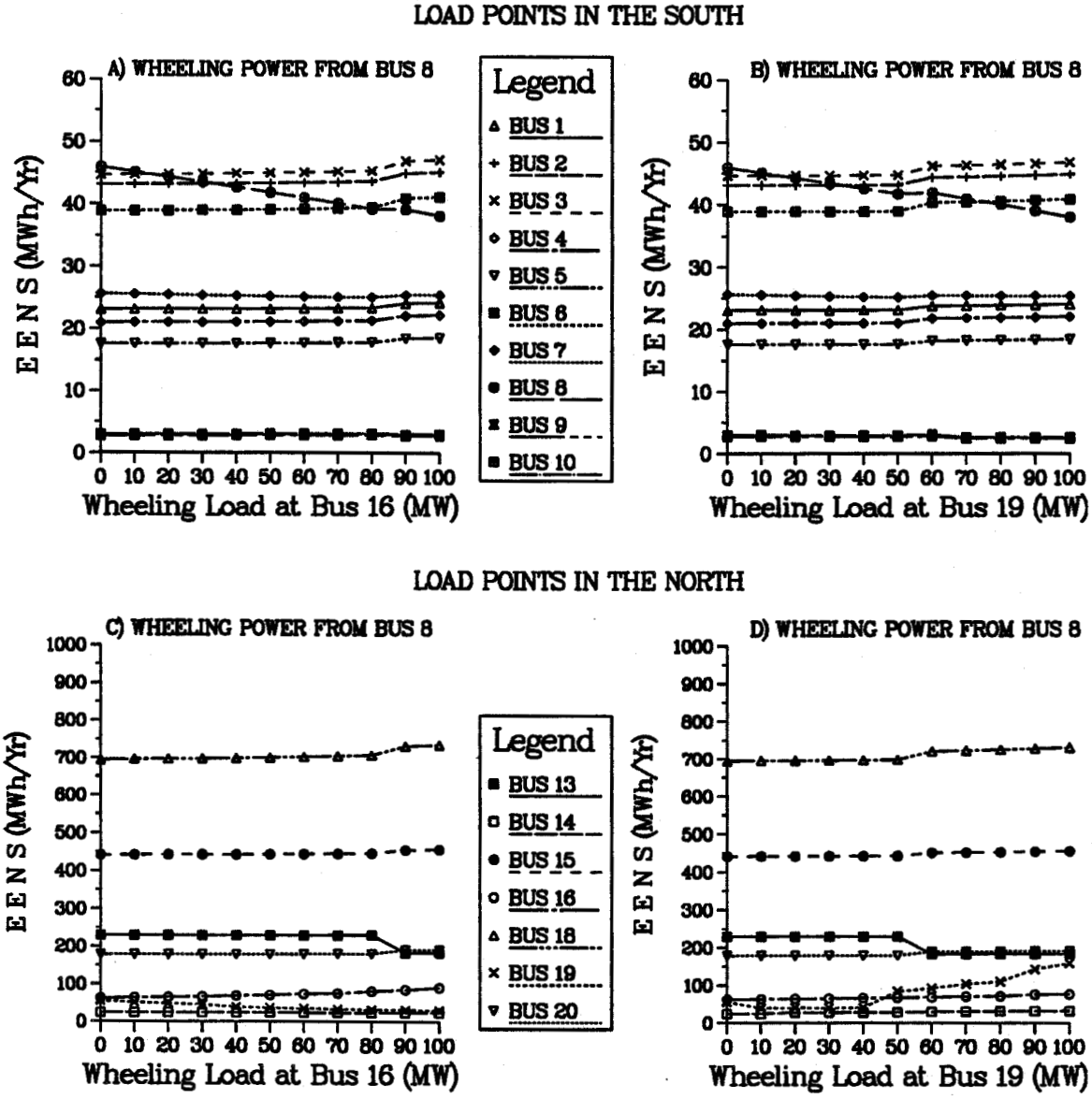

Figure 5.27: Variation In EENS At The Load Points With Intra-system Wheeling Power From The South Region To The North Region Of The IEEE-RTS

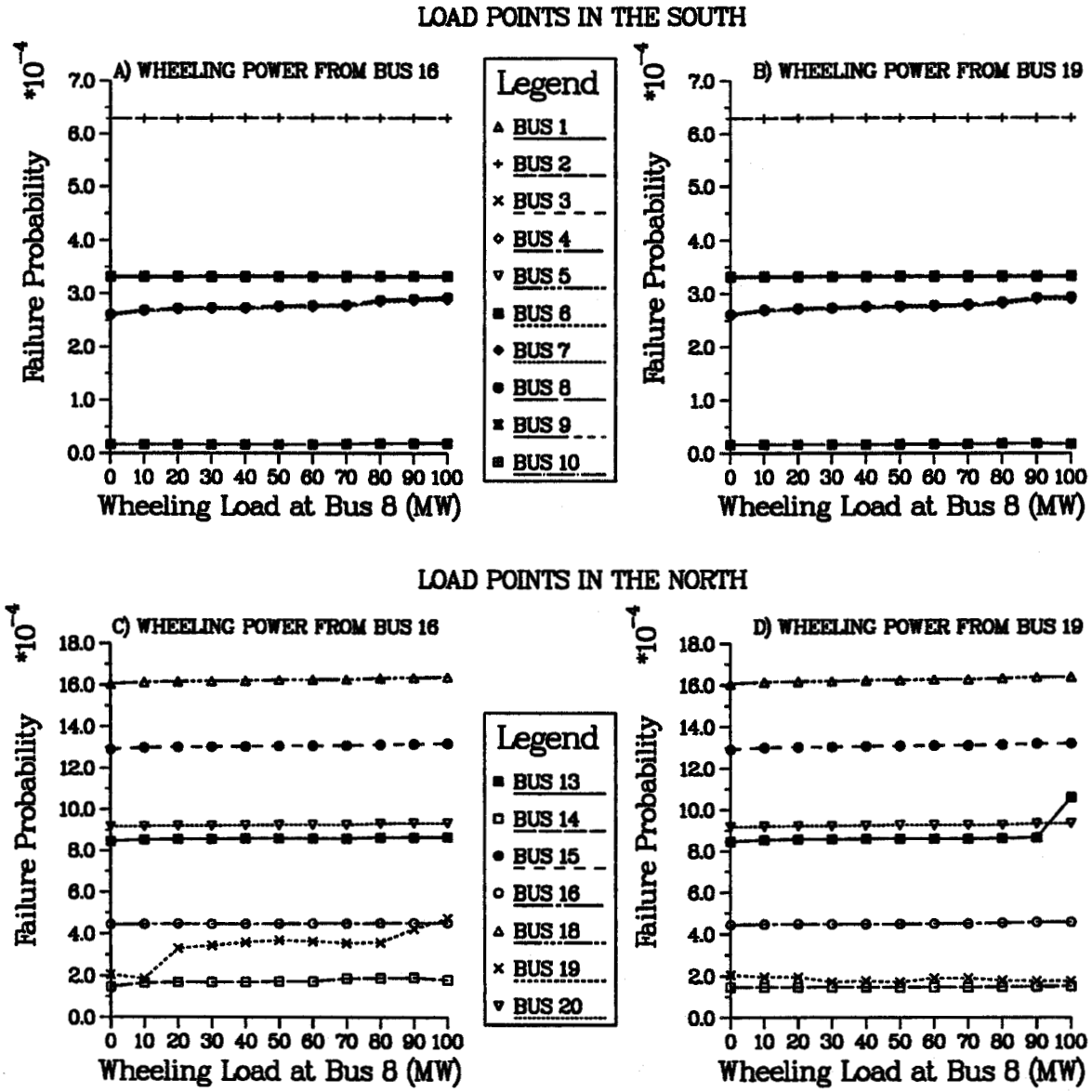

Figure 5.28: Variation In Load Point Failure Probability With Intra-system Wheeling Power From The North Region To The South Region Of The IEEE-RTS

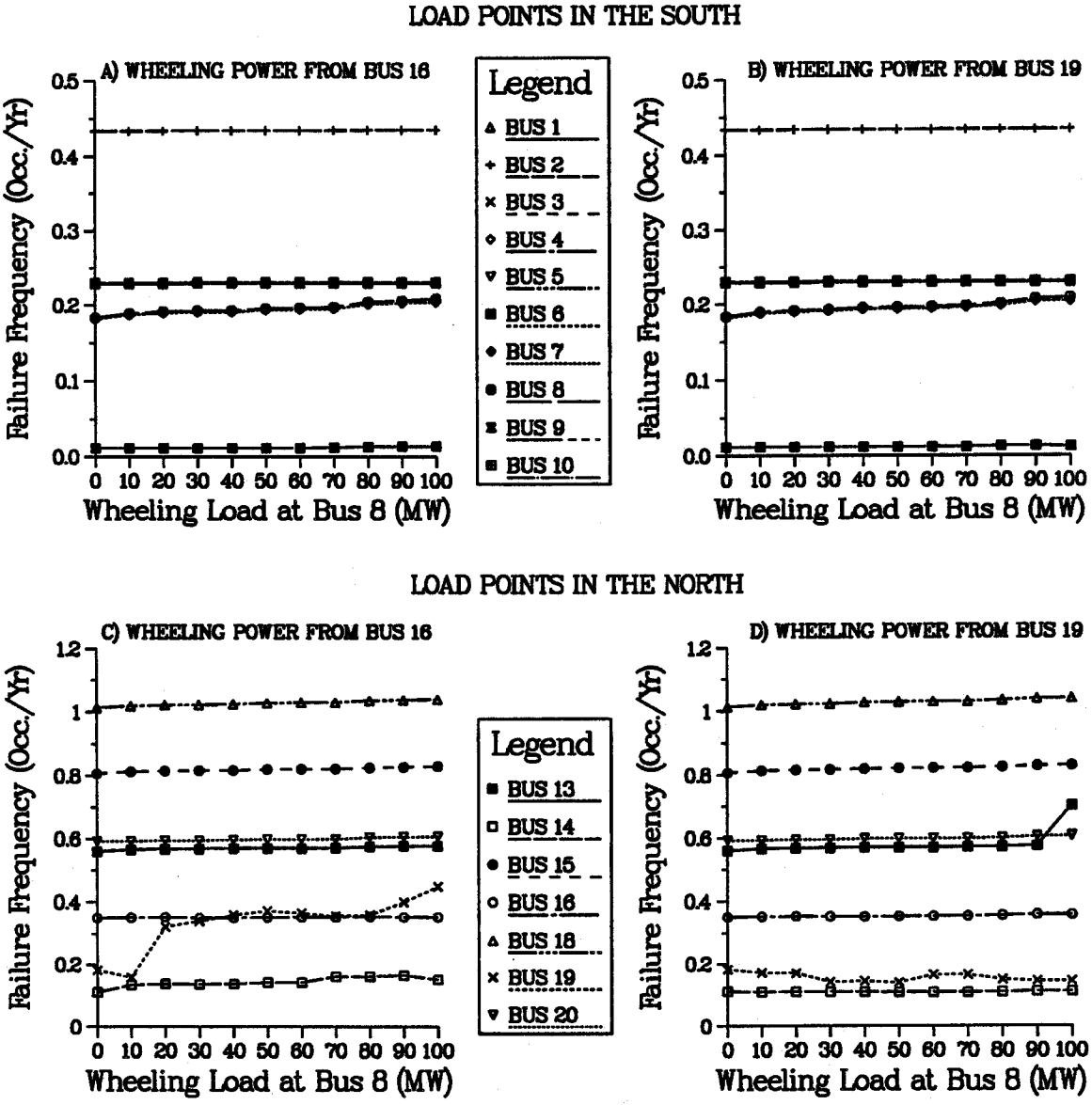

Figure 5.29: Variation In Load Point Failure Frequency With Intra-system Wheeling Power From The North Region To The South Region Of The IEEE-RTS

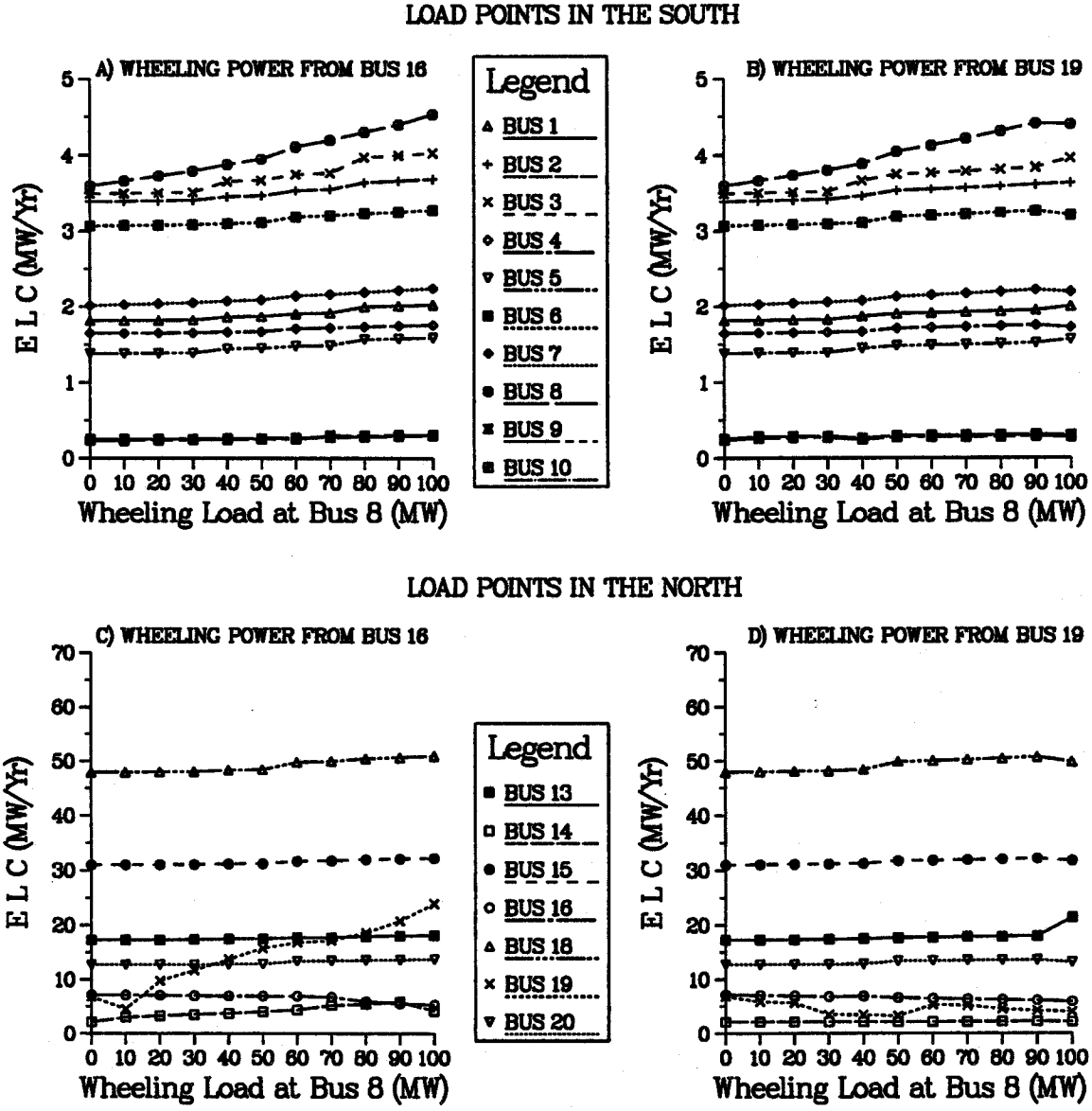

Figure 5.30: Variation In ELC At The Load Points With Intra-system Wheeling Power From The North Region To The South Region Of The IEEE-RTS

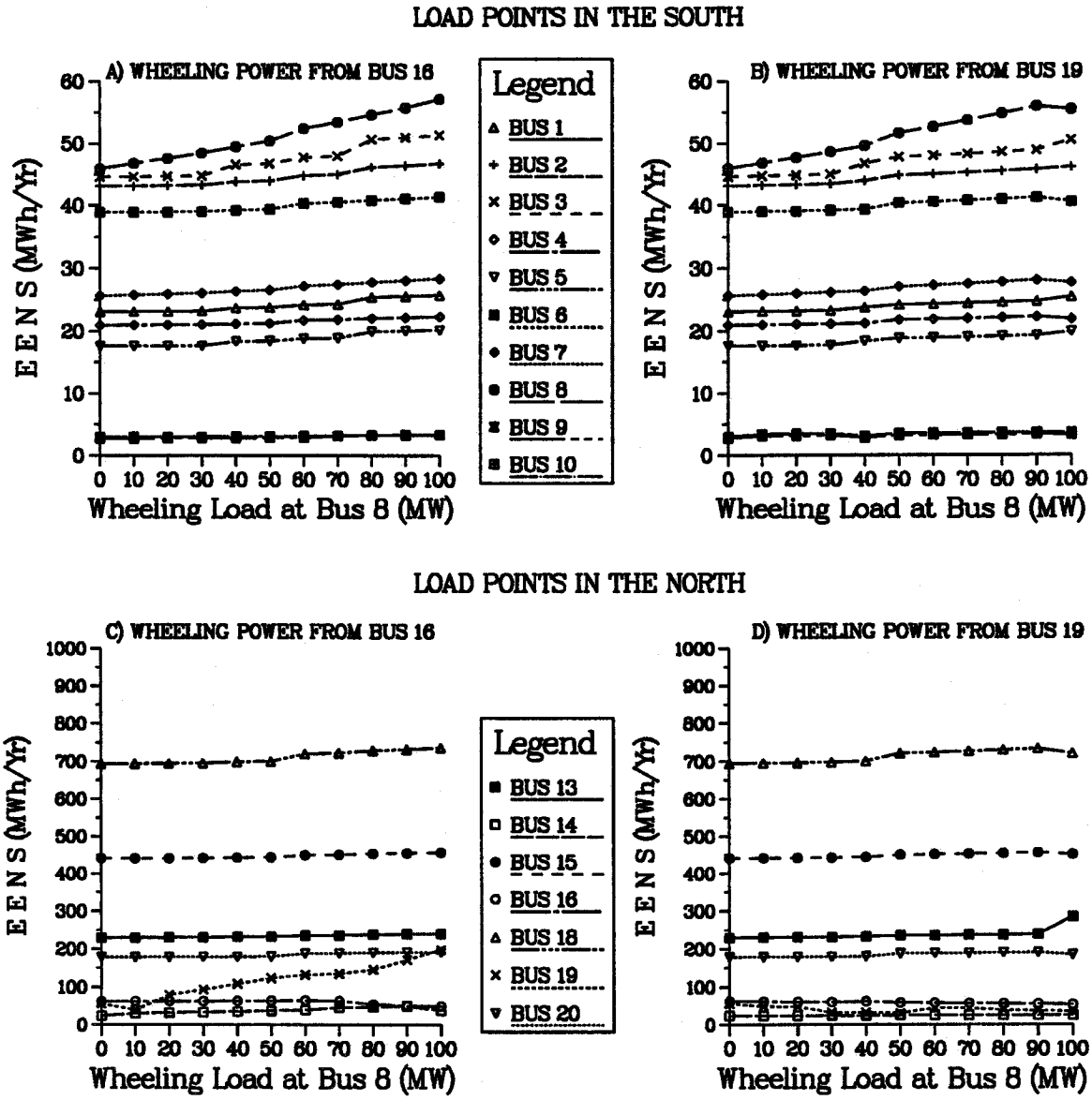

Figure 5.31: Variation In EENS At The Load Points With Intra-system Wheeling Power From The North Region To The South Region Of The IEEE-RTS

operations are fairly well confined to the load points in the region where the wheeling takes place. For example, it can be seen from Figures 5.16-5.19, that the indices of most of the load points in the north region remain virtually unaffected by the wheeling operations in the south region. Similarly from Figures 5.20-5.23, wheeling operations in the north do not cause any significant variation in the indices for the load points in the south region. This indicates the ability of the two regions of the IEEE-RTS to effectively accommodate wheeling operations independently undertaken in their respective regions without affecting the existing levels of adequacy at the load points in the neighbouring region. Generally, adequacy at the load points directly involved in the wheeling operation are the ones most affected although the effects can spread to immediate neighbouring load points as well. Whilst an improvement in adequacy is noticed at the wheeling source, the wheeling sink and the load points surrounding it generally experience a deterioration in adequacy. It can be seen from Figures 5.20-5.23 that wheeling from bus 18 to supply a wheeling load at bus 13 reduces the level of adequacy at several load points in the IEEE-RTS. This happens because introduction of the wheeling load close to the swing bus intensifies the adverse effects of swing bus overload conditions, which account for the bulk of the inadequacy experienced, particularly at the load points in the north region of the IEEE-RTS. On the other hand, wheeling in the opposite direction favours the test system as additional wheeling supplies provided close to the swing bus tend to minimise the occurrence of the swing bus overload conditions.

Similar observations can be made from Figures 5.24-5.27 and Figures 5.28-5.31 which show the impact on load point indices of wheeling from the south to the north and vice-versa respectively across the north-south boundary of the IEEE-RTS. The impacts of wheeling from the south to the north are generally minimal and are favourable at a number of load points in most of the cases shown in Figures 5.24-5.27. This is because by introducing a wheeling source in the south region, which is a net generation importing area, the region's dependence on supplies from the north is reduced; hence this releases generation supplies for use in the north to suppress the occurrence of swing bus overload conditions. The resulting impact is particularly significant when the wheeling load is located at bus 16 which is further away from the swing bus than bus 19. Wheeling from the north to the south, on the other hand, causes a considerable deterioration at several

load points in the south region as shown in Figures 5.28-5.31. This is expected, because by introducing a wheeling load in the south region, that region's dependency on supplies from the north region increases; and it should be recognised that these additional supplies would have to be transported through existing transmission facilities exposed to various risks of failure. Though the effects on the failure probability and frequency indices are not very apparent from Figures 5.28 and 5.29, the impact on ELC and EENS indices shown in Figures 5.30 and 5.31 respectively can be seen to be quite significant. The ELC and EENS indices are therefore more responsive to the impacts of intra-system wheeling operations on adequacy at the load points of a utility system.

5.4.2.2. System Indices

Figures 5.32-5.37 show the variation in the overall system indices of the IEEE-RTS when up to 100 MW of power is wheeled to and from different parts of the system.

Figures 5.32 and 5.33 respectively show the impacts on the BPII and the SI of wheeling operations undertaken separately within the north and south regions of the IEEE-RTS. It can be observed that the impacts due to wheeling within the south region are relatively minimal compared to the impacts due to wheeling within the north region. This can be attributed to the comprehensive nature of the transmission system in the IEEE-RTS which enables the system to cope fairly well with the wheeling operations in the south region without encountering serious transmission capacity limitation problems. Wheeling operations involving load points in the north region, however, are noted to be sensitive to the proximity of the wheeling source and sink locations to the swing bus. It should be recalled that capacity deficiencies account for the bulk of inadequacy in the IEEE-RTS and these frequently lead to swing bus overload conditions mainly affecting load points in the north region. Hence introduction of a wheeling source close to the swing bus tends to suppress the occurrence of the swing bus overload conditions thus producing a considerable improvement in overall system adequacy. When the wheeling source is located further away from the swing bus or the wheeling load is introduced close to the swing bus, a reduced level of improvement in overall system adequacy is obtained. It can be seen from Figures 5.32 and 5.33, that wheeling within the north region from bus 18 to bus 13, for example, produces an increase in the overall system indices as

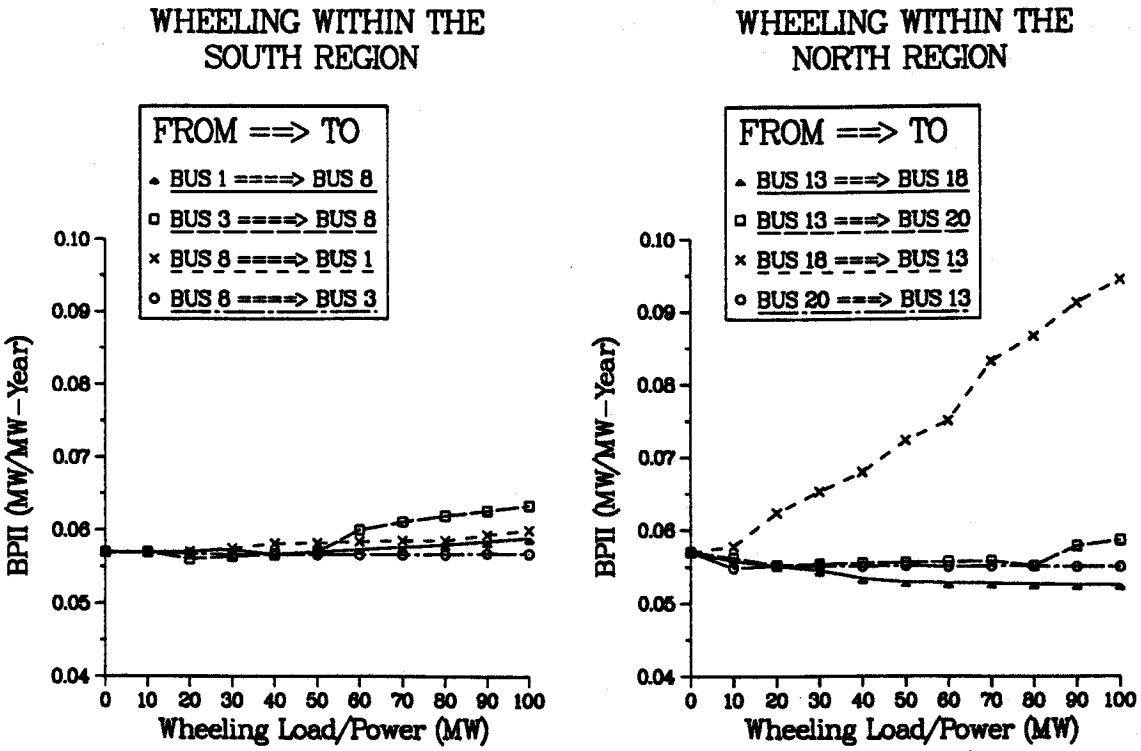

Figure 5.32: Variation In BPII With Intra-system Wheeling Power Within The North And South Regions Of The IEEE-RTS

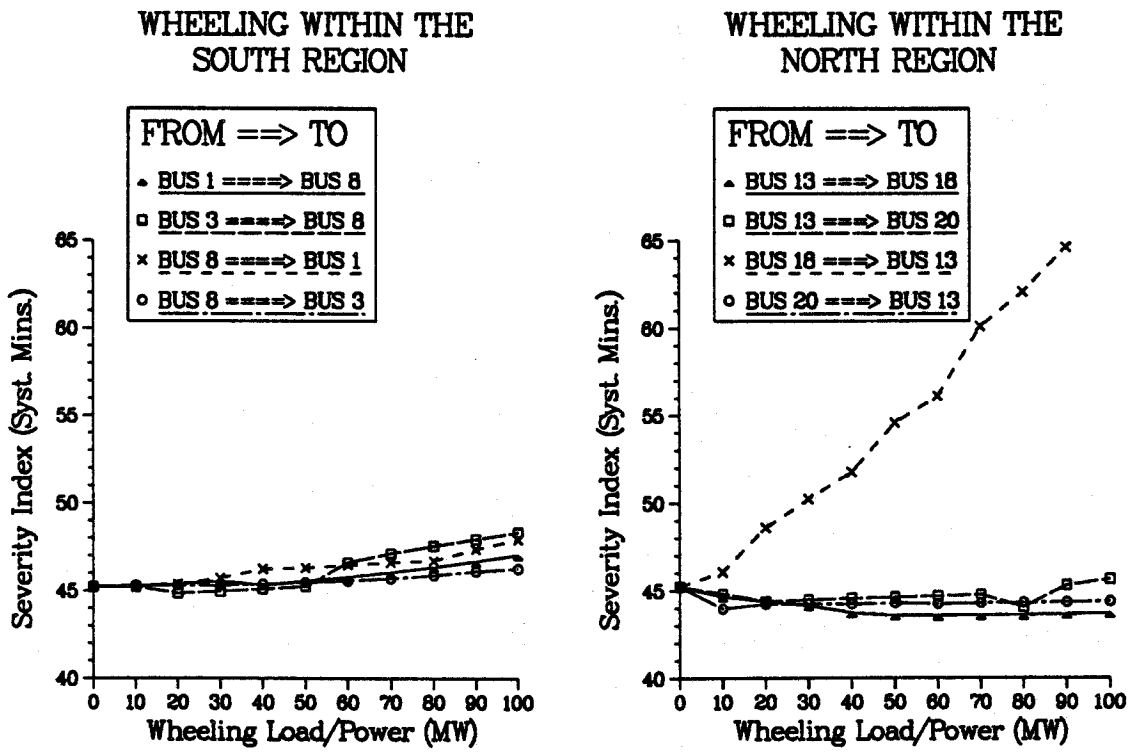

Figure 5.33: Variation In Severity Index With Intra-system Wheeling Power Within The North And South Regions Of The IEEE-RTS

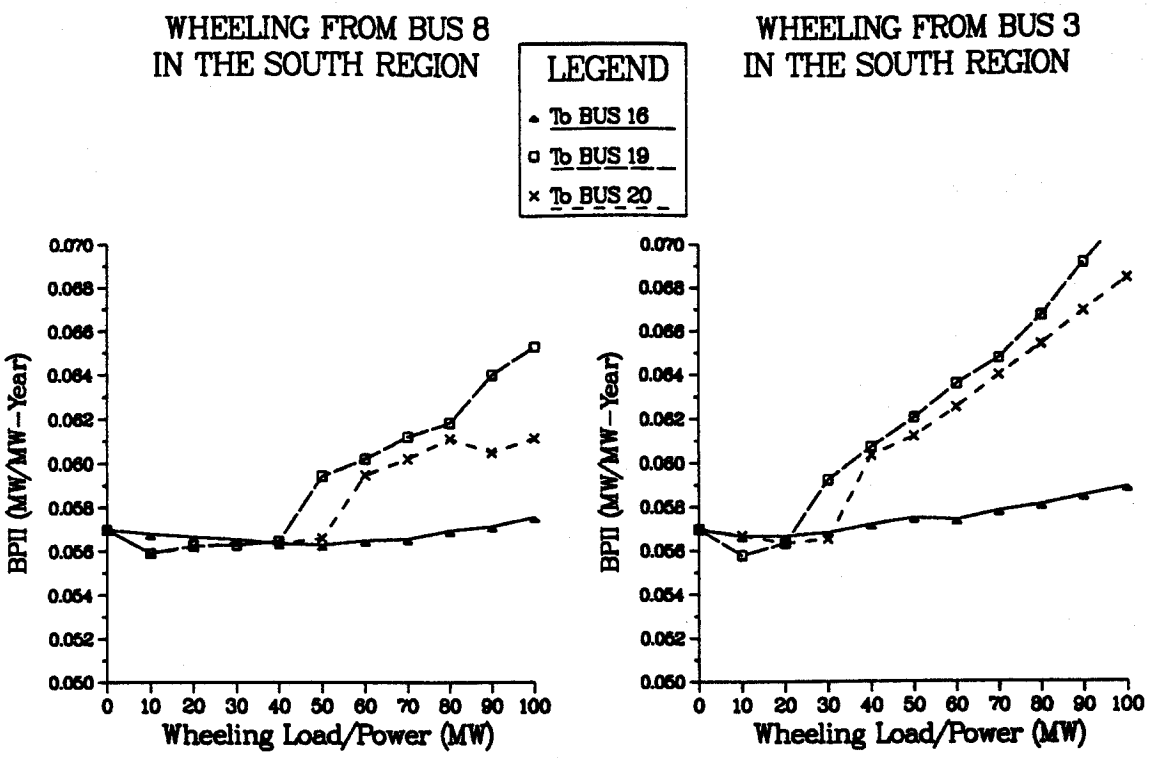

Figure 5.34: Variation In BPII With Intra-system Wheeling Power From The South Region To The North Region Of The IEEE-RTS

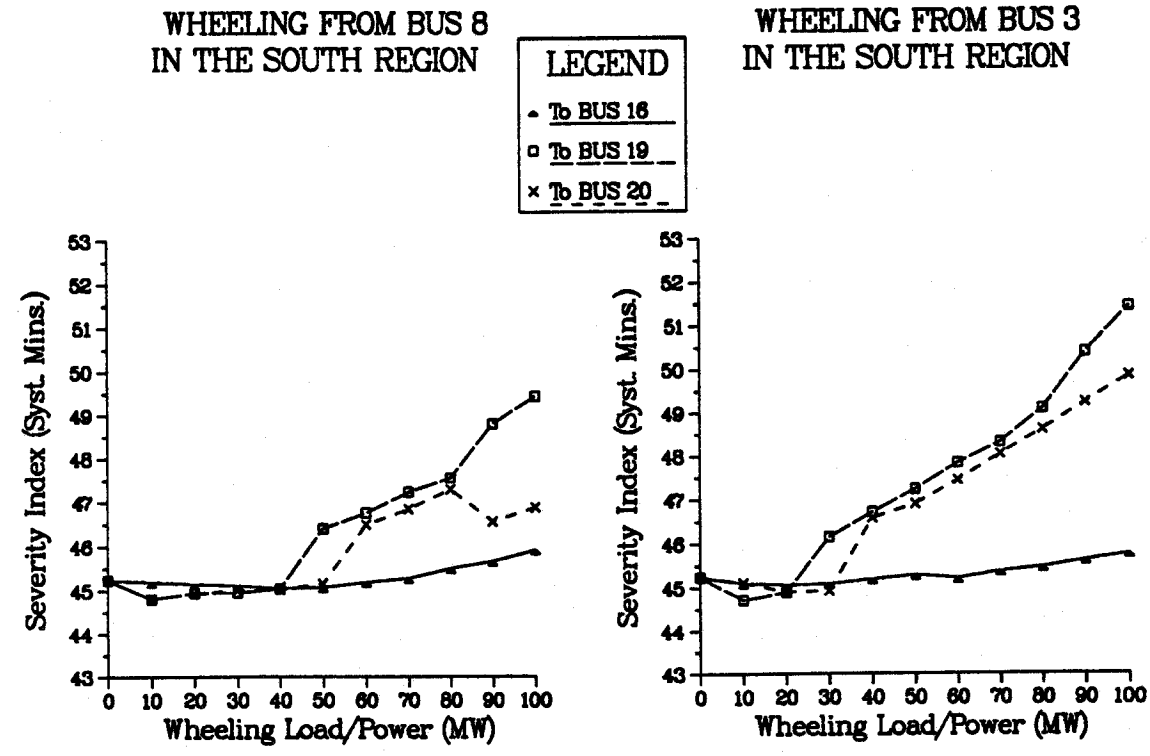

Figure 5.35: Variation In Severity Index With Intra-system Wheeling Power From The South Region To The North Region Of The IEEE-RTS

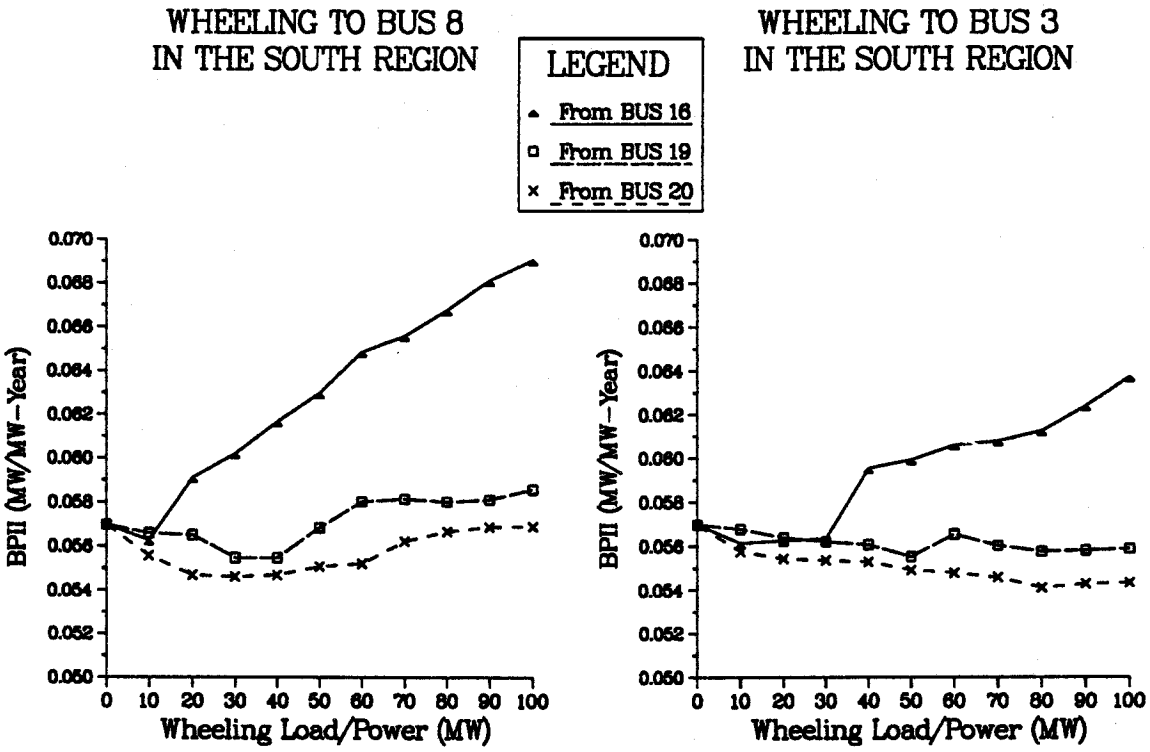

Figure 5.36: Variation In BPII With Intra-system Wheeling Power From The North Region To The South Region Of The IEEE-RTS

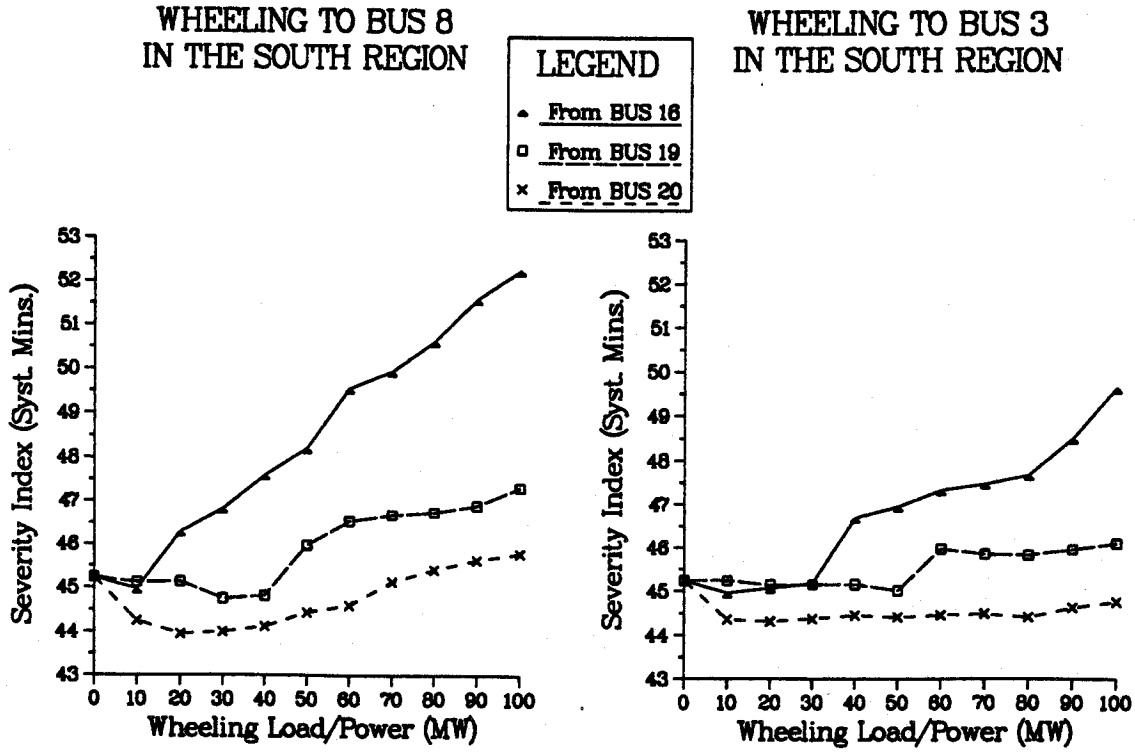

Figure 5.37: Variation In Severity Index With Intra-system Wheeling Power From The North Region To The South Region Of The IEEE-RTS

the wheeling source is located far away from the swing bus and the wheeling load at bus 13 is quite close to the swing bus.

Similar observations can be made from Figures 5.34-5.37 which show the impact on the overall system indices when the wheeling operations are carried out across the north-south boundary in both directions. Referring to the single-line diagram of the IEEE-RTS shown in Figure 3.2, bus 20 is directly connected through a double circuit to bus 23 which served as the swing bus in the analyses, and buses 19 and 16 are further away from it. It can therefore be seen from Figures 5.36 and 5.37 that as the wheeling source gets closer to the swing bus, lower values of overall system indices are obtained. Similarly, introducing the wheeling loads further away from the swing bus also produces relatively lower values of overall system indices as shown in Figures 5.34 and 5.35.

5.5. Summary

This chapter introduces the concept of quantitatively assessing the impact of intra-system wheeling on power system adequacy, and methods for modelling intra-system wheeling conditions in composite system adequacy analysis are proposed. These methods were applied using the COMREL program to determine the impact of intra-system power wheeling operations on the composite system indices of the two test systems. The Expected Load Curtailed (ELC) and the Expected Energy Not Supplied (EENS) indices are shown to be more responsive indices for predicting the impact of intra-system wheeling operations on load point adequacy.

A wide range of impacts on the load point and overall system indices are produced by the various wheeling operations considered. The results obtained clearly show that the impact on the indices due to a specific wheeling operation depends largely on the existing composite generation and transmission system configuration of the utility system. Depending on the relative locations of the wheeling source and the wheeling sink, the wheeling impact can either lead to an improvement or a deterioration in load point adequacy and overall system adequacy and in some situations may have relatively little effect on the indices. Load points directly involved in the wheeling operations are shown to be the ones most affected by the wheeling operations.

The studies illustrated in this chapter clearly show that it is extremely important to quantitatively assess the implications of wheeling operations prior to establishing formal contracts. The investigations should cover detailed examination of load point and overall system adequacy prior to wheeling in order to provide a datum against which to assess the implications of possible options.

6. POWER WHEELING CONSIDERATIONS IN COMPOSITE SYSTEM ANALYSIS OF INTERCONNECTED POWER SYSTEMS

6.1. Introduction

One of the primary objectives of interconnecting two or more power systems is to improve the adequacy of generating capacity in the interconnected systems [42]. The risk associated with generating capacity in the interconnected systems is determined from the probabilities of simultaneous occurrences of capacity outages in the various systems [18]. Interconnection enables each associated system to operate at a given risk level with a lower reserve than would be required without interconnection [43, 44]. The actual benefits of interconnecting power systems, however, depends on the installed capacity in each system and a number of factors [18] related to the tie line characteristics, the operating load levels in each system and the interconnection agreements.

Wheeling of energy through a system is one of the many possible uses and benefits of interconnection. A wheeling situation arises when assistance is required from a power system which is not directly interconnected with the assisted system. This chapter discusses some of the composite system reliability considerations which arise when power wheeling is practised in interconnected power systems.

6.2. Power Wheeling Concepts in Interconnected Power Systems

The concept of power wheeling in interconnected systems can be illustrated using the three interconnected power systems shown in Figure 6.1.

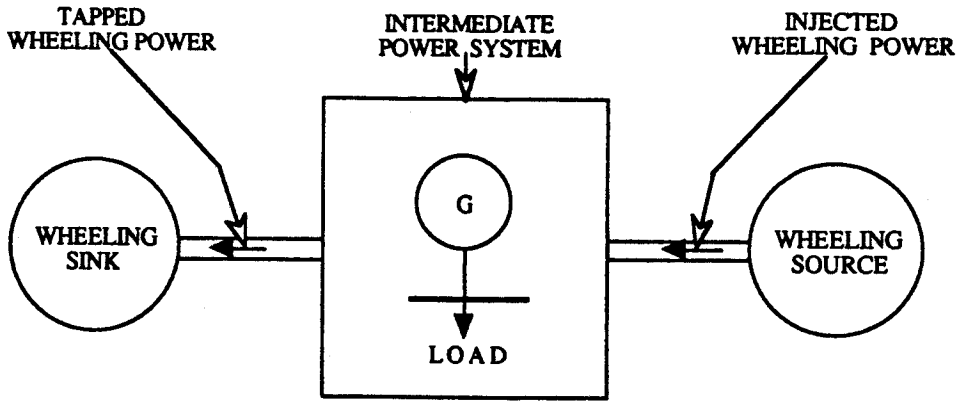

Figure 6.1: Illustration Of Power Wheeling Concept In Interconnected Systems

The wheeling source represents the system providing the energy whilst the wheeling sink represents the system receiving the energy. These two systems are not directly interconnected, but are both connected to a third system which is situated between them and is denoted as the Intermediate Power System (IPS) in Figure 6.1. An agreement with the IPS is required in order for its transmission facilities to be utilised to transport the wheeling power from the assisting system (i.e. the wheeling source) to the assisted system (i.e. the wheeling sink). Once an agreement for the transaction is reached, the wheeling power can be injected into the IPS which then passes it on to the wheeling sink at the respective interconnection points in accordance with the terms of the contract.

The objective of the analyses in this chapter is to examine the impact of wheeling operations on the composite system indices of the IPS which renders the wheeling service. Results of the analyses utilising the RBTS and the IEEE-RTS respectively as intermediate power systems are presented and illustrated. The COMREL program is used to perform these analyses.

6.3. Modelling Considerations for Power Wheeling in Interconnected Systems

6.3.1. Wheeling Source & Power

The energy/power to be provided is assumed to originate from an imaginary generating bus which is directly connected to the IPS. This bus is denoted as the wheeling source and is external to the IPS. The wheeling power is modelled as a 100% available generating unit located at the wheeling source. The rated capacity of the unit is equal to the contracted wheeling power.

6.3.2. Wheeling Sink & Load

The IPS is connected to an imaginary load bus (denoted as the wheeling sink) which is external to the IPS and which represents the location at which the energy/power is received by the assisted power system. The connection of the wheeling sink to the IPS is made through a buffer bus as shown in Figure 6.2. An ideal wheeling situation is realised in this analysis, when the wheeling sink is able to receive all the contracted energy/power without experiencing any of the curtailment effects in the IPS. This condition, however, is difficult to satisfy in all situations. The configuration shown in Figure 6.2 is used to connect the wheeling sink as it minimises the load curtailment impacts that could affect the wheeling sink as a result of outage events in the IPS. Adequacy indices at the wheeling sink can be used as indicators to determine satisfactory wheeling situations. The failure probability and expected energy not supplied indices obtained at the wheeling sink for wheeling operations examined in this thesis are provided in Appendix D.

The entire wheeling load at the sink is considered to be firm load and it is assumed to be always equal to the input power from the wheeling source. The percentage of curtailable load at the wheeling sink is therefore specified to be zero. Both the sink and the source are considered to be separate power systems and external to the IPS. Therefore, in computing the indices for the IPS, only the loads and facilities belonging to the IPS are considered and the load at the wheeling sink is not utilised when computing the IPS peak load.

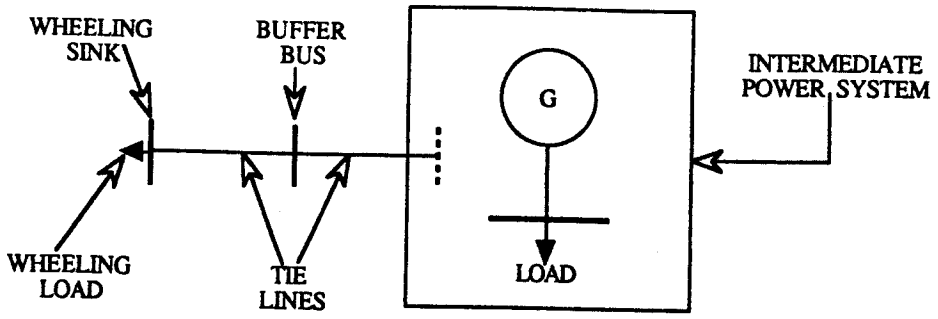

Figure 6.2: Interconnection Configuration Of The Wheeling Sink

6.3.3. Tie Lines

Tie lines with adequate transmission capacity to transport the entire range of the wheeling power considered are assumed to exist for interconnecting the wheeling source and the wheeling sink with the IPS. The failure rates of these tie lines are assumed to be zero (i.e.λ=0.0) thus assuming 100% availability. This condition is required in order to avoid the situation where due to external tie line unavailability, the assistance from the wheeling source fails to get to the IPS but the wheeling sink continues to draw its quota of power at the expense of the IPS or vice versa. There is also a wide range of possible contractual options which could be examined. These options, however, are not examined in this thesis. The analyses performed were based on the assumption that a fixed amount of wheeling power is constantly made available by the source throughout the study period and this is passed on simultaneously to the wheeling sink.

6.3.4. Load Model and System Studies

Annual reliability indices were computed to determine the impact of power wheeling on load point and overall system adequacy of the IPS. The 4-step and 7-step load models were utilised for the analysis involving the RBTS and the IEEE-RTS respectively. The wheeling load was however kept constant at all load levels throughout

each study period. The DC load flow technique was used for the analysis. Contingency enumeration was restricted to only system elements of the IPS and this included simultaneous outage combinations identical to those used to obtain the base case results in Chapter 3.

6.4. Discussion of Results

The impact of power wheeling on the composite system indices of the test systems used to represent the intermediate power system (IPS) are illustrated and presented in this section. The results obtained show trends similar in several respects to the results discussed in Chapter 5 for the intra-system wheeling analyses. The discussions in this chapter will therefore highlight the similarities and the slight differences that exist between the two sets of results. The failure probability and the expected energy not supplied (EENS) indices are used to illustrate the impacts on load point adequacy and the severity index is used to illustrate the impact on overall system adequacy.

6.4.1. Results for the RBTS

6.4.1.1. Load Point Indices

The impact on load point failure probability and the EENS indices of wheeling up to 50 MW of power through the RBTS are shown in Figures 6.3-6.8. Figures 6.3-6.4, 6.5-6.6 and 6.7-6.8 respectively show the results obtained when the wheeling sink is connected to buses 2, 3 and 5, and with the wheeling source connected to different points in the RBTS.

The results show that wheeling operations in which the wheeling source is connected to either bus 1 or bus 2 in the north generally produce the worst impacts on load point adequacy. This conforms with the observations made in Chapter 5 regarding the intra-system wheeling cases that, the RBTS is better able to cope with wheeling if the wheeling load is introduced at points close to the conventional generation locations within the RBTS. This is reaffirmed by the results in Figures 6.3 and 6.4 which show respectively the impact on the load point failure probability and the EENS indices when the wheeling sink is connected to bus 2 (a conventional generation location) and the

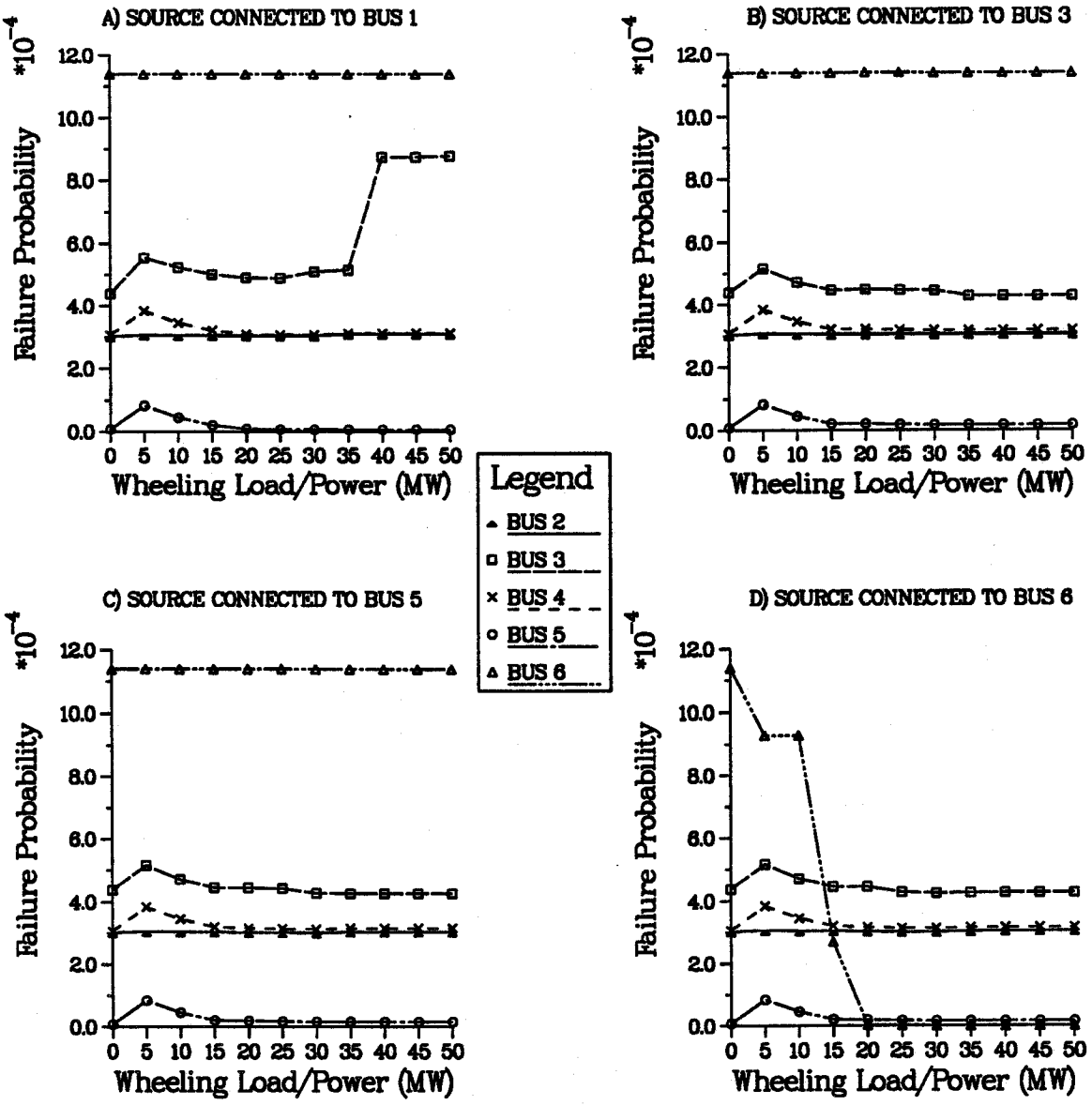

Figure 6.3: Variation In Load Point Failure Probability With Wheeling Power/load - Wheeling Sink Connected To Bus 2 Of The RBTS

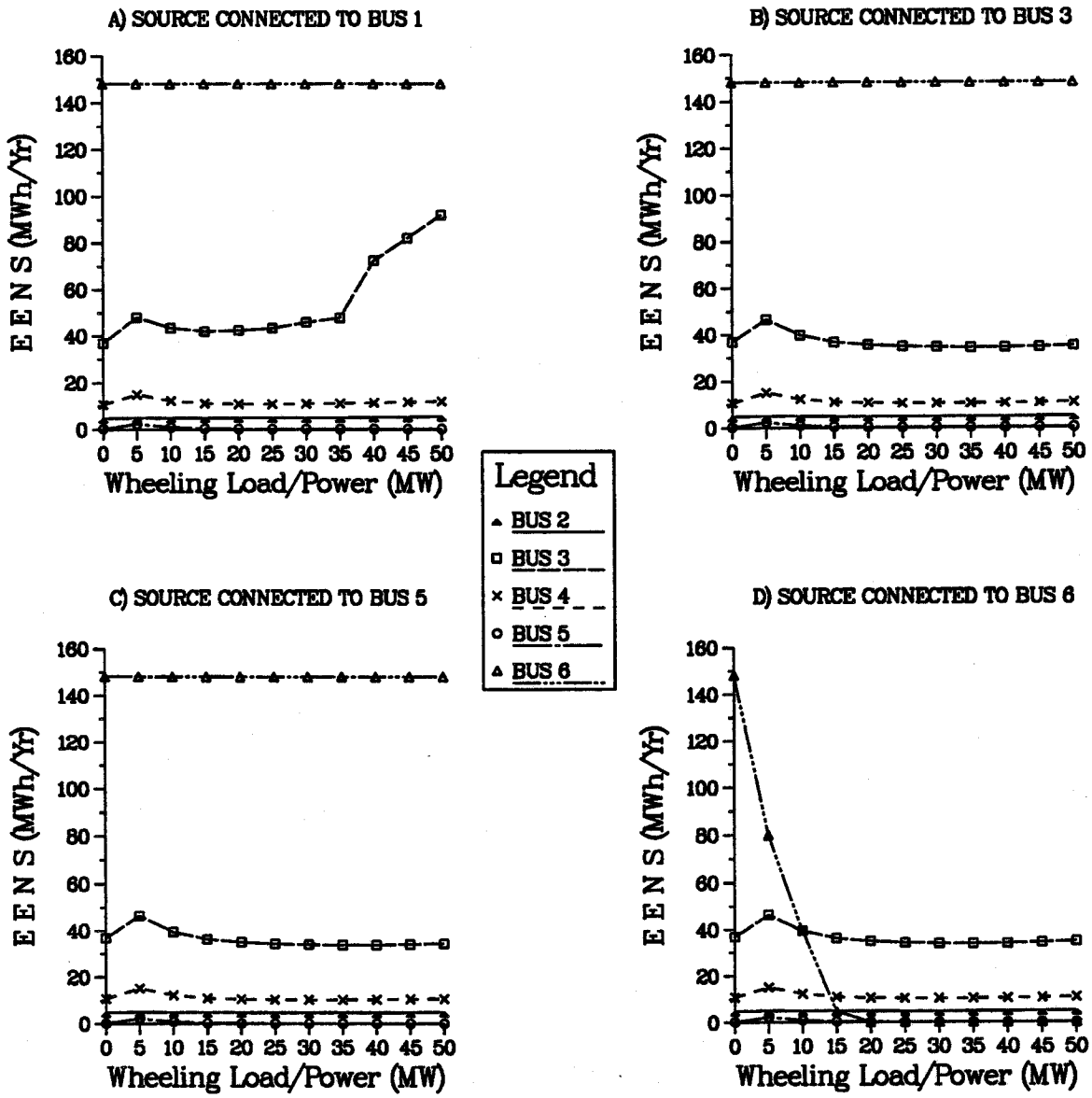

Figure 6.4: Variation In EENS At The Load Points With Wheeling Power/load - Wheeling Sink Connected To Bus 2 Of The RBTS

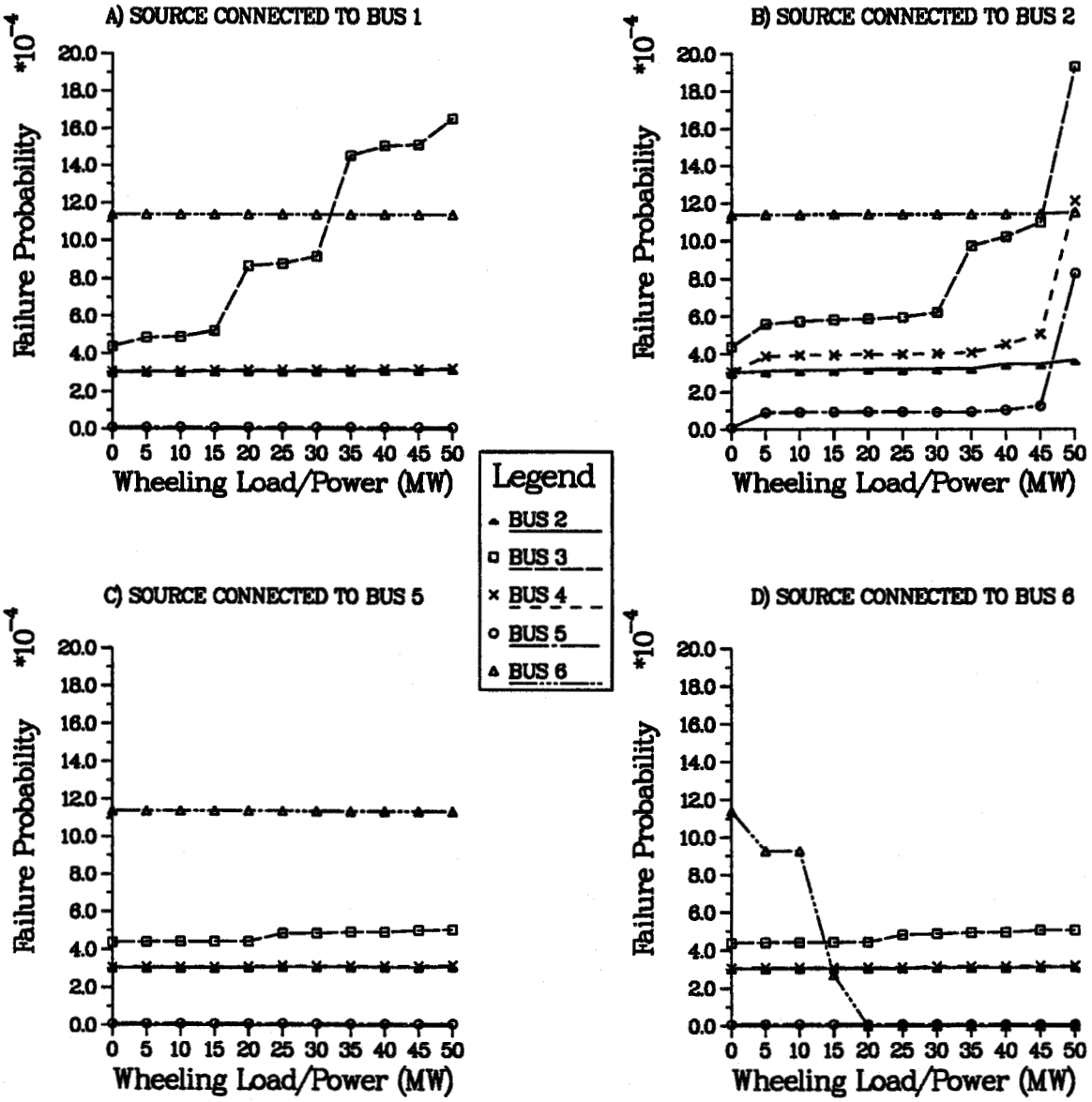

Figure 6.5: Variation In Load Point Failure Probability With Wheeling Power/load - Wheeling Sink Connected To Bus 3 Of The RBTS

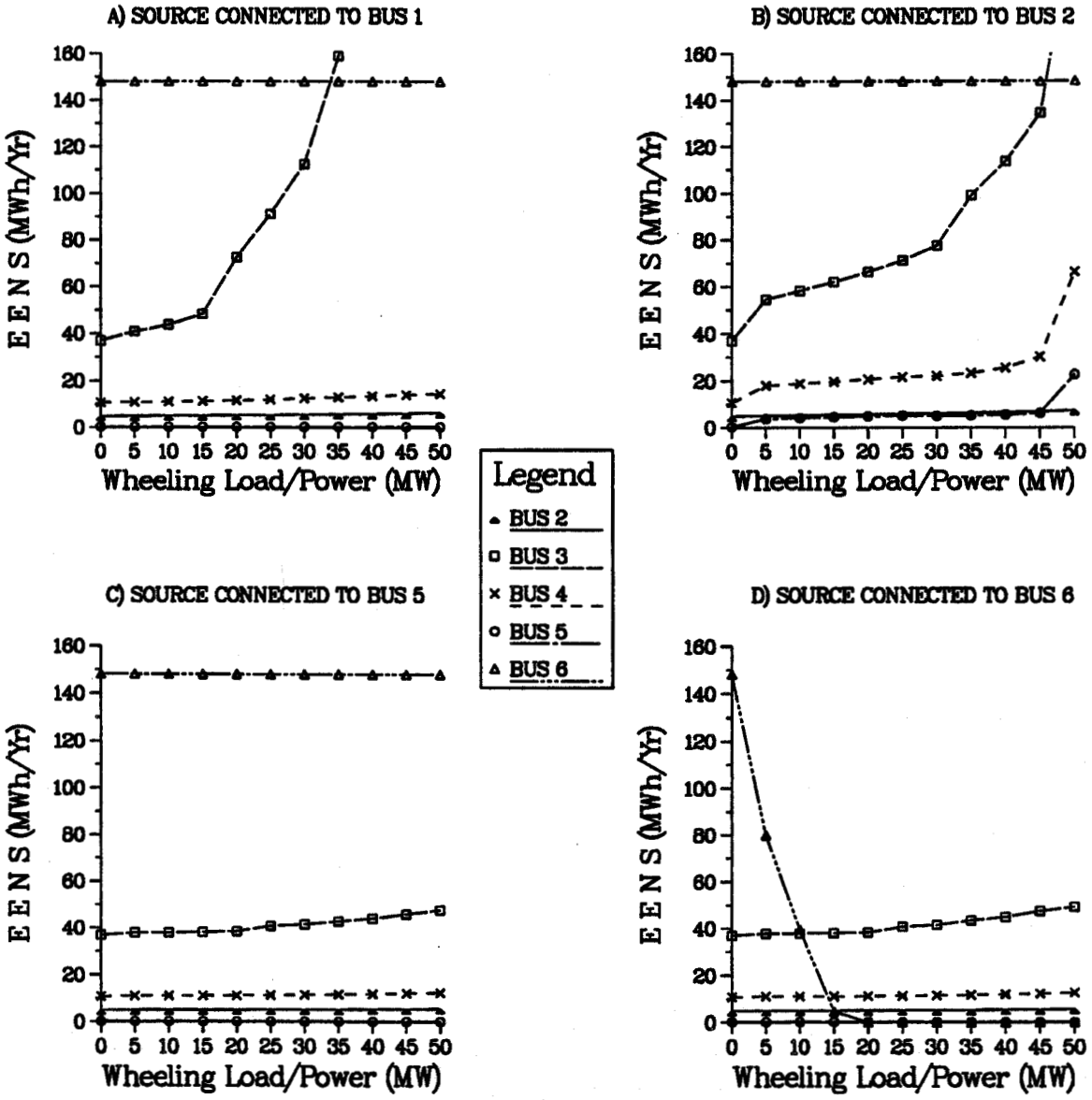

Figure 6.6: Variation In EENS At The Load Points With Wheeling Power/load - Wheeling Sink Connected To Bus 3 Of The RBTS

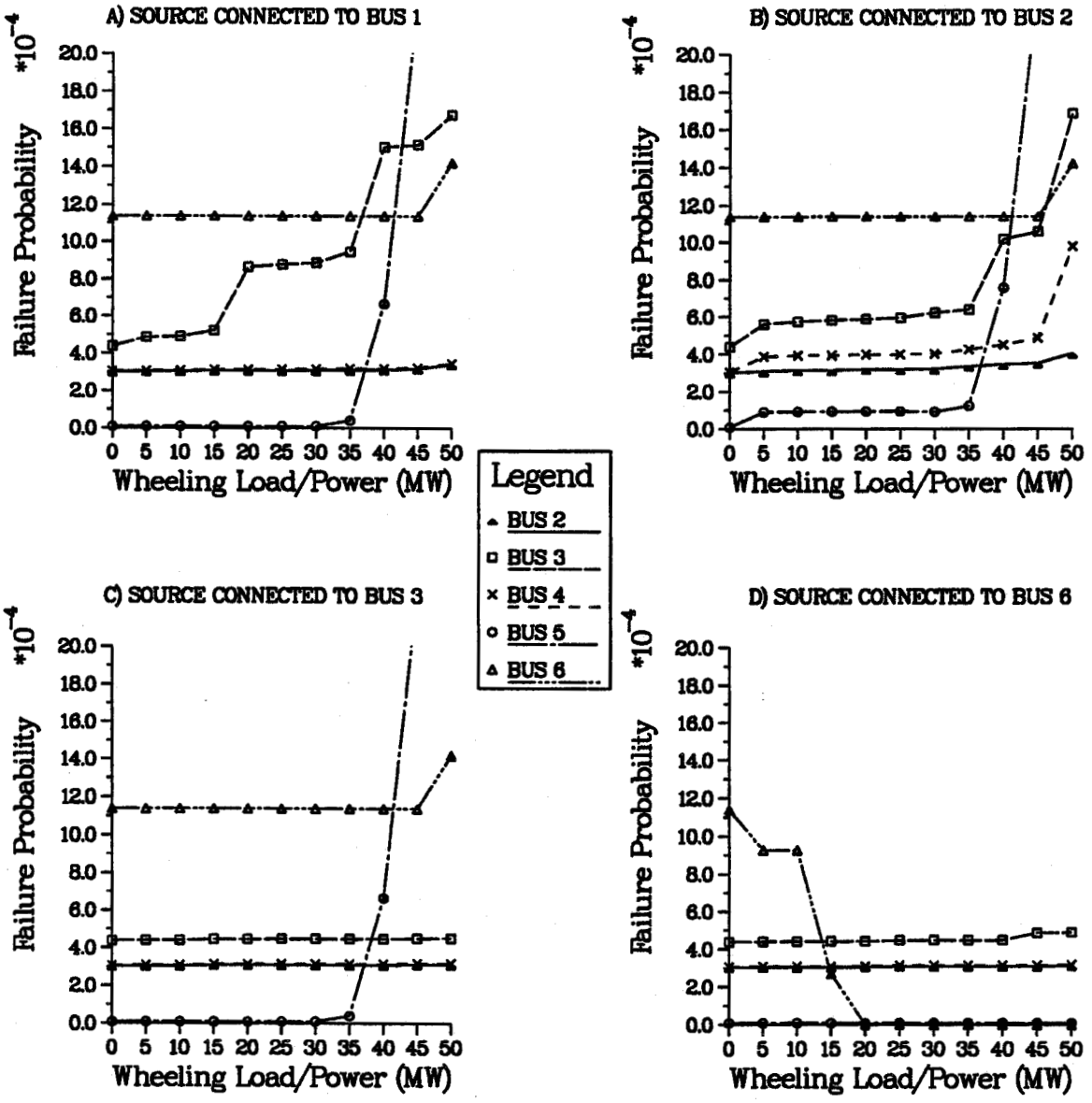

Figure 6.7: Variation In Load Point Failure Probability With Wheeling Power/load - Wheeling Sink Connected To Bus 5 Of The RBTS

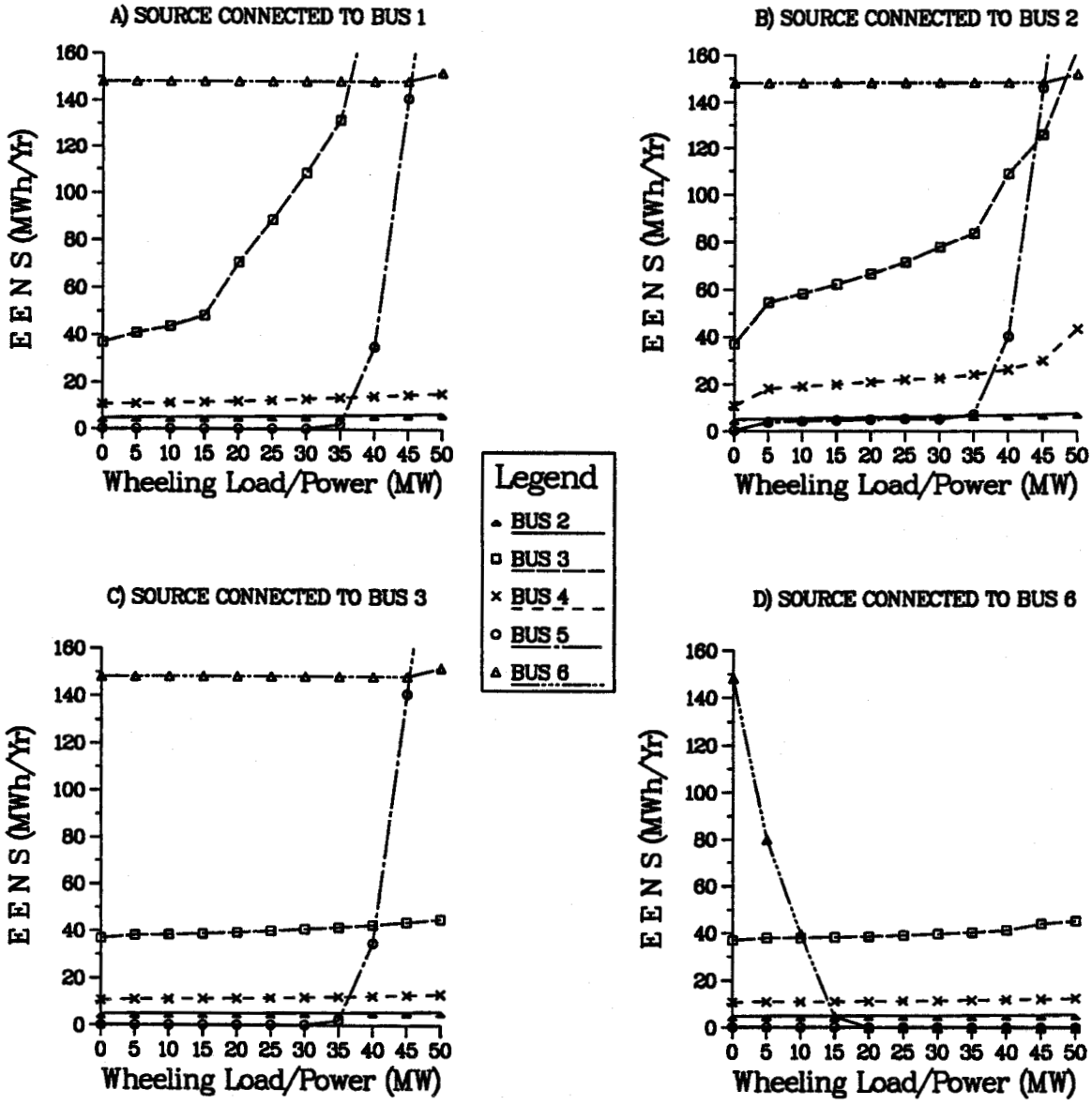

Figure 6.8: Variation In EENS At The Load Points With Wheeling Power/load - Wheeling Sink Connected To Bus 5 Of The RBTS

wheeling source is connected to buses 1, 3, 5 and 6. The relatively more efficient distribution of power flow achieved in the RBTS network as a result of these wheeling operations accounts for the system's ability to cope fairly well with the entire range of wheeling power considered.

Connection of the wheeling sink to either bus 3 or bus 5 also produces some effects on load point adequacy depending upon the point of interconnection of the wheeling source with the IPS. It should be noted that bus 3 alone accounts for over 50% of the load in the southern section of the RBTS. Therefore connecting the sink to that load point tends to increase the pressure on the transmission facilities required to transport power to that part of the system. This system condition accounts for the considerably higher inadequacy indices recorded at bus 3. As can be seen from Figures 6.5 and 6.6, the indices for bus 3 increase dramatically with wheeling power (load) particularly when the source is connected to the conventional generation locations. As expected, adequacy at bus 6 remains virtually unaffected throughout the wheeling scenario in all the cases, except when the source is connected to that load point.

6.4.1.2. Severity Index Variations

Figure 6.9 shows variations in the system severity index associated with the various wheeling operations. The figures labelled A, B and C show the results for wheeling operations with the sink connected to RBTS buses 2, 3 and 5 respectively.

The severity index variations determined for wheeling operations with the source connected to buses 1 and 2 can be seen in Figure 6.9 to be considerably higher for all cases compared to the results obtained for all the other wheeling operations examined. Wheeling from bus 6 resulted in an initial significant drop in the severity index up to the point of wheeling 15 MW of power, and then remained virtually constant at this level through the rest of the wheeling scenario. These observations are generally similar to those shown in Figure 5.14 for the intra-system wheeling operations.

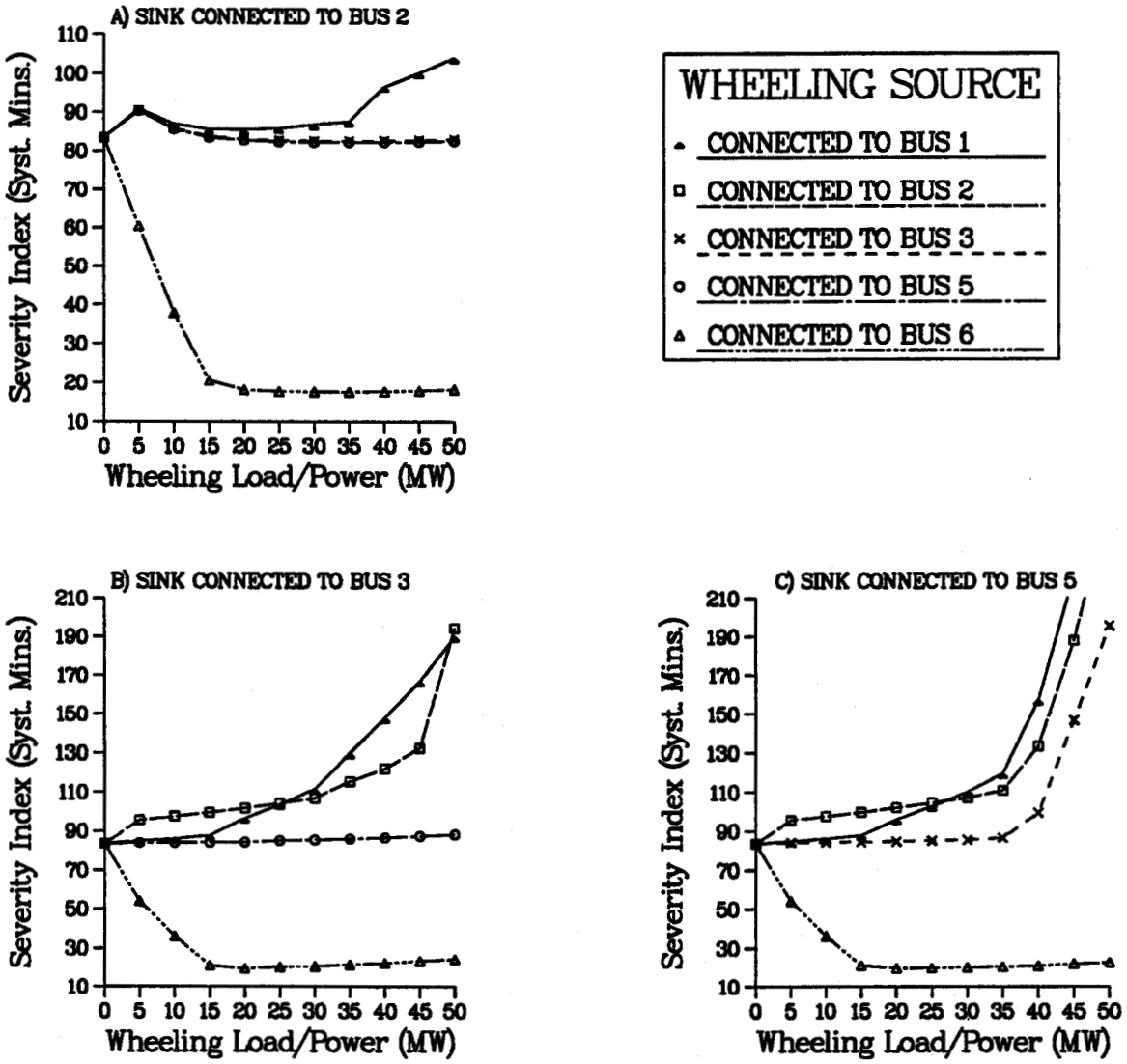

Figure 6.9: Variation In Severity Index With Wheeling Power/load For Wheeling Operations In The Interconnected RBTS

6.4.2. Results for the IEEE-RTS

6.4.2.1. Load Point Indices

The variations in the load point failure probability and EENS indices when up to 100 MW of power is wheeled through the interconnected IEEE-RTS are shown in Figures 6.10-6.17. Figures 6.10 and 6.11 show the impacts when the wheeling source and the sink are connected to buses 3 and 8 in the southern region of the test system. The impacts of similar wheeling operations involving buses 13 and 17 in the northern region are also shown in Figure 6.12 and 6.13.

A comparison of these two sets of results shows that both regions are able to accommodate the wheeling operations in their respective regions fairly well without significantly affecting the existing levels of adequacy at the load points in the neighbouring region. This agrees with the observations made with regard to the intra-system wheeling operations. The impact of wheeling operations in which the wheeling source and the sink are interconnected in separate regions of the IEEE-RTS are also shown in Figures 6.14-6.16. It can be observed that the worst impacts are experienced when the wheeling source is interconnected in the north region and the sink in the south region. This is because the southern region of the IEEE-RTS, under normal circumstances, is a net importer of power from the northern region. The connection of the sink to any point in the southern region therefore increases the region's dependency on supplies from the north. As a result, the provision of additional supplies to effectively satisfy the increased demand in the south tends to rely on the availability of sufficient composite generation and transmission capacity in the system, which is reflected in the calculated reliability indices.

It was noted in Chapter 5, that load points serving as wheeling sources generally experienced the most improvement in adequacy. The results of this analysis however show that this does not generally apply to wheeling in interconnected systems especially when the wheeling source is connected to pure load buses in the IPS. Referring to Figures 5.16-5.19 in Chapter 5 for example, a consistent drop in the value of the indices at bus 3 (or bus 8) is realised with increasing wheeling power when the load point is made a wheeling source and re-defined as a PV-bus. These improvements are, however, absent

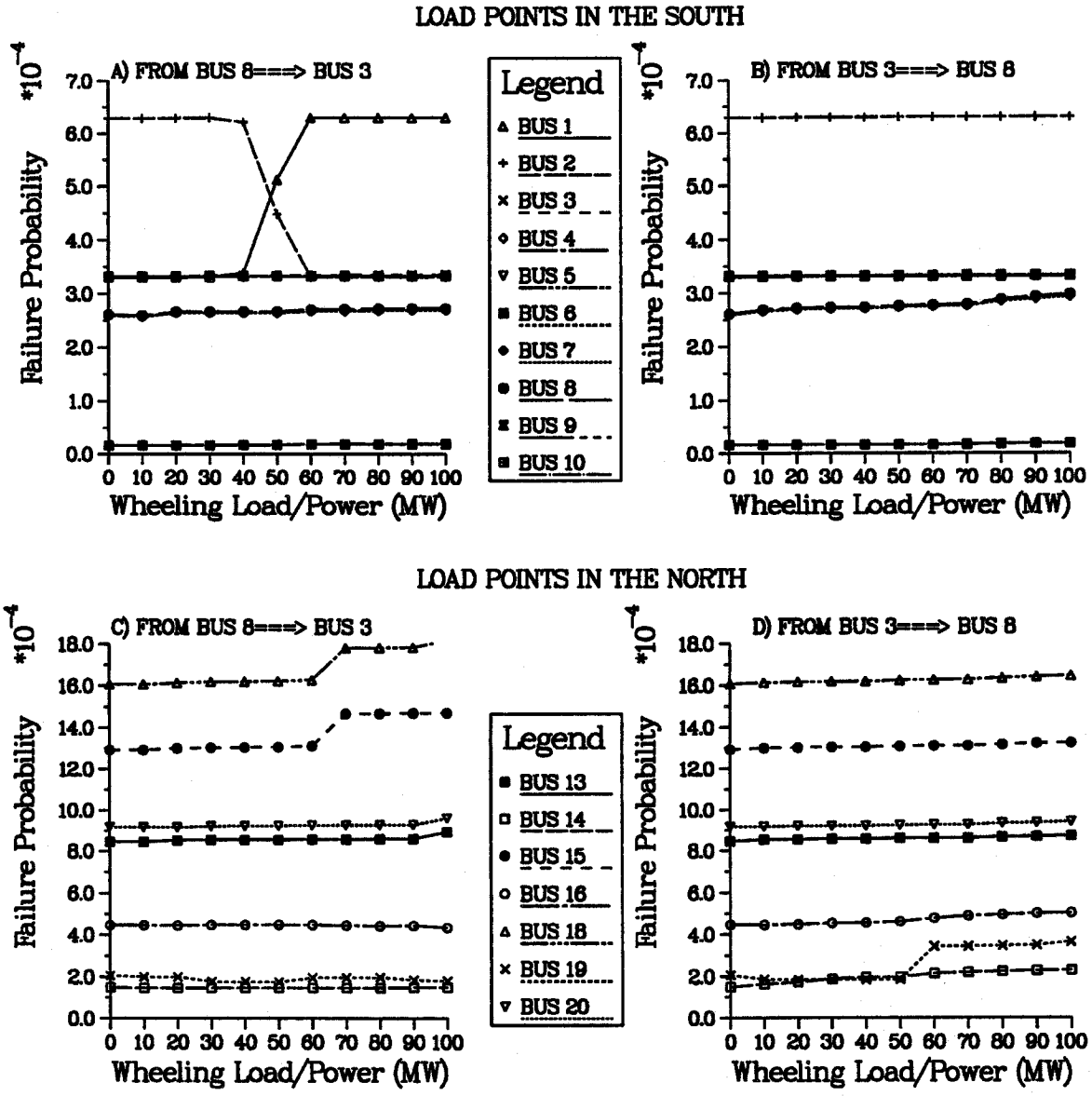

Figure 6.10: Variation In Load Point Failure Probability With Wheeling Power/load - Wheeling Interconnections In The South Region Of The IEEE-RTS

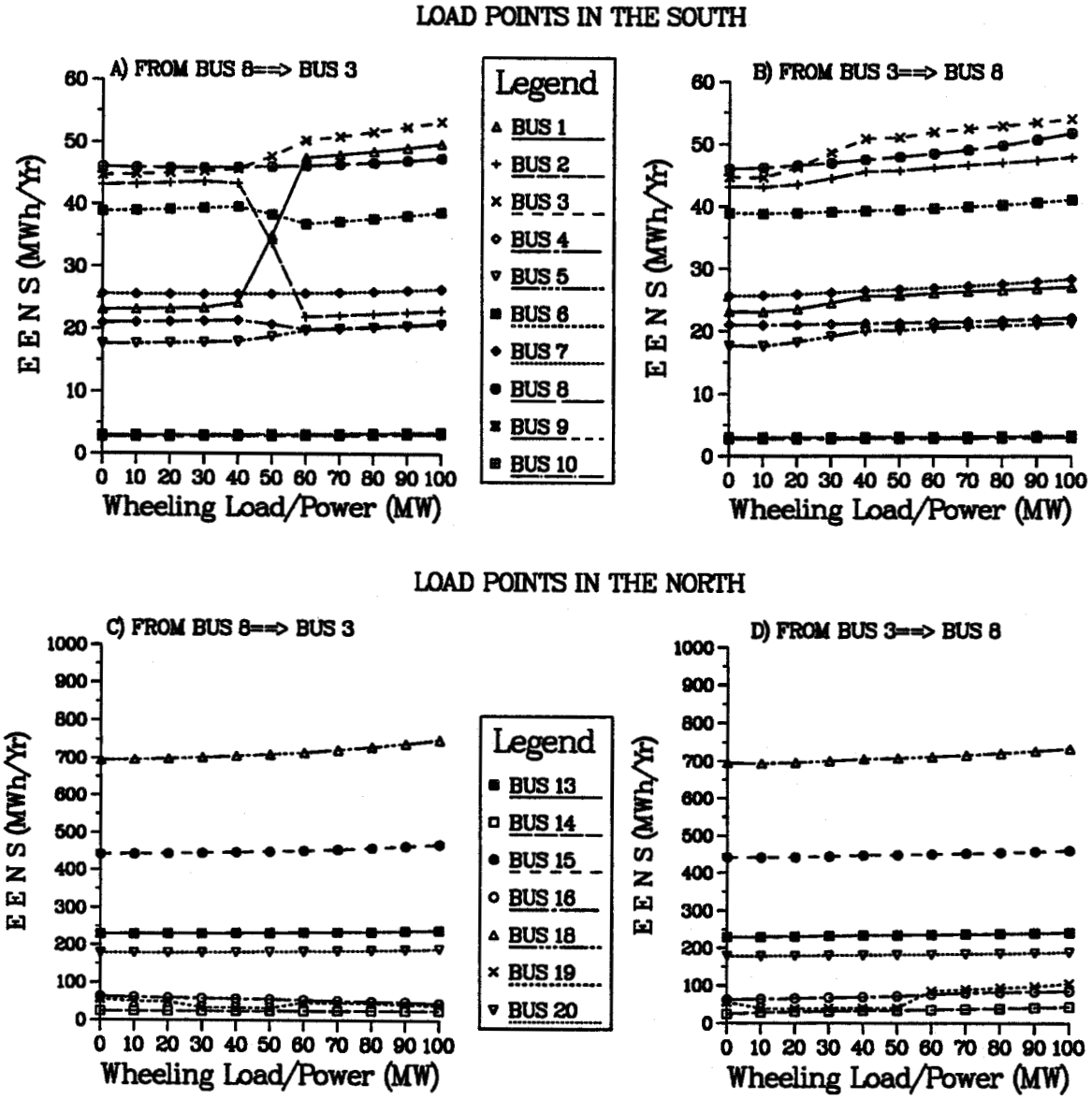

Figure 6.11: Variation In EENS At The Load Points With Wheeling Power/load - Wheeling Interconnections In The South Region Of The IEEE-RTS

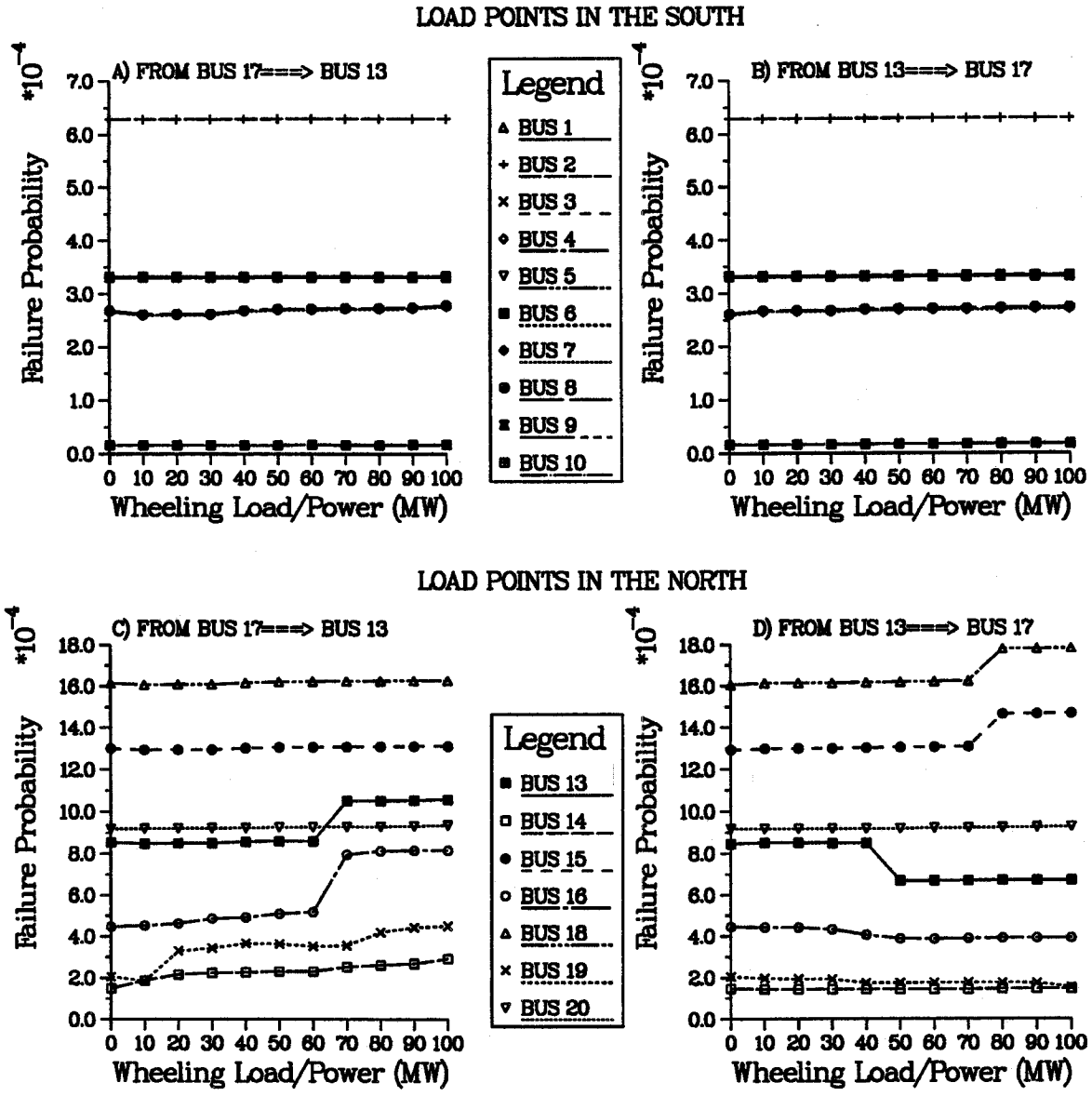

Figure 6.12: Variation In Load Point Failure Probability With Wheeling Power/load - Wheeling Interconnections In The North Region Of The IEEE-RTS

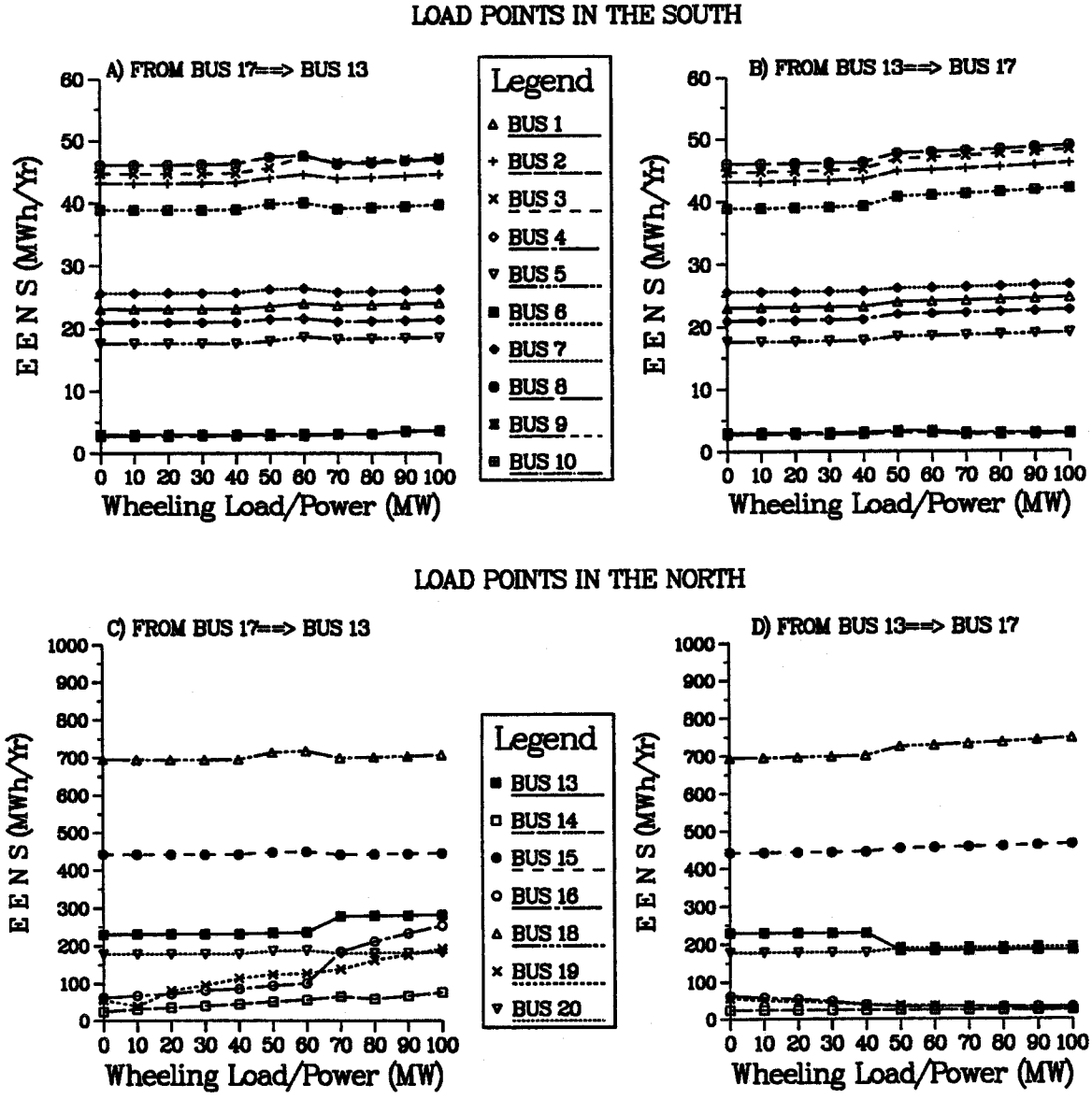

Figure 6.13: Variation In EENS At The Load Points With Wheeling Power/load - Wheeling Interconnections In The North Region Of The IEEE-RTS

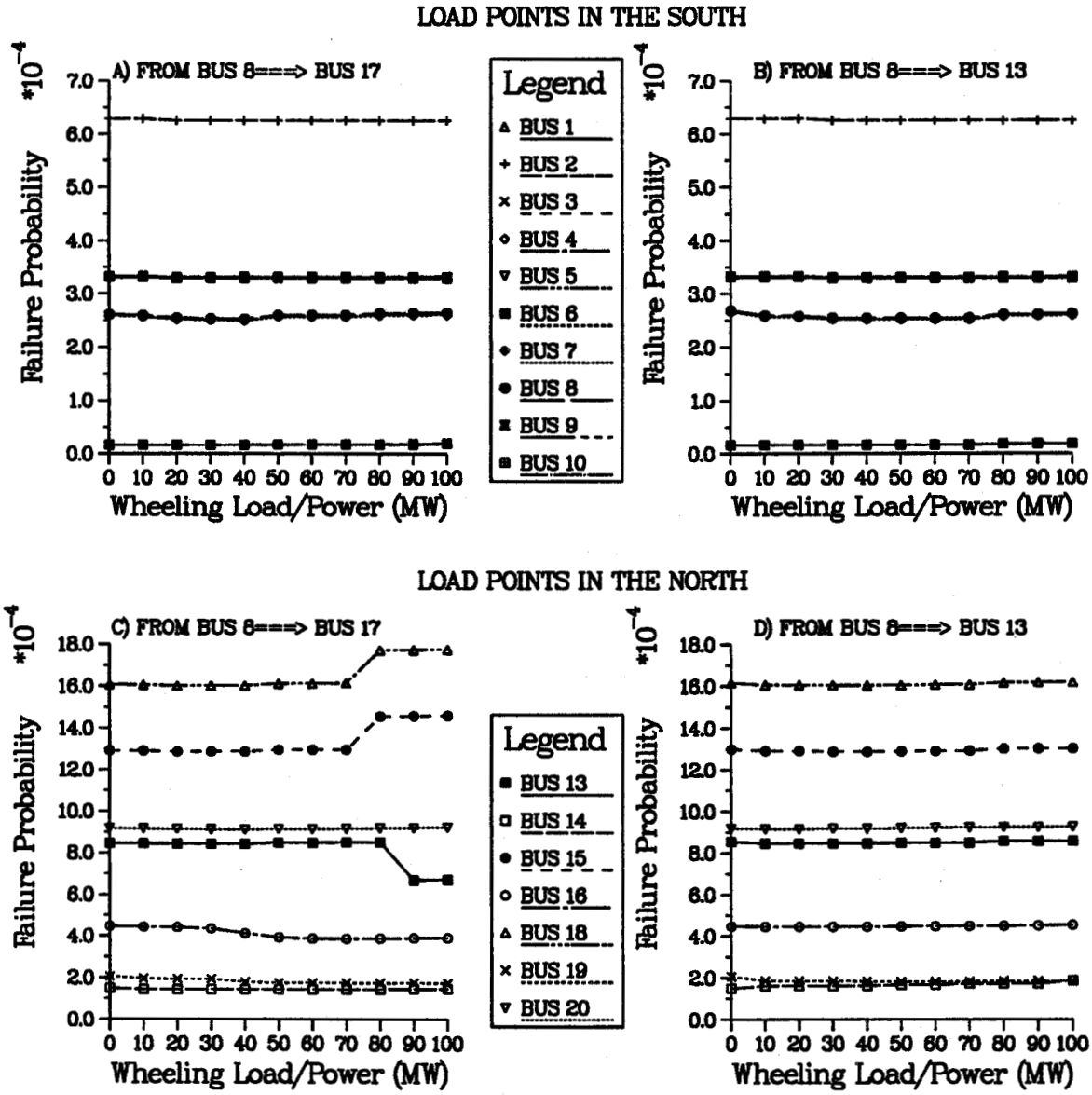

Figure 6.14: Variation In Load Point Failure Probability With Wheeling Power/load - Wheeling Source Connected In The South Region And Wheeling Sink Connected In The North Region Of The IEEE-RTS

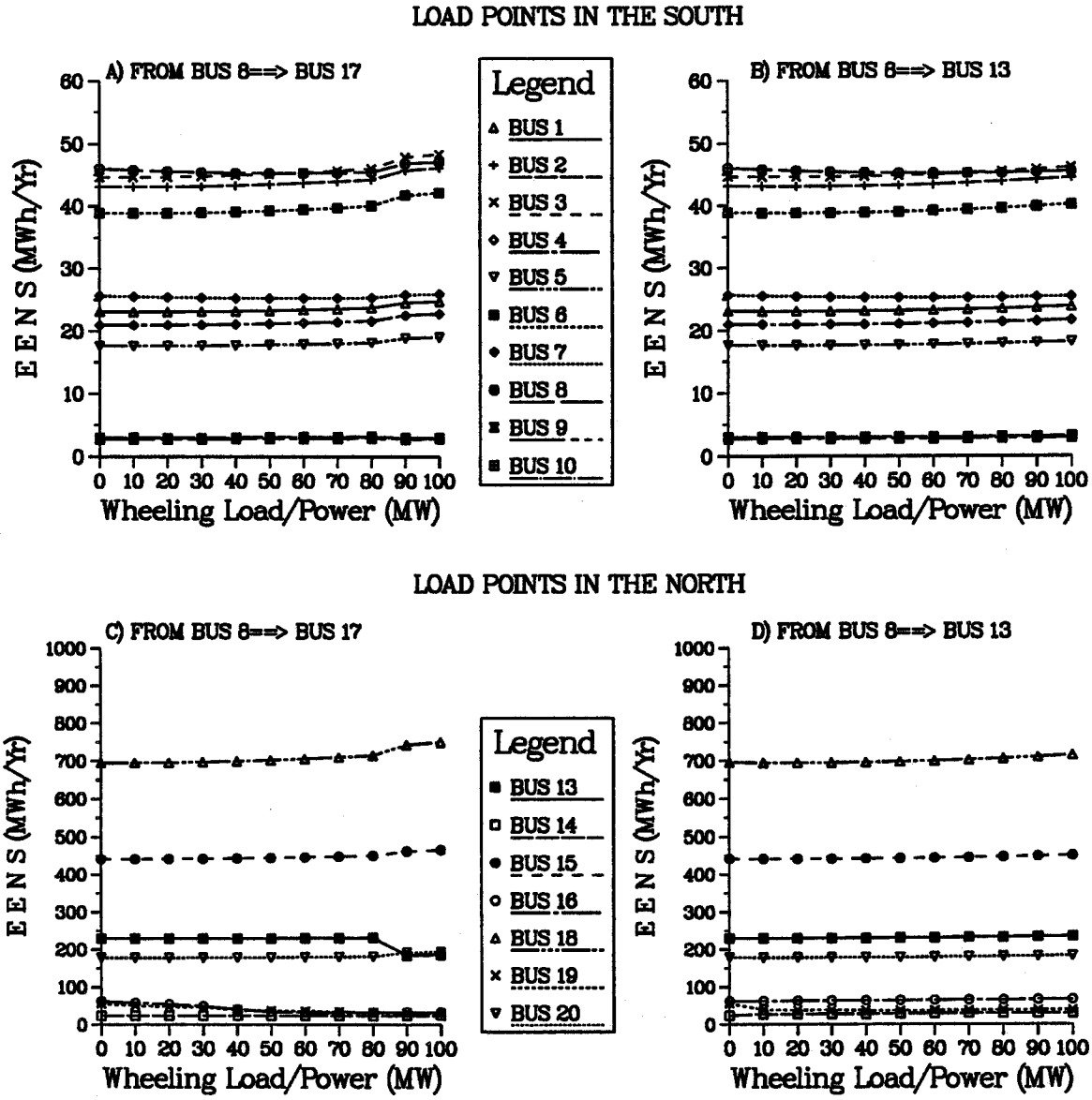

Figure 6.15: Variation In EENS At The Load Points With Wheeling Power/load - Wheeling Source Connected In The South Region And Wheeling Sink Connected In The North Region Of The IEEE-RTS

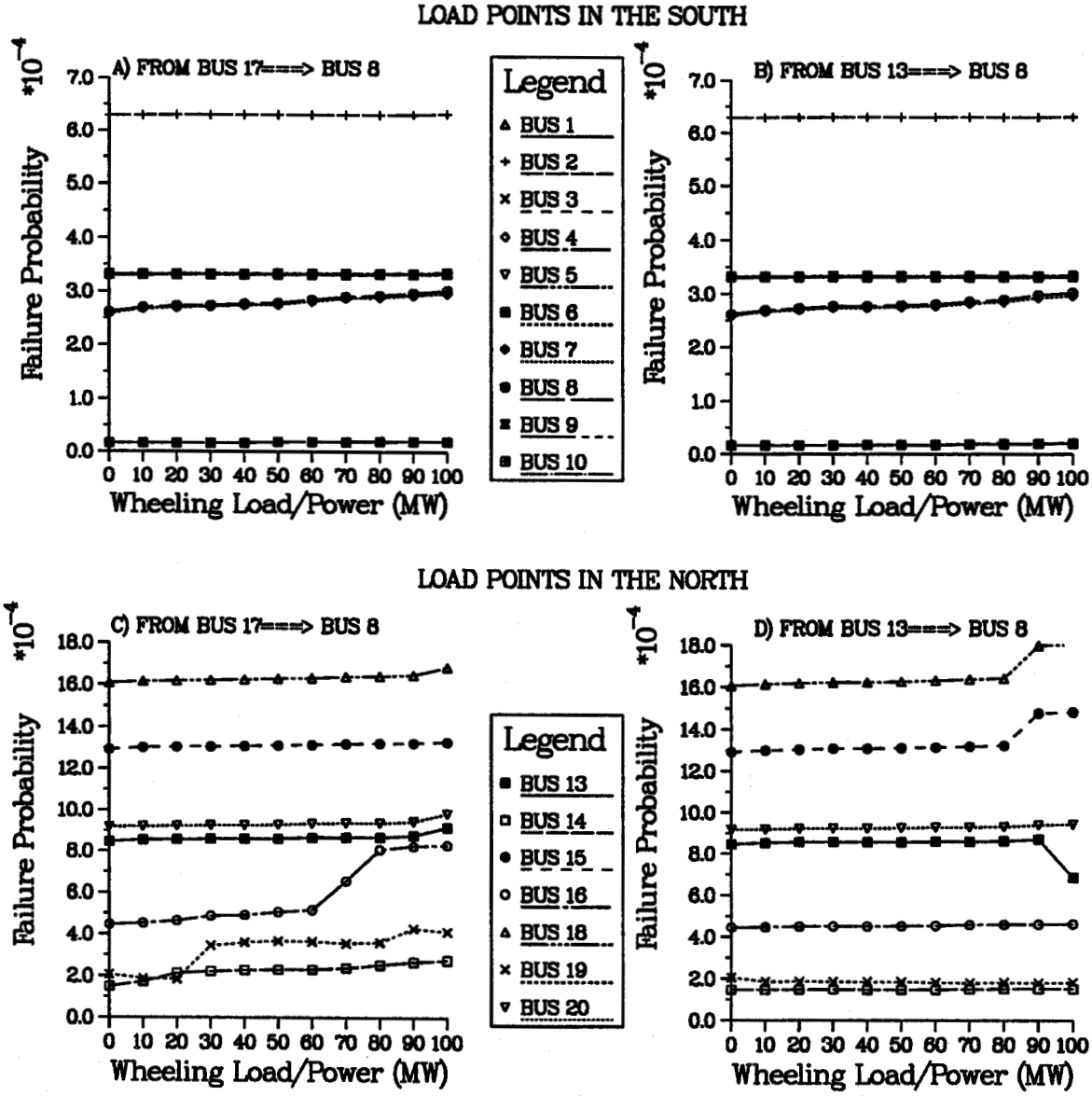

Figure 6.16: Variation In Load Point Failure Probability With Wheeling Power/load - Wheeling Source Connected In The North Region And Wheeling Sink Connected In The South Region Of The IEEE-RTS

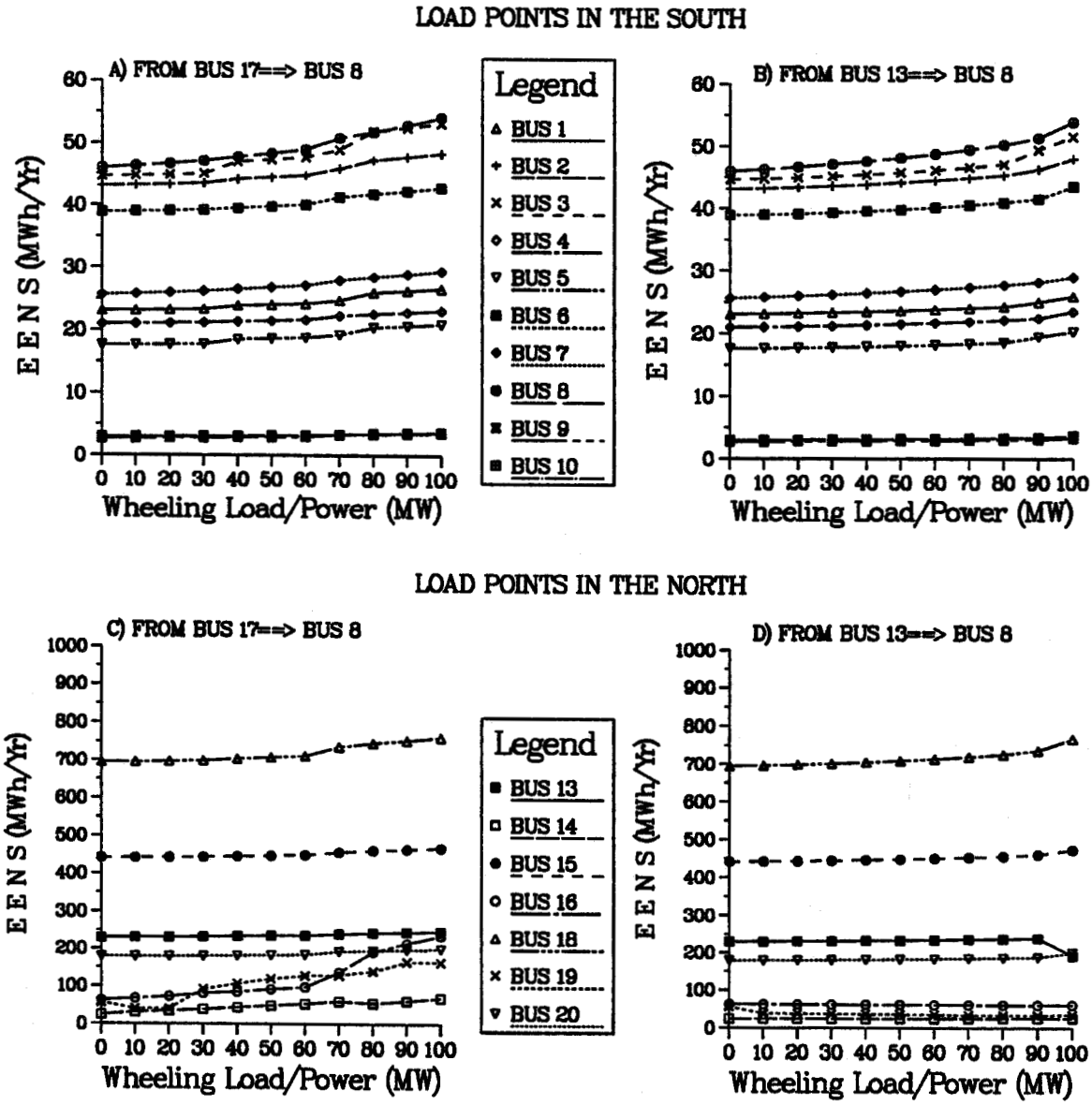

Figure 6.17: Variation In EENS At The Load Points With Wheeling Power/load - Wheeling Source Connected In The North Region And Wheeling Sink Connected In The South Region Of The IEEE-RTS

from Figures 6.10 and 6.11 when the buses retain their PQ-bus characteristics and are directly connected to the wheeling source as required in the interconnected systems analysis. The connection of the wheeling sink to a load point however leads to a deterioration in adequacy at the load point as noted previously.

6.4.2.2. Severity Index Variations

The severity index variations obtained for the different wheeling operations in the interconnected IEEE-RTS are shown in Figures 6.18-6.20.

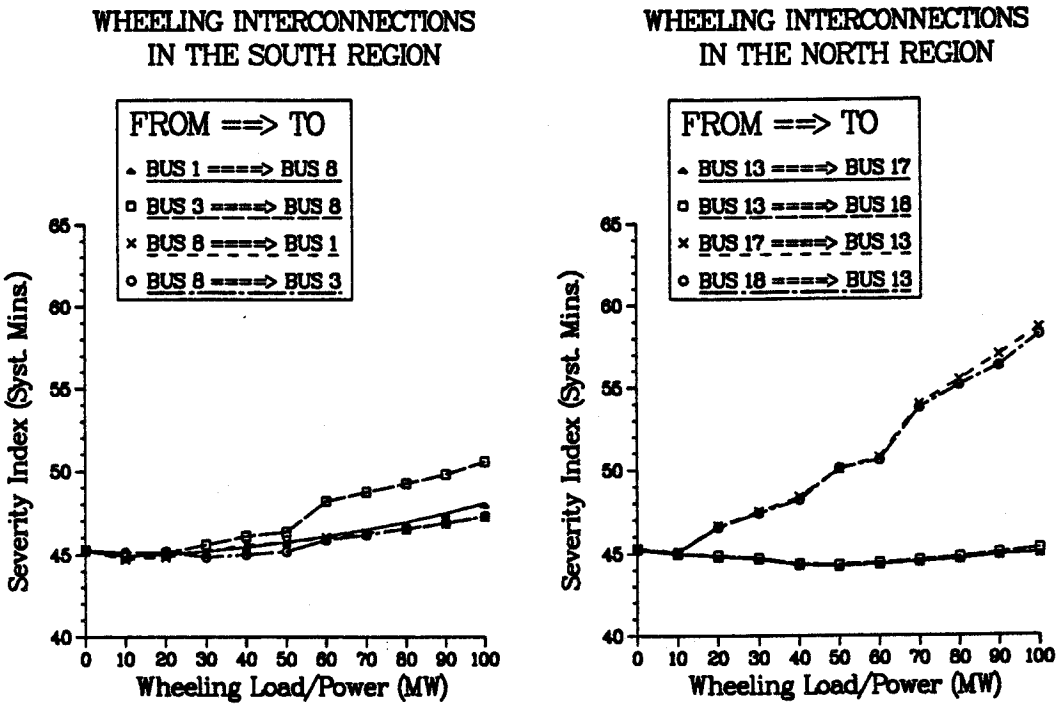

Figure 6.18: Variation In Severity Index With Wheeling Power/load For Wheeling Operations Within The North And South Regions Of The IEEE-RTS

The trends obtained are similar to those discussed for the intra-system wheeling operations and are mainly influenced by the proximity of the wheeling source (or load) to the swing bus (i.e. bus 23). It can be seen from Figure 6.18 that wheeling operations in which the sink is connected close to the swing bus (i.e. buses 8 and 13) produced the most adverse impacts on overall system adequacy. Conversely, the lowest severity index values result when the wheeling source is interconnected at a point close to the swing bus.

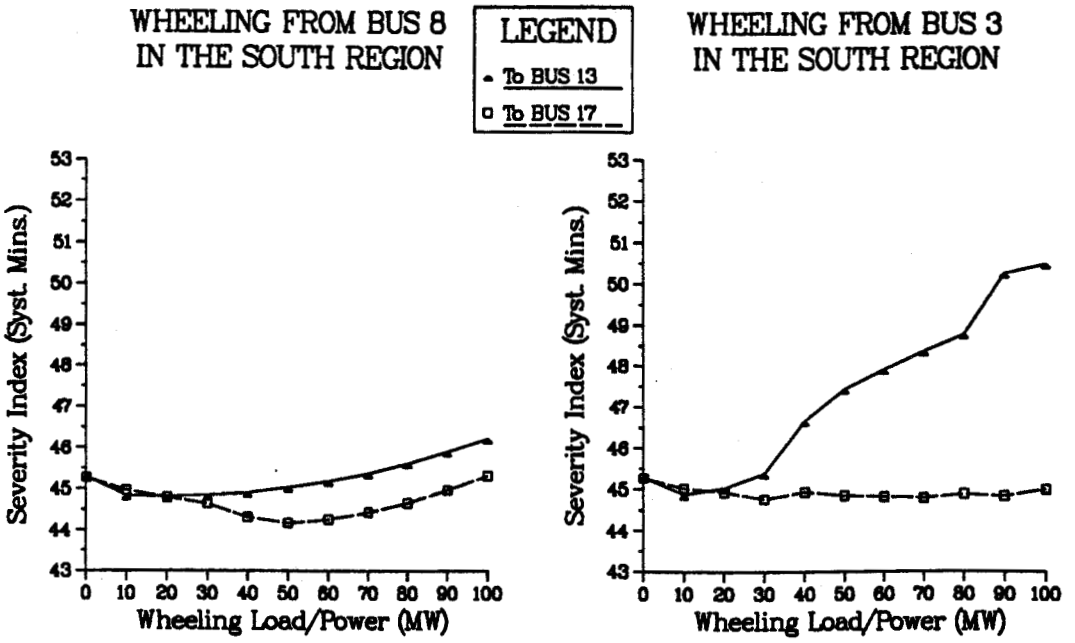

Figure 6.19: Variation In Severity Index With Wheeling Power/load For Wheeling Operations With The Source Connected To The South Region And The Sink Connected To The North Region Of The IEEE-RTS

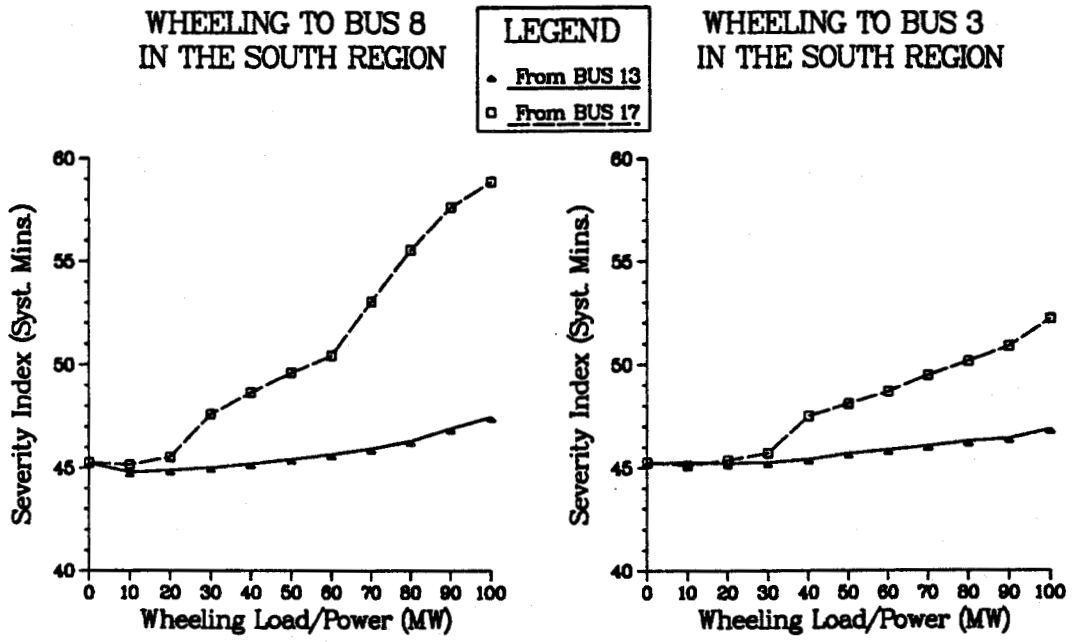

Figure 6.20: Variation In Severity Index With Wheeling Power/load For Wheeling Operations With The Source Connected To The North Region And The Sink Connected To The South Region Of The IEEE-RTS

6.5. Sensitivity Analysis

6.5.1. Effects on Wheeling Impacts of Varying the Peak Load of the Intermediate Power System

Sensitivity studies were performed to determine the effect on the severity or intensity of the wheeling impacts of varying the peak load in the intermediate power system. The load at various load points in the test systems was varied proportionally to realise a suitable range of system peak load values and the wheeling analysis was then repeated in each case to determine the impact on the severity index. The severity index values computed are compared with similar values obtained for the IPS when it is not interconnected and not engaged in any wheeling transactions (i.e. stand-alone system). Wheeling operations resulting in severity index values lower than that of the stand-alone system are considered to be favourable whilst those producing higher values can be considered to be unfavourable to the IPS.

The results shown in Figures 6.21 and 6.22 represent the wheeling effects on the severity index of the interconnected RBTS when operated at a range of peak load levels. The results of similar wheeling analyses involving the IEEE-RTS are shown in Figures 6.23 and 6.24.

From Figures 6.21 it can be observed that the severity index values obtained beyond 15 MW of power wheeling are lower than those obtained for the stand-alone RBTS when operating at any of the peak load levels considered. Similar results were obtained for the IEEE-RTS given wheeling power does not exceed 70-80 MW in the wheeling operations shown in Figure 6.23. Furthermore, it can be observed from both figures that the adequacy gains resulting from the wheeling transactions increase as the peak load level increases. It can therefore be concluded that wheeling options that are favourable to the IPS generally tend to be more attractive and beneficial when the IPS is subjected to higher system load stress.

On the other hand, Figures 6.22 and 6.24 respectively show typical results of wheeling transactions whose impacts adversely affect the level of adequacy in the

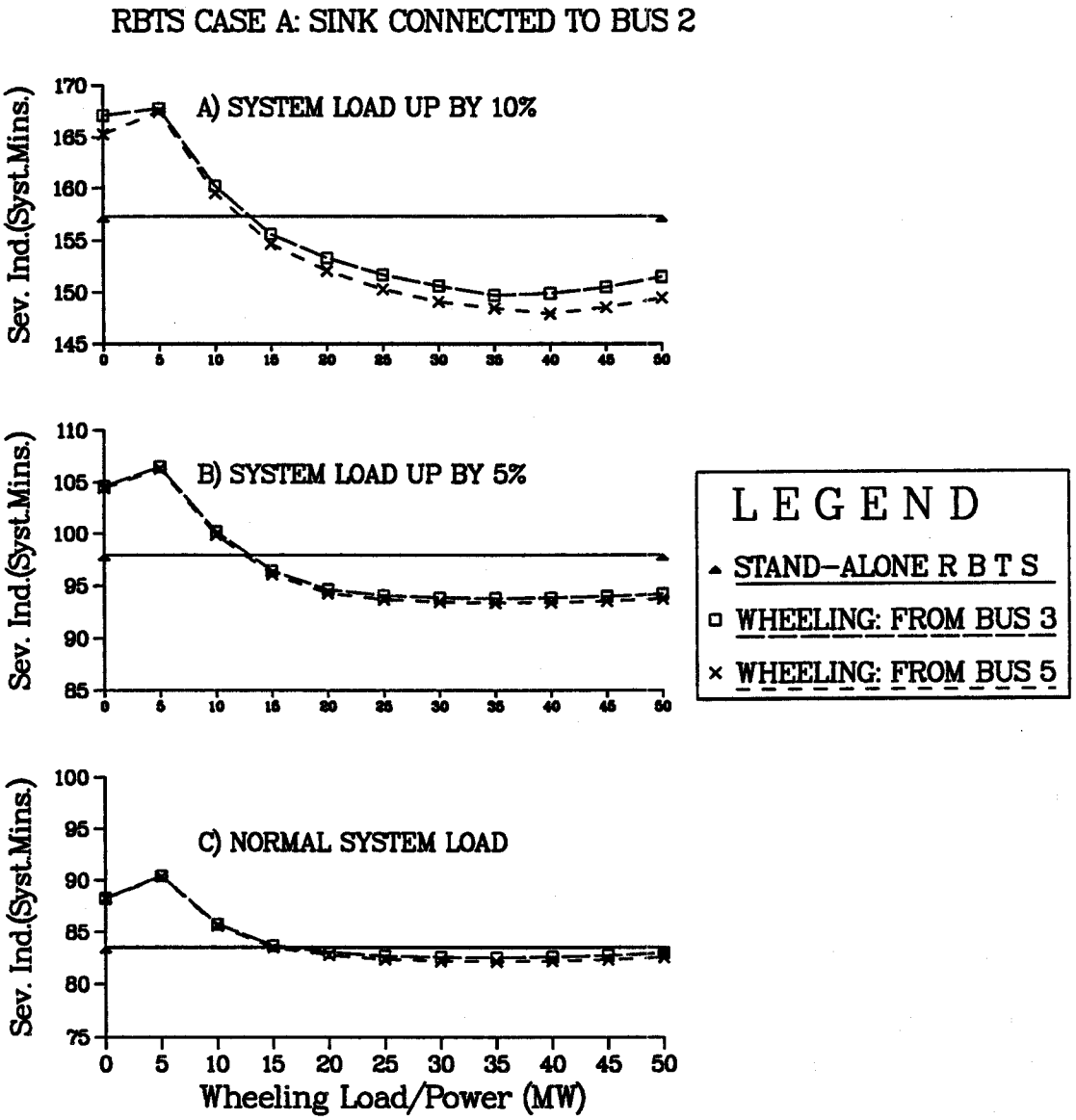

Figure 6.21: Sensitivity Study - RBTS Case A: Comparison Of Severity Index Variation With Wheeling Power/load At Varying IPS Peak Load Levels

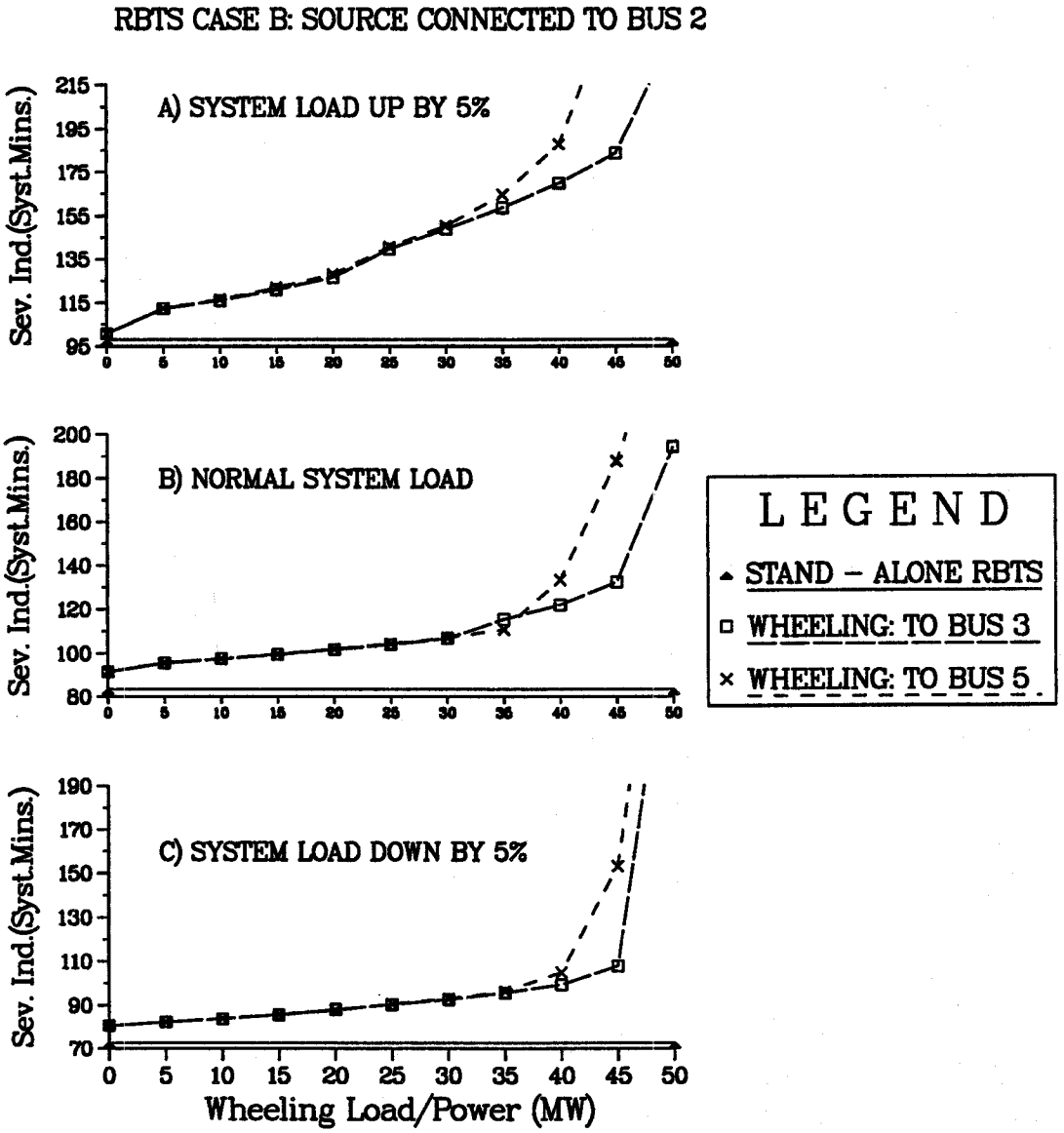

Figure 6.22: Sensitivity Study - RBTS Case B: Comparison Of Severity Index Variation With Wheeling Power/load At Varying IPS Peak Load Levels

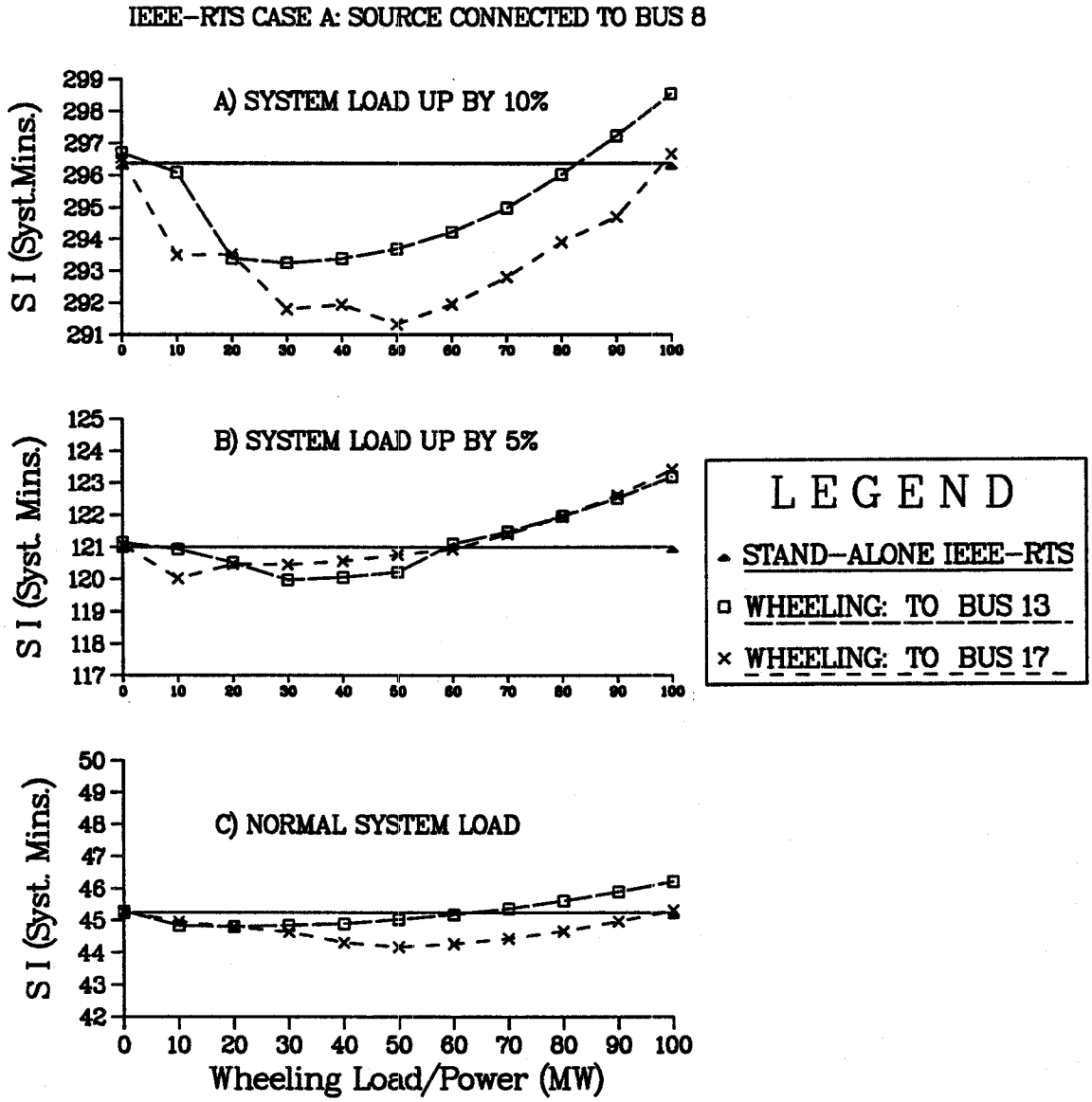

Figure 6.23: Sensitivity Study - IEEE-RTS Case A: Comparison Of Severity Index Variation With Wheeling Power/load At Varying IPS Peak Load Levels

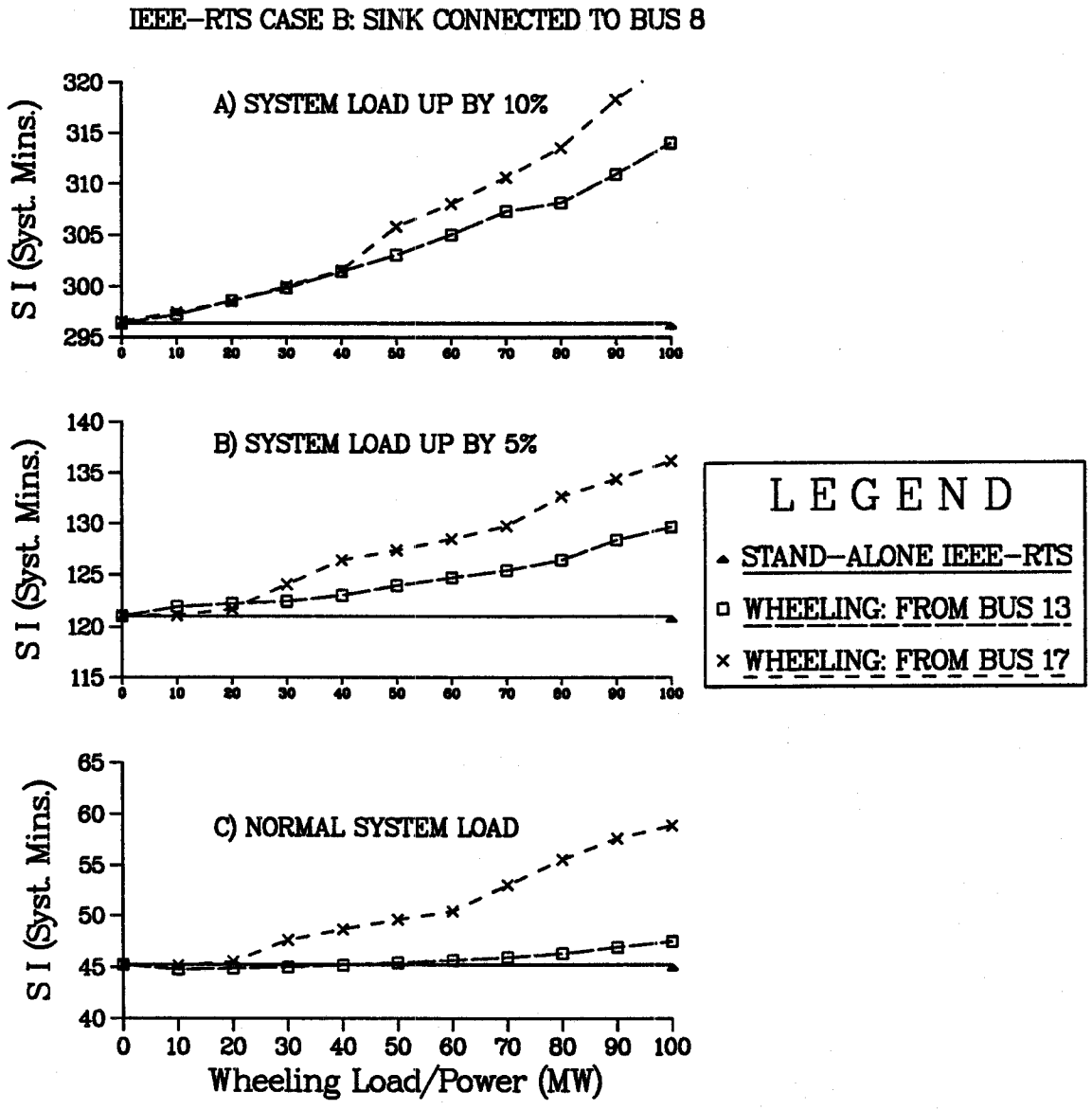

Figure 6.24: Sensitivity Study - IEEE-RTS Case B: Comparison Of Severity Index Variations With Wheeling Power/load At Varying IPS Peak Load Levels

interconnected RBTS and the IEEE-RTS. These transactions are therefore regarded as unfavourable wheeling options. It can be seen from both figures that the severity index values increase steadily with wheeling power, and consistently remain above the corresponding stand-alone system values. The rate at which the severity index increases with the wheeling power is generally not uniform, but can be observed to be higher at higher system load levels. This is expected because at higher system loads, the deterioration in overall system adequacy is intensified due to increased transmission capacity constraints which are reflected in the reliability indices.

6.6. Summary

The concept of power wheeling in interconnected systems has been introduced in this chapter. Methods for modelling this type of wheeling situation in composite system analysis have been presented and utilised. These methods were used, together with the COMREL program, to determine the impacts of wheeling on the composite reliability indices of the system providing the wheeling service (i.e. the IPS)

The impacts of power wheeling in the interconnected system were found to be similar to the impacts associated with intra-system power wheeling. Different impacts on load point and overall composite system indices are produced by different wheeling options. The reliability impacts associated with a particular wheeling option can either be favourable or unfavourable to the IPS depending upon the composite generation and transmission configuration of the system. Sensitivity studies performed show that wheeling options that have the potential to reduce the level of overall system inadequacy are generally more attractive and more beneficial to the IPS at higher peak load levels.

7. SUMMARY AND CONCLUSIONS

Composite system adequacy evaluation of a power system involves an assessment of the adequacy of the combined generation and transmission facilities in regard to their ability to supply adequate, dependable and suitable electrical energy to the major load points. One of the main objectives of the work described in this thesis was to provide a general review of the methods used for composite system adequacy analysis and to highlight the major differences, advantages and limitations associated with the methods.

In Chapter 2, several computer programs currently available for composite system analysis are cited [1-9] and briefly examined. These programs were classified as being based either on the analytical approach, which usually employs the contingency enumeration technique, or on Monte Carlo simulation. The analytical models produce exact solutions, but the simplifying assumptions normally required for analytical tractability limits their ability to effectively represent complex systems. Monte Carlo methods, on the other hand, are flexible and can allow easy incorporation of complex system features; but only provide estimates of the expected values of the indices. Two computer programs developed at the University of Saskatchewan and used in the research work described in this thesis are also described in this chapter. The COMREL program is based on the contingency enumeration technique whilst the MECORE program utilises the random sampling approach typical of Monte Carlo methods.

The COMREL and MECORE programs were utilised in Chapter 3 to compute the composite system reliability indices for two test systems, the Roy Billinton Test System (RBTS) and the IEEE-Reliability Test System (RTS), in order to illustrate the features associated with the two methods for composite system adequacy analysis and to provide a comparative test of the programs and techniques. The 6-bus RBTS is a relatively small

system developed for educational purposes at the University of Saskatchewan. The 24-bus IEEE-RTS is a much larger and relatively more complex system with characteristics approaching those of a practical power system.

The results of the studies conducted show the MECORE program to be more effective computationally in the analysis of the more complex IEEE-RTS. The COMREL program was however more effective computationally in the analysis of the RBTS because of that system's simplicity and the reduced number of system states involved. It can be concluded from the studies performed that depending on a number of factors including system complexity, the required level of accuracy and the computational facilities available, one method may be found to be more appropriate and generally more convenient than the other. Recent developments in computer programs for composite system analysis seek to combine the best features of each of the two methods [7, 9, 45] in order to create more efficient computational tools.

A second major objective of this research work was to investigate the composite system reliability impacts associated with Non-Utility Generation (NUG) and power wheeling transactions in power utility systems. This has not been previously examined and there is no evidence of any detailed study available in the literature. It is believed that quantification of the reliability impacts can provide an important insight into the positive and negative aspects of NUGs and power wheeling and enhance the existing methods used in the power industry for evaluating these options.

System studies are described in Chapter 4 of this thesis which utilise the COMREL and the MECORE programs to determine the impact of NUGs on the composite system adequacy indices of the RBTS and the IEEE-RTS. The results obtained show that the introduction of NUGs at different locations in the utility system have different impacts on load point and overall system adequacy depending upon the existing composite utility generation and transmission configuration. The results also indicate that NUGs can serve as suitable alternatives to conventional power system reinforcement in the form of utility generation and transmission facilities. A comparison of the results obtained from the two programs illustrate that a power utility's operational practices and philosophies, such as the load curtailment policy, can have considerable influence on the benefits accruing

from the NUG facilities. The influence is most significant when the adequacy of the system load points are determined.

Intra-system and inter-system power wheeling concepts are introduced in Chapters 5 and 6 respectively. Methods for modelling each type of wheeling condition are presented. These methods were used together with the COMREL program to determine the impact on the composite system indices of the RBTS and the IEEE-RTS.

The reliability impacts associated with intra-system and inter-system wheeling were found to be similar in several respects. The results obtained for both cases indicate that different impacts on load point and overall system indices are produced by different wheeling options. Depending upon the relative locations of the wheeling source and the wheeling sink (in the utility system), the wheeling impact can either lead to an improvement or a deterioration in load point adequacy or overall system adequacy or may not significantly affect the indices of the utility system. Utility system load points that are directly involved in the wheeling operations are the ones mostly affected. Sensitivity studies performed show that wheeling options that have the potential to reduce the level of overall system adequacy are generally more attractive and beneficial to the utility system when operating at higher peak load levels.

In conclusion, the results of the studies conducted in this thesis show that NUGs operation and wheeling transactions can have considerable reliability impacts on utility systems. The energy related indices such as the expected energy not supplied index and the severity index are the most responsive indices for measuring these impacts. It is possible to use these indices as a basis to evaluate the reliability worth associated with NUGs and wheeling options. Finally, it can be concluded that understanding the reliability performance at the different locations within the utility system and of the entire system is an important requirement which should be satisfied prior to embarking on the utilisation of NUGs and wheeling options.

REFERENCES

1. DeSieno, C.F and Stine, L.L., "A Probabilistic Method for Determining the Reliability of Electric Power Systems", *IEEE Transactions on Power Apparatus and Systems, Vol. PAS-83*, February 1964, pp. 174-181.

2. Noferi, P.L., Paris, L. and Salvaderi, L., "Monte Carlo Methods for Power System Reliability Evaluation in Transmission or Generatiion Planning", *Proceedings 1975 Reliability and Maintainability Symposium, Washington DC,* .

3. Dodu, J.C. and Merlin, A., "An Application of Linear Programming to the Planning of Large Scale Power System: The MEXICO Model", *Proceedings of the 5th PSCC, Cambridge, England*, September 1975.

4. Marks, G.E., "A Method of Combining High Speed Contingency Load Flow Analysis with Stochastic Probability Methods to Calculate a Quantitative Measure of Overall Power System Reliability", *IEEE PES Winter Power Meeting, New York*, January 1978.

5. Meliopoulos, A.P., "Bulk Power System Reliability Assessment with the RECS Program", *Proceedings 1985 PICA Conference*, , pp. 38-46.

6. Cunha, S.H.F., Pereira, M.V.F., Oliveira, G.C. and Pinto, L.M.V.G., "Composite Generation and Transmission Reliability Evaluation in Large Scale Hydroelectric Systems", *IEEE Transactions on Power Apparatus and Systems, Vol. PAS-104, No.10*, October 1985, pp. 2657-2663.

7. Pereira, M.V.F. and Pinto, L.M.V.G., "A New Computational Tool for Composite System Reliability Evaluation", *IEEE PES Summer Meeting, San Diego, Paper No.91 SM 443-2 PWRS*, July/August 1991.

8. Billinton, R., "Composite System Adequacy Assessment - The Contingency Enumeration Approach", *IEEE (Power Engineering Society) Tutorial Course, Course Text 90EH0311-1-PWR: Reliability Assessment of Composite Generation and Transmission Systems*, 1989, pp. 29-35.

9. Billinton, R. and Li, W., "A Novel Method for Incorporating Weather Effects in Composite System Adequacy Evaluation", *IEEE Transactions on Power Systems, Vol. .6, No.3*, August 1991, pp. 1154-1160.

10. Mukeri, R., Neugebauer, W., Ludorf, R.P. and Catelli, A., "Evaluation of Wheeling and Non-Utility Generation (NUG) Options Using Optimal Power Flows", *IEEE Power Engineering Review, Vol. 12, No.2*, February 1992.

11. Grover, M.S. and Billinton, R., "Substation and Switching Station Reliability Evaluation", *CEA Transactions Vol. 13 (Pt 3), Paper No.74-SP-153*, 1974.

12. Grover, M.S. and Billinton, R., "A Computerised Approach to Substation and Switching Station Reliability Evaluation", *IEEE Transactions on Power Apparatus and Systems, Vol. PAS-93, No. 5*, Sept./Oct. 1974, pp. 1488-1497.

13. Billinton, R. and Medicherla, T.K.P., "Station Originated Multiple Outages in the Reliability Analysis of a Composite Generation and Transmission System", *IEEE Transactions on Power Apparatus and Systems, Vol. PAS-100, No. 8*, August 1981, pp. 3870-3878.

14. Ford, L.R. and Fulkerson, D.R., *Flows in Network,* Princeton Universty Press, N.J., 1962.

15. Billinton, R. and Allan, R.N., *Reliability Evaluation of Engineering Systems,* Plenum Press, New York, 1983.

16. Singh, C. and Billinton, R., *System Reliability Modelling and Evaluation,* Hutchinson & Co.(Publishers) Ltd, 3 Fitzroy Square, London W1, 1977.

17. Endrenyi, J., *Reliability Modelling in Electric Power Systems,* Marcel Dekker, Inc., 270 Madison Avenue, New York, NY. 10016, 1987.

18. Billinton, R. and Allan, R.N., *Reliability Evaluation of Power Systems,* Plenum Press, New York & London, 1984.

19. Billinton, R., "Composite System Reliability Evaluation", *IEEE Transactions on Power Apparatus and Systems, Vol. PAS-88, No. 4*, April 1969, pp. 276-281.

20. Rubinstein, R.Y., *Simulation and the Monte Carlo Method,* John Wiley & Sons, Inc., 1981.

21. EPRI, "Composite System Reliability Evaluation: Phase I - Scoping Study", *Report EL-5290*, December 1987.

22. Medicherla, T.K.P, " Reliability Evaluation of Composite Generation And Transmission Systems", Master's thesis, University of Saskatchewan, Saskatoon, May 1982.

23. Kumar, S., "Adequacy Evaluation of Composite Power System", Master's thesis, University of Saskatchewan, Saskatoon, July 1984.

24. Khan, E., "Fast Adequacy Assessment of Composite Power Systems", Master's thesis, University of Saskatchewan, Saskatoon, May 1988.

25. Stott, B. and Alsac, O., "Fast Decoupled Load Flow", *IEEE Transactions on Power Apparatus and Systems, Vol. PAS-93*, May/June 1974, pp. 859-869.

26. Billinton, R. and Kumar, S., "Effects of Higher-Level Independent Generator Outages in Composite System Adequacy Evaluation", *IEE Proceedings, Vol. 134, Part C*, August 1986, pp. 17-26.

27. Lian, G., " The Application of the Monte Carlo Simulation Method to Terminal Stations", Master's thesis, University of Saskatchewan, Saskatoon, November 1990.

28. Billinton, R. and Li, W., "Hybrid Approach for Reliability Evaluation of

Composite Generation and Transmission Systems Using Monte-Carlo and Enumeration Technique'', *IEE Proceedings-C, Vol. 138, No. 3*, May 1991, pp. 233-241.

29. Billinton, R. and Li, W., ''Consideration of Multi-state Generating Unit Models in Composite System Adequacy Assessment Using Monte Carlo Simulation'', *Canadian Journal for Electrical & Computer Enegineering, Vol. 17, No.1*, 1992, pp. 24-28.

30. IEEE Committee Report, ''IEEE Reliability Test System'', *IEEE Transactions on Power Apparatus and Systems, Vol. PAS-98*, 1979, pp. 2047-2054.

31. Billinton, R., Kumar, S., Chowdhury, K., Chu, K., Debnath, K., Goel, L., Khan, E., Kos, P., Nourbakhsh, G. and Oteng-Adjei, J., ''A Reliability Test System for Educational Purposes - Basic Data'', *IEEE Transactions on Power Systems, Vol. 4, No.3*, August 1989, pp. 1238-1244.

32. Billinton, R. and Salvaderi, L., ''A Comparison Between Two Fundamentally Different Approaches to Composite System Reliability Evaluation'', *IEEE Transactions on Power Apparatus and Systems, Vol. PAS-104, No.12*, December 1985, pp. 3486-3492.

33. Hallaron, S.A., ''Utility Involvement in Cogeneration and Small Power Production since PURPA'', *Power Engineering* , September 1985, pp. 44-47.

34. Harkins, H.C., ''PURPA New Horizons for Electric Utilities and Industry'', *IEEE Transactions on Power Apparatus and Systems, Vol. PAS-100, No.6*, June 1981, pp. 2784-2789.

35. Kirky, K.A., Rich, J.F. and Mahoney, P.J., ''Cogeneration Systems Evaluation: A Case Study'', *IEEE Transactions on Power Apparatus and Systems, Vol. PAS-100, No.6*, June 1981, pp. 2790-2795.

36. Palmer, J.D., ''Cogeneration From Waste Energy Streams - Four Energy Conversion Systems Described'', *IEEE Transactions on Power Apparatus and Systems, Vol. PAS-100, No.6*, June 1981, pp. 2831-2836.

37. Caramanis, M.C., Tabor, R.D., Nochur, K.S. and Schweppe, F.C, ''Non-Dispachable Technologies as Decision Variables in Long Term Generation Expansion Models'', *IEEE Transactions on Power Apparatus and Systems, Vol. PAS-101*, August 1982, pp. 2658-2667.

38. Merril, H.M., ''Cogeneration - A Strategic Evaluation'', *IEEE Transactions on Power Apparatus and Systems, Vol. PAS-102, No.2*, February 1983, pp. 463-471.

39. Chowdhury, A.A., *Unconventional Energy Sources in Power System Reliability Evaluation,* PhD dissertation, University of Saskatchewan, Saskatoon, February 1988.

40. Dialynas, E.N., ''Impact of Cogeneration and Small Power Producing Facilities on the Power System Reliability Indices'', *IEEE Winter Power Meeting Paper No. 89 WM 007-6 EC*, 1989.

41. Noyes, R., *Generation of Steam and Electric Power,* Noyes Data Corporation, Park Ridge, New Jersey., 1978.

42. Watchorn, C.W., "The Determination and Allocation of the Capacity Benefits Resulting from Interconnecting Two or More Generating Systems", *AIEE Transactions, 69, Part II*, (1950), pp. 1180-1186.

43. Cook, V.M., Galloway, C.D., Steinberg, M.J. and Wood, A.J., "Determination of Reserve Requirements of Two Interconnected Systems", *AIEE Transactions, PAS-82, Part III*, (1963), pp. 110-116.

44. Billinton, R. and Bhavaraju, M.P., "Load Loss Approach to the Evaluation of Generating Capacity Reliability of Two Interconnected Systems", *CEA Transactions, Spring Meeting*, March (1967).

45. Pereira, M.V.F., Maceira, M.E.P., Oliveira, G.C. and Pinto, L.M.V.G., "Combining Analytical Models and Monte-Carlo Techniques in Probabilistic Power System Analysis", *IEEE PES Summer Meeting, San Diego, Paper No.91 SM 459-8 PWRS*, July/August 1991.

Appendix A

DATA OF THE RBTS

BASE MVA = 100
BASE KV = 230

Table A.1: Bus Data

Bus No.	Load (p.u.) P	Q	P_g (p.u.)	Q_{max} (p.u.)	Q_{min} (p.u.)	V_0 (p.u.)	V_{max} (p.u.)	V_{min} (p.u)
1	0.00	0.000	1.000	0.50	-0.40	1.05	1.05	0.97
2	0.20	0.000	1.200	0.75	-0.40	1.05	1.05	0.97
3	0.85	0.000	0.000	0.00	0.00	1.00	1.05	0.97
4	0.40	0.000	0.000	0.00	0.00	1.00	1.05	0.97
5	0.20	0.000	0.000	0.00	0.00	1.00	1.05	0.97
6	0.20	0.000	0.000	0.00	0.00	1.00	1.05	0.97

Table A.2: Line Data

Line No.	Buses From	To	R	X	B/2	Tap	Current Rating (p.u.)	Failures per Year	Repair Time (Hrs)
1	1	3	0.0342	0.1800	0.10600	1.0	0.85	1.50	10.0
2	2	4	0.1140	0.6000	0.03520	1.0	0.71	5.00	10.0
3	1	2	0.0912	0.4800	0.02820	1.0	0.71	4.00	10.0
4	3	4	0.0228	0.1200	0.00705	1.0	0.71	1.00	10.0
5	3	5	0.0228	0.1200	0.00705	1.0	0.71	1.00	10.0
6	1	3	0.0342	0.1800	0.01060	1.0	0.85	1.50	10.0
7	2	4	0.1140	0.6000	0.03520	1.0	0.71	5.00	10.0
8	4	5	0.0228	0.1200	0.00705	1.0	0.71	1.00	10.0
9	5	6	0.0228	0.1200	0.00705	1.0	0.71	1.00	10.0

Table A.3: Generator Data

Unit No.	Bus No.	Rating (MW)	Failures per Year	Repair Time (Hrs)
1	1	40.00	6.00	45.00
2	1	40.00	6.00	45.00
3	1	10.00	4.00	45.00
4	1	20.00	5.00	45.00
5	2	5.00	2.00	45.00
6	2	5.00	2.00	45.00
7	2	40.00	3.00	60.00
8	2	20.00	2.40	55.00
9	2	20.00	2.40	55.00
10	2	20.00	2.40	55.00
11	2	20.00	2.40	55.00

Appendix B

DATA OF THE 24-BUS IEEE-RTS

BASE MVA = 100

Table B.1: Bus Data

Bus No.	Load (p.u.) P	Load (p.u.) Q	P_g (p.u.)	Q_{max} (p.u.)	Q_{min} (p.u.)	V_0 (p.u.)	V_{max} (p.u.)	V_{min} (p.u)
1	1.08	0.220	1.720	1.20	-0.75	1.02	1.05	0.95
2	0.97	0.200	1.720	1.20	-0.75	1.02	1.05	0.95
3	1.80	0.370	0.000	0.00	0.00	1.00	1.05	0.95
4	0.74	0.150	0.000	0.00	0.00	1.00	1.05	0.95
5	0.71	0.140	0.000	0.00	0.00	1.00	1.05	0.95
6	1.36	0.280	0.000	0.00	0.00	1.00	1.05	0.95
7	1.25	0.250	3.000	2.70	0.00	1.02	1.05	0.95
8	1.71	0.350	0.000	0.00	0.00	1.00	1.05	0.95
9	1.75	0.360	0.000	0.00	0.00	1.00	1.05	0.95
10	1.95	0.400	0.000	0.00	0.00	1.00	1.05	0.95
11	0.00	0.000	0.000	0.00	0.00	1.00	1.05	0.95
12	0.00	0.000	0.000	0.00	0.00	1.00	1.05	0.95
13	2.65	0.540	5.500	3.60	0.00	1.02	1.05	0.95
14	1.94	0.390	0.000	3.00	-0.75	1.00	1.05	0.95
15	3.17	0.640	2.100	1.65	-0.75	1.02	1.05	0.95
16	1.00	0.200	1.450	1.20	-0.75	1.02	1.05	0.95
17	0.00	0.000	0.000	0.00	0.00	1.00	1.05	0.95
18	3.33	0.680	4.000	3.00	-0.75	1.02	1.05	0.95
19	1.81	0.370	0.000	0.00	0.00	1.00	1.05	0.95
20	1.28	0.260	0.000	0.00	0.00	1.00	1.05	0.95
21	0.00	0.000	3.500	3.00	-0.75	1.02	1.05	0.95
22	0.00	0.000	2.500	1.45	-0.90	1.02	1.05	0.95
23	0.00	0.000	6.600	4.50	-1.75	1.02	1.05	0.95
24	0.00	0.000	0.000	0.00	0.00	1.00	1.05	0.95

Table B.2: Line Data

Line No.	Buses From	To	R	X	B/2	Tap	Current Rating (p.u.)	Failures per Year	Repair Time (Hrs)
1	1	2	0.0026	0.0139	0.2306	1.0	1.93	0.240	16.00
2	1	3	0.0546	0.2112	0.0286	1.0	2.08	0.510	10.00
3	1	5	0.0218	0.0845	0.0115	1.0	2.08	0.330	10.00
4	2	4	0.0328	0.1267	0.0172	1.0	2.08	0.390	10.00
5	2	6	0.0497	0.1920	0.0260	1.0	2.08	0.480	10.00
6	3	9	0.0308	0.1190	0.0161	1.0	2.08	0.380	10.00
7	3	24	0.0023	0.0839	0.0000	1.0	2.08	0.020	768.00
8	4	9	0.0268	0.1037	0.0141	1.0	2.08	0.360	10.00
9	5	10	0.0228	0.0883	0.0120	1.0	2.08	0.340	10.00
10	6	10	0.0139	0.0605	1.2295	1.0	1.93	0.330	35.00
11	7	8	0.0159	0.0614	0.0166	1.0	2.08	0.300	10.00
12	8	9	0.0427	0.1651	0.0224	1.0	2.08	0.440	10.00
13	8	10	0.0427	0.1651	0.0224	1.0	2.08	0.440	10.00
14	9	11	0.0023	0.0839	0.0000	1.0	6.00	0.020	768.00
15	9	12	0.0023	0.0839	0.0000	1.0	6.00	0.020	768.00
16	10	11	0.0023	0.0839	0.0000	1.0	6.00	0.020	768.00
17	10	12	0.0023	0.0839	0.0000	1.0	6.00	0.020	11.00
18	11	13	0.0061	0.0476	0.0500	1.0	6.00	0.400	11.00
19	11	14	0.0054	0.0418	0.0440	1.0	6.00	0.390	11.00
20	12	13	0.0061	0.0476	0.0500	1.0	6.00	0.400	11.00
21	12	23	0.0124	0.0966	0.1015	1.0	6.00	0.520	11.00
22	13	23	0.0111	0.0865	0.0909	1.0	6.00	0.490	11.00
23	14	16	0.0050	0.0389	0.0409	1.0	6.00	0.380	11.00
24	15	16	0.0022	0.0173	0.0364	1.0	6.00	0.330	11.00
25	15	21	0.0063	0.0490	0.0515	1.0	6.00	0.410	11.00
26	15	21	0.0063	0.0490	0.0515	1.0	6.00	0.410	11.00
27	15	24	0.0067	0.0519	0.0546	1.0	6.00	0.410	11.00
28	16	17	0.0033	0.0259	0.0273	1.0	6.00	0.350	11.00
29	16	19	0.0030	0.0231	0.0243	1.0	6.00	0.340	11.00
30	17	18	0.0018	0.0144	0.0152	1.0	6.00	0.320	11.00
31	17	22	0.0135	0.1053	0.1106	1.0	6.00	0.540	11.00
32	18	21	0.0033	0.0259	0.0273	1.0	6.00	0.350	11.00
33	18	21	0.0033	0.0259	0.0273	1.0	6.00	0.350	11.00
34	19	20	0.0051	0.0396	0.0417	1.0	6.00	0.380	11.00
35	19	20	0.0051	0.0396	0.0417	1.0	6.00	0.380	11.00
36	20	23	0.0028	0.0216	0.0228	1.0	6.00	0.340	11.00
37	20	23	0.0028	0.0216	0.0228	1.0	6.00	0.340	11.00
38	21	22	0.0087	0.0678	0.0712	1.0	6.00	0.450	11.00

Table B.3: Generator Data

Unit No.	Bus No.	Rating (MW)	Failures per Year	Repair Time (Hrs)
1	22	50.00	4.42	20.00
2	22	50.00	4.42	20.00
3	22	50.00	4.42	20.00
4	22	50.00	4.42	20.00
5	22	50.00	4.42	20.00
6	22	50.00	4.42	20.00
7	15	12.00	2.98	60.00
8	15	12.00	2.98	60.00
9	15	12.00	2.98	60.00
10	15	12.00	2.98	60.00
11	15	12.00	2.98	60.00
12	15	155.00	9.13	40.00
13	7	100.00	7.30	50.00
14	7	100.00	7.30	50.00
15	7	100.00	7.30	50.00
16	13	197.00	9.22	50.00
17	13	197.00	9.22	50.00
18	13	197.00	9.22	50.00
19	1	20.00	19.47	50.00
20	1	20.00	19.47	50.00
21	1	76.00	4.47	40.00
22	1	76.00	4.47	40.00
23	1	20.00	19.47	50.00
24	1	20.00	19.47	50.00
25	1	76.00	4.47	40.00
26	1	76.00	4.47	40.00
27	23	155.00	9.13	40.00
28	23	155.00	9.13	40.00
29	23	350.00	7.62	100.00
30	18	400.00	7.96	150.00
31	21	400.00	7.96	150.00
32	16	155.00	9.13	40.00

Appendix C

LOAD DATA

Table C.1: 100 Points Load Data

Study Period (p.u.)	Peak Load (p.u.)	Study Period (p.u.)	Peak Load (p.u.)	Study Period (p.u.)	Peak Load (p.u.)	Study Period (p.u.)	Peak Load (p.u.)
0.0000	1.0000	0.0002	0.9933	0.0003	0.9866	0.0004	0.9800
0.0006	0.9733	0.0008	0.9666	0.0010	0.9599	0.0015	0.9532
0.0024	0.9466	0.0034	0.9399	0.0040	0.9332	0.0058	0.9265
0.0076	0.9199	0.0081	0.9132	0.0100	0.9065	0.0137	0.8998
0.0160	0.8931	0.0189	0.8865	0.0239	0.8798	0.0290	0.8731
0.0333	0.8664	0.0401	0.8597	0.0464	0.8531	0.0517	0.8464
0.0614	0.8397	0.0718	0.8330	0.0823	0.8264	0.0906	0.8197
0.1004	0.8130	0.1122	0.8063	0.1254	0.7996	0.1353	0.7960
0.1452	0.7863	0.1574	0.7796	0.1704	0.7729	0.1823	0.7662
0.1918	0.7596	0.2005	0.7529	0.2114	0.7462	0.2232	0.7395
0.2339	0.7329	0.2436	0.7262	0.2561	0.7195	0.2670	0.7128
0.2773	0.7061	0.2909	0.6995	0.3030	0.6928	0.3163	0.6861
0.3300	0.6794	0.3448	0.6727	0.3616	0.6661	0.3769	0.6594
0.3934	0.6527	0.4094	0.6460	0.4260	0.6394	0.4420	0.6327
0.4591	0.6260	0.4771	0.6193	0.4932	0.6126	0.5089	0.6060
0.5242	0.5993	0.5390	0.5926	0.5501	0.5859	0.5625	0.5792
0.5742	0.5726	0.5869	0.5659	0.5992	0.5592	0.6134	0.5525
0.6265	0.5459	0.6415	0.5392	0.6544	0.5325	0.6706	0.5259
0.6881	0.5191	0.7043	0.5125	0.7218	0.5058	0.7410	0.4991
0.7603	0.4924	0.7810	0.4857	0.7992	0.4791	0.8158	0.4724
0.8302	0.4657	0.8473	0.4590	0.8599	0.4523	0.8758	0.4457
0.8880	0.4390	0.9029	0.4323	0.9159	0.4256	0.9293	0.4190
0.9420	0.4123	0.9549	0.4056	0.9647	0.3989	0.9721	0.3922
0.9783	0.3856	0.9827	0.3789	0.9867	0.3722	0.9905	0.3655
0.9949	0.3588	0.9977	0.3522	0.9991	0.3455	1.0000	0.3388

Appendix D

WHEELING SINK ADEQUACY INDICES

The failure probability and EENS indices obtained at the wheeling sink for the different wheeling operations in the interconnected RBTS and the IEEE-RTS are shown in Tables D.1 and D.2 respectively. These results can be used as indicators to determine satisfactory wheeling operations.

Table D.1: Wheeling Sink Failure Probability and EENS Indices for Wheeling Operations in the Interconnected RBTS

Wh. Sink Connected To:	Failure Probability (Wheeling Power/Load)		E E N S (MWh/Yr) (Wheeling Power/Load)	
	5 MW	50 MW	5 MW	50 MW
Bus 2	0.00000000	0.00000000	0.0000	0.0001
Bus 3	0.00000013	0.00000181	0.0008	0.5897
Bus 5	0.00000107	0.00000149	0.0464	0.4988
**Bus 6	0.00092654	0.00092657	40.5819	405.8260

**NB: Bus 6 is therefore unsuitable for wheeling sink connections.

Table D.2: Wheeling Sink Failure Probability and EENS Indices for Wheeling Operations in the Interconnected IEEE-RTS

Wh. Sink Connected To:	Failure Probability (Wheeling Power/Load)		E E N S (MWh/Yr) (Wheeling Power/Load)	
	10 MW	100 MW	10 MW	100 MW
Bus 1	0.00000000	0.00000000	0.0000	0.0000
Bus 3	0.00000000	0.00000005	0.0000	0.0080
Bus 8	0.00000001	0.00000014	0.0001	0.0115
Bus 13	0.00001025	0.00001025	0.1104	0.9349
Bus 17	0.00000000	0.00000000	0.0000	0.0000
Bus 18	0.00000773	0.00000798	0.0642	0.5897